Neural changes associated with spinal cord and external peripheral nerve stimulation for the treatment of neuropathic lower limb pain

Thesis submitted in accordance with the requirements of the University of Liverpool for the degree of Doctor in Philosophy by Danielle Hewitt

March 2022

Contents

Declaration

No part of this work was submitted in support of any other applications for degree or qualification at this or any other university or institute of learning.

Acknowledgements

I would firstly like to thank my supervisor, Dr Andrej Stancak, for his invaluable knowledge, expertise, and guidance during every stage of my PhD. I could not have asked for a better supervisor. I am also grateful to Dr Nick Fallon, Dr Chris Brown and Dr Bernhard Frank for their insight and support.

I would like to thank every member of my research group, with a special thanks to Jess Henderson, Alice Newton-Fenner, Adam Byrne, John Tyson-Carr and Tyler Mari, who provided moral support, technical assistance, and an endless supply of coffee and snacks. It has been an absolute pleasure.

Thank you to Abbott and MRC for funding this project, and the pain and neuromodulation team at The Walton Centre for their help with identifying patients for these studies. I am also deeply grateful to all study participants, without whom this work would not be possible.

Finally, I am thankful to my family for their unwavering support and encouragement over the years, which helped me to believe that this was possible.

I dedicate this thesis to my partner, Jordan, who has supported me throughout every stage of my academic journey so far. Doing this PhD would have been so much harder without your reassurance, optimism, and much-needed morning coffees. Thanks for everything.

List of abbreviations

In alphabetical order:

ACC	Anterior cingulate cortex
Ag-AgCl	Silver-silver chloride
ALE	Activation-likelihood estimation
ANOVA	Analysis of variance
BESA	Brain electrical source analysis
CLARA	Classical LORETA analysis recursively applied
CO_2	Carbon dioxide
CPSS	Chronic pain after spinal surgery
CRPS	Complex regional pain syndrome
CT	C-tactile
EEG	Electroencephalography
EN-PNS	External non-invasive peripheral nerve stimulation
ERD	Event-related desynchronisation
ERP	Event-related potential
ERS	Event-related synchronisation
fMRI	Functional magnetic resonance imaging
fNIRS	Functional near-infrared spectroscopy
GABA	Gamma-aminobutyric acid
GRADE	Grading of recommendations, assessment, development and evaluations
HFS	High-frequency stimulation
HTMR	High-threshold mechanoreceptors
Hz	Hertz
ICA	Independent component analysis
IPG	Implantable pulse generator
LEP	Laser-evoked potential
LFS	Low-frequency stimulation
LORETA	Low-resolution electromagnetic tomography
LTD	Long-term depression
LTMR	Low-threshold mechanoreceptor
LTP	Long-term potentiation
mA	Milliamperes

MCC	Midcingulate cortex
MEG	Magnetoencephalography
MI	Primary motor cortex
mJ	MegaJoule
MS	Multiple sclerosis
Nd:YAG	Neodimium Yttrium–Aluminium–Grenat
Nd:YAP	Neodimium Yttrium-Aluminium-Perovskite
NHS	National Health Service
PENS	Percutaneous electrical nerve stimulation
PET	Positron-emission tomography
PNS	Peripheral nerve stimulation
RA	Rapidly adapting
SA	Slowly adapting
SCS	Spinal cord stimulation
SD	Standard deviation
SEP	Somatosensory-evoked potential
SI	Primary somatosensory cortex
SI/MI	Primary sensorimotor cortex
SII	Secondary somatosensory cortex
SPECT	Single-photon emission computed tomography
TENS	Transcutaneous electrical nerve stimulation
Tm:YAG	Thulium Yttrium-Aluminium-Grenat
TMS	Transcranial magnetic stimulation
TSE	Temporal-spectral evolution
V	Voltage
VAS	Visual analogue scale
µs	Microseconds
µV	Microvolt

List of figures

List of tables

Abstract

Danielle Hewitt, Neural changes associated with spinal cord and external peripheral nerve stimulation for the treatment of neuropathic lower limb pain.

Spinal cord stimulation (SCS) and external low-frequency peripheral nerve stimulation (LFS) are palliative neurostimulation interventions for intractable neuropathic pain. However, understanding of the neural mechanisms underlying SCS and LFS is limited. Neurostimulation parameters such as waveform type and intensity modulate peripheral and central nociceptive pathways, which influence their therapeutic effects. The current thesis aimed to investigate the effects of varying intensities of burst and tonic SCS on resting cortical oscillations and somatosensory processing, and the temporal dynamics of LFS on somatosensory processing.

Effects of SCS on oscillatory dynamics were assessed in patients using burst and tonic SCS for neuropathic leg pain. Spontaneous resting oscillations and event-related desynchronisation during brushing of a pain-free leg were examined at four SCS intensities. Temporal effects of LFS applied to the radial nerve were examined using source dipole modelling in healthy volunteers at varying intensities. Change in resting EEG and nociceptive processing were investigated after LFS.

Results of four empirical studies pointed towards intensity-related changes in cortical activation during both SCS and LFS. Greater intensities of SCS and LFS were associated with decreased cortical excitability primarily in central and parietal scalp regions. Facilitatory effects of stimulation intensity were also identified in sensorimotor sources. Cortical activation changes during processing of somatosensory input were found between burst and tonic SCS.

Intensity-related changes in cortical excitability during SCS and LFS may be partially explained by the Gate Control Theory and long-term depression, respectively. Coexistence of attenuated cortical excitability and sensorimotor facilitation suggests that these neurostimulation interventions do not have simple gating effects. Results support different underlying mechanisms between burst and tonic SCS which are engaged during somatosensory input. Findings have important clinical implications for the palliative treatment of neuropathic pain syndromes.

Chapter 1

1 Spinal cord stimulation and peripheral nerve stimulation for neuropathic pain

1.1 Chronic pain

Pain is defined as "an unpleasant sensory and emotional experience associated with, or resembling that associated with, actual or potential tissue damage" (Raja et al., 2020). When pain persists or recurs over a period of 3 months or more, it is regarded as chronic (Treede et al., 2015). Chronic pain affects between 20–40% of people worldwide (Fayaz et al., 2016). In the UK, the annual incidence rate of chronic pain has been estimated at 8.3%, with a recovery rate of 5.4% (The British Pain Society, 2010).

Chronic pain has considerable negative impacts on quality of life, employment prospects, physical functioning, professional life and personal relationships (Hadi et al., 2019). The economic cost of chronic pain is difficult to quantify, but has been estimated at £10 billion in the UK (Maniadakis & Gray, 2000). Globally, the greatest cause of years lived with disability is chronic back and neck pain (Rice et al., 2016; World Health Organisation, 2020). In the UK, low back pain has the second biggest impact on disability-adjusted life years (World Health Organisation, 2020).

Pain can be divided into three broad categories: nociceptive, resulting from tissue damage, neuropathic, resulting from nerve damage, and nociplastic, resulting from a sensitized nervous system. Chronic pain can span multiple pain categories, which in turn determine clinical diagnosis, approach, and treatment options. Patients with neuropathic pain syndromes may be suitable candidates for neurostimulation interventions.

1.1.1 Neuropathic pain

Neuropathic pain is defined as pain caused by a lesion or disease in the somatosensory system (Treede et al., 2008). Neuropathic pain syndromes affect approximately 7–10% of the general population (van Hecke et al., 2014), with significant impacts on quality of life and functioning (Smith & Torrance, 2012).

Diagnosis of neuropathic pain requires a history of central or peripheral nervous system injury and a neuroanatomically plausible distribution of pain symptoms (Treede et al., 2019). Neuropathic pain symptoms may be spontaneous or evoked, as an increased response to a painful stimulus (hyperalgesia) or as a painful response to nonpainful stimuli (allodynia) (Finnerup et al., 2016; Scholz et al., 2019). Verbal descriptors of neuropathic pain include lancinating, shooting, electrical-like, stabbing and burning sensations, which can be experienced alongside sensory deficits of numbness, tingling and pricking (Cohen et al., 2021).

The origin of neuropathic pain can be peripheral, central, or both. The broad range of causes of neuropathic pain include physical trauma, vascular and metabolic disorders, infection, inflammation, genetic abnormalities and other pathological processes affecting peripheral and central nervous system structures (Devor, 2013). Such conditions result in changes in the nervous system, including ectopic hyperexcitability and abnormal impulse generation at the site of injury (reviewed in Devor, 2013). First-line treatment for neuropathic pain syndromes is pharmacological management. Patients who do not have effective pain relief from pharmacological treatments may be candidates for neurostimulation, with the primary indications being chronic pain after spinal surgery, complex regional pain syndrome and peripheral neuropathy.

1.1.2 Chronic low back pain after spinal surgery

Low back pain is defined as "pain, muscle tension or stiffness below the costal margin and above the inferior gluteal folds, with or without leg pain" (Koes et al., 2006). Back pain can be axial, radicular, or referred. Axial back pain is mechanical pain within the region of the lower back (L1–5) that worsens with movement and is not specific to the anatomical structure responsible for the pain (Alshelh et al., 2021; Bogduk, 2009; Urits et al., 2019). Radicular pain is that which radiates along the nerve into the leg and/or foot (Bogduk, 2009; Patel & Perloff, 2018; Urits et al., 2019). Axial pain is generally nociceptive, while radicular pain has a greater neuropathic component (Alshelh et al., 2021; Bogduk, 2009). Referred pain is the spread of pain to distal sites not innervated by the affected area (Bogduk, 2009). Low back pain may develop as a result of spinal canal tumours, arthritis, herniated or degenerated discs, stenosis, or instability (Long, 2013). Chronic low back pain that does not resolve

with time can be treated with surgical procedures such as spinal fusion, laminectomy, or decompression.

Chronic pain after spinal surgery (CPSS), also known as failed back surgery syndrome or lumbar post-laminectomy syndrome, is persistent or recurrent axial and/or radicular pain after surgery (Schug et al., 2019; Thomson, 2013). Prevalence for CPSS is estimated at 20% of patients who undergo spinal surgery (Inoue et al., 2017). CPSS can develop in patients for whom surgery was not indicated, where the surgery did not correct the original abnormality, or where a complication of surgery occurs and generates pain (Long, 2013). Complications of lumbar surgery include leakage of spinal fluid, nerve root injury, surgically-induced instability, infection and excessive scar formation (Long, 2013; Sebaaly et al., 2018). Risk factors for CPSS include psychological and social patient-related factors such as history of anxiety, depression and poor coping strategies, surgical factors of poor candidate selection, revision surgery and improper planning, and postoperative factors such as surgical complications and disease progression (Sebaaly et al., 2018).

1.1.3 Complex regional pain syndrome

Complex regional pain syndrome (CRPS) is a type of chronic primary pain characterised by severe, continuing regional pain which is seemingly disproportionate to the inciting event (Nicholas et al., 2019). CRPS can be separated into two distinctive forms: CRPS type I (previously known as reflex sympathetic dystrophy), where there is no demonstrable nerve damage, and CRPS type II (previously known as causalgia), where nerve damage can be identified as an initial cause of the condition (Harden et al., 2010). Those at a greater risk of developing CRPS are Caucasian women aged over 60 years, with a high household income and private insurance (Misidou & Papagoras, 2019; Sandroni et al., 2003). Although CRPS is separated into two types, nerve conduction studies show no significant difference in symptoms between groups (Harden et al., 1999).

CRPS occurs predominantly in one extremity, with multiple extremities affected in up to 7% of patients, although pain is not restricted to a specific dermatome (Sandroni et al., 2003; Veldman et al., 1993). The Budapest clinical diagnostic criteria for CRPS includes: positive sensory abnormalities including spontaneous pain, hyperalgesia or allodynia; vascular abnormalities including vasodilation,

vasoconstriction, temperature and/or skin colour asymmetry; oedema, including swelling and sweating changes; and motor and trophic changes, including decreased range of motion, stiffness, motor dysfunction, and nail or hair changes (Harden et al., 2010). Clinical diagnosis of CRPS relies on a patient experiencing at least one symptom from three or more categories.

For CRPS type I, the most common inciting event is trauma affecting distal extremities, which can originate from a fracture, contusion, strain or post-surgical condition, or less commonly from spinal cord injuries or cerebrovascular events (Binder & Baron, 2013). CRPS occurs in two phases: an acute "warm" phase with the onset of inflammation, during which time patients experience constant, deep pain that exacerbates with movement, and a later chronic "cold" phase as the inflammation subsides, where patients experience pain during rest, sensory deficits and sympathetic nervous system dysfunction (Bussa et al., 2017; Misidou & Papagoras, 2019). Aberrant inflammatory mechanisms, vasomotor dysfunction and plasticity in the peripheral and central nervous system have been suggested as mechanisms involved in the development and persistence of CRPS (Marinus et al., 2011).

1.1.4 Peripheral neuropathy

Painful peripheral neuropathies are a heterogenous group of conditions which include neuropathic pain due to peripheral nerve damage (Scadding & Koltzenburg, 2013). Causes of peripheral neuropathy are vast and can be broadly divided into symmetrical polyneuropathies and asymmetrical mononeuropathies or oligoneuropathies. Mononeuropathies include traumatic (including amputation stump pain and post-operative neuropathies), metabolic and nutritional (including beriberi and diabetes mellitus), drug-related and other mononeuropathies. Polyneuropathies include hereditary (including amyloid neuropathy and Fabry's disease), inflammatory (e.g. Guillian-Barré syndrome), and infectious polyneuropathies (e.g. human immunodeficiency virus) (Scadding & Koltzenburg, 2013).

Symptoms of peripheral neuropathy include sensory and motor alterations of numbness and tingling in the extremities, burning, stabbing or shooting pain in affected areas, loss of balance and coordination, twitching, paralysis, muscle weakness, and spontaneous, stimulus-independent pain

(NHS, 2019; Scadding & Koltzenburg, 2013). Sensory symptoms are mostly confined to affected peripheral nerves, although patients may experience secondary hyperalgesia outside of the injured dermatome (Binder & Baron, 2013). Due to the heterogeneity in clinical conditions producing peripheral neuropathy, a symptom-oriented approach is taken with diagnosis (Binder & Baron, 2013).

1.2 Spinal cord stimulation for neuropathic pain

1.2.1 Background of SCS

The first report of spinal cord stimulation (SCS, historically referred to as dorsal column stimulation) in humans was by Shealy, Mortimer, & Reswick (1967) in the case of a patient with upper abdomen and lower chest pain following bronchogenic carcinoma. SCS was shown to reduce deep and spontaneous pain whilst sparing mechanical pinprick sensation. This approach was inspired by the Gate Control Theory (Melzack & Wall, 1965) (see section 1.4.3). The first fully implantable SCS device was created by Medtronic in 1981, and the first rechargeable implanted pulse generator was released by Boston Scientific in 2004.

1.2.2 Indications for SCS

In the UK, SCS is recommended as a palliative treatment option for adults with chronic pain of neuropathic origin, including CPSS and CRPS, who continue to experience chronic pain for at least six months despite conventional medical management, and who have had a successful trial of stimulation (National Institute for Health and Care Excellence, 2008). In this case, chronic pain is optimised as measuring at least 50 mm on a 0 to 100 mm visual analogue scale.

The British Pain Society suggests that, in patients with CPSS, SCS may be an alternative intervention to repeat operation or increased opioid use (National Institute for Health and Care Excellence, 2008). In patients with radicular pain, approximately 50% of patients receiving conventional SCS achieve clinically significant pain relief (Grider et al., 2016; Kumar et al., 1996, 2008; North et al., 1991). In contrast, little to no efficacy is evident in patients with a primarily axial pain distribution (Kumar et al., 2008; Oakley, 2006). SCS is established as a cost-effective treatment for patients with neuropathic leg and back pain secondary to CPSS (Brinzeu et al., 2019; Farber et al., 2017; Hollingworth et al., 2011).

In CRPS, the British Pain Society states that SCS may be considered for pain management when conventional treatments including pharmacotherapy and nerve blocks fail to provide adequate pain relief (National Institute for Health and Care Excellence, 2008). SCS is a favourable and effective modality with high-level (1B+) evidence for treating pain symptoms and improving quality of life in patients with CRPS (Visnjevac et al., 2017). In the UK, SCS is a cost-effective adjunctive treatment to conventional medical management for CRPS (Kemler et al., 2010).

1.2.3 Procedure for SCS

The procedure for SCS implantation and programming has been recently described in detail (Sheldon et al., 2021). SCS implantation is a two-step procedure involving a screening trial implant and a permanent implant. During the trial period, which can last from 5 days up to 1 month, an epidural lead with multiple electrodes is placed over the dorsal column of the spinal cord and connected to an external pulse generator. The external pulse generator delivers electrical stimulation at programmed settings which are determined according to patient needs. A successful trial period, defined as a 50% reduction in pain and an acceptance of the stimulation by the patient, is the prerequisite to progress to permanent implant in the UK (National Institute for Health and Care Excellence, 2008). During the permanent implant, the epidural lead is connected to an implantable pulse generator (IPG) and therapeutic programmes are determined (see ***Figure 1.1***).

SCS has four programmable parameters: contact selection, amplitude, pulse width, and frequency. SCS leads are comprised of electrodes which generate an electric field when programmed in combinations of anodes and cathodes. Contact or electrode selection determines the size of stimulation coverage and depth and accounts for anatomical variations. Perception threshold, the minimum intensity required to induce paraesthesia, is a function of the spinal level of implanted electrodes, of the mediolateral position in the spinal canal and of the contact separation of the electrodes (He et al., 1994). Differences in perception threshold between spinal levels result from varying depths of cerebrospinal fluid (He et al., 1994). Frequency is defined as the number of pulses per second. Amplitude determines the strength and intensity of perception, as a measure of power output from the IPG measured in current (milliamperes, mA) or voltage (V). Amplitude is varied

according to patient need and is dependent on the type of stimulation. Once the optimal amplitude is determined, a therapeutic range is set with upper and lower limits, within which the patient can adjust independently. Pulse width determines the size of the electric field, with increased pulse width resulting in greater neuronal recruitment and wider areas of anatomical coverage (Miller et al., 2016; Yearwood et al., 2010). Pulse width directly correlates with amplitude, and the resultant charge per pulse determines the threshold for neuronal activation and action potential propagation (Crosby et al., 2015a; Miller et al., 2016).

Figure 1.1 Spinal cord stimulation devices. Left: Permanent SCS IPG (St Jude Medical Prodigy MRI™ IPG: Abbott, Texas, USA) which is capable of both BurstDR™ and tonic stimulation. Right: External pulse generator used for trial implants (St. Jude Medical™ Invisible Trial System: Abbott, Texas, USA), clinician programmer, for setting SCS contacts, amplitude, pulse width and frequency, and patient programmer, for switching the device on and off, changing therapeutic programmes and modifying intensity within predetermined limits.

Conventional tonic stimulation utilises single pulses of electrical stimulation typically at a frequency of 40–100 Hz, pulse width between 200 and 500 μs (Sheldon et al., 2021). During tonic SCS programming, the target stimulation range is determined for a patient. Minimum amplitude is typically the lowest value perceived by a patient, while maximum amplitude is the level at which stimulation induces uncomfortable sensations (Sheldon et al., 2021). The aim is to find an intensity that produces a tingling sensation known as paraesthesia over the painful area that is comfortable for the patient.

Paraesthesia-free SCS waveforms are set below sensory threshold. This thesis investigated conventional tonic stimulation and the burst waveform (BurstDR™, Abbott, Texas, USA) (De Ridder

et al., 2013). Burst stimulation consists of a series or packet of monophasic pulses of increasing amplitude followed by a brief quiescent period, after which the pattern repeats (De Ridder et al., 2010). Unlike other forms of burst SCS, the charge builds up over successive pulses and is passively recharged at the end of each packet (De Ridder et al., 2020; Falowski, 2018).

1.2.4 Advantage over alternative treatments

Alternative treatments to SCS are dependent on the patient's condition and symptoms, but commonly include pharmaceutical or surgical options. Treatments for neuropathic pain aim to achieve >30–50% pain reduction, an improvement in sleep and quality of life, and the recovery and maintenance of social activities, relationships and the ability to work (Binder & Baron, 2016).

First-line treatment for neuropathic pain is pharmaceutical management with tricyclic antidepressants, selective serotonin reuptake inhibitors, anticonvulsants or topical treatments such as capsaicin (Bates et al., 2019). UK guidelines recommend initial treatment of amitriptyline, duloxetine, gabapentin or pregabalin as initial treatment for all neuropathic pain syndromes except trigeminal neuralgia (National Institute for Health and Care Excellence, 2021c). These drugs have strong GRADE (Grading of Recommendations, Assessment, Development and Evaluations) recommendation for use in all neuropathic pain conditions due to high or moderate-high quality of evidence, low-moderate to moderate-to-high tolerability and safety, and moderate effect size (Finnerup et al., 2015). If initial treatment is not effective or not tolerated, another of the initial treatment drugs can be offered. Tricyclic antidepressants and selective serotonin reuptake inhibitors have common side effects of decreased appetite, gastrointestinal disorders, headache, vision disorders, somnolence and nausea (National Institute for Health and Care Excellence, 2021a). Anticonvulsant medications such as pregabalin and gabapentin are associated with common side effects of reduced appetite, impaired cognition, gastrointestinal discomfort, mood changes, movement disorders and sleep impairment (National Institute for Health and Care Excellence, 2021d, 2021b).

If pain is exacerbated or treatment is inadequate, stronger medications or a combination of treatments can be recommended (Bates et al., 2019). Opiates are not recommended, except for acute rescue therapy or in a specialist setting (National Institute for Health and Care Excellence, 2021c).

Strong opiates have weak GRADE recommendation for use and as such are third-line drugs for all neuropathic pain conditions, with moderate quality of evidence, moderate effect sizes, and low-to-moderate tolerability and safety (Finnerup et al., 2015). Opiates such as tramadol have side effects that include confusion, dizziness, drowsiness, euphoric mood, hallucination, respiratory depression, and headache (National Institute for Health and Care Excellence, 2021e).

Primary surgical treatment aims to treat the underlying cause of pain. It can be associated with further damage, leading to CPSS, or may not effectively treat the pain. CPSS is estimated to occur in 20% of patients who undergo spinal surgery (Inoue et al., 2017; Weir et al., 2020). In a systematic review of the long-term use of opiates after lumbar spinal fusion for chronic lower back pain, opioid use was found to persist in more than one in three patients, suggesting a continued need for pain management (Vraa et al., 2022).

Neurostimulation is recommended as a fourth-line treatment for neuropathic pain, prior to low-dose opioids (Bates et al., 2019). For chronic neuropathic pain after spinal surgery, SCS has been shown to provide better pain relief and improve health-related quality of life and functional capacity than conventional pharmacological management (Kumar et al., 2007). In a review of safety, appropriateness, fiscal neutrality and effectiveness of SCS for CPSS, it was suggested that SCS should be considered before long-term systemic opioid therapy or repeat spinal surgery (Krames et al., 2011). In patients with CRPS, clinical effectiveness of SCS has been investigated versus conventional medical management of physical therapy. A randomised controlled trial of 36 patients showed a significant improvement in health-related quality of life, and greater reduction in pain intensity was observed for SCS and physical therapy versus physical therapy only (Kemler et al., 2000).

1.3 Peripheral nerve stimulation for neuropathic pain

1.3.1 Background of PNS

Electrical stimulation has been used for many years to treat pain, dating back to the use of eels to treat pain from arthritis, gout and headaches in around 47CE (Cambiaghi & Sconocchia, 2018). In the late 1800s, Gaiffe developed a transcutaneous electrical nerve stimulator which relieved pain

when applied to the head, while Althaus reported that direct electrical stimulation of peripheral nerves reduced surgical pain in the extremities (reviewed in Ottestad and Orlovich, 2020).

The modern era of neuromodulation was conceptualised based on the Gate Control Theory (Melzack and Wall, 1965) (see section 1.4.3). Subsequently, the first report of pain relief after peripheral electrical stimulation (PNS) came from Wall and Sweet, who reported that nonpainful electrical PNS suppressed acute mechanical pain perception in the infraorbital nerve, and reduced pressure pain in affected nerve regions in patients with chronic cutaneous pain (Wall & Sweet, 1967). The first full permanent implant was attributed to Sweet and Wepsic (Sweet & Wepsic, 1968). Commercially available electrodes, leads and IPGs for PNS inserted in open surgery were developed in the 1980s (Ottestad & Orlovich, 2020). A percutaneous technique for inserting electrodes was subsequently developed for occipital neuralgia by placing an electrode in the proximity of the nerve (PENS) (Weiner & Reed, 1999).

More recently, external PNS devices have been developed, which present a non-invasive treatment option. One such method, external non-invasive peripheral nerve stimulation (EN-PNS), delivers cutaneous electrical stimulation to affected peripheral nerves at low frequencies of 1–2 Hz. Early reports support the effectiveness of 1.5–2.5 Hz electrical stimulation to treat a range of pain conditions, including back pain, headache, trigeminal neuralgia, vascular disease and cancer pain (Rutkowski et al., 1975). Low frequency external peripheral nerve stimulation (LFS) has since been shown to reduce pain from acute experimental stimuli in healthy volunteers (Ellrich & Schorr, 2004; Klein et al., 2006; Magerl et al., 2018; Rottmann et al., 2008), relieve symptoms of neuropathic pain (Johnson et al., 2015; Johnson & Goebel, 2016), and suppress mechanical hyperalgesia (Johnson et al., 2021).

1.3.2 Indications for LFS

Treatments utilising invasive PNS are effective for neuropathic pain conditions restricted to a single area or dermatome, and successful treatment has been reported in conditions such as occipital neuralgia (Weiner & Reed, 1999), neuropathic pain (Law et al., 1980; Reverberi et al., 2009), chronic migraine (Matharu et al., 2004), CRPS (Frederico & da Silva Freitas, 2020; Goroszeniuk et al., 2014),

and cranial neuralgias (Slavin et al., 2006). In the UK, PENS is accredited to treat refractory neuropathic pain based on evidence of short-term efficacy (National Institute for Health and Care Excellence, 2013).

Due to the emerging nature of this treatment, external, non-invasive LFS is not widely available as a treatment option in the UK. Indications for LFS match that of invasive PNS. External, non-invasive LFS has been used in patients with a diagnosis of CRPS or peripheral neuropathy (Johnson et al., 2015, 2021; Johnson & Goebel, 2016).

1.3.3 Procedure for LFS

LFS is applied transcutaneously to peripheral nerves using a small diameter ball or concentric electrode. LFS frequency is set between 1–2 Hz, with a pulse width of 0.1–2 μs (Biurrun Manresa et al., 2010; Chen & Sandkühler, 2000; Torta et al., 2020; Vo & Drummond, 2014). LFS intensity is determined by increasing stimulation amplitude to reach a moderately painful intensity (Liu et al., 1998). An optimal intensity of fourfold pain threshold has been recommended in humans (Jung et al., 2009). A combination of high intensity and small diameter electrode allows a high current density, which preferentially activates Aδ nerve fibres (Inui et al., 2002; Liu et al., 1998; Sandkühler et al., 1997). Treatment durations of 20-minutes are suggested for optimal LFS, with a total of 1200 pulses per block (Jung et al., 2009).

1.3.4 Advantages over alternative treatments

Alternative treatments for CRPS and peripheral neuropathic pain are pharmacological management, as described, and other neurostimulation treatments.

LFS is less invasive than classical PNS treatment. Invasive PNS involves percutaneous placement of an electrode over one or more individual nerves or dermatomes, connected to an IPG and battery. A randomised controlled trial of PNS in 94 patients with neuropathic pain found a mean pain reduction of 27% in the treatment group compared to 2% in the control group (Deer et al., 2016). Invasive PNS is associated with a myriad of risks, with common side effects of skin infection, inadequate stimulation and lead migration. In a multicentre trial of 157 patients undergoing PNS for

chronic migraine, 70.7% (111) of patients experienced one or more adverse events, with 8.6% of incidents requiring hospitalisation and 40.7% requiring surgical intervention (Dodick et al., 2015).

While LFS is not yet widely available as a treatment option in the UK, initial reports support the effectiveness as a pain treatment. Kothari & Goroszeniuk (2006) reported a case series in which 86% of 240 patients tested with a 5-minute session of LFS reported "excellent" pain relief. An observational study of 20 patients using LFS for CRPS or neuropathic pain after peripheral nerve injury found that 40% of patients showed significant short-term pain relief over 6 weekly treatment sessions (Johnson et al., 2015). This effect was sustained by a subset of patients in the long term (Johnson & Goebel, 2016). However, it should be noted that a recent randomised controlled trial did not find a statistically significant reduction of spontaneous pain with LFS (Johnson et al., 2021).

Alternative non-invasive electrical stimulation devices are commercially available such as transcutaneous electrical nerve stimulation (TENS). TENS uses a higher frequency of 50–100 Hz and large, flat electrodes, resulting in a low current density and preferential activation of Aβ fibres. Overall, TENS is neither supported nor refuted by the literature as a treatment for intractable neuropathic pain. Systematic reviews of the therapeutic effects of TENS in a range of chronic pain conditions, including neuropathic pain, report a lack of consensus on the harm or benefit of TENS on pain management, disability and health-related quality of life due to methodological limitations and low-quality data (Gibson et al., 2019).

1.4 Neurobiology of pain

To investigate neural mechanisms of neurostimulation methods, it is essential to understand the neurobiology of pain.

1.4.1 Peripheral mechanisms of cutaneous nociception

Somatosensory processing starts with activation of cutaneous sensory neurons. One type, low-threshold mechanoreceptors (LTMRs), lead to the perception of innocuous touch. Another type, high-threshold mechanoreceptors (HTMRs), are classed as nociceptors and respond to noxious (injurious or possibly injurious) stimuli.

Cutaneous senses include tactile, thermal, pain and itch submodalities. Cutaneous sensations relayed to the somatosensory cortex from the neck down are conveyed by fibres of primary sensory neurons located in dorsal root ganglia. Sensations from the face are relayed by cranial nerves located in trigeminal root ganglia. These fibres comprise cell bodies of peripheral afferents innervating the skin (see ***Table 1.1.*** and ***Figure 1.2***).

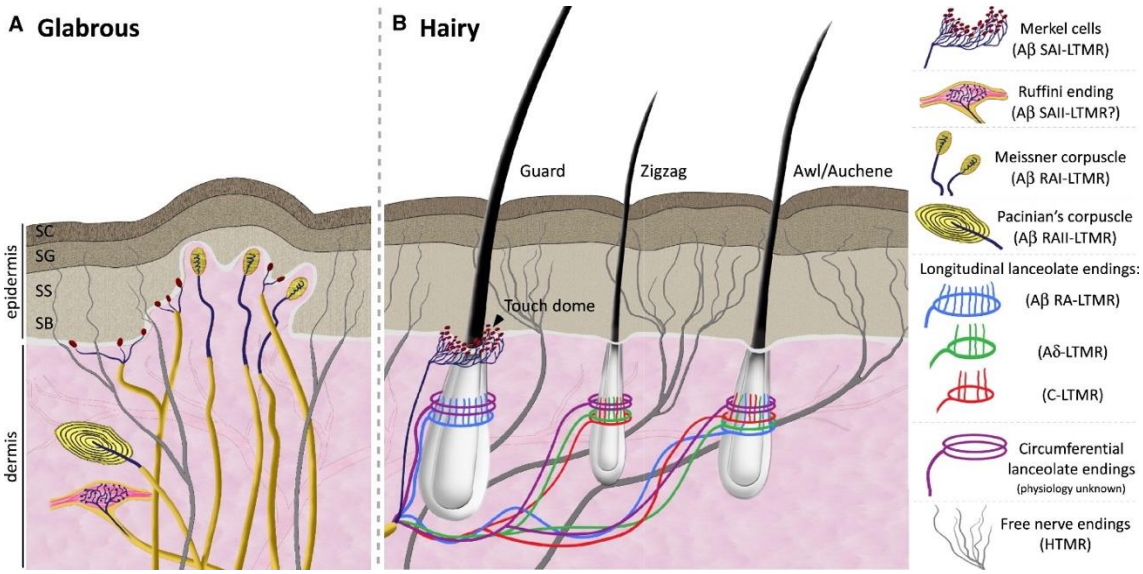

Figure 1.2. Organisation of cutaneous mechanoreceptors in the skin. From Abraira & Ginty (2013).

Aβ fibres are tactile cutaneous afferents which have a large diameter and a thick myelin sheath to rapidly conduct information from non-noxious mechanical stimuli (reviewed in Abraira & Ginty, 2013). Touch perception via Aβ fibres in glabrous (non-hairy) skin relies on four different receptors: Pacinian corpuscles, Meissner's corpuscles, Merkel's disks and Ruffini endings, known as LTMRs (McGlone & Reilly, 2010). Cutaneous receptors are classified by speed of adaptation: Pacinian and Meissner's corpuscles are rapidly adapting (RA), responding to initial and final contacts of stimuli, while Merkel's disks and Ruffini endings are slowly adapting (SA), continuously firing to constant stimuli. Receptors are also defined by the size of their receptive fields. Meissner's corpuscles and Merkel's disks near the surface of the skin have small receptive fields. Pacinian corpuscles and Ruffini endings located deeper in the skin have large receptive fields. Myelination of sensory axons determines the speed of impulse conduction.

Table 1.1. Cutaneous sensory afferents, reviewed in Abraira & Ginty (2013), McGlone & Reilly (2010) and Smith & Lewin (2009).

Class	Subtype	Conduction velocity	Myelination	Skin type	End organ	Stimuli
Aβ	SAI-LTMR	16–96m/s	Thick	Hairy, glabrous	Merkel's disc, guard hair	Mechanical fine touch
	SAII-LTMR	20–100m/s	Thick	Glabrous	Ruffini corpuscle	Stretch
	RAI-LTMR	26–91m/s	Thick	Glabrous	Meissner's corpuscle	Skin deformation
	RAII-LTMR	30–90m/s	Thick	Glabrous	Pacinian corpuscle	Vibration
Aδ	HTMR	2–10 m/s	Thin	Hairy, glabrous	Free nerve endings	Noxious heat and mechanical
	LTMR	5–30m/s	Thin	Hairy	Free nerve endings, zigzag and auchene hair	Mechanical, non-noxious cold
C	HTMR	0.2–1.5 m/s	Unmyelinated	Hairy, glabrous	Free nerve endings	Noxious heat, cold, mechanical
	LTMR/C-tactile	0.2–2m/s	Unmyelinated	Hairy	Zigzag and auchene hair	Pleasant mechanical, non-noxious heat, rapid cooling

LTMRs in Aβ, Aδ and C-type categories innervate hairy skin. Hairy skin LTMRs are associated with hair follicles. Merkel cells, the cellular substrate of SAI-LTMRs (Halata et al., 2003), are found at a higher density in sensitive areas of the skin, including glabrous skin of the fingers and lips, and at a lower density in hairy skin (reviewed in Abraira & Ginty, 2013).

A population of LTMR C fibres, known as C-tactile (CT) afferents, respond preferentially to low force, slowly moving mechanical stimuli in hairy skin. First described in humans using microneurography by Johansson et al. (1988), CT-afferents have primarily been found in hairy skin (Vallbo et al., 1993), with only preliminary evidence of CT-afferents in glabrous skin (Watkins et al., 2020). These neurons have been suggested to code for pleasant, affective touch (Löken et al., 2009).

Nociceptors are primary afferents which protect the skin against potential or actual damage. There are two major classes of nociceptors: Aδ and C fibres (Bessou & Perl, 1969; Burgess & Perl, 1967). Aδ fibres are medium diameter, thinly myelinated afferents which respond with high acuity to noxious mechanical and thermal stimuli within their small receptive fields (Burgess & Perl, 1967). Aδ nociceptors adapt slowly to stimuli (Koltzenburg et al., 1997). C fibres are thin, unmyelinated afferents which slowly conduct noxious mechanical, heat and chemical stimuli (Bessou & Perl, 1969). Polymodal C fibres have large receptive fields and poor localisation. Aδ and C nociceptors do not have specialised end organ structures and terminate as free nerve endings in the epidermis in glabrous and hairy skin (Kruger et al., 1981; Smith & Lewin, 2009).

Aδ nociceptors in hairy skin can be subdivided into Type I (HTMRs) and Type II (LTMRs) nociceptors (Treede et al., 1998, 1995). Type I Aδ nociceptors respond to mechanical and chemical stimuli, as well as maintained heat stimuli. These Type I Aδ nociceptors likely mediate the first pain evoked by intense mechanical stimuli (Basbaum et al., 2009; Treede et al., 1998). Type II Aδ nociceptors have a lower heat threshold but high mechanical threshold, which mediate the first acute pain response to noxious heat (Basbaum et al., 2009).

A population of HTMR C fibres can be sensitized after inflammation due to injury. This population has been termed “silent” C fibres as they usually do not respond to mechanical or thermal stimuli (Handwerker et al., 1991; Schaible & Schmidt, 1983; Schmidt et al., 1995) but can become responsive to mechanical or heat stimuli after sensitisation (Kress et al., 1992; Prato et al., 2017).

1.4.2 Central projections of cutaneous sensory afferents

Cell bodies of primary sensory neurons from the body are located in the dorsal root ganglion. Dorsal root ganglion cells project to the periphery and to the central nervous system, with centrifugal branches terminating in the spinal cord. Primary afferent fibres innervating areas of the body are grouped together into fascicles of axons forming the peripheral nerves. Central projections of primary afferent fibres differ for those responding to tactile and noxious stimuli, although some mixing between tracts does occur (reviewed in Gardner & Johnson, 2013 and McGlone & Reilly, 2010).

The spinal cord is composed of grey matter, including cell bodies and dendrites of neurons and glial cells, and white matter, consisting primarily of axons (Amaral & Strick, 2013). The spinal cord grey matter is organised into anatomically distinct laminae, numbered from I to X based on cytoarchitecture (Gardner & Johnson, 2013; Rexed, 1952). Spinal grey matter is further subdivided into functionally distinct regions of the dorsal horn, intermediate zone and ventral horn; laminae I–VI comprise the dorsal horn and have the closest association with nociception (Gardner & Johnson, 2013). Neurons in lamina I receive nociceptive or thermal inputs from Aδ or C fibres. Neurons in lamina II and III are interneurons that receive inputs from Aδ and C fibres and make connections with other laminae. Neurons in laminae III–V receive tactile input from Aβ fibres. Additionally, neurons in lamina V, known as wide-dynamic range neurons, respond to multiple stimulus modalities including low-threshold mechanical stimuli, visceral stimuli and noxious stimuli.

First-order neurons of tactile primary afferents (Aβ fibres) project to deep laminae (III, IV, and V), and ascend the spinal cord to form dorsal columns (Gardner & Johnson, 2013). Information from the legs and trunk are conveyed in medial tracts of the gracile fasciculus, which synapse with second-order neurons in the gracile nucleus. Information from the arms and trunk are conveyed in lateral tracts comprising the cuneate fasciculus, which synapse with second-order neurons in cuneate nucleus. Dorsal column fibres are initially arranged segmentally but rearrange somatotopically (Brodal, 1992). Second-order neurons decussate in the medulla to form the medial lemniscus tract which ascends to the thalamus. The dorsal column system transmits tactile and proprioceptive information from Aβ and Aα fibres (Brodal, 1992). Fibres of the medial lemniscus terminate in ventral posterior nuclei (*nucleus ventralis caudalis* in humans) of the thalamus, with the medial zone receiving trigeminal nerve fibres from the head and face, and the lateral zone receiving fibres from dorsal column nuclei (Gardner & Johnson, 2013). Neurons of the ventral posterior nucleus transmit cutaneous information via the internal capsule to the primary somatosensory cortex (SI) in the postcentral gyrus and the secondary somatosensory cortex (SII) on the upper bank of the Sylvian fissure (Brodal, 1992).

The first synapse in ascending nociceptive pathways is the dorsal horn, where nociceptive afferents terminate (Brodal, 1992). First-order neurons of noxious primary afferents ascend the dorsal

horn of the spine and synapse to form the dorsolateral fasciculus or Lissauer's tract (Light & Perl, 1977). Aδ fibres enter the posterior marginalis and nucleus proprius of the dorsal horn (laminae I, III and IV) and synapse onto second-order neurons, which decussate and ascend to the thalamus via the anterolateral system to form the spinothalamic tract. C fibres project to the substantia gelatinosa of the dorsal horn (superficial laminae I and II) and synapse onto interneurons, which relay to secondary afferents in the posterior marginalis or nucleus proprius, and ascend to the thalamus to form the spinothalamic tract (Gardner & Johnson, 2013). C fibres synapsing with interneurons in lamina II send axons dorsally into lamina I, and ventrally to other interneurons which synapse onto spinothalamic cells in laminae V, VII and VIII, as well as sending axon collaterals to spinal segments above and below via the tract of Lissauer (Brodal, 1992).

The spinothalamic tract projects from neurons in lamina I, V and VII to convey noxious, thermal and visceral information from nociceptive-specific (Aδ and C fibres), wide dynamic range neurons and visceral neurons (Basbaum & Jessell, 2013). Fibres in the spinothalamic tract are arranged somatotopically (Gardner & Johnson, 2013). The spinothalamic tract terminates in medial and lateral thalamic nuclei (Brodal, 1992). Lateral thalamic nuclei are made up of the ventroposterior medial nucleus, ventroposterior lateral nucleus and posterior nucleus and are thought to be involved in processing the location of pain stimuli (Gardner & Johnson, 2013). Medial thalamic nuclei are comprised of the central lateral nucleus and intralaminar complex. Nociceptive information from the thalamus projects to SI and SII (Brodal, 1992).

1.4.3 Gate Control Theory

The Gate Control Theory of pain (Melzack & Wall, 1965) posited that the substantia gelatinosa in the spinal dorsal horn acts as a gating mechanism to modulate synaptic transmission of nociceptive information from peripheral fibres to central processing. Interneurons of the substantia gelatinosa modulate input to spinal transmission cells based on the balance between large (Aβ) and small diameter (Aδ) nerve fibre inputs, with large fibres inhibiting transmission (closing the 'gate') and small fibres facilitating transmission (opening the 'gate').

According to the Gate Control Theory, high intensity stimuli cause an unbalanced small fibre input to transmission cells via the presynaptic gate in the substantia gelatinosa due to selective adaptation of large fibres (Melzack & Wall, 1965). Unbalanced small fibre input reduces presynaptic inhibition of sensory inputs, thus opening the spinal gate. When spinal transmission cell output reaches or exceeds a critical level, the so-called action system is activated, resulting in pain experience. The critical level is determined by the net input of afferent impulses reaching the spinal transmission cells. Simultaneous somatosensory stimuli (such as touch, vibration or electrical stimulation) activating Aβ fibres may increase the action of inhibitory interneurons, producing a disproportionate relative increase of large diameter fibre over small diameter fibre activity, suppressing the transmission and closing the spinal gate to reduce the subsequent experience of pain. The Gate Control Theory also suggested a mechanism of descending pain modulation (Melzack & Wall, 1965). A mechanism in the central nervous system, named the central control trigger, activates brain processes that exert control over the gate control system via descending fibres to influence the transmission of sensory information. Therefore, the Gate Control Theory postulates that the brain receives information about pain via a gate controlled system which is influenced by injury signals, afferent impulses, and descending control (Wall, 1978).

Shortcomings of the Gate Control Theory have been described extensively (Mendell, 2014; Nathan, 1976) ***(see 1.6.1.3)***. Limitations include oversimplifications and flaws in descriptions of spinal cord architecture and descending pain modulation (reviewed in Mendell, 2014; Sufka & Price, 2002). Despite its limitations, the Gate Control Theory remains an important early account of the neural interactions underlying nociceptive transmission.

1.4.4 Primary and secondary hyperalgesia

Injury to the skin results in the local release of chemicals from non-neuronal cells and terminals of primary afferent fibres that facilitate the inflammatory process, which can, in turn, potentiate nociceptor responses (Ringkamp et al., 2013; Treede et al., 1992). Increased responsiveness to mechanical and heat stimuli at the site of injury is known as primary hyperalgesia, while increased

responsiveness in an adjacent zone outside the site of injury is known as secondary hyperalgesia (Hardy et al., 1950; Treede et al., 1992; Woolf, 2011).

Primary hyperalgesia of mechanical and heat stimuli is mediated by peripheral sensitisation of primary afferent nociceptors (LaMotte et al., 1983; Ringkamp et al., 2013). After a thermal injury, stimulus-response functions for heat pain at the site of injury are shifted to the left, indicating a decrease in threshold and an increase in sensation (Bessou & Perl, 1969; Raja et al., 1984). In uninjured adjacent skin, no increase in heat responsiveness is observed. Primary hyperalgesia to heat stimuli is mediated by sensitisation of nociceptors (LaMotte et al., 1982; Meyer & Campbell, 1981). Sensitisation of nociceptors is dependent on tissue type and the nature of injury; heat hyperalgesia for thermal injuries on the glabrous skin of the hand are thought to be coded for by mechanical and heat sensitive type I Aδ fibres (Meyer & Campbell, 1981), while heat hyperalgesia for thermal injuries on hairy skin are mediated by sensitisation of mechanical and heat sensitive C fibres (Campbell & Meyer, 1983). Thresholds to mechanical stimulation for mechanical and heat sensitive C- and A-fibres are not changed by heat or mechanical injury, but mechanical-insensitive A fibres develop mechanical sensitivity after inflammation (Campbell et al., 1988; Thalhammer & LaMotte, 1982). Inflammation results in enhanced responses to suprathreshold mechanical stimuli, spontaneous activity and expanded receptive fields of mechanical and heat sensitive A fibres (Andrew & Greenspan, 1999; Reeh et al., 1987; Thalhammer & LaMotte, 1982).

Secondary hyperalgesia is accounted for by central sensitisation, an abnormal state of responsiveness or increased gain of the nociceptive system (Latremoliere & Woolf, 2009; Woolf, 1983). Secondary hyperalgesia is specific to mechanical stimuli (Hardy et al., 1950; Treede et al., 1992; Woolf, 2011). Two forms of mechanical hyperalgesia have been observed: stroking and punctate hyperalgesia. Stroking hyperalgesia, also known as dynamic hyperalgesia or allodynia, is the perception of pain from a normally innocuous mechanical stimulus such as a brush (Ringkamp et al., 2013). Stroking hyperalgesia is mediated by sensitisation of second-order neurons in the dorsal horn to the input of LTMRs (Koltzenburg et al., 1992; LaMotte et al., 1991). Punctate hyperalgesia is heightened pain associated with probes or pinpricks applied to the skin (Ringkamp et al., 2013). Punctate hyperalgesia appears to be mediated by small-diameter Aδ fibres which are insensitive to

capsaicin and heat and project via sensitized mechano-specific interneurons to central pain-signalling neurons (Fuchs et al., 2000; Magerl et al., 2001). Anaesthesia or cooling over the area of primary hyperalgesia can block the development of allodynia, whereas punctate hyperalgesia persists, suggesting that allodynia is dependent on ongoing discharge from the sensitized area while punctate hyperalgesia is dependent on input from the primary area of injury (LaMotte et al., 1991). Central sensitisation has been linked to pain hypersensitivity in neuropathic pain, which is characterised by symptoms of allodynia and mechanical hyperalgesia (Ringkamp et al., 2013; Treede et al., 1992).

Activity-dependent synaptic plasticity in the dorsal horn can be modified in the form of long-term depression (LTD) and long-term potentiation (LTP). In contrast to central sensitisation, where activity in affected synapses enhance activity in non-activated synapses, LTD and LTP modify the efficacy of activated synapses only. LTD, a decrease in synaptic strength, can be induced with repetitive LFS (1–2 Hz) in the hippocampus and other areas of the central nervous system (Bliss & Cooke, 2011; Dudek & Bear, 1992; Mulkey & Malenka, 1992). LTD can be induced in the nociceptive system after repetitive LFS of Aδ fibres in the spinal dorsal horn both *in vitro* (Chen & Sandkühler, 2000; Ikeda et al., 2000; Kim et al., 2015; Sandkühler et al., 1997) and *in vivo* (Liu et al., 1998).

LTP, an increase in synaptic strength, can be elicited with conditioning high-frequency stimulation (HFS, ~100 Hz) at many synapses in the central nervous system, most notably in the hippocampus (Bliss & Collingridge, 1993; Bliss & Lomo, 1973; Lømo, 2003). HFS of primary afferent fibres in the dorsal horn induces LTP of Aδ (Randić et al., 1993) and C fibre responses (Ikeda et al., 2003, 2006; Liu et al., 2009; Svendsen et al., 1997). In addition to HFS, LTP of C fibres has been shown to be induced by natural noxious stimuli in spinalised rats (Sandkühler & Liu, 1998) and following nerve injury in intact rats (Zhang et al., 2004). LTP in the dorsal horn can be inhibited and reversed with LFS (Ikeda et al., 2000; Liu et al., 1998; Sandkühler et al., 1997).

1.5 Representation of pain in the brain

Sensory impulses from the dorsal column pathway, transmitting signals from LTMRs, terminate in the thalamus and project to SI and SII (Brodal, 1992). SI and SII receive somatotopically organised projections from thalamic nuclei and send fibres to the association areas in the posterior

parietal cortex. Somatosensory impulses are also transmitted to other cortical regions including the motor cortex (MI) in the precentral gyrus (Brodal, 1992). Sensory inputs from the spinothalamic tract conveying noxious and thermal information terminate in the thalamus and project primarily to SII, midcingulate cortex (MCC) and the insula (Dum et al., 2009). In humans, activation of these regions in response to pain stimuli have been investigated using neuroimaging and electrophysiology techniques.

1.5.1 Distinct brain responses to acute pain

Neuroimaging studies measuring haemodynamic changes using functional magnetic resonance imaging (fMRI), functional near-infrared spectroscopy (fNIRS) and positron-emission tomography (PET) have identified a wide network of cortical and subcortical areas activated during pain.

Pain-related neural activation patterns are consistent across a range of stimuli used to induce acute pain sensations. In a large co-ordinate-based activation-likelihood estimation (ALE) meta-analysis of 222 fMRI studies, Xu et al. (2020) reported pain-related activation in bilateral SII, left insula, bilateral thalamus, bilateral brainstem, bilateral amygdala, right middle frontal gyrus, and left MCC. Activation in these regions was consistent regardless of stimulation technique, induction location, and participant sex. Likewise, in an ALE meta-analysis of 138 fMRI datasets, Jensen et al. (2016) reported clusters with a significant likelihood of activation during pain in the bilateral thalamus, bilateral insula, left SI, left SII, right ACC, right prefrontal cortex and cerebellum. Duerden & Albanese (2013) found common activation in 140 neuroimaging studies in the left thalamus, right ACC, bilateral anterior insula, and left dorsal posterior insula across studies using noxious stimuli. Here, the right insula and ACC had the greatest likelihood of activation, followed by the left insula, bilateral SII, prefrontal cortex and SI/posterior parietal cortex. A systematic review and meta-analysis of 18 fNIRS studies comparing noxious with innocuous stimulation in healthy volunteers found greater engagement of sensorimotor regions compared to prefrontal regions during noxious stimuli (Hall et al., 2021).

Pain-related cortical activation differs according to the stimulus used to elicit pain. In the aforementioned meta-analysis, Xu et al. (2020) contrasted brain activation for thermal versus non-thermal pain modalities, and electrical versus mechanical pain modalities. Thermal experiments were associated with stronger convergence of activation in bilateral MCC, while non-thermal experiments were associated with stronger convergence in the right insula and left Rolandic operculum. Widespread overlap between activations was observed in bilateral supramarginal gyrus (including SII), bilateral thalamus, bilateral MCC, right middle frontal gyrus, bilateral putamen, bilateral supplementary motor area and right amygdala. Similarly, a smaller, early ALE meta-analysis reported a consistent network of thermal pain-related activity of the mid-ACC, bilateral thalamus, insula, opercula cortices, posterior parietal cortex, premotor cortex, supplementary motor area, and cerebellum (Farrell et al., 2005). Electrical pain stimulation is associated with convergence of activation in bilateral thalamus, right MCC, right Rolandic operculum and left postcentral gyrus, while mechanical pain stimulation shows consistent clusters of activation in bilateral insula, bilateral supramarginal gyrus (consisting of SII and inferior parietal lobule), bilateral thalamus and right MCC (Xu et al., 2020).

Neural activation during pain has been previously suggested to form a pain 'neuromatrix' (Melzack, 1999) or 'Neurologic Pain Signature' (Wager et al., 2013). Engagement of varying regions during pain are assumed to result from different underlying processes. Different brain regions may be preferentially involved in various aspects of pain processing. SI and SII encode the spatial, temporal and intensive properties of somatosensory stimuli (Bornhövd et al., 2002; Coghill et al., 1999). Together with lateral thalamic nuclei and posterior insula, these regions are associated with the sensory-discriminative aspects of pain (Baliki et al., 2009; Maihöfner & Handwerker, 2005; Segerdahl et al., 2015; Treede et al., 1999). Medial thalamic nuclei, ACC, anterior insula cortex and prefrontal cortex are associated with affective-emotional pain processing (Maihöfner & Handwerker, 2005; Treede et al., 1999). The ACC is particularly implicated in the negative affective dimension of pain (Tölle et al., 1999; Xiao & Zhang, 2018).

1.5.2 Altered brain structure and function in patients with chronic pain

Alterations in brain structure and function in patients living with chronic pain compared to pain-free individuals have been reported in a multitude of studies. A full review of the literature is beyond the scope of this thesis; therefore, the following is a selective review of major findings on altered brain structure and function in chronic pain based on systematic reviews and meta-analyses.

Patients with chronic pain have been shown to have differences in the volume of grey and white matter, although evidence is mixed and often inconsistent. Systematic reviews of changes in brain structure in patients with chronic low back pain have identified both increases and decreases of regional grey matter volume in regions including SI and SII, dorsolateral prefrontal cortex, cerebellum, ACC, temporal lobes, insula, precuneus and cuneus in chronic low back pain (Kregel et al., 2015; Ng et al., 2017). Selected studies report a decrease in global grey matter, while others report no difference compared to pain-free controls (Ng et al., 2017). In a co-ordinate based meta-analysis with pain of mixed aetiologies, reduced grey matter was found in a wide network of regions in the right hemisphere including the inferior frontal gyrus, insula, dorsal striatum, ACC, MCC, superior temporal gyrus, thalamus, middle frontal gyrus, and increased grey matter volume in right hippocampus and parahippocampal gyrus, compared to controls (Smallwood et al., 2013). In a small qualitative systematic review of 12 studies investigating patients with neuropathic pain after spinal cord injury, Huynh et al. (2020) found bidirectional alterations in grey matter volume of ACC, SI, MI and thalamus. In the few studies investigating changes in white matter structure in patients with low back pain, conflicting findings have been reported, with some studies reporting increases in white matter structure, while others report decreased white matter or no difference from controls (Ng et al., 2018; Kregel et al., 2015).

Changes in structural and functional connectivity have also been identified in patients with chronic pain. Patients with chronic low back pain show greater resting-state activation in the medial prefrontal cortex, cingulate cortex, amygdala and insula (Kregel et al., 2015). In a systematic review of studies using graph theory to characterise changes in connectivity between mixed aetiologies of chronic pain and healthy controls, global level differences in connectivity were found, with decreased structural transitivity, as well as changes in betweenness centrality, intramodular degree and rich club

organisation in patients with chronic pain (Lenoir et al., 2021). The direction of change was found to be dependent on the specific brain region. In contrast, path length, modularity, degree and hub disruption index did not differ between groups. Disrupted default mode network connectivity has also been consistently reported in patients with chronic pain (Kregel et al., 2015). The default mode network, which is engaged during resting wakefulness, consists of functionally correlated brain areas including the ventromedial and lateral prefrontal, posteromedial and inferior parietal, lateral and medial temporal cortex and subcortical structures including the amygdala and striatum (Alves et al., 2019). Alterations in the default mode network may predict the transition from acute to chronic pain (Pfannmöller & Lotze, 2019).

Similarities have been reported between the processing of acute pain in individuals living with chronic pain and healthy controls. A meta-analysis examining differential brain responses to acute noxious stimuli found no significant difference in activation between patients with chronic pain and healthy volunteers (Xu et al., 2021). Comparatively, Kregel et al. (2015) reported increased activity in pain-related regions and decreased activity in regions mediating an analgesic response in patients with chronic low back pain compared to controls. In contrast to acute pain, hallmark symptoms of neuropathic pain including spontaneous pain and allodynia may be reflected in alterations in brain function. Experience of allodynia in patients with neuropathic pain is associated with greater likelihood of activation in left supramarginal gyrus, the right caudal-anterior insula, and the left ACC, and reduced activation in left posterior and right anterior insula, the right supplementary motor area, right MCC and right SII compared to experimental pain in healthy volunteers (Friebel et al., 2011). Studies investigating both allodynia and hyperalgesia in neuropathic pain are associated with significantly stronger likelihood of activation in bilateral SII, ipsilateral cingulate cortex, prefrontal cortex, contralateral basal ganglia and cerebellum, and weaker activation likelihood in ipsilateral insula, contralateral cingulate cortex, bilateral thalamus and basal ganglia, compared to acute pain in healthy volunteers (Lanz et al., 2011). In later investigations using mixed pain aetiologies versus acute pain, no difference in activation likelihood was found (Tanasescu et al., 2016).

Treatment for chronic pain can elicit changes in brain function. In an ALE meta-analysis of 62 fMRI and 13 PET studies in patients undergoing treatment for chronic pain, SI, MI, thalamus, insula, and ACC showed significantly decreased activity after the treatments compared to baseline (Kim et al., 2021). Increased glucose uptake, blood flow and opioid-receptor binding potentials were observed in SI, MI, thalamus, and insula. Changes in the dopaminergic pathway and descending inhibitory system have also been implicated in chronic pain. Konno & Sekiguchi (2018) stated that decreased activation of the ACC, prefrontal cortex, and nucleus accumbens in chronic low back pain patients may be related to decreased function of the descending inhibitory system.

1.5.3 Electrophysiological markers for pain

Electrophysiological changes measured with electroencephalography (EEG) during somatosensory stimulation comprise phase-locked and oscillatory changes. Changes which are phase-locked to an event can be examined with event-related potentials (ERPs), while non-phase-locked, oscillatory changes can be examined during rest as relative or absolute band power, or following tasks using the event-related desynchronisation (ERD) transformation.

1.5.3.1 Somatosensory- and laser-evoked potentials associated with pain

In the pain domain, electrical and laser stimuli have been used to examine event-related changes to noxious stimuli.

Somatosensory-evoked potentials (SEPs) are ERP deflections that are usually evoked by electrical stimulation of peripheral nerves (Dawson, 1947; Dawson & Scott, 1949). The latency and amplitude of SEPs vary depending on the area of the body being stimulated. Early SEP components with a peak latency of less than 40 ms after stimulation of upper limbs, or 60 ms after stimulation of lower limbs, originate from SI (Allison et al., 1992; Valeriani et al., 2000a, 2001). Mid-latency SEPs up to 200 ms originate from bilateral SII and supplementary motor area or ACC (Cruccu et al., 2008; Stancak et al., 2003; Valeriani et al., 2000a, 2001; Vrána et al., 2005). SEPs from nonpainful and painful electrical stimuli originate from similar sources (Valeriani et al., 2000a). SEP amplitudes are enhanced with graded intensities of nonpainful and noxious stimuli (Derbyshire et al., 1997; Iannetti et al., 2008; Loggia et al., 2012; Shimojo et al., 2000; Valeriani et al., 2000a).

Laser-evoked potentials (LEPs) are measured in response to laser stimuli. LEPs have been extensively described and consist primarily of series of positive and negative deflections: N1/P1 and N2-P2. The N1/P1 is a lateralised potential, peaking at 150–180 ms over temporal regions and inverting phase at the midline, which is generated by the operculo-insular cortex and potentially also SI (García-Larrea et al., 2003). The N2-P2 complex which is maximal over the vertex between 200–380 ms is generated by ACC/MCC and the operculo-insular cortex (García-Larrea et al., 2003). However, the N2 and P2 components may have different origins, with the P2 component also involving deeper source dipoles in medial temporal cortex (Stancak et al., 2016, 2018; Stancak & Fallon, 2013). LEP latencies differ between stimulation sites: for stimuli applied to the hand, normative N2 latencies have been estimated between 200–277 ms, while P2 latencies have been estimated between 248–380 ms (Truini et al., 2005). These LEPs primarily reflect activation of Aδ fibres (Bromm & Treede, 1984; García-Larrea et al., 2003). Ultra-late potentials in the interval 700–1000 ms after stimuli may reflect afferent volleys from C fibres (Hu et al., 2014; Iannetti et al., 2003; Opsommer et al., 2001).

1.5.3.2 Alterations of pain-related components in neuropathic pain

Alterations in pain-related EEG components in patients living with chronic pain compared to pain-free individuals have been reported in a wealth of studies. A full review of the literature is beyond the scope of this thesis; therefore, the focus is on major findings and reviews of alternations in pain-related ERP components in patients with neuropathic pain syndromes.

Variations of pain-related components in patients with neuropathic pain have been investigated by comparing responses to stimuli applied to the affected region versus the unaffected region of the body. Alterations in pain-related components indicate reduced integrity of nociceptive pathways (Cruccu et al., 2010; Haanpää et al., 2011). SEPs have been used extensively in clinical applications to evaluate disorders in somatosensory pathways in the central and peripheral nervous system (Cruccu et al., 2008). Pain-related SEPs from concentric electrodes show reduced peak-to-peak amplitude and longer N1 latency in patients with neuropathic pain compared to healthy controls (Hansen et al., 2012).

LEPs are recommended for the assessment and diagnosis of peripheral and central neuropathic pain syndromes (Cruccu et al., 2010; Haanpää et al., 2011). LEPs can be absent, reduced in amplitude or delayed in latency in patients with neuropathic pain (Pazzaglia & Valeriani, 2009). Abnormalities in pain-related LEP components are more pronounced in patients who experience spontaneous pain, and have been related to Aδ fibre deafferentation (Garcia-Larrea et al., 2002). In the only systematic review of pain-related ERP components in chronic pain versus healthy controls, Lenoir et al. (2020) described increased latency and reduced amplitude of the LEP N2-P2 complex in two studies in patients with neuropathic pain.

1.5.3.3 Spontaneous oscillatory changes in waking EEG

Amplitude suppressions and enhancements in the theta (4–7 Hz), alpha (8–13 Hz) and beta (14–30 Hz) frequency bands are associated with changes in wakefulness, vigilance level, task performance and external stimuli.

Adult human EEG in waking states is characterised by a predominance of oscillations in the alpha band (Chang et al., 2011). Alpha rhythms describe frequencies which occur in the 8–13 Hz range, with an amplitude of up to 50 μV, which are observed over occipital, parietal, and sensorimotor cortices (Kropotov, 2009). Occipital alpha rhythms (9–11 Hz) which are dominant in EEG recordings with eyes closed are attenuated with eyes opening, drowsiness, and mental tasks (Adrian & Matthews, 1934; Berger, 1929, as cited in Kropotov, 2009; Nunez et al., 2001). Increased alpha rhythms during eyes closed are proposed to result from decreased visual input to the occipital cortex (Kropotov, 2009). Alpha band power increases over parietal-occipital regions have been observed during cued attention (Foxe & Snyder, 2011), indicating a suppression of visual processing. Occipital alpha rhythms have been proposed to reflect an idling or inactive cortical region (Adrian & Matthews, 1934), corresponding to fMRI studies showing a negative correlation between alpha band oscillations and metabolic activity (Feige et al., 2005).

Alpha rhythms over sensorimotor cortices focused around 10 Hz (8–13 Hz) are known as mu rhythms. Mu rhythms originating from SI are observed in the absence of movement and are attenuated during voluntary movement, motor imagery or tactile stimulation (Chatrian et al., 1959; Gastaut,

1952; Salmelin & Hari, 1994c). Originally conceived as an indication of cortical idling (Pfurtscheller et al., 1996b), mu rhythms are postulated to reflect sensorimotor processing in frontoparietal networks (Pineda, 2005). Sensorimotor mu and occipital alpha rhythms have been shown to be independent phenomena originating from different sources (Andrew & Pfurtscheller, 1997; Pineda, 2005), suggesting that alpha rhythms reflect local and global brain dynamic processes resulting from functional segregation and integration (Nunez et al., 2001).

Beta band oscillations are observed over sensorimotor and frontal cortices (Kropotov, 2009). Sensorimotor beta oscillations are maximal over C3, Cz and C4 electrodes and have been localised to S1/M1 (Salmelin & Hari, 1994c). Alongside mu rhythms, amplitude attenuation of 20 Hz cortical oscillations has been found following tactile or peripheral nerve stimulation (Kuhlman, 1978; Pfurtscheller, 1981). Beta oscillations are sensitive to gamma-aminobutyric acid (GABA), with enhanced beta band oscillations on the induction of GABA agonists (Jensen et al., 2005; Jensen & Mazaheri, 2010).

Theta band oscillations are observed in the frontal midline regions during cognitive tasks and attention-related processes (Kropotov, 2009). Theta band power increases with greater working memory load, leading to the suggestion that theta oscillations represent top-down memory processes (Klimesch, 1999; Klimesch et al., 2008). The functional role of theta band oscillations includes cognitive-affective functions such as attentional processing, sensory-motor integration, navigation, and memory (Karakaş, 2020).

1.5.3.4 Electrophysiological markers for somatosensory processing

Somatosensory stimuli are associated with amplitude increases or decreases in various oscillatory frequency bands (Chatrian et al., 1959; Pfurtscheller & Aranibar, 1977; Pfurtscheller & Lopes da Silva, 1999; Stančák, 2006). Increased power of cortical oscillations, known as event-related synchronisation (ERS), and decreased power of cortical oscillations, known as ERD, reflect decreased or increased synchrony of underlying neuronal populations, respectively (Pfurtscheller, 1977, 1992; Pfurtscheller & Aranibar, 1977). ERPs are assumed to represent the responses of cortical neurons due to changes in afferent activity, while ERD/S reflect changes in local interactions between neurons and

interneurons (Pfurtscheller & Lopes da Silva, 1999). ERD in alpha and beta frequency bands are considered as a correlate of cortical activation (Pfurtscheller & Lopes da Silva, 1999), while ERS is considered to reflect active inhibition of task-irrelevant stimuli (Fry et al., 2016; Jensen & Mazaheri, 2010; Neuper & Pfurtscheller, 2001b) or cortical idling (Pfurtscheller, 1992; Pfurtscheller et al., 1996a, 1996b). ERD is suggested to indicate notification of sensory event and subsequent opening of sensory channels, which may aid in the transmission of neuronal information within sensorimotor and association cortices (Stančák, 2006).

Somatosensory stimuli are followed by 10 and 20 Hz ERD located over the contralateral and ipsilateral primary sensorimotor cortex (SI/MI) around 250–400 ms after stimulus onset (Cheyne et al., 2003; Gaetz & Cheyne, 2006; Hirata et al., 2002; Neuper & Pfurtscheller, 2001b; Nikouline et al., 2000; Pfurtscheller, 1992; Stancak et al., 2003). Contralateral 10 Hz ERD is typically stronger than ipsilateral ERD, which appears approximately 150ms later (Stančák, 2006; Stancak et al., 2003). During ERD, ERS of 20 Hz oscillations over the contralateral precentral cortex occurs at a latency of 450–700 ms after stimuli (Brovelli et al., 2002; Cheyne et al., 2003; Gaetz & Cheyne, 2006; Neuper & Pfurtscheller, 2001b; Pfurtscheller, 1981; Salenius et al., 1997; Salmelin & Hari, 1994c; Stancak et al., 2003). This is followed by 10 Hz ERS localised to the postcentral gyrus approximately 150 ms later (Salmelin & Hari, 1994c). Post-stimulus 20 Hz ERS has been linked to MI inhibition (Chen et al., 1999; Jensen et al., 2005; Salmelin & Hari, 1994c) which may serve to prepare for new inputs and limit overactivation (Kropotov, 2009). Movement observation and real and imagined movements attenuate the post-stimulus 20 Hz ERS rebound (Cheyne et al., 2003; Salenius et al., 1997). ERD/S after somatosensory stimulation is also found in regions corresponding to the supplementary motor area (Brovelli et al., 2002; Ohara et al., 2004; Stancak et al., 2003) and SII (Della Penna et al., 2004; Forss et al., 2001; Palva et al., 2005). Somatosensory brushing stimuli administered at slow velocities of 3cm/s are also associated with ultra-late slow-wave oscillations around 6 Hz ERS over frontal areas of the scalp (Ackerley et al., 2013). The amplitude of 10 Hz and 20 Hz ERD/S can distinguish weak from strong stimuli, but does not scale linearly with stimulus intensity (Iannetti et al., 2008; Stancak et al., 2003).

Painful laser and electrical stimuli are followed by 10 and 20 Hz ERD peaking around 500–800 ms and 340 ms, respectively (Chien et al., 2014; Hu et al., 2013; Ohara et al., 2004; Ploner et al., 2017; Raij et al., 2004; Stančák, 2006). Sources of these effects are similar to those for nonpainful somatosensory stimuli (Cheyne et al., 2003; Salmelin & Hari, 1994b; Stancak & Pfurtscheller, 1996). Post-stimulus 20 Hz ERS has not been reported following noxious laser stimulation (Ohara et al., 2004; Raij et al., 2004; Stančák et al., 2005), suggesting that 20 Hz rebound is linked to involvement of the dorsal column system (Stančák, 2006).

1.5.3.5 Electrophysiological markers for chronic pain

Changes in oscillatory dynamics measured with EEG and magnetoencephalography (MEG) have been reported in pathological conditions, including chronic pain. Patients with chronic pain show increased power of cortical oscillations in frequency bands including theta (4–7 Hz) (Lim et al., 2016; Sarnthein et al., 2006; Stern et al., 2006; Vučković et al., 2014), alpha (8–13 Hz) (Kisler et al., 2020; Sarnthein et al., 2006; Vučković et al., 2014), beta (16–30 Hz) (Lim et al., 2016; Sarnthein et al., 2006; Stern et al., 2006), and delta (1–4 Hz) frequency bands (Sarnthein et al., 2006). Augmented theta and beta power in chronic pain patients compared to healthy controls have been localised to pain-associated areas including the insula, ACC, prefrontal cortex, SI and SII (Fallon et al., 2018; Lim et al., 2016; Stern et al., 2006).

Abnormal theta rhythms have been suggested to reflect alterations in local or long-range communication between functionally specialised neuronal assemblies (Schnitzler & Gross, 2005). A shift of dominant resting oscillatory activity from the alpha band towards the theta band has been proposed as a contributing factor in the development or maintenance of various pathologies including chronic pain (Llinás et al., 1999, 2005). Dominant low-frequency oscillations in the thalamo-cortico-thalamic network, known as thalamocortical dysrhythmia, is suggested to maintain pain by disrupting the normal state-dependent flow of information between the thalamus and cortex, leading to disturbances of sensation, motor performance and cognition (Jones, 2010).

1.6 Neural effects of SCS

1.6.1 Physiological effects of tonic SCS

SCS was originally based on the Gate Control Theory (Melzack & Wall, 1965), which postulated that electrical stimulation of large diameter (Aβ) fibres would produce an inhibitory effect on processing of signals from small diameter (Aδ and C) fibres (Joosten & Franken, 2020; Shealy et al., 1967).

In line with the Gate Control Theory, conventional tonic stimulation induces antidromic stimulation of Aβ fibres in the dorsal column and paraesthesia over the affected nerves (Barolat et al., 1991; Melzack & Wall, 1965; North et al., 1991; Parker et al., 2012; Shealy et al., 1967). The balance between large and small diameter fibres which modulate the transmission of noxious stimuli is mediated by interneurons in the upper laminae of the spinal dorsal horn. Tonic SCS modulates nociceptive signalling through the release of GABA. In rat models of neuropathic pain, tonic stimulation decreases intracellular GABA levels (Janssen et al., 2012), increases extracellular GABA levels (Cui et al., 1997; Linderoth et al., 1994; Stiller et al., 1996), and reduces the release of excitatory amino acids glutamate and aspartate (Cui et al., 1997). In preclinical studies, administration of $GABA_B$ receptor antagonists abolish the analgesic effects of SCS, while $GABA_B$ receptor agonist baclofen increases the therapeutic effects of SCS (Ren et al., 1996). In humans, SCS combined with sub-effective doses of baclofen can improve treatment prospects for patients who do not respond to SCS alone (Lind et al., 2004, 2008; Schechtmann et al., 2010).

1.6.1.1 Supraspinal effects of SCS measured with electrophysiology

Electrophysiological techniques including EEG, MEG, and transcranial magnetic stimulation (TMS) have been utilised to investigate supraspinal effects of SCS in humans.

Supraspinal effects of SCS have been investigated as alterations in cortical SEPs or somatosensory evoked magnetic fields (SEFs) to innocuous electrical stimulation of Aβ fibres, measured with EEG and MEG, respectively. Observation of changes in SEPs during SCS have primarily shown an inhibitory effect of SCS on somatosensory processing. In patients using permanent or trial implants of SCS chronic pain of lower limbs, SCS is associated with attenuation of

short- and mid-latency SEP components for innocuous tibial nerve stimulation (Buonocore et al., 2012; Buonocore & Demartini, 2016; De Andrade et al., 2010; Poláček et al., 2007; Urasaki et al., 2014; Wolter et al., 2013). Comparable effects have been reported with MEG as reduced SEF amplitudes to posterior tibial nerve stimulation (115 and 150 ms latency) and median nerve stimulation (90–100 ms latency) after SCS implantation (Theuvenet et al., 1999). Attenuated SEPs during SCS have been localised to SI and SII using source dipole modelling (Poláček et al., 2007). Attenuated long-latency SEPs from tibial nerve stimulation have also been reported with SCS (Blair et al., 1975; Poláček et al., 2007). For sural nerve stimulation, long-latency SEPs localised to the MCC are enhanced during SCS compared to SCS off (Poláček et al., 2007). Few studies with mixed pathologies report no effect of SCS on tibial or median nerve SEP components (Doerr et al., 1978; Mazzone et al., 1994).

Changes in oscillatory dynamics have been investigated during SCS with MEG and EEG. In 30 patients with CPSS, Sufianov et al. (2014) reported a predominance of delta and theta band activity of a greater amplitude than controls, which decreased after SCS implant. Oscillatory changes may indicate treatment response. Patients who underwent an unsuccessful SCS trial showed greater mean spectral power in the high theta range (7–9 Hz), compared to healthy controls and patients with a successful SCS trial, who showed a predominance of alpha (9–11 Hz) band power (Schulman et al., 2005). Using TMS in 5 patients with chronic neuropathic leg pain, SCS has also been shown to induce changes in cortical excitability, with increases in intracortical facilitation during SCS off compared to SCS on, which was related to degree of perceived pain (Schlaier et al., 2007).

1.6.1.2 Effects of SCS on haemodynamic responses

Effects of SCS in humans have been investigated with functional neuroimaging techniques based on haemodynamic principles, including fMRI, PET and single-photon emission computed tomography (SPECT).

Studies investigating SCS with fMRI have primarily been conducted during the SCS trial period as permanent implants are often a contraindication for fMRI. Activation has been reported in somatosensory processing regions during blocks of SCS on, compared to SCS off, in areas including

the SI, SII, cingulate cortex and posterior parietal cortex (Deogaonkar et al., 2016; Kiriakopoulos et al., 1997; Stancak et al., 2008). In an investigation of 8 patients with chronic leg and back pain after spinal surgery, SCS was associated with increased activation of SI/MI somatotopically corresponding to the affected foot and/or perineal region, contralateral posterior insula, and the ipsilateral SII, and decreased activation in bilateral MI and ipsilateral SI corresponding to the shoulder, elbow and hand (Stancak et al., 2008). Widespread deactivation has been reported during SCS in regions including bilateral medial thalamus, cingulate cortex, ipsilateral dorsal premotor cortex, bilateral anterior insula, ipsilateral SI and contralateral SII, contralateral hypothalamus and parahippocampal gyrus (Moens et al., 2012). In a connectivity analysis of 10 patients with CRPS or CPSS, Deogaonkar et al. (2016) reported decreased connectivity between left SII and right middle cingulate, and increased connectivity between left superior precentral cortex and left supramarginal cortex with optimal SCS.

Effects of SCS on cortical processing have also been investigated with PET and SPECT, with changes in a wide network of pain and somatosensory associated regions. Increased regional cerebral blood flow with SCS has been noted particularly in the bilateral prefrontal cortex (Kishima et al., 2010) as well as ACC and contralateral temporal lobe, while reductions have been observed in contralateral parietal cortex (Kunitake et al., 2005). In a comparison of good and poor SCS responders prior to SCS implant, good SCS responders had reduced regional cerebral blood flow in the thalamus and precuneus compared to poor responders (Nagamachi et al., 2006).

1.6.1.3 Problems with the Gate Control Theory and SCS

Some mechanisms of SCS cannot be explained by the Gate Control Theory. The dorsal columns alone do not mediate the effects of SCS, as tonic SCS reduces pain hypersensitivity and allodynia after dorsal column transection (Barchini et al., 2012; El-Khoury et al., 2002). Tonic SCS engages supraspinal processes which exert descending modulation of pain, with activation of brainstem nuclei including the locus coeruleus and nucleus raphe magnus and rostral ventromedial medulla (Saadé et al., 1986; Song et al., 2013; Tazawa et al., 2015). Paraesthesia, resulting from orthodromic activation of Aβ fibres during tonic SCS, does not seem to be a requirement for pain

relief. Paraesthesia-free waveforms such as burst stimulation are equally or more effective than tonic SCS (De Ridder et al., 2010, 2013; Deer et al., 2018).

1.6.2 Physiological effects of burst SCS

The mechanisms underlying burst SCS are different to those of conventional tonic stimulation. Burst SCS does not appear to modulate the dorsal column pathway. In an investigation of anesthetised rats, burst SCS did not increase spontaneous activity in the gracile nucleus of the dorsal column (Tang et al., 2014). Pain-relieving effects of burst SCS are not mediated by GABAergic mechanisms. In a rat model of cervical radiculopathy, burst and tonic stimulation were shown to reduce spinal neuronal firing, although contrary to tonic stimulation, neuronal firing during burst SCS was not attenuated by $GABA_B$ receptor agonists (Crosby et al., 2015b).

Few human studies comparing burst and tonic waveforms have been conducted. De Ridder et al. (2013) investigated sources of resting oscillatory changes in 5 patients during burst, tonic and no stimulation. Burst SCS was associated with an increase in synchronised activity in bilateral dorsal ACC in the low alpha band (8–10 Hz), and in left dorsolateral prefrontal cortex in low alpha (8–10 Hz) and high beta band (18.5–30 Hz), compared to tonic SCS. Compared to SCS off, burst stimulation was associated with greater synchronised activity in the low alpha band in dorsal ACC, and decreased gamma band (30.5–44 Hz) activity in the parahippocampal gyrus. Tonic stimulation was associated with decreased high beta band power in posterior cingulate cortex and gamma band power in posterior insula compared to SCS off. De Ridder & Vanneste (2016) reported a subsequent region-of-interest conjunction and functional connectivity analysis of data described in De Ridder et al. (2013). Common mechanisms between tonic and burst stimulation were found, with increased theta band power in SI, inferior parietal area and supramarginal gyrus extending into SII, posterior cingulate cortex and the parahippocampal area, and increased gamma band power in the pregenual ACC extending into the ventromedial prefrontal cortex. The ratio of oscillatory power between pregenual ACC and ventromedial prefrontal cortex ratio was reduced after burst stimulation in comparison to tonic and baseline in the gamma frequency band.

More recently, Yearwood et al. (2019) reported results from 7 patients taking part in a randomised controlled trial comparing burst and tonic stimulation who underwent PET scanning prior to implant and after 12 weeks each of burst and tonic stimulation. Increased metabolic rate was found in anterior and posterior cingulate cortices, and decreased metabolic rate was found in subgenual ACC, during burst compared to tonic stimulation. Reduced pain vigilance after implant was associated with decreased metabolic rate in ventromedial prefrontal cortex/subgenual ACC during burst stimulation and decreased metabolic rate in retrosplenial cortex and the thalamus during tonic stimulation.

Burst SCS has been argued to modulate both affective-motivational and sensory-discriminative aspects of pain by engaging both the medial and lateral spinothalamic tracts (De Ridder et al., 2013; De Ridder & Vanneste, 2016). In contrast, tonic stimulation is proposed to modulate activity in the lateral spinothalamic tract only as a result of engagement of the dorsal column pathway (De Ridder & Vanneste, 2016; Joosten & Franken, 2020).

1.7 Neural effects of LFS

1.7.1 Mechanisms of action

The mechanism underlying the therapeutic effects of LFS has been proposed as LTD. LTD, and its counterpart process LTP, can be observed at many sites in the central nervous system (Bliss & Lomo, 1973; Dudek & Bear, 1992; Mulkey & Malenka, 1992). LTP was originally identified in the rabbit hippocampus (Bliss & Lomo, 1973), and as such was inferred to have role in learning and memory (Bliss & Collingridge, 1993). Likewise, LTD has been identified in the hippocampus, and has thus been suggested as a forgetting process (Bliss & Cooke, 2011).

In a seminal study, it was found that LTD could be induced in the spinal dorsal horn of the rat (Sandkühler et al., 1997). Repetitive 1 Hz LFS of primary afferent Aδ fibres reduced excitatory postsynaptic potential amplitude in the substantia gelatinosa for at least 2 hours after stimulation. Reduction in excitatory postsynaptic potentials started shortly after the induction of LFS and continued to decline with increasing pulses by an average of 41% compared to baseline. LFS at lower Aβ intensities induced only a transient depression of synaptic transmission which lasted around 30

minutes (Liu et al., 1998; Sandkühler et al., 1997), suggesting that strong intensities activating Aδ fibres were essential to induce LTD.

1.7.2 Effects of LFS on nociception and pain perception

Animal models of neuropathic pain have been used to study the effects of LFS on nociception. Nociceptive LTD is associated with reduced pain behaviour and reduced mechanical allodynia in a rat neuropathic pain model (Xing et al., 2007). LFS of peripheral nerve fibres in humans is associated with a sustained, homotopic decrease in perceived pain to noxious electrical pain stimuli (Aymanns et al., 2009; Jung et al., 2009; Klein, 2004; Lindelof et al., 2010), and a reversal of increased pain perception from HFS (Klein, 2004; Magerl et al., 2018). Klein (2004) reported that LFS resulted in a 27% reduction in perceived pain for at least one hour after stimulation. Reduced pain perception after LFS is homotopic: confined to conditioned synapses (Aymanns et al., 2009; Rottmann et al., 2008) or receptive fields (Jung et al., 2011). Further studies have supported the use of LFS for acute pain, with evidence of LTD in somatosensory processing of masseter inhibitory reflexes (Ellrich & Schorr, 2002), blink reflexes (Ellrich & Schorr, 2002; Yekta et al., 2006) and supraorbital nerve afferents (Ellrich & Schorr, 2004), as well as subjective reports of both sensory and affective components of pain (Klein, 2004; Rottmann et al., 2010a).

1.7.3 Effects of LFS on electrophysiological and haemodynamic measures

Changes in pain-related neural activity after LFS have been interpreted as indirect correlates of nociceptive LTD. LFS has consistently been shown to decrease the amplitude of SEPs recorded with EEG to noxious electrical test stimuli (Ellrich & Schorr, 2004; Jung et al., 2012; Rottmann et al., 2008). Ellrich & Schorr (2004) found a sustained reduction in N2 and P2 SEP components during acute pain after LFS of trigeminal nerve afferents, accompanied by a reduction in pain perception. A later study using source dipole modelling investigated the effects of LFS versus no stimulation on cortical activation patterns for electrical pain stimuli (Jung et al., 2012). SEPs in response to electrical test stimuli elicited an N1 component located in the contralateral temporal region, and N2 and P2 components in the cingulate cortex. N1 and N2 components were unaffected by LFS, while P2 dipole magnitude was significantly reduced after LFS, compared to a control of no stimulation. Maximal

reduction in SEP amplitude and subjective pain ratings have been observed after 1200 pulses of 1 Hz stimulation at four times pain threshold (Jung et al., 2009).

Neural activation changes resulting from LFS have also been investigated using fMRI. Rottmann, Jung, Vohn, et al. (2010) reported significantly reduced activation in bilateral SI and SII, right insula, ACC, superior temporal cortex, prefrontal cortex and right inferior parietal lobule during electrical pain stimulation after LFS in comparison to baseline.

1.8 Interim summary

In summary, SCS and LFS are analgesic neurostimulation interventions for intractable neuropathic pain syndromes. There are important gaps in the literature which must be addressed; namely, the effects of stimulation parameters such as waveform and intensity. EEG can be used to investigate changes in somatosensory processing during neurostimulation, as discussed in the following chapter.

Chapter 2

2 Methods of EEG for measurement of pain-associated activity

2.1 Types of stimulation to investigate somatosensory processing

Somatosensory processing can be explored by applying stimuli to the periphery. Stimuli can comprise heat, mechanical or electrical modalities.

2.1.1 Tactile Brushing Stimuli

Mechanical stimuli applied to healthy skin at low intensities are associated with activation of Aβ mechanoreceptors. Static mechanical stimuli used in experiments can include punctate probes or pressure devices. Dynamic mechanical stimulation administered with a brush involve a complex sequence of mechanical events: as a brush moves across the skin, the skin in front of the brush is stretched, the skin under the brush is indented and the skin behind the brush is stretched (Edin et al., 1995). This complex process activates multiple Aβ mechanoreceptors in the glabrous and hairy skin, particularly slowly-adapting type II units, as well as slowly-adapting type I and rapidly-adapting type I units (Abraira & Ginty, 2013; Edin et al., 1995). Gentle brushing stimuli applied to the hairy skin can also activate CT fibres when delivered at velocities of 1–10cm/s, with optimal responses at 3cm/s (Johansson et al., 1988; Löken et al., 2009; Vallbo et al., 1993).

2.1.2 Electrical Stimuli

Electrical stimuli are quantifiable, controlled, have a fast onset and offset, and can be repeated without tissue damage (Berge, 2013). Electrical stimuli bypass peripheral receptors and activate cutaneous nerve fibres via an electrical potential difference across the nerve fibre membrane, with the classes of fibres activated dependent on stimulus parameters such as intensity (Berge, 2013; Burke et al., 1975). At low, nonpainful intensities around detection threshold, electrical stimuli activate Aβ fibres (Burke et al., 1975; Sang et al., 2003), as large diameter fibres have low thresholds and are the most sensitive to electrical stimulation (Collins et al., 1960). Repeated stimuli at higher, painful

intensities also recruit Aδ fibres, and greater intensities activate C fibres (Burke et al., 1975; Collins et al., 1960; Sang et al., 2003).

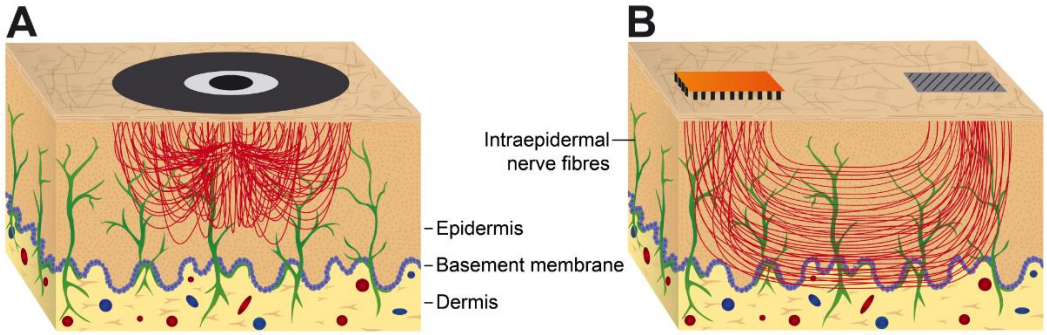

Figure 2.1 Schematic drawing of the distribution of current density in surface concentric (A) and intraepidermal matrix (B) electrodes based on finite element modelling. Both electrode designs induce high current density in superficial layers of the skin where free nerve endings are located. From Mücke et al. (2014).

Direct electrical current flowing through two electrodes stimulates the nerve at the cathode and resists excitation at the anode (Tsui, 2008). Electrodes have been designed to preferentially activate Aδ fibres without co-activation of Aβ fibres (***Figure 2.1***). These designs include concentric electrodes, consisting of a cathode surrounded by an anode, matrix electrodes, consisting of multiple cathodes and a separate anode, and intraepidermal pin electrodes (Bromm & Meier, 1984; Hansen et al., 2012; Inui et al., 2002; Kaube et al., 2000; Mücke et al., 2014; Nilsson & Schouenborg, 1999). A common element of these electrodes is a small cathode area, resulting in a high current density at the dermoepidermal junction which decreases uniformly below the cathode towards the anode, and is highest at the centre of the cathode for diameters smaller than 4 mm (Lelic et al., 2012; Mørch et al., 2011). In contrast, larger cathode diameters penetrate deeper layers of the skin (Mørch et al., 2011). The inter-electrode distance may not significantly influence the current distribution in the skin where separate anode and cathodes are used (Tsui, 2008), while for concentric electrode designs, small anode areas and a small distance between anodes and cathodes are required to limit current spreading to deeper tissue layers (Poulsen et al., 2021).

LFS is delivered with a range of electrodes with small-diameter cathodes to elicit preferential activation of Aδ fibres in humans (Klein, 2004; Magerl et al., 2018; Mücke et al., 2014). In clinical populations, LFS has been applied with pen electrodes with a small-diameter cathode tip, connected to a distal surface electrode which serves as the anode (***Figure 2.2***) (Johnson et al., 2015, 2021). Activation of Aδ fibres during LFS is supported by subjective reports that the stimulus elicits sharp, pricking sensations (Ellrich & Schorr, 2004; Jung et al., 2012). The electrode design allows a high current density at relatively low stimulus intensities, ranging from 2.3–5 × pain threshold, or 10–20 × detection threshold (Aymanns et al., 2009; Biurrun Manresa et al., 2010; Ellrich & Schorr, 2002; Klein, 2004; Rottmann et al., 2008). Optimal stimulus parameters for eliciting LTD-like effects on human pain perception have been determined as 1 Hz, 1200 pulses and an intensity of 4× pain threshold, corresponding to 15× detection threshold (Jung et al., 2009).

Figure 2.2 Pen electrode with 4mm diameter cathode used to deliver LFS.

2.1.3 Laser Heat Stimuli

Acute heat pain can be evoked using contact or radiant sources (Gracely, 2013). Contact heat pain can be induced with objects heated in water baths or with contact thermodes, which are applied to the skin. Radiant heat sources typically involve infrared light sources delivered by a laser stimulus (Gracely, 2013).

Laser stimuli were introduced for pain research in the mid-1970s (Carmon et al., 1978; Mor & Carmon, 1975). Laser stimuli deliver brief heat pulses (1–100ms) that selectively activate Aδ- and C fibre nociceptors (Bromm & Treede, 1984; García-Larrea et al., 2003). Due to selective nociceptor activation, LEPs recorded with EEG have been widely accepted as the most reliable clinical tool in diagnosing hypoalgesia or neuropathic pain (Valeriani et al., 2012). Perception thresholds for laser stimuli applied to the hand are 5.7±2.6 mJ/mm^2 (Truini et al., 2005). Laser stimuli are sensitive to

skin pigmentation, as the absorption of stimuli is greater in darker, black ink-marked, or tattooed skin (Leandri et al., 2006). Laser stimuli cannot be repeated in the same spot due to increases in skin temperature which can heighten the risk of tissue damage (Madden et al., 2016).

Types of laser stimuli include high power carbon dioxide (CO_2) lasers, and solid-state lasers such as Neodimium Yttrium–Aluminium–Grenat (Nd:YAG), Neodimium Yttrium-Aluminium-Perovskite (Nd:YAP) and Thulium Yttrium-Aluminium-Grenat (Tm:YAG). High power CO_2 lasers are the most commonly investigated and have been tested extensively with regards to energy distribution and peripheral fibre activation (Mor & Carmon, 1975; Perchet et al., 2008; Plaghki & Mouraux, 2003). Solid-state lasers have advantages over CO_2 lasers of compactness, shorter pulse duration, shorter wavelength (1–2 μm) and easier optic fibre transmission (Perchet et al., 2008). Shorter wavelength of solid-state lasers allows deeper penetration into the skin than CO_2 lasers (Valeriani et al., 2012). In a comparison of CO_2 and Nd-YAP lasers, Nd-YAP lasers were recommended for clinical and experimental settings due to earlier latencies and larger amplitudes of evoked potentials, which suggested a more synchronised nociceptive afferent volley compared to CO_2 lasers (Perchet et al., 2008).

2.2 General Principles of EEG

2.2.1 Genesis of electrical potentials in the brain

Electrical activity is the human brain is conducted by billions of neurons (Azevedo et al., 2009). Neurons communicate using action potentials, discrete voltage spikes that travel down the axon towards axon terminals, known as dendrites. Neurotransmitters are released at dendrites and bind to receptors on the postsynaptic cell membrane, altering the permeability of the membrane to specific ions and leading to a change in potential (Hämäläinen et al., 1993). This process creates a dipole: a pair of positive and negative charges separated by a short distance. Action potentials in excitatory or inhibitory presynaptic neurons result in excitatory postsynaptic potentials or inhibitory postsynaptic potentials, respectively (Speckmann et al., 2011).

Action potentials generate fields of short duration (<2 ms) and nearby neurons do not often fire synchronously and summate, so voltage generated by action potentials is often undetectable at the

scalp (Buzsáki et al., 2012). Excitatory or inhibitory postsynaptic potentials occur relatively slower, lasting for hundreds of milliseconds, allowing synchronous firing due to an overlap in time (Buzsáki et al., 2012). Postsynaptic potentials that occur around the same time with the same polarity and in spatial alignment can summate, and when this happens the signals can be recorded at the scalp level with EEG. Signals that are not in spatial alignment are cancelled out before the signals reach the scalp; thus, signals recorded by EEG are likely to originate from pyramidal cells in the cortex due to their perpendicular orientation to the surface of the cortex which generates an open field (Nunez & Srinivasan, 2006). A single EEG electrode provides estimates of synchronous synaptic activity averaged over several centimetres of the cortex containing between 100 million and 1 billion neurons (Nunez & Srinivasan, 2006).

2.2.2 EEG acquisition

To acquire EEG, electrodes are positioned on the scalp, and conductive gel, paste or liquids are used to achieve low impedances. Electrodes are commonly positioned according to a derivative of the International 10–20 System, which places electrodes at 10% and 20% points along lines of latitude and longitude on the head using anatomical landmarks of the nasion, inion and left and right pre-auricular points (Jasper, 1958; Klem et al., 1999). Standardised placement allows consistency between studies which can aid interpretation and comparison of findings. Alternative placement systems can be used, particularly for dense electrode arrays, such as the geodesic arrangement where all electrodes are placed equidistant to one another. Many sensors in geodesic arrangements have corresponding electrodes in the International 10–20 System (Luu & Ferree, 2005).

As the amplitude of the raw EEG is very small, ranging between 10–100 μV in adults, the signal is amplified by a factor of 10,000–50,000 for accurate measurement (Luck, 2014). Amplified signals are digitised for storage, display, and analysis on a computer. EEG is recorded as the potential for current to pass from one electrode (the active electrode) to another (Luck, 2014). This requires the use of reference and ground electrodes. Due to noise in the ground circuit, a differential amplifier is used in which activity at active electrode sites is computed as the difference between active-ground electrodes and reference-ground electrodes (Luck, 2014).

Reference sites chosen for recording can be differentially affected by volume conduction of combinations of neuronal generators. Therefore, techniques can be used to obtain reference-free data. One method to do so is the common average reference, which uses the unweighted average of all channels as the reference (Lehmann, 1984, 1987). Only signals that are common to all sites remain in the common average reference, while isolated signals are cancelled out. This method limits the effects of single electrode references which can be too close to extreme maximal or minimal potential values. The common average has been shown to perform well as an estimate of reference-independent potentials in simulation studies, particularly when used with high-density electrode arrays (Srinivasan et al., 1998). Another method is to implement the surface Laplacian transformation which reflects an estimate of the current density entering or exiting the scalp (Hjorth, 1975; Nunez & Srinivasan, 2006; Perrin et al., 1989). The Laplacian transformation is derived from the second spatial derivative of the potential field in the local curvature in $\mu V/cm^2$, whereby each electrode is referenced to a weighted average of neighbouring electrodes (Hjorth, 1975) or as a spline interpolation of potentials measured at a discrete set of electrode locations (Nunez et al., 1994; Perrin et al., 1989). Laplacian approaches emphasize superficial sources from radial dipoles in proximal gyral surfaces which are more likely to produce large potentials on the scalp surface (Nunez & Srinivasan, 2006). This technique is most recommended with high density arrays for the localisation of neuronal current sources (Nunez & Srinivasan, 2006).

Studies involving clinical pain populations in the current thesis utilised a 63-channel system with actively-shielding Ag-AgCl electrodes (BrainProducts GmbH, Germany). **Figure *2.3*** illustrates the locations of electrodes on the head using this system. This system uses an electrolyte gel as the conductive medium to lower skin-to-electrode impedances and improve conduction of electrical signals. Electrodes were positioned based on the International 10–20 system and placed according to three anatomical landmarks: the nasion and 2 preauricular points. Actively-shielding electrodes, which use preamplifiers built into the electrode housing, reduce sensitivity to induced noise from electrical devices in the vicinity (Metting van Rijn et al., 1990). Fpz was used as the ground electrode. Data were sampled at 1000 Hz and filtered from 0.1–200 Hz.

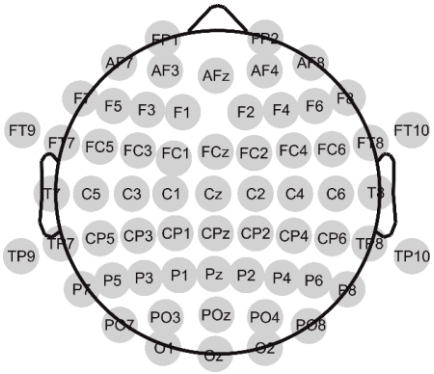

Figure 2.3. Distribution of 63 electrodes across the scalp for the gel-based BrainProducts cap.

Studies using healthy volunteers in the current thesis utilised a 128-electrode sponge-based geodesic sensor net (Magstim EGI, UK). **Figure *2.4*** illustrates the locations of electrodes on the head using this system. The high-density system gives coverage of the whole head including the forehead and suborbital regions of the face. Saline solution was used as the conductive medium and electrodes were placed in a geodesic arrangement according to three anatomical landmarks: the nasion and 2 preauricular points. Electrode Cz was used as the initial reference, and COM was used as the isolated common/ground electrode. Electrical signals were recorded at 1000 Hz and filtered from 0.1–200 Hz.

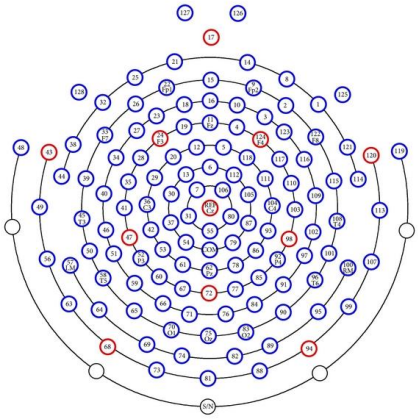

Figure 2.4. Distribution of 128 electrodes across the scalp for the sponge-based EGI net.

2.2.3 Correcting EEG artifacts

After recording, EEG data must be inspected for artifacts from non-cerebral sources which can obscure the cortically generated signal. Artifacts can be physiological, generated from the participant, or non-physiological, generated by the equipment or environment. Common physiological

artifacts are eye blinks and eye movements, muscle movements, tongue artifacts, breathing and sweat potentials (Luck, 2014). Non-physiological artifacts can be caused by hardware issues and electrical interference, with the most common electrical interference caused by the alternating mains power supply at 50 Hz in Europe and 60 Hz in the United States (Luck, 2014).

Artifacts should be minimised during data acquisition, but any artifacts that remain are identified during data processing. Manual artifact rejection is carried out by scanning the continuous data and marking segments which contain artifacts for rejection. Alternatively, regularly occurring artifacts such as eye movements and heartbeats can be removed using adaptive artifact correction in the Brain Electrical Source Analysis software (BESA, GmbH) (Berg & Scherg, 1994; Ille et al., 2002). The adaptive artifact correction method uses a spatial filter to separate neural activity from artifacts without distorting the data. Segments are considered to represent brain activity if the correlation between data and artifact topography does not exceed a certain threshold, and if the signal amplitudes are below a specified threshold. Segments that do not meet this criterion are subject to principal component analysis, which decomposes the data into an independent, linear combination of brain and artifact activities so that estimated artifact signals can be subtracted from the raw data (Ille et al., 2002; Lagerlund et al., 1997).

An alternative approach to artifact removal is independent component analysis (ICA) which can be implemented in the EEGlab toolbox (Delorme & Makeig, 2004). ICA uses blind source separation to decompose data into temporally independent components (Makeig et al., 1996). In this approach, EEG data is assumed to be a mix of signals from independent brain sources which can be separated into a set of maximally independent, physiologically and functionally distinct, sources (Makeig et al., 2004). Decomposition into independent components allows separation of contributions from non-brain artifacts including eye movements, line noise and muscle activities (Jung et al., 2000). A limitation of the ICA method is that the quality of decomposition is dependent on the quality of data (Makeig et al., 2004).

2.2.4 Event-related Potentials

Event-related potentials (ERPs) are time-locked changes in EEG which are evoked by the onset of an event or stimulus (Lopes da Silva, 2011b). It is generally accepted that ERPs are signals generated by neural populations that are time-locked to the stimulus which are in addition to the ongoing EEG activity (Lopes da Silva, 2011b). ERP analysis is therefore based on the assumptions that the electrical response evoked by stimuli is time-locked to the stimulus and that the ongoing activity is stationary noise that can be removed by averaging over many trials (Lopes da Silva, 2011b). ERPs studied in relation to pain include SEPs, usually evoked by electrical stimulation applied to peripheral nerves, and LEPs, evoked by noxious laser stimuli.

ERPs are seldom visible on a single trial level and are isolated from ongoing EEG by averaging over many trials. Averaging over many trials increases the signal-to-noise ratio of the data by minimising the contribution of voltage fluctuations that are not time-locked to the event or stimulus of interest (Boudewyn et al., 2018). Signal-to-noise ratio of EEG improves as a function of the square root of the number of trials (Luck, 2014). The number of trials necessary for an ERP experiment is not fixed and depends on the quality of the data, sample size, effect size under investigation and the amount of time required for data to be collected (Boudewyn et al., 2018).

The process for averaging involves extracting fixed-length epochs from the continuous data which are time-locked to the event of interest. Epochs involve a baseline period prior to the event of 100–200 ms, followed by a period after the event of 500–1500 ms, dependent on the component under examination (Luck, 2014). After extracting epochs, baseline correction can be performed by subtracting the mean baseline voltage from the entire waveform. The purpose of baseline correction is to correct for voltage offsets and gradual drifts in the data caused by factors such as skin potentials and static changes which vary slowly over time (Luck, 2014). Next, artifact-free epochs are averaged with respect to the time-locked event by summing all single-trial waveforms and dividing by the number of trials.

ERPs can be analysed based on latency (ms) or amplitude (μV) of positive and negative voltage deflections which make up the waveform, known as components (Luck, 2014). The amplitude

of an ERP can be measured at the peak, or more accurately as the mean or area amplitude over the component (Luck, 2014). The benefit of measuring the mean or area under the curve amplitude rather than peak amplitude for monophasic deflections is that latency jitter does not impact the mean amplitude. Deviations in component amplitudes and/or latencies can be used to make neurophysiological inferences about a process or population. Standard nomenclature for ERPs is the polarity of the waveform, P (positive) or N (negative), followed by either the post-stimulus latency or order of the component (Luck, 2014).

A drawback of the ERP technique is that deflections which are not phase-locked to an event may be cancelled out during averaging. In this case, time-frequency analyses may be more appropriate (Tallon-Baudry et al., 1996).

2.2.5 Time-frequency analysis

2.2.5.1 Cortical rhythms and their generators

The earliest human EEG studies by Berger (1929–1933) (as cited in Kropotov, 2009) and Adrian & Matthews (1934) noted that awake subjects with eyes closed produced dominant 10 Hz oscillations, which Berger named "waves of the first order" or alpha rhythms. These rhythms were blocked with eye opening and under mental effort, leading to "waves of the second order" or beta rhythms (Kropotov, 2009). It is now accepted that EEG is an oscillatory, time-varying signal that varies in frequency. Ongoing, spontaneous EEG during the resting state can vary with changes in wakefulness, vigilance level, task performance, and drug effects (Dumermuth & Molinari, 1987). Neural oscillations are rhythmic fluctuations in the excitability or synchronicity of neuron populations. Factors that influence the basic phenomena of synchronous oscillations are the intrinsic membrane properties of neurons, interconnectivity between network elements, synaptic processes that subserve specific inputs and feedback and feedforward loops and modulating influences from neurotransmitters (Lopes da Silva & Pfurtscheller, 1999).

2.2.5.2 Quantifying amplitudes of spontaneous cortical oscillations

EEG can be analysed quantitatively based on frequency, time, amplitude, phase, and morphology. To analyse changes in the frequency domain, EEG data is split into frequency bands. Classical bands for EEG analysis are delta (1–4 Hz), theta (4–7 Hz), alpha (8–13 Hz), beta (14–30 Hz), and gamma (>30 Hz), with the most relevant for somatosensory processing and nociception being alpha, beta and theta bands. These boundaries can vary across individuals and states (Gevins, 1987).

Spectral analysis involves quantification of the frequency content of a signal or the distribution of signal power over frequency, measured in power (Kropotov, 2009). There are many approaches to the decomposition of oscillatory data, including band-pass filters, Fourier transformation or wavelet transformations. Each method entails a trade-off between temporal and frequency resolution, whereby the higher the frequency resolution, the lower the temporal resolution, and vice versa (Cohen, 2014).

Fourier transformations, including the Welch power method, involve correlating the EEG time series with standard sine and cosine waves and tabulating the energy accounted for by each of those waves (Gevins, 1987; Welch, 1967). The sum of the energy of the waves equals the power spectrum, while the inverse tangent of their ratio represents the phase spectrum (Gevins, 1987). One such method, the Fast Fourier Transform, is an efficient algorithm for computing the Fourier series which assumes that an input signal is one period of a periodic signal which is stationary and slowly varying (Kropotov, 2009). When computing the power spectra, data is cut into overlapping or non-overlapping segments of various lengths and the power spectrum of each data segment is computed. The choice of time segment influences the frequency resolution, as segments must be long enough to capture at least one cycle of the lowest frequency of interest, but not too long that transient higher frequency activity is missed (Cohen, 2014). Changes in power spectra can be examined as an average over the whole recording interval or as gradual changes over time by using a windowed Fourier transform (Kropotov, 2009). Three minutes is the minimum duration of EEG recording for a stable power spectrum (Kropotov, 2009).

Power can be analysed in terms of absolute or relative power. Absolute power is a measure of the amount of power of a specific frequency. Absolute power can vary between subjects based on neurophysiological, anatomical and physical properties of the brain and surrounding tissue (Kropotov, 2009). The power spectrum of EEG is not equal across frequency bands. Lower frequency bands typically have greater amplitudes compared to higher frequency bands (Chang et al., 2011). As a result, power spectra must be scaled to obtain a more normally distributed value, with a common method being the logarithm transformation (Gasser et al., 1982; Gevins, 1987). An alternate method to absolute spectral power is relative power. Relative power of each frequency band can be examined by dividing the absolute power of each band by the total power, or by the sum of powers in the frequency band of interest.

In contrast to Fourier analysis, wavelet analysis allows examination of how rhythms in EEG change over time. Wavelet analysis involves decomposing EEG into finite length oscillating waveforms, called wavelets (Kropotov, 2009). To compute a wavelet transform, the original EEG timeseries is convolved with a scaled and translated version of a mother wavelet function, leading to a new signal of wavelet coefficients (Herrmann et al., 2005). The result is improved time resolution but reduced frequency resolution in comparison to Fourier transformation (Herrmann et al., 2005). The most commonly used mother wavelet functions are Morlet or Gabor wavelets, complex functions that consist of a sine wave windowed in time by a Gaussian taper (Cohen, 2014; Herrmann et al., 2005).

Oscillations at frequencies not sampled in the Fourier or wavelet transformation may spread power to sampled frequencies (Kropotov, 2009). This phenomenon of spectral leakage can be reduced using single tapers such as Blackman, Hann or Hamming windows. The Hamming window is a raised cosine with non-zero endpoints, which tapers the data at the beginning and end of the segment (Cohen, 2014). Alternatively, multiple tapers such as discrete prolate spheroidal sequence, also known as Slepian windows, can be used to achieve better control over the frequency smoothing and are beneficial for noisy data with a relatively small number of trials, or for examining frequencies over 30 Hz (Cohen, 2014; Slepian, 1978).

2.2.5.3 Quantifying event-related changes in cortical oscillations

Short-lasting amplitude changes of spontaneous oscillations which are time-locked to sensory, motor, or cognitive events can be investigated with the ERD method. The ERD method involves selecting frequency bands of interest, squaring the amplitude samples to obtain power samples, averaging power samples across all trials, and averaging over all time samples to smooth the data and reduce variability (Pfurtscheller & Aranibar, 1977; Pfurtscheller & Lopes da Silva, 1999).

ERD can be quantified by comparing oscillatory power in a specific frequency band during an event compared to a reference or baseline interval with the following equation:

$$D\% = \left(100 * \frac{A - R}{R}\right)$$

where *D* represents the percentage power change during epochs following the event onset *(A)* relative to the preceding baseline or reference period *(R).* Positive *D* values correspond to relative power decreases (ERD), considered to signify cortical activation (Pfurtscheller, 1977; Pfurtscheller & Aranibar, 1977). Negative *D* values correspond to relative increases of cortical band power (ERS), considered to signify cortical idling or inhibition (Lopes da Silva & Pfurtscheller, 1999; Pfurtscheller, 1992). A drawback to the ERD method is that nonlinearity during quantification results in skewed data, which may violate normality assumptions in parametric statistical tests (Graimann & Pfurtscheller, 2006).

An alternative way to quantify oscillatory changes is temporal-spectral evolution (TSE) method (Salmelin & Hari, 1994c). The TSE method involves selecting frequency bands of interest, which are band-pass filtered, averaged over trials and rectified. The result is that signal amplitude at a certain scalp location and in a specific frequency band is displayed as a function of time. Increase and decrease of TSE curves corresponds to changes in ERS and ERD (Pfurtscheller, 1999). Similar to ERD, the TSE method allows the identification of event-related oscillatory activity which is time- but not phase-locked to the event.

2.2.6 Source dipole analysis

Electrical activity of the brain consists of ionic currents generated by cellular sources. These ionic currents cause electric and magnetic fields that can be measured in the brain and surrounding tissues, diminishing in strength with distance. The forward problem is the determination of an observed potential distribution at the scalp given a set of intracerebral current sources (Lopes da Silva, 2011a). Solving the forward model requires a head model which accurately characterises the conduction of electrical potentials in the human head. The first head models were comprised of homogenous spheres (Frank, 1952), followed later by spherical head models of multiple shells which used different conductivities for each medium, and more realistic head models such as the boundary element method and finite element models (Lopes da Silva, 2011a). The inverse problem of EEG is the determination of intracerebral sources contributing to an observed measured potential at the scalp. The inverse problem has no unique solution, as infinite combinations of intracerebral sources can result in the same potential distribution observed with EEG (Lopes da Silva, 2011a). The problem is underdetermined due to the number of EEG sensors in comparison to the number of cortical macrocolumns being estimated (Lopes da Silva, 2011a). Methods of source localisation known as inverse solutions can be used to overcome the inverse problem.

Methods for source localisation can be separated into dipole versus distributed techniques. Source dipole modelling assumes that the observed field on the scalp is generated by only one or a few equivalent current dipole in the brain (Michel & Brunet, 2019). Nonlinear multidimensional optimisation procedures are used to determine the dipole parameters that best explain the observed potentials. In this thesis, source dipole modelling was carried out using BESA with a 4-shell ellipsoidal head model (Scherg, 1992; Scherg & Berg, 1996). Each dipole in this model is specified by 6 parameters: coordinates in 3-dimensional space, 2 angles that specify its orientation and the strength of the source. Dipoles are fitted using a sequential strategy from the earliest peak in recorded potentials until the addition of another dipole does not explain any more of the residual variance (Scherg, 1992; Scherg & Berg, 1996; Stancak et al., 2002). Source models should agree with proven knowledge about underlying brain activity, and source waveform time courses should be distinctly

different from those of other sources (Scherg et al., 2010). Accuracy of dipole source localisation methods have reported mean errors of 6–20mm (Akalin Acar & Makeig, 2013; Chen et al., 2007; Cohen et al., 1990; Cuffin et al., 1991).

Distributed source modelling estimates a spatial distribution of neural current consistent with the measured EEG over the cortical surface. Distributed source models typically use minimum norm or weighted minimum norm solutions, which require that current distribution over all solution points have minimum energy and that the forward solution of this distribution optimally explains the data (Hämäläinen et al., 1993; Michel & Brunet, 2019). One such method is low-resolution electromagnetic tomography (LORETA) algorithm. The LORETA method assumes that neighbouring neurons are simultaneously and synchronously activated and selects the smoothest of all possible 3-dimensional current distributions, resulting in a tomography with a degree of dispersion (Pascual-Marqui et al., 1994). A variant of the LORETA algorithm, classical LORETA analysis recursively applied (CLARA), uses an iterative application of weighted LORETA images to reduce the source space per iteration and resolve closely neighbouring sources (Hyder et al., 2015).

2.2.7 Electrode selection for data analysis

EEG datasets are rich sources of information in terms of electrodes, time samples and frequency components. Comparison over all electrode sites, time points and frequency components lead to inflation of Type I error rate, so data used for statistical analysis must be constrained to choose only those showing a significant effect with correction for multiple comparisons. One way to select electrodes, time samples or frequency bands is based on prior research if the components being measured are well defined (Luck, 2014). Alternatively, mass univariate approaches such as false discovery rate correction and permutation approaches can be used. False discovery rate correction controls for the total proportion of bogus effects in a set of values (Benjamini & Hochberg, 1995). False discovery rate correction is recommended for studies with focal or broadly distributed effects (Groppe et al., 2011). Permutation statistics examine random partitions of the data to estimate the null distribution (Maris & Oostenveld, 2007). This allows determination of the t-value required to exceed what is expected by chance. Permutation-based testing is recommended for use when the effects of

interest are robust, sample size is large, or effects of interest are likely to only cover a small proportion of the null hypothesis, and when strong control of family-wise error is necessary (Groppe et al., 2011).

2.2.8 Pitfalls of EEG

EEG has excellent temporal resolution (~1 ms) due to the direct nature of recordings of neural activity (Luck, 2014). This allows for the disentangling of neural processes that occur between stimuli and responses, which is not possible with behavioural measures such as reaction times and pain ratings. The direct recording of neural activity with EEG is an advantage over other neuroimaging methods which measure changes in haemodynamic function as a proxy for neural activity, such as PET and fMRI. These methods measure changes in the proportion of oxygenated and deoxygenated blood in regions of the brain, based on the assumption that neural activity is associated with increased blood flow to that area (Logothetis, 2008). Blood flow to a region is much slower than the neural activity itself, resulting in poor temporal resolution in the magnitude of several seconds (Luck, 2014).

Electrical fields recorded at the scalp are subject to volume conduction effects. The voltage at the scalp is dependent on the position and orientation of the generator dipole, as well as the resistance and shape of the head. Electricity spreads through the path of least resistance, and increased resistance with the skull results in smearing of the signal recorded with EEG (Hämäläinen et al., 1993). Magnetic fields are not affected by the scalp, resulting in a better spatial resolution with MEG in contrast to EEG. However, MEG is insensitive to radially oriented dipoles, whereas EEG collects data from radial and tangential sources (Hämäläinen et al., 1993). The poor spatial resolution of EEG poses an obstacle of inferring the location of neuronal activity in the cortex from the volume-conducted signal measured at the scalp. As discussed, this inverse problem is ill-posed due to an infinite number of solutions to the measured signal. To resolve the inverse problem, solutions such as source analysis can be applied to estimate the location of dipoles, although definitive identification of electrical potentials is not possible from EEG alone.

Chapter 3

3 Research Problems and Hypotheses

3.1 Research problems

Neurostimulation treatments are palliative interventions for intractable neuropathic pain syndromes which are not improved with conventional medical management. However, a proportion of patients do not obtain clinically significant long term pain relief (Grider et al., 2016; Johnson et al., 2015, 2021; Johnson & Goebel, 2016; Kumar et al., 1996, 2008; North et al., 1991). The general effects of neurostimulation on somatosensory processing are well established, although the effects of stimulation parameters such as waveform and intensity are poorly understood. Parameters of electrical stimulation methods modulate the effects on peripheral and central pathways, which impact their therapeutic effects for reducing neuropathic pain. This thesis is focused on two parallel streams of neurostimulation research: a well-established intervention for neuropathic pain, SCS, and a novel method, LFS.

SCS is an established intervention for the palliative treatment of chronic neuropathic pain, although knowledge of the underlying mechanisms is limited (***See 1.6***). Conventional tonic SCS has been proposed to exert therapeutic effects via multiple mechanisms, including inhibition of somatosensory processing by concurrent impulses in the dorsal horn, as well as via supraspinal processes and descending inhibition (Linderoth & Foreman, 2017). Mechanisms underlying the newer burst waveform are still under debate. Limited studies point towards alternative mechanisms for tonic and burst waveforms which are reflected at spinal levels (Crosby et al., 2015b; Tang et al., 2014) and in the brain (De Ridder et al., 2013; De Ridder & Vanneste, 2016; Saber et al., 2021; Yearwood et al., 2019). Greater resting alpha and beta band power has been reported during trial stimulation of burst compared to tonic SCS; although differences during trial implant may not reflect long-term changes in oscillatory dynamics (De Ridder et al., 2013; De Ridder & Vanneste, 2016). Augmented theta band power has been implicated as a factor contributing to chronic pain (Llinás et al., 1999, 2005), and successful SCS treatment has been associated with decreased theta band power (Schulman et al.,

2005; Sufianov et al., 2014). Tonic SCS has been shown to inhibit neural processing of somatosensory inputs (Bentley et al., 2016; Sankarasubramanian et al., 2019) ***(see 1.6.1.1)***. To date, no studies have investigated the effects of burst and tonic SCS on oscillatory correlates of somatosensory processing. Examination of the effects of burst and tonic SCS on spontaneous oscillations and on processing of somatosensory input in the brain in theta, alpha and beta frequency bands is necessary to further delineate supraspinal mechanisms underlying the two waveforms.

The effects of SCS intensity on neural oscillatory dynamics are poorly understood. Somatosensory stimuli are associated with decreased alpha and beta band power over SI/MI (Chatrian et al., 1959; Pfurtscheller & Aranibar, 1977; Pfurtscheller & Lopes da Silva, 1999; Stančák, 2006) ***(see 1.5.3.4)***. Stronger stimulus intensities may result in greater amplitude attenuation, but do not encode fine intensity gradations (Iannetti et al., 2008; Stancak et al., 2003). Stimuli presented concurrently result in an inhibition of nociceptive and tactile somatosensory processing (Gandevia et al., 1983; Kakigi & Jones, 1986; Mancini et al., 2015), and the degree of inhibition is dependent on stimulus intensity (Lim et al., 2012). Understanding of the effects of SCS intensity is crucial, as intensity is one of a number of parameters that determine electrical dose for SCS (Abejón et al., 2015; Miller et al., 2016; Tan et al., 2016). Optimising electrical dose is crucial for effective pain relief with SCS (Chakravarthy et al., 2021; Paz-Solís et al., 2022). Currently, the method for SCS dose titration is a process of trial and error between the programmer and patient. Further understanding of the SCS therapeutic window, particularly for paraesthesia-free waveforms, is of vital importance. It is expected that SCS intensity will have a variable effect on cortical oscillations in the alpha, beta and theta bands, and the relationship between intensity and cortical oscillations may differ between burst and tonic SCS.

LFS is an emerging intervention for peripheral neuropathic pain which has been shown to reduce acute and chronic pain perception (Johnson et al., 2015; Johnson & Goebel, 2016; Jung et al., 2009; Klein, 2004; Lindelof et al., 2010; Magerl et al., 2018). The underlying mechanism of LFS is proposed to be LTD of nociception, which is specific to high intensities activating Aδ fibres (Liu et al., 1998; Sandkühler et al., 1997; Sdrulla et al., 2015). However, cortical effects that occur during LFS conditioning have not been investigated in humans. Peripheral electrical stimulation evokes SEPs

originating from nociceptive and somatosensory processing regions, including SI, bilateral SII and ACC or MCC, which increase in amplitude with greater stimulus intensities (Valeriani et al., 2000a) ***(See 1.5.3.1)***. The concept of LTD denotes that processing of somatosensory input reduces during LFS. Animal models have shown that LTD occurs steadily over the duration of LFS (Liu et al., 1998; Randić et al., 1993; Sandkühler et al., 1997). To understand the direct effects of LFS, it is important to examine the regions mediating the effects of LFS on cortical somatosensory processing during LFS conditioning. Furthermore, to investigate changes in cortical somatosensory processing that are specific to LTD, it is crucial to compare the effects of noxious intensities of LFS to stimulation at nonpainful intensities.

It is not known if cortical changes during LFS correlate with post-stimulation decreases in nociceptive processing or resting oscillatory activity. In humans, LFS is associated with reduced acute pain perception (Jung et al., 2009; Klein, 2004; Lindelof et al., 2010; Magerl et al., 2018) and attenuated SEP amplitude (Ellrich & Schorr, 2004; Jung et al., 2009, 2012; Magerl et al., 2018) to noxious test stimuli delivered following LFS. However, previous studies have compared LFS to a control condition of no stimulation ***(See 1.7)***, raising the possibility that changes in pain perception and SEPs could be due to reduced stimulus saliency and habituation. Therefore, to thoroughly investigate the effects of LFS on acute pain perception and pain-related neural activity, it is vital to compare the effects of LFS to an ineffective sham condition, and at varying LFS intensities.

3.2 Hypotheses

H_1 Burst and tonic SCS waveforms will have different effects on cortical somatosensory processing, with decreased alpha and beta band power in frontal and midline regions, and changes in theta band power, during burst SCS compared to tonic SCS.

H_2 Increasing SCS intensities will be associated with increased alpha and beta band power in sensorimotor regions and reduced theta band power in frontal central regions during rest and during somatosensory processing.

H_3 Low frequency stimulation delivered at high intensities will attenuate cortical somatosensory processing, with a systematic decrease in SEP amplitude in regions associated with nociceptive processing during stimulation.

H_4 Low frequency stimulation will attenuate post-stimulation nociceptive processing, indicated by reduced amplitude LEPs, and increased power of alpha and beta band resting cortical oscillations.

3.3 *Thesis chapters*

Chapter 4 describes a study utilising resting EEG which investigated the cortical oscillatory dynamics of four intensities of SCS in patients with chronic neuropathic pain (H_2). SCS was administered at four intensities: no stimulation, low, medium and therapeutic intensities. Changes in the power of resting oscillations were collected from patients using burst and tonic stimulation during each SCS intensity to investigate the effect of varying SCS waveforms and SCS intensities on cortical oscillatory activity (H_1, H_2).

Chapter 5 examines the effect of SCS intensity on cortical oscillations during dynamic brushing stimulation in patients with chronic neuropathic pain (H_2). SCS was administered at four intensities: no stimulation, low, medium and therapeutic intensities. The ERD method was used to investigate cortical activation changes during brushing at each intensity. Alterations in brushing-related ERD were evaluated in patients using either burst or tonic stimulation to investigate the interaction between SCS waveform and intensity (H_1, H_2).

Chapter 6 describes a sham-controlled ERP and resting EEG study in healthy volunteers which investigated the spatiotemporal characteristics of LFS of the radial nerve on somatosensory processing, and changes in nociceptive processing and resting cortical oscillations associated with LFS. A source dipole model was developed to describe the sources contributing to LFS. Changes in source dipole magnitude during LFS were used as an indirect correlate of LTD of somatosensory processing (H_3). Noxious laser stimuli were applied to radial and ulnar surfaces of the hand before and after active or sham LFS to examine the effect of LFS on nociceptive processing (H_3). Resting EEG

was recorded before and after active and sham LFS to investigate alterations in the power of cortical oscillations after LFS (*H_4*).

Chapter 7 describes an ERP and resting EEG study in healthy volunteers which investigated the spatiotemporal profiles of cortical activity during four intensities of LFS and amplitudes of cortical oscillations following LFS. A source dipole model was developed to describe the sources contributing to LFS of the radial nerve, and changes in source dipole magnitude during LFS were used as an indirect correlate of LTD of somatosensory processing (*H_3*). Administration of LFS at four intensities, varying from perception to moderately painful intensities, allowed investigation of the effects of LFS intensity on somatosensory processing (*H_3*). Resting EEG was recorded at the start of the experiment and after each LFS intensity to examine post-stimulation effects of LFS on cortical oscillations (*H_4*).

Chapter 8 comprises a general discussion of all experimental findings. The implications of the findings are discussed in the context of the current opinions in the field of neuromodulation, and future directions are considered.

Chapter 4

Oscillatory changes during graded intensities of burst and tonic spinal cord stimulation in neuropathic pain patients

Danielle Hewitt[1], Adam Byrne[1,2], Jessica Henderson[1], Kathryn Wilford[3], Rajiv Chawla[3], Manohar Lal Sharma[3], Bernhard Frank[3], Christopher Brown[1], Nicholas Fallon[1], Andrej Stancak[1]

[1] Department of Psychological Sciences, University of Liverpool, Liverpool, UK.

[2] Institute for Risk and Uncertainty, University of Liverpool, Liverpool, UK.

[3] The Walton Centre NHS Foundation Trust, Liverpool, UK.

This experiment investigated the effect of burst and tonic SCS intensities on resting cortical oscillations in patients with chronic neuropathic pain.

The roles of the co-authors are summarised below:

Danielle Hewitt: Conceptualisation, Methodology, Software, Investigation, Formal analysis, Writing - Original Draft, Writing - Review & Editing. **Adam Byrne:** Investigation, Writing - Review & Editing. **Jessica Henderson:** Investigation, Writing - Review & Editing. **Kathryn Wilford:** Resources. **Rajiv Chawla:** Resources. **Manohar Lal Sharma:** Resources. **Bernhard Frank:** Conceptualisation, Resources, Funding acquisition. **Nicholas Fallon:** Conceptualisation, Writing - Review & Editing. **Christopher Brown:** Conceptualisation, Writing - Review & Editing. **Andrej Stancak:** Conceptualisation, Software, Formal analysis, Writing - Original Draft, Writing - Review & Editing, Supervision, Funding acquisition.

4 Oscillatory changes during graded intensities of burst and tonic spinal cord stimulation in neuropathic pain patients

4.1 Abstract

SCS is a palliative neurostimulation treatment for neuropathic pain. Tonic stimulation has been proposed to exert its therapeutic effects via multiple mechanisms, including inhibition of somatosensory processing by concurrent impulses in the dorsal horn, while newer waveforms such as burst may have alternative mechanisms. Moreover, the impact of SCS intensity on oscillatory activity is poorly understood. This study investigated the effect of varying intensities of burst and tonic SCS on resting EEG oscillations.

Twenty-one patients using SCS (11 burst, 10 tonic) for unilateral neuropathic leg pain participated. Oscillatory activity was recorded continuously with a 64-channel EEG system during 4 SCS intensities: 'Therapeutic' (100%), 'Medium' (66%), 'Low' (33%) and 'Off'. Log-transformed absolute band power was computed in theta (4-7 Hz), alpha (8-13 Hz) and beta (16-24 Hz) frequency bands. Repeated-measures ANOVAs assessed differences in oscillatory band power between SCS intensities. Independent t-tests investigated differences in band power between burst and tonic SCS.

SCS intensities were associated with changes in band power in alpha and beta frequency bands. In the alpha band (8-11 Hz), posterior parietal electrodes showed significantly greater band power at low and medium intensities compared to no stimulation and therapeutic SCS intensity. In the beta band (21-24 Hz), greater band power was found in right midline electrodes at the therapeutic intensity compared to lower SCS intensities. Burst SCS showed widespread reductions in alpha and beta band power compared to tonic stimulation, although differences were not statistically significant.

Results suggest a nonlinear effect of SCS intensity on resting oscillatory activity. Augmented beta band power at the highest therapeutic intensity and in the alpha band at lower intensities point towards cortical inhibition in somatosensory processing regions. Burst and tonic SCS may have similar effects on spontaneous oscillatory activity, although further investigation with a larger, homogeneous sample is warranted to elucidate the underlying mechanisms of action.

4.2 *Introduction*

SCS is a palliative neurostimulation treatment for neuropathic pain conditions including chronic pain after spinal surgery and complex regional pain syndrome. While the clinical effectiveness of conventional SCS is well established (Duarte et al., 2020; Scalone et al., 2018; Visnjevac et al., 2017), a considerable number of patients do not experience long-term pain relief (Geurts et al., 2013). Novel stimulation waveforms such as burst stimulation may match or exceed the effectiveness of conventional tonic stimulation (De Ridder et al., 2013; de Vos et al., 2014; Deer et al., 2018; Schu et al., 2014).

SCS was developed as a direct application of the Gate Control Theory (Melzack & Wall, 1965), which postulates that activation of low-threshold Aβ fibres in the dorsal column close a spinal gate to inhibit nociceptive transmission (Melzack & Wall, 1965; Shealy et al., 1967; Sun et al., 2021). Tonic SCS delivers single repetitive electrical pulses (40–100 Hz) to the spinal cord, resulting in paraesthesia over the painful area. In line with the Gate Control Theory, tonic SCS inhibits ascending nociceptive transmission from wide dynamic range cells (Yakhnitsa et al., 1999) with the release of neurotransmitters such as gamma-aminobutyric acid (GABA) in the spinal dorsal horn (Cui et al., 1997; Stiller et al., 1996). Comparatively, burst SCS utilises trains of 5 monophasic pulses administered at 40 Hz interburst and 500 Hz intraburst frequencies which are charge balanced after each pulse train and delivered below sensory threshold (De Ridder et al., 2010, 2013, 2020). Burst SCS does not activate Aβ fibres (Crosby et al., 2015b) or increase spontaneous activity in the gracile nucleus (Tang et al., 2014), suggesting that unlike tonic stimulation, burst does not drive the dorsal column pathway. Alternative mechanisms of burst stimulation have been suggested, such as fibre threshold accommodation (Arle et al., 2020) and engagement of the medial pain pathway (De Ridder et al., 2013; De Ridder & Vanneste, 2016; Yearwood et al., 2019). Consequently, greater effectiveness of burst stimulation compared to tonic stimulation may result from different mechanisms of action.

EEG has been used to investigate changes in ongoing neural activity in patients with chronic pain. Numerous studies have reported greater resting band power in patients with chronic pain in theta (4–7 Hz), alpha (8–13 Hz) and beta frequency bands (16–24 Hz) (Lim et al., 2016; Pinheiro et al.,

2016; Sarnthein et al., 2006; Stern et al., 2006; Vučković et al., 2014). Alpha band power has been related to cortical idling (Klimesch et al., 1998; Pfurtscheller et al., 1996b) or active suppression of irrelevant stimuli (Foxe & Snyder, 2011), with decreased alpha activity during states of alertness and sensory processing. Increased theta band power has been suggested as a contributing factor in the development or maintenance of a number of pathologies including chronic pain (Llinás et al., 1999, 2005). Successful SCS treatment is associated with reduced theta power in animal models of neuropathic pain (Koyama et al., 2018) and in humans (Schulman et al., 2005; Sufianov et al., 2014). Combined, this suggests that alterations in neural oscillatory power may have clinical relevance for the treatment of chronic pain with SCS.

Alterations in oscillatory power have been observed between different SCS waveforms (Goudman et al., 2020; Telkes et al., 2020), although few studies have investigated the effects of burst stimulation on resting EEG in humans. Using a small subset of SCS-naïve patients undergoing trial stimulation, De Ridder and colleagues reported that burst SCS was associated with increased low alpha band power in sources localised to the dorsal ACC, and increased alpha and beta band power in the prefrontal cortex, compared to tonic stimulation (De Ridder et al., 2013; De Ridder & Vanneste, 2016). This effect differed across frequency subbands, with significant effects restricted to low-alpha (8–10 Hz), mid-beta (18.5–21.5 Hz) and high-beta subbands (21.5–30 Hz). Dissociations in the frequency of cortical rhythms have likewise been reported following voluntary movement, with distinct topographic representations of lower (8–10 Hz) and upper (10–12 Hz) alpha frequency components (Pfurtscheller et al., 2000). Similarly, distinct resonance frequencies have been reported in the beta band for voluntary movement and electrical stimulation of upper versus lower limbs (Neuper & Pfurtscheller, 2001a; Pfurtscheller et al., 1999). Therefore, burst and tonic stimulation may differently affect subcomponents of alpha and beta frequency bands, although due to the small patient group in the aforementioned studies, a thorough investigation of changes in cortical oscillatory power between burst and tonic SCS is warranted.

The intensity of SCS may interact with its effect on somatosensory processing. Graded intensities of painful and nonpainful stimuli applied to the periphery are associated with enhanced amplitude of evoked potentials (Derbyshire et al., 1997; Iannetti et al., 2008; Loggia et al., 2012;

Shimojo et al., 2000; Valeriani et al., 2000a) and greater haemodynamic responses in somatosensory processing regions (Geuter et al., 2020; Oertel et al., 2012; Peyron et al., 2000; Su et al., 2019). With regards to SCS, stimulation intensity is determined by amplitude. SCS amplitude influences the number of fibres recruited by stimulation and contributes to overall electrical charge transfer (Miller et al., 2016). Electrical charge transfer has been shown to be a critical factor in SCS effectiveness; increased intensity is associated with reduced neuronal firing to noxious stimuli and nonlinear increases in the responsiveness of wide dynamic range neurons for burst SCS (Crosby et al., 2015a), and a greater reversal of nociceptive behaviours in animal studies with tonic SCS (Sato et al., 2014; Yang et al., 2014). However, it is not known how SCS intensity will affect cortical oscillatory activity, or if intensity will differentially modulate cortical activity during burst and tonic stimulation.

The current study sought to investigate the effects of SCS on cortical oscillations during rest under four intensities of SCS and in two SCS waveforms. Firstly, the study aimed to investigate whether differences in resting cortical oscillations would be found between tonic and burst stimulation in theta (4–7 Hz), alpha (8–13 Hz) or beta (16–24 Hz) frequency bands. Secondly, the study aimed to investigate the effect of SCS intensity on cortical oscillations at four intensities: low, medium, therapeutic and no stimulation. As somatosensory stimuli can differently affect subcomponents of alpha and beta frequency bands (Neuper & Pfurtscheller, 2001a; Pfurtscheller et al., 1999, 2000), we investigated the effect of SCS type and intensity on single frequency components within each predefined frequency band. We predicted that greater SCS intensities would be associated with increased band power in alpha and beta frequency bands and reduced band power in the theta band. Due to the previous evidence of greater engagement of the medial pain system during burst SCS (De Ridder & Vanneste, 2016; Yearwood et al., 2019), we hypothesized that burst SCS would be associated with decreased alpha and beta band power in frontal and midline regions compared to tonic SCS.

Table 4.1. Clinical patient characteristics for Study 1.

ID	Age	Sex	Diagnosis	Pain Duration	SCS Type	SCS Duration	Lead	Lead location	IPG	Freq (Hz)
1	63	F	Neuropathic radicular right leg pain	228	Burst	30	Octrode	T10–T12	Prodigy	40
2	46	F	Neuropathic right leg pain secondary to MS	108	Burst	29	Lamitrode Tripole	T10–T12	Prodigy	40
3	68	F	Bilateral neuropathic leg secondary to MS	168	Burst	48	Octrode x2	T9–T11	Prodigy	40
4	73	M	Neuropathic left foot pain	336	Tonic	57	Lamitrode	T11–T12	Eon-C	54
5	59	M	Neuropathic radicular left leg pain	48	Tonic	2	Lamitrode Tripole	T9–T10	Prodigy	40
6	53	M	Bilateral lower limb neuropathic pain	267	Tonic	2	Lamitrode Tripole	T9–T10	Prodigy MRI	40
7	52	M	Bilateral neuropathic leg pain secondary to MS	60	Burst	30	Lamitrode Tripole	T10–T12	Prodigy	40
8	61	F	Neuropathic bilateral leg pain	84	Tonic	1	Octrode	T9–T12	Prodigy	30
9	50	F	Right foot CRPS	26	Tonic	50	Octrode x 2	T9–T11	Prodigy	50
10	76	M	Neuropathic right foot pain	96	Tonic	47	Lamitrode Tripole	T12–L1	Prodigy	60
11	50	M	Neuropathic radicular left leg pain	84	Burst	1	Octrode	T9–T11	Prodigy	40
12	39	M	Neuropathic left foot and ankle pain	84	Burst	1	Octrode x 2	T8–T11	Prodigy	40
13	37	F	Neuropathic radicular left leg pain	60	Tonic	16	Octrode x 2	T8–T11	Prodigy	50
14	30	F	Neuropathic radicular left leg pain	72	Tonic	1	Lamitrode Tripole	T8–T9	Prodigy	40
15	55	F	Neuropathic left foot and ankle pain	240	Burst	24	Octrode	T10–T12	Prodigy	40
16	75	F	Neuropathic radicular left leg pain	420	Burst	8	Octrode x 2	T8–T12	Prodigy	40
17	52	M	Neuropathic radicular left leg pain	192	Burst	12	Lamitrode Tripole	T9–T10	Prodigy	40
18	52	F	Neuropathic radicular left leg pain	60	Burst	12	Octrode x 2	T9–T12	Prodigy	40
19	52	F	Neuropathic radicular left leg pain	48	Burst	12	Octrode x 2	T8–T10	Prodigy	44
20	36	F	Left foot and ankle CRPS-II	66	Burst	12	Octrode	T10–T12	Prodigy	40
21	44	M	Neuropathic radicular right leg pain	96	Tonic	19	Octrode	T10–T12	Prodigy	50

Pain duration and SCS duration measured in months. IPG = implantable pulse generator. Freq = frequency in hertz (Hz).

4.3 Methods

4.3.1 Subjects

Twenty-one patients (11 females, aged 53.5 ± 12.8 years (mean ± SD)) with unilateral neuropathic lower limb pain were recruited from The Walton Centre NHS Foundation Trust, Liverpool, UK. All participants had previously been implanted with Abbott (Texas, USA) SCS in conventional tonic (N=10) or BurstDR waveforms (N=11). The procedure used was approved by the Liverpool Central North West Research Ethics Committee, and all participants gave fully informed written consent at the start of the experiment in accordance with the Declaration of Helsinki. Participants were reimbursed with £40 for their time and inconvenience on completion of the study.

Patient characteristics are summarised in ***Table 4.1***. All patients fulfilled criteria for neuropathic pain, determined by the Neuromodulation team prior to permanent implantation of SCS devices at The Walton Centre NHS Foundation Trust. Mean duration of SCS implant was 19.71 ± 18.15 months, and mean duration of symptoms was 134.95 ± 106.26 months. A one-way ANOVA showed that there was no significant difference of symptom duration ($F(1,19) = .10$, $p > .05$) or SCS duration ($F(1,19) = 2.46$, $p > .05$) between patients using burst and tonic SCS. Analgesic medications were not withdrawn prior to participating; 16 patients were using pain medication, with 13 patients using 2 or more pain medications.

4.3.2 Experimental protocol

Experimental procedures were carried out in a single 2-hour session in the Pain Research Laboratory, Pain Relief Institute, Aintree University Hospital NHS Foundation Trust (Liverpool, UK). SCS were switched off using the patient handheld programmer from the time of arrival until the experiment began while EEG was applied to the head, a duration of approximately 40 minutes.

Participants were seated in a comfortable chair in a quiet room. EEG was recorded during 4 five-minute blocks. During the experiment, participants were instructed to keep their eyes closed and stay awake. Blocks were varied by SCS intensity determined using the patient programmer: normal therapeutic intensity, medium (66% of the therapeutic level), low (33% of the therapeutic level) and no stimulation (off). Block order was varied pseudo-randomly for each participant, and participants

were unaware of the order of blocks during the experiment. After each block, participants were able to open their eyes, and SCS was turned off for two minutes.

Next, clinical and demographic data including age, duration of pain and duration of SCS treatment were collected verbally from patients. Patients self-completed the Neuropathy Pain Scale and Pain Catastrophising Scale by hand or using a tablet. Pain diaries were collected for 7 days following the visit to assess average and worst daily pain scores using a visual analogue scale from no pain (0) to worst imaginable pain (10).

4.3.3 EEG acquisition

Whole-scalp EEG was continuously recorded using a 63-channel system (BrainProducts GmbH, Munich, Germany). Actively shielding Ag-AgCl electrodes were mounted on an electrode cap (actiCap snap, BrainProducts) according to the International 10–20 system (Jasper, 1958). The cap was aligned with respect to three anatomical landmarks of two preauricular points and the nasion. Electrolyte gel was applied to achieve electrode-to-skin impedances of below 50 kΩ throughout the experiment. A recording band-pass filter was set at 0.001–200 Hz with a sampling rate of 1000 Hz. Electrode FCz was used as a reference electrode, and electrode FPz was used as the ground electrode. EEG average reference was applied, and signals were digitised at 1 kHz with a BrainAmp DC amplifier (actiChamp), connected to BrainVision Recorder 2.0 running on a Windows 10 laptop.

4.3.4 Spectral analysis of EEG signals

EEG data were processed using EEGLab (Delorme & Makeig, 2004). Continuous EEG data were re-referenced to the common average (Lehmann, 1987) and filtered using 1 Hz high pass and 100 Hz low pass filters. For each participant, data were visually inspected for movement and muscle artifacts. Intervals containing motion, electrode or muscle artifacts were marked and excluded from further analysis. Electrode channels with large artifacts were interpolated to a maximum of <10% electrodes. The average duration of resting data remaining after artifact correction for each condition were: no-stimulation 296.19 ± 8.34 seconds, low-intensity 294.29 ± 15.68 seconds, medium-intensity 293.91 ± 15.05 seconds, therapeutic-intensity 296.19 ± 6 seconds. A repeated-measures ANOVA

showed that the duration of resting data was not significantly different between SCS intensity ($F(3,57) = 0.26$, $p > .05$) or SCS types ($F(1,19) = 0.15$, $p > .05$).

Average spectral band-power in 4-min resting EEG recordings were calculated using FieldTrip (Oostenveld et al. 2011: http://fieldtriptoolbox.org). Power spectra were computed using a fast Fourier transform in non-overlapping 4-s segments. Data were smoothed using a Hanning window. Spectral power was estimated in the range 1–100 Hz with a frequency resolution of 0.25 Hz. Mean absolute power values were transformed using a decadic logarithmic transform. In light of the presence of SCS artifacts at stimulation frequencies between 40–60 Hz (see Table 1), only frequency components between 1–30 Hz were considered for statistical analysis. Log-transformed absolute band power in single (1 Hz) frequency components within alpha (8–13 Hz), beta (16–24 Hz) and theta (4–7 Hz) frequency bands were evaluated in each of the four SCS intensity conditions for burst and tonic stimulation.

4.3.4.1 Statistical analysis

Grand average topographic plots were visually inspected to identify electrode clusters showing prominent changes in frequency bands of interest: alpha (8–13 Hz), beta (16–24 Hz) and theta (4–7 Hz) frequency bands.

A permutation analysis with 2000 repetitions, implemented in the *statcond.m* program in the EEGLab package (Delorme & Makeig, 2004), was utilised to identify electrode clusters and frequency components showing a significant main effect of SCS Intensity within each frequency band. Permutation analysis provides a data-driven approach to test effects across all frequency components whilst controlling for multiple comparisons with no loss in statistical power (Maris & Oostenveld, 2007). For each frequency band, electrode clusters and single frequency components that exceeded a predefined threshold on the calculated *p*-values ($p < .05$) for the main effect of Intensity were selected for further analysis. Log-transformed absolute band power in frequency components and electrode clusters exceeding permutation tests were entered into 1×4 repeated-measures ANOVAs with 4 SCS intensities (off, low, medium and therapeutic). Pairwise comparisons were computed to further investigate significant main effects.

Similarly, unpaired t-tests were used to assess the effect of SCS Type (burst or tonic). Electrode clusters and frequency components exceeding permutation testing with 2000 repetitions ($p < .05$) were selected for analysis. Electrode clusters and frequencies showing a significant main effect of SCS Type or Intensity were entered into mixed methods ANOVAs to analyse the presence of an interaction between conditions. For all comparisons, the Huynh-Feldt correction was used where necessary to tackle a violation of the sphericity assumption in the data, denoted by ε.

4.4 Results

4.4.1 Subjective reports

Patients' level of pain on the day of the experiment was collected using the Neuropathy Pain Scale. Patients reported a mean pain score of 45.7 ± 18.2 out of a maximum 100 points. Patients' completed the Pain Catastrophizing Scale, reporting a mean score of 16.35 ± 13.32 out of a maximum 52 points. A one-way ANOVA showed no significant difference in neuropathic pain scores ($F(1, 19) = .050$, $p > .05$) or Pain Catastrophizing scores ($F(1, 19) = 1.33$, $p > .05$) between patients using burst and tonic SCS. In the 7 days following the experiment, pain diaries were collected. Five patients did not complete the pain diaries. In the completed diaries, mean average daily pain was 5.1 and mean strongest pain was 6.4 out of 10 (maximum pain). A one-way ANOVA showed no significant difference between mean average ($F(1, 13) = 4.3$, $p > .05$) and strongest ($F(1, 13) = 4.2$, $p > .05$) pain ratings between patients using burst and tonic SCS. Due to the absence of significant between-group effects, no further analyses of subjective reports were conducted.

4.4.2 Effect of SCS Intensity

The effect of SCS intensity was evaluated separately for each frequency band. For each frequency band, electrodes showing band-power maxima and minima were grouped into clusters. Statistical probability values were subject to permutation analysis with 2000 permutations and a statistical threshold of $p = .05$. Absolute band power in frequency components and electrode clusters exceeding permutation tests were entered into individual repeated measures ANOVAs with four levels of SCS intensity (off, low, medium and therapeutic) and a between-subjects factor of SCS type (burst or tonic stimulation).

In the theta band, topographic maps showed relatively strong band-power minima in frontal midline, bilateral central parietal and central midline electrodes (Figure 1B). Regions showing band-power minima were grouped into 4 clusters (**Figure *4.1***A). No significant effect of SCS intensity was found in any of the predefined electrode clusters in the theta frequency band (**Figure *4.1***B-C).

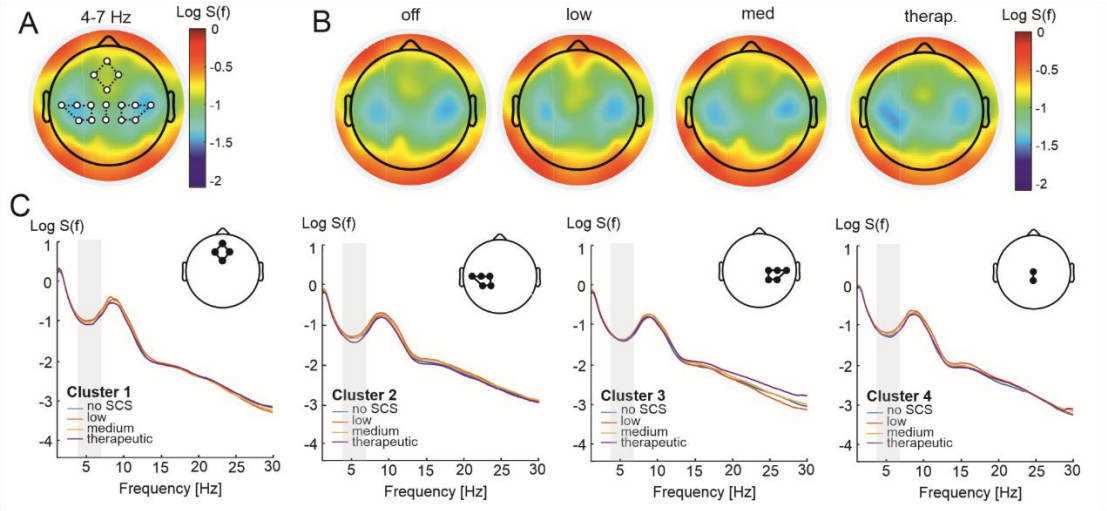

Figure 4.1. Power spectral density in the theta band at 4 SCS intensities. **A.** Electrodes were selected from grand average topographic plots as areas showing maximal changes in spectral power in the 4–7 Hz alpha band. **B.** Topographic plots of 4–7 Hz band power at 4 SCS intensities. **C.** Logarithmic power spectral density (log S(f)) in all 4 predefined clusters.

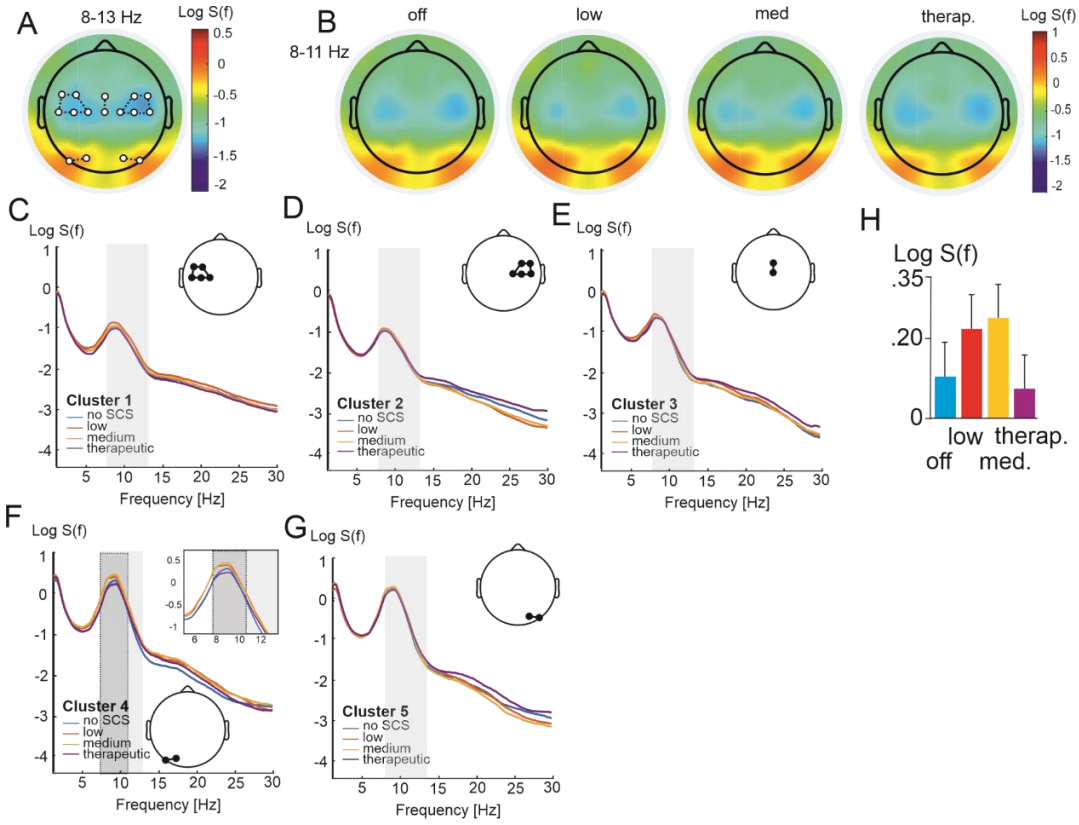

Figure 4.2: Power spectral density in the alpha band at 4 SCS intensities. **A.** Electrodes were selected from grand average topographic plots as areas showing maximal changes in spectral power in the 8–13 Hz alpha band. **B.** Significant differences in band power between SCS intensities were identified in Cluster 4 within the 8–11 Hz band using permutation analysis. **C**–**G.** Power spectral density in all 5 predefined clusters. **H.** Bar graph showing significant changes in band power in 8–11 Hz band in Cluster 4. Error bars show standard error of the mean.

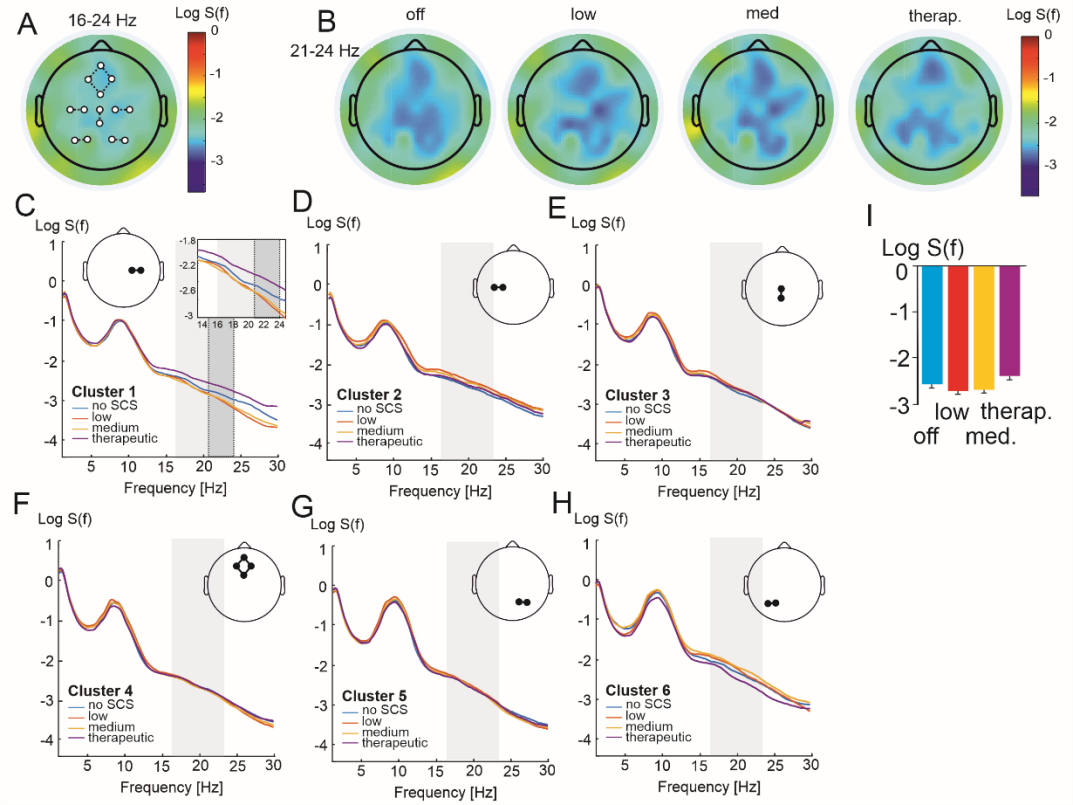

Figure 4.3. Power spectral density in the beta band at 4 SCS intensities. **A.** Electrodes were selected from grand average topographic plots as areas showing maximal changes in spectral power in the 16–24 Hz beta band. **B.** Significant differences in band power between SCS intensities were identified in Cluster 1 within the 21–24 Hz band using permutation analysis. **C–H.** Power spectral density in all 6 predefined clusters. **I.** Bar graph showing significant changes in band power in 21–24 Hz band in Cluster 1. Error bars show standard error of the mean.

Topographic maps of alpha band power were featured by relatively strong band-power minima in bilateral central and central midline electrodes, and relatively weak band-power maxima in bilateral posterior parietal electrodes (**Figure 4.2**A). A repeated-measures ANOVA showed that a cluster of electrodes overlying left posterior parietal scalp regions (PO7 and PO3) showed statistically significant amplitude changes across SCS intensities at 8-11 Hz ($F(3,57) = 3.2$, $p = .031$; **Figure 4.2**F). This effect was due to greater band power during medium intensity SCS ($p = .023$) compared

to no stimulation, and greater band power during low (p = .029) and medium intensities (p = .011) compared to the strongest, therapeutic intensity (**Figure 4.2H)**.

Topographic maps of beta band power were featured by band-power minima in frontal and central midline, bilateral central, and parietal electrodes. **Figure 4.3**A shows electrode clusters selected for analysis in the beta band. Repeated measures ANOVAs showed statistically significant amplitude changes across SCS intensities in right midline electrodes (C2 and C4) at 21-24 Hz ($F(3,57) = 3.3$, p = .043, ε = .73; Figure 3C). This effect was due to greater band power at the therapeutic intensity compared to low SCS intensity (p = .029) (**Figure 4.3I**).

4.4.3 Effect of SCS Type

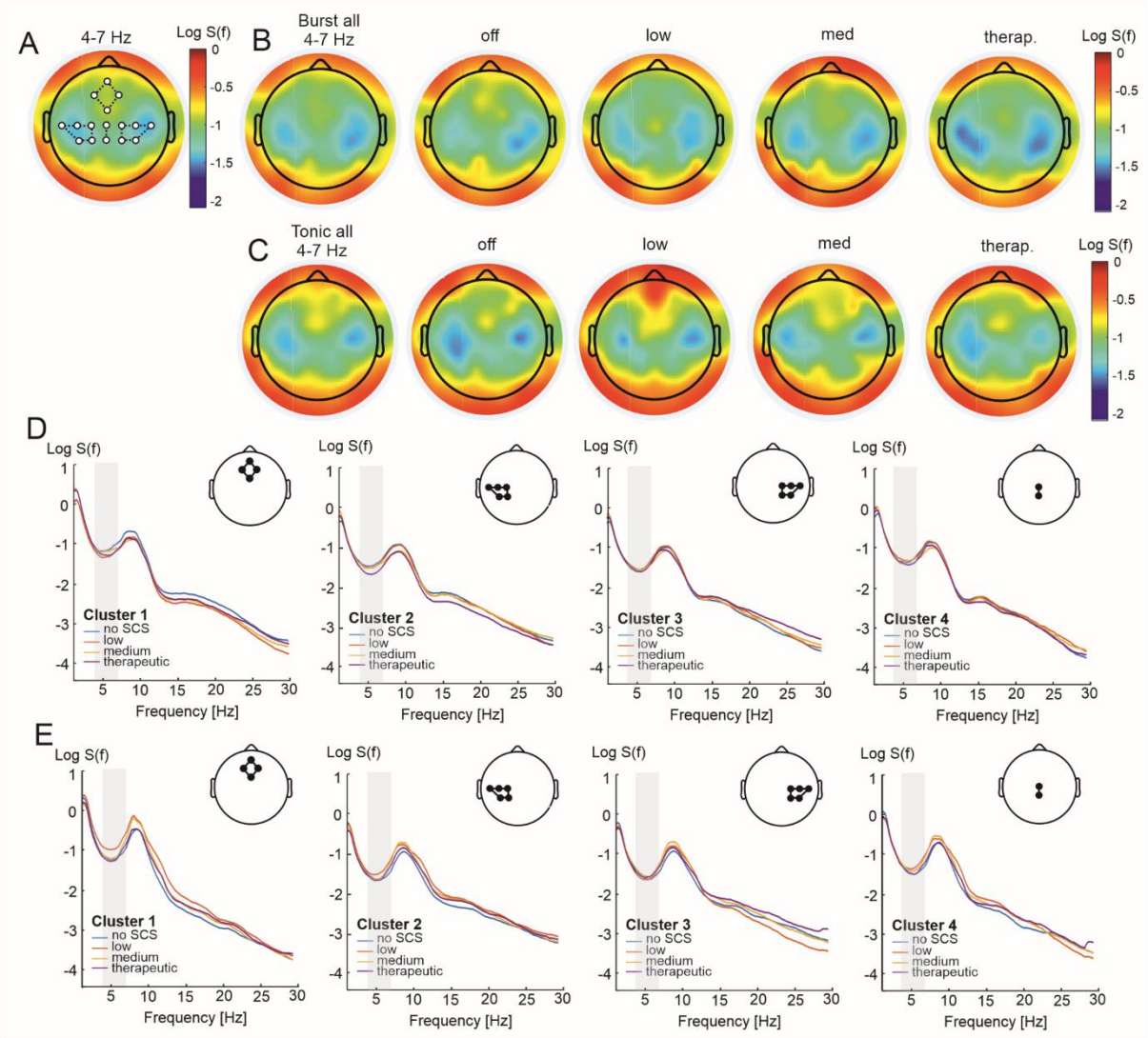

Figure 4.4. Power spectral density in the theta band in patients using burst and tonic SCS during 4 SCS intensities. **A.** Electrodes were selected from grand average topographic plots as areas showing maximal changes in spectral power in the 4–7 Hz theta band. **B.** Topographic plots of 4-7 Hz band

power during 4 intensities of burst SCS. **C.** Topographic plots of 4–7 Hz band power during 4 intensities of tonic SCS. **D.** Power spectral density in all 4 predefined clusters for burst SCS. **E.** Power spectral density in all 4 predefined clusters for tonic SCS.

Band power changes between SCS types were investigated in theta (**Figure 4.4**), alpha (**Figure 4.5**) or beta frequency bands (**Figure 4.6**). The effect of stimulation type in predefined electrode clusters and frequency components were evaluated using unpaired Student t-tests. Statistical probability values were subject to permutation analysis with 2000 permutations and a statistical threshold of $p = .05$. No electrode clusters showed a significant interaction effect in theta, alpha or beta frequency bands.

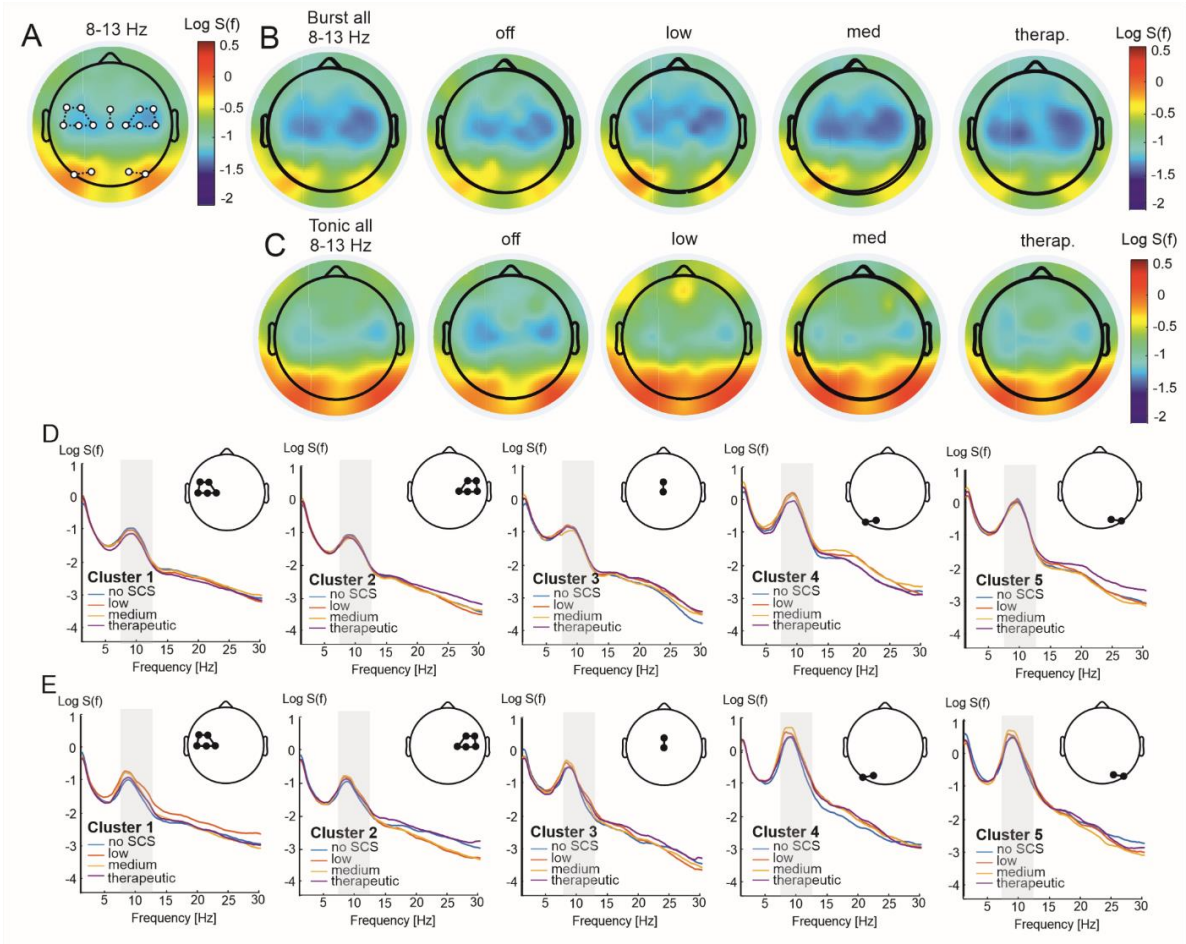

Figure 4.5. Power spectral density in the alpha band in patients using burst and tonic SCS during 4 SCS intensities. **A.** Electrodes were selected from grand average topographic plots as areas showing maximal changes in spectral power in the 8–13 Hz alpha band. **B.** Topographic plots of 8–13 Hz band power during 4 intensities of burst SCS. **C.** Topographic plots of 8–13 Hz band power during 4 intensities of tonic SCS. **D.** Power spectral density in all 5 predefined clusters for burst SCS. **E.** Power spectral density in all 5 predefined clusters for tonic SCS.

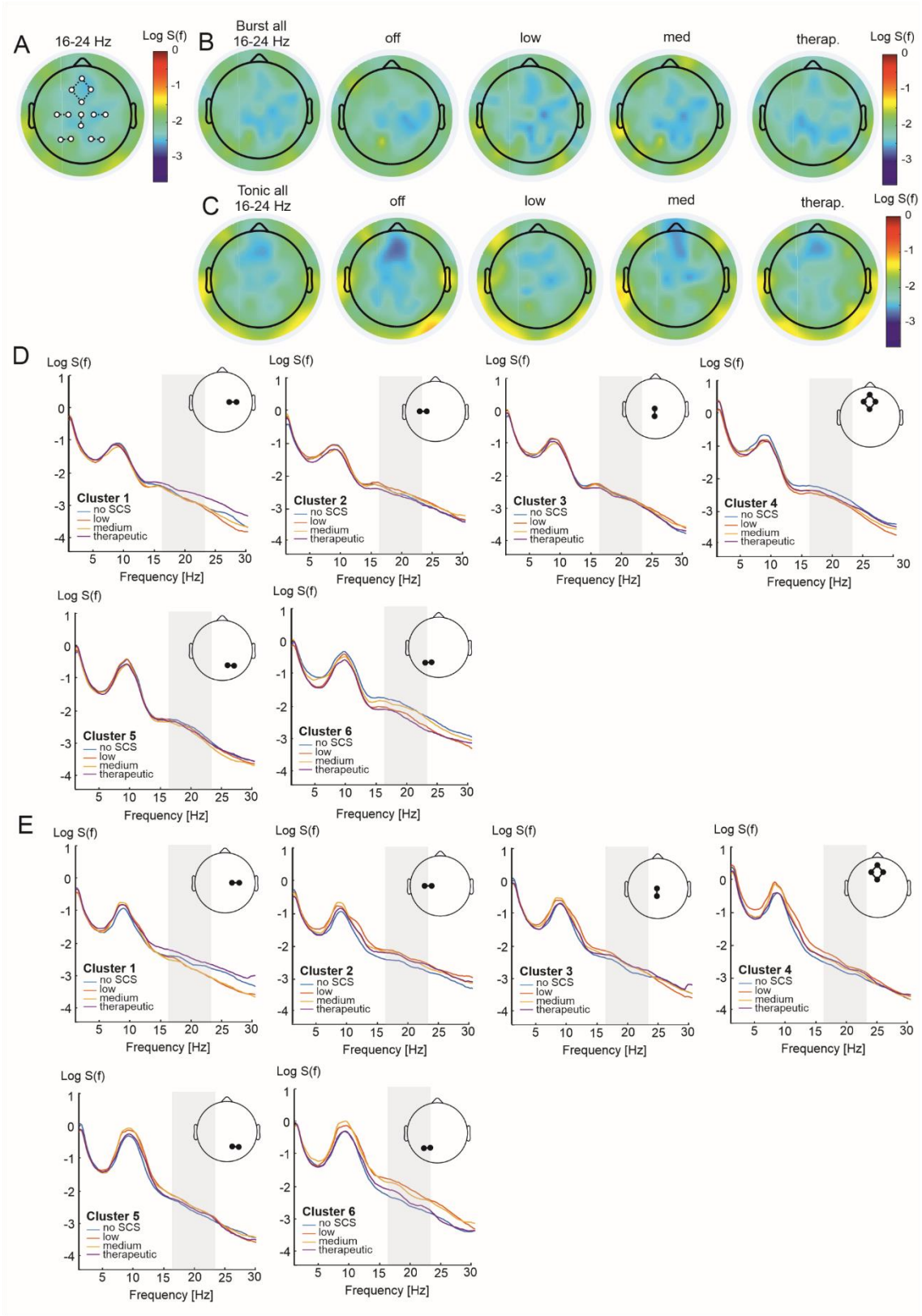

Figure 4.6. Power spectral density in the beta band in patients using burst and tonic SCS during 4 SCS intensities. **A.** Electrodes were selected from grand average topographic plots as areas showing maximal changes in spectral power in the 16–24 Hz beta band. **B.** Topographic plots of 16–24 Hz band power during 4 intensities of burst SCS. **C.** Topographic plots of 16–24 Hz band power during 4

intensities of tonic SCS. **D.** Power spectral density in all 6 predefined clusters for burst SCS. **E.** Power spectral density in all 6 predefined clusters for tonic SCS.

4.4.4 Interaction between SCS Type and Intensity

Electrode clusters showing a significant main effect of SCS intensity were entered into a 2×4 repeated measures ANOVA to investigate an interaction between SCS type and intensity. No electrode clusters showed a significant interaction effect in theta (**Figure 4.4**), alpha (**Figure 4.5**) or beta frequency bands (**Figure 4.6**).

4.5 Discussion

The current study investigated the effects of burst and tonic SCS on the power of resting cortical oscillations at four SCS intensities: low, medium, therapeutic and no stimulation. Significant effects of SCS intensity were found most notably in the beta frequency band (21–24 Hz), with increased band power in right midline electrodes during the strongest, therapeutic intensity compared to lower intensities. Increased alpha band (8–11 Hz) power was observed in posterior parietal electrodes at low and medium intensities compared to no stimulation and therapeutic intensity. No statistically significant changes in band power were found between patients using burst stimulation compared to those using tonic stimulation.

As predicted, therapeutic SCS intensities were associated with greater beta band power compared to lower SCS intensities in right midline electrodes. Sensorimotor beta oscillations, which arise from MI (Salmelin & Hari, 1994c), are associated with sensorimotor processing and integration (Barone & Rossiter, 2021; Guerra et al., 2016). Beta oscillations are tightly linked with inhibitory functions; increased concentrations of GABA increase beta band power over SI/MI during rest (Hall et al., 2010; Jensen et al., 2005; Muthukumaraswamy et al., 2013), after median nerve stimulation (Baker & Baker, 2003) and after motor responses (Muthukumaraswamy et al., 2013), while GABA antagonists reverse the effect (Baker & Baker, 2003). Increased extracellular GABA levels (Cui et al., 1997; Linderoth et al., 1994; Stiller et al., 1996) and decreased intracellular GABA levels (Janssen et al., 2012) are found in the spinal dorsal horn during tonic SCS. Induction of GABA agonists also improves the effectiveness of SCS in patients with chronic neuropathic pain (Lind et al., 2004, 2008;

Schechtmann et al., 2010), supporting an inhibitory role of SCS on spinal transmission. SCS has been shown to reduce intracortical facilitation in excitatory glutamatergic circuits during TMS over the motor cortex in patients with chronic neuropathic pain (Schlaier et al., 2007). Therefore, increased beta at therapeutic SCS intensities suggests greater inhibition or reduced facilitation of sensorimotor processing compared to subtherapeutic intensities.

SCS intensity modulated resting oscillations in the alpha band, with augmented alpha band power in posterior parietal scalp regions at low and medium intensities compared to no stimulation and the therapeutic intensity. The reason for this relationship is unclear but suggest that SCS intensity does not have linear effect on resting cortical oscillations. SCS has previously been shown to inhibit somatosensory processing (Blair et al., 1975; Buonocore et al., 2012; Buonocore & Demartini, 2016; De Andrade et al., 2010; Poláček et al., 2007; Theuvenet et al., 1999; Wolter et al., 2013) and modulate cortical excitability (Bocci et al., 2018; Schlaier et al., 2007). Correspondingly, increased alpha band power suggests decreased cortical excitability or active inhibition of task-irrelevant regions during low and medium SCS intensities (Jensen & Mazaheri, 2010; Klimesch et al., 2007; Pfurtscheller, 2003). It is possible that these oscillatory changes indicate fluctuations in cortical excitability during lower levels of SCS which are abolished at stronger intensities. However, whether this effect is related to the therapeutic benefit of SCS remains to be investigated.

No significant differences in resting oscillations were observed between burst and tonic SCS, although patients using burst stimulation showed lower absolute band power in comparison to those using tonic stimulation. This is contrary to previous studies showing increases in alpha and beta band power in anterior cingulate and prefrontal cortex sources compared to tonic stimulation (De Ridder et al., 2013; De Ridder & Vanneste, 2016). Inconsistencies with previous studies could be due to crucial differences in study design and population. De Ridder et al. (2013) and De Ridder & Vanneste (2016) utilised a within-subjects design during the trial stimulation period in a small group of five patients who were naïve to SCS. In the current study, while only patients with unilateral neuropathic pain were recruited, the causes of pain were heterogenous, and patients had been treated with permanent SCS for varying lengths of time. Differences between burst and tonic SCS have been proposed to reflect greater modulation of the medial pain pathway with burst stimulation (De Ridder et al., 2013; De

Ridder & Vanneste, 2016; Yearwood et al., 2019). However, as the present study found no significant oscillatory changes between stimulation types, it is not known if differences in cortical oscillations are associated with long-term pain relief or if they reflect short-term effects of stimulation.

The absence of a varying effect of intensity on resting oscillations in burst and tonic SCS may indicate a shared mechanism between stimulation types. Shared mechanisms between burst and tonic SCS have been highlighted, with both waveforms modulating theta rhythms in SI, SII and posterior cingulate cortex, and gamma rhythms in the pregenual ACC (De Ridder & Vanneste, 2016). Differences in the effects of intensity by burst and tonic SCS could be anticipated based on the strength-duration curve: the amplitude needed for neural activation in dorsal columns. The strength-duration curve for tonic stimulation has been investigated thoroughly, with stimulation set at an electrical charge which produces optimal paraesthesia perception (Abejón et al., 2015; Miller et al., 2016; Tan et al., 2016). Burst SCS, in comparison, is set below sensory threshold and is not thought to engage the dorsal column pathway (Crosby et al., 2015b; Tang et al., 2014). Stimulation below activation threshold produces no action potentials, despite considerable charge being delivered (Miller et al., 2016). The strength-duration curve is not linear; increases in amplitude produce very slow increases in neural activation followed by sharper increases until the maximal intensity tolerable (Miller et al., 2016). Thus, it is reasonable that intensity may be differentially affected by SCS waveforms. Further investigations with a larger sample could investigate the relationship between tonic and burst SCS whilst matching electrical dose between the two waveforms.

A recent review argued that optimising electrical dose is crucial for effective pain relief with SCS (Chakravarthy et al., 2021). Electrical dose consists of frequency, pulse width and amplitude. SCS with optimised dosing parameters yields significant reductions in back, leg and overall pain, as well as energy savings compared to non-optimised electrical doses (Paz-Solís et al., 2022). The importance of intensity has been recognised with the advent of closed-loop SCS devices which continually vary subject's programmed settings for optimal stimulation (Levy et al., 2019; Mekhail et al., 2020; Pilitsis et al., 2021). This is based on the measurement of evoked compound action potentials, a quantitative measure of spinal recruitment of Aβ fibres in the spinal cord, in order to vary stimulation amplitude in line with postural changes which can affect the amount of charge delivered

to targets (Parker et al., 2012; Pilitsis et al., 2021). Closed-loop SCS systems are in their infancy, but initial studies show increased therapeutic efficacy compared to standard, tonic stimulation (Levy et al., 2019; Mekhail et al., 2020). As burst does not activate Aβ fibres (Crosby et al., 2015b; Tang et al., 2014), it is unlikely to work via this mechanism, although a framework for incorporating closed-loop systems with sub-perception SCS has recently been outlined (Vallejo et al., 2021). In summary, further understanding of the SCS therapeutic window, particularly for paraesthesia-free waveforms, is of vital importance.

A potential limitation of the current study is the short duration between intensity conditions. The washout period of tonic and burst SCS is poorly understood, and may differ according to stimulation type (Meuwissen et al., 2018) or stimulus energy (Abejón et al., 2015; Miller et al., 2016). To take this into account, SCS intensities were varied between participants and followed by a short wash-out period of no stimulation. Another drawback of the current study is related to the intrinsic differences between stimulation types. While participants were unaware of the SCS intensity during the recording, patients using tonic stimulation would have had greater awareness of therapeutic intensities due to the presence of paraesthesia, compared to patients using sub-perception burst stimulation. This limitation has been recognised in previous investigations, particularly in randomised controlled trials with tonic stimulation where blinding of patients is challenging (reviewed in Duarte et al., 2020). However, due to the lack of a statistically significant difference in cortical oscillatory activity between burst and tonic stimulation, the results do not appear to have been influenced by the presence of paraesthesia.

SCS is an effective, yet often last-option, treatment for chronic neuropathic pain. Technological advances and new waveforms are providing further insights into the mechanisms underlying the therapeutic effects of SCS. Results suggest that SCS intensity has a nonlinear effect on somatosensory processing, with greater intensities sufficient to achieve a therapeutic benefit facilitating and inhibiting sensorimotor cortices. Future studies should seek to clarify if cortical oscillatory changes during SCS correlate with symptom relief.

Chapter 5

Effects of Burst and Tonic Spinal Cord Stimulation Intensity on Neural Responses to Innocuous Brushing Stimuli in Neuropathic Pain

Danielle Hewitt[1], Adam Byrne[1,2], Jessica Henderson[1], Kathryn Wilford[3], Rajiv Chawla[3], Manohar Lal Sharma[3], Bernhard Frank[3], Christopher Brown[1], Nicholas Fallon[1], Andrej Stancak[1]

[1] Department of Psychological Sciences, University of Liverpool, Liverpool, UK.

[2] Institute for Risk and Uncertainty, University of Liverpool, Liverpool, UK.

[3] The Walton Centre NHS Foundation Trust, Liverpool, UK.

This experiment investigated the effect of burst and tonic SCS intensities on cortical oscillations during dynamic brushing stimulation in patients with chronic neuropathic pain.

This paper has been submitted for publication in Neuromodulation. The format of the text has been modified to match the style of this thesis.

The roles of the co-authors are summarised below:

Danielle Hewitt: Conceptualisation, Methodology, Software, Investigation, Formal analysis, Writing - Original Draft, Writing - Review & Editing. **Adam Byrne:** Investigation, Writing - Review & Editing. **Jessica Henderson:** Investigation, Writing - Review & Editing. **Kathryn Wilford:** Resources. **Rajiv Chawla:** Resources. **Manohar Lal Sharma:** Resources. **Bernhard Frank:** Conceptualisation, Resources, Funding acquisition. **Nicholas Fallon:** Conceptualisation, Writing - Review & Editing. **Christopher Brown:** Conceptualisation, Writing - Review & Editing. **Andrej Stancak:** Conceptualisation, Software, Formal analysis, Writing - Original Draft, Writing - Review & Editing, Supervision, Funding acquisition.

5 Effects of Burst and Tonic Spinal Cord Stimulation Intensity on Neural Responses to Innocuous Brushing Stimuli in Neuropathic Pain

5.1 Abstract

SCS is an effective treatment for intractable neuropathic pain. One mechanism underlying pain relief during SCS may be the inhibition of somatosensory processing by concurrent impulses in the dorsal column. However, the mechanisms underlying burst SCS and the effect of SCS intensity are poorly understood. We investigated the effect of varying intensities of burst and tonic SCS on cortical oscillatory responses to brushing.

Twenty patients using SCS (11 burst, 9 tonic) for unilateral neuropathic leg pain participated. Brushing was administered to a pain-free leg during four SCS intensities: therapeutic (100%), medium (66%), low (33%), and no stimulation. Whole-brain EEG was continuously recorded. Changes in spectral power during brushing were evaluated using the ERD method in alpha (8-13 Hz), beta (16-24 Hz) and theta (4-7 Hz) frequency bands. Repeated-measures ANOVAs assessed changes in ERD between patients using burst or tonic SCS at each of the four SCS intensities.

Brushing was accompanied by ERD in frequencies between 4-24 Hz. Patients using tonic SCS showed attenuated ERD over right sensorimotor electrodes in the theta band, and over right frontal and left sensorimotor electrodes in the alpha band, compared to burst SCS. Conversely, a greater reduction of brushing-related ERD was observed in burst SCS in left frontal electrodes in the alpha band compared to tonic SCS. Stronger intensities of burst and tonic SCS diminished ERD in theta and alpha bands in parietal electrodes, and in central electrodes in the beta band, with the strongest suppression at medium intensity.

Results suggest that burst and tonic SCS are mediated by both different and shared mechanisms. Attenuated brushing-related ERD with tonic SCS suggests a gating of cortical activation by afferent impulses in the dorsal column, while burst may engage different pathways. Shared mechanisms of reduced brushing-related ERD at stronger intensities points towards a nonlinear effect of SCS on somatosensory processing.

5.2 *Introduction*

SCS is a palliative neurostimulation treatment for the relief of intractable neuropathic pain. SCS is a cost-effective (Farber et al., 2017) method to reduce neuropathic pain (Duarte et al., 2020; Kriek et al., 2017; Visnjevac et al., 2017) and improve quality of life (Amirdelfan et al., 2018; Eldabe et al., 2010; Scalone et al., 2018; Visnjevac et al., 2017). However, only 62% of patients who undergo permanent SCS implantation experience adequate pain relief (Taylor et al., 2014), and an estimated 30% of all implanted devices are removed (Simopoulos et al., 2019). The reason for ineffectiveness could be, in part, due to our limited understanding of the therapeutic mechanisms of SCS.

SCS was originally developed as a direct application of the Gate Control Theory (Melzack & Wall, 1965), whereby antidromic activation of Aβ fibres in the dorsal column close a spinal "gate" to inhibit the transmission of nociceptive input, and orthodromic activation of Aβ fibres results in paraesthesia in the painful area (Holsheimer, 2002; Joosten & Franken, 2020; Melzack & Wall, 1965; Shealy et al., 1967). Accordingly, tonic SCS suppresses the transmission of nociceptive signals from wide dynamic range cells (Yakhnitsa et al., 1999) through the release of gamma-aminobutyric acid (GABA) in the dorsal horn (Cui et al., 1997). Enhanced GABA concentrations during SCS have been found alongside reduced tactile allodynia in neuropathic pain models (Stiller et al., 1996; Wallin et al., 2002), and administration of $GABA_B$ agonists can improve the response to tonic SCS in rats (Cui et al., 1998; Wallin et al., 2002) and humans (Lind et al., 2004, 2008; Schechtmann et al., 2010). Taken together, the literature suggests that tonic SCS works by gating the transmission of noxious stimuli.

Conventional tonic SCS utilises continuous repetitive electrical pulses (20–100 Hz) administered to the spinal cord using epidurally placed electrodes powered by a battery. Recent technological advances have resulted in novel stimulation paradigms such as high frequency and burst stimulation. Burst SCS, in particular, utilises trains of 5 monophasic pulses, with an intraburst frequency of 500 Hz and interburst frequency of 40 Hz (De Ridder et al., 2010, 2013, 2020). Burst SCS has been shown to match or exceed the effectiveness of conventional tonic stimulation (De Ridder et al., 2013; de Vos et al., 2014; Deer et al., 2018; Schu et al., 2014). Improved efficacy may be due to differences in the underlying mechanisms between waveforms. As burst is set below

perceptual threshold, it does not produce paraesthesia and may not activate Aβ afferents in the dorsal column (Tang et al., 2014). Furthermore, while both burst and tonic SCS reduce spinal neuronal firing (Tang et al., 2014), burst SCS does not act via spinal GABAergic mechanisms (Crosby et al., 2015b). Therefore, there is evidence that the spinal mediators of burst SCS differ from tonic stimulation.

The intensity of SCS may interact with its effect on somatosensory processing. Stimulation intensity or amplitude influences the number of fibres recruited by stimulation, and is one of multiple parameters that determines electrical charge transfer (Miller et al., 2016). Electrical charge transfer has been shown to be a critical factor in SCS effectiveness, as increased intensity is associated with reduced neuronal firing to noxious stimuli and nonlinear increases in the responsiveness of wide dynamic range neurons for burst SCS (Crosby et al., 2015a), and a greater reversal of nociceptive behaviours in animal studies with tonic SCS (Sato et al., 2014; Yang et al., 2014). In an early electrophysiological study, Blair et al. (1975) reported selective amplitude decreases of late SEP components at minimal therapeutic intensities, with higher intensities abolishing SEPs entirely. However, it is not known how intensity may affect somatosensory processing during burst SCS.

EEG can be used to investigate changes in ongoing neural activity. Increased power has been reported in patients with chronic pain in theta (4–7 Hz) (Lim et al., 2016; Sarnthein et al., 2006; Stern et al., 2006; Vučković et al., 2014), alpha (8–13 Hz) (Kisler et al., 2020; Sarnthein et al., 2006; Vučković et al., 2014), beta (16–30 Hz) (Lim et al., 2016; Sarnthein et al., 2006; Stern et al., 2006), and delta (1–4 Hz) frequency bands (Sarnthein et al., 2006). Augmented theta and beta power in chronic pain patients compared to healthy controls have been localised to pain-associated areas including the insula, ACC, prefrontal cortex, SI and SII (Fallon et al., 2018; Lim et al., 2016; Stern et al., 2006). Successful SCS treatment is associated with reduced theta power in neuropathic pain models (Koyama et al., 2018) and in humans (Schulman et al., 2005; Sufianov et al., 2014). Alterations in oscillatory power have been observed between different SCS waveforms; burst SCS was associated with increased low alpha band power (8–10 Hz) in sources localised to the dorsal ACC, and increased alpha and beta band power (18.5–30 Hz) in the prefrontal cortex, compared to tonic stimulation (De Ridder et al., 2013; De Ridder & Vanneste, 2016). Greater activation of the ACC has led to the suggestion that burst SCS modulates affective, motivational aspects of pain via

engagement of the medial pain pathway (De Ridder et al., 2013; De Ridder & Vanneste, 2016; Yearwood et al., 2019). This suggests that alterations in neural oscillatory power may have clinical relevance for the treatment of chronic pain with SCS.

Processing of sensory, cognitive, or motor stimuli can result in relative decreases or increases in EEG oscillatory power in given frequency bands. Decreases in oscillatory power, known as ERD, are related to states of activation within the sensorimotor system (Pfurtscheller, 1977; Pfurtscheller & Aranibar, 1977). Comparatively, increases in oscillatory power, ERS, are related to idling of a cortical area (Pfurtscheller, 1992) or cortical inhibition (Salmelin & Hari, 1994a). Presence of alpha and beta ERD over contralateral and ipsilateral SI/MI has been shown during tactile brushing stimuli (Cheyne et al., 2003; Fallon et al., 2013; Gaetz & Cheyne, 2006), as well as electrical (Hirata et al., 2002; Lemm et al., 2009; Nikouline et al., 2000; Pfurtscheller et al., 2002; Stancak et al., 2003) and vibrotactile stimulation (Bardouille et al., 2010). The effects of SCS on ERD have yet to be investigated, however, tonic SCS has been shown to inhibit somatosensory processing of innocuous nerve stimulation (Blair et al., 1975; Buonocore et al., 2012; Buonocore & Demartini, 2016; De Andrade et al., 2010; Poláček et al., 2007; Theuvenet et al., 1999; Wolter et al., 2013). Due to differences in the spinal mechanisms between tonic and burst SCS, there may be differences in the pattern of ERD reflecting differences in cortical activation during stimulation.

The current study sought to investigate the effects of SCS on amplitude changes of cortical oscillations evaluated using the ERD method during brushing of the leg. Specifically, the study aimed to investigate whether somatosensory ERD evoked during brushing in theta (4–7 Hz), alpha (8–12 Hz) or beta (16–24 Hz) frequency bands would be diminished during SCS, and if differences in ERD would be found between tonic and burst stimulation. Secondly, the study aimed to investigate the effect of SCS intensity on ERD during brushing at four intensities: low, medium, therapeutic, and off. We predicted that somatosensory ERD in alpha and beta frequency bands would be present during brushing when SCS was off, and ERD would diminish with increasing stimulation intensity. Due to the previous evidence of differences between SCS types, with burst SCS predominantly engaging the medial pain system (De Ridder & Vanneste, 2016; Yearwood et al., 2019), we hypothesized that

differences between tonic and burst SCS in brushing-related ERD would be found in frontal and midline regions.

5.3 Methods

5.3.1 Subjects

Twenty-one patients with unilateral neuropathic lower limb pain were recruited from The Walton Centre NHS Foundation Trust, Liverpool, UK. All participants had previously been implanted with Abbott (Texas, USA) spinal cord stimulators in conventional tonic (N=10) or burst waveforms (N=11). One subject was excluded due to incomplete data. The final sample included 20 participants (11 females) with a mean age of 52.5 ± 12.3 years (mean ± SD). The procedure used was approved by the Liverpool Central North West Research Ethics Committee, and all participants gave fully informed written consent at the start of the experiment in accordance with the Declaration of Helsinki. Participants were reimbursed with £40 for their time and inconvenience on completion of the study.

Patient characteristics are summarised in ***Table 5.1***. All patients fulfilled criteria for neuropathic pain, determined by the Neuromodulation team prior to permanent implantation of SCS devices at The Walton Centre NHS Foundation Trust. Mean duration of SCS implant was 17.85 months, and mean duration of symptoms was 124.90 months. A one-way ANOVA showed that there was no significant difference of symptom duration ($F(1,19) = .09$, $p > .05$) or SCS duration ($F(1,19) = 2.36$, $p > .05$) between patients using Burst and Tonic SCS. Target stimulation amplitude was available for 10 patients and ranged from 0.2–6.3 mA. Analgesic medications were not withdrawn prior to participating; 15 patients were using pain medication, with 13 patients using 2 or more pain medications.

Table 5.1. Clinical patient characteristics for Study 2.

ID	Age	Sex	Diagnosis	Pain Duration	SCS Type	SCS Duration	Lead	Lead location	IPG	Freq (Hz)
1	63	F	Neuropathic radicular right leg pain	228	Burst	30	Octrode	T10–T12	Prodigy	40
2	46	F	Neuropathic right leg pain secondary to MS	108	Burst	29	Lamitrode Tripole	T10–T12	Prodigy	40
3	68	F	Bilateral neuropathic leg secondary to MS	168	Burst	48	Octrode x2	T9–T11	Prodigy	40
4	59	M	Neuropathic radicular left leg pain	48	Tonic	2	Lamitrode Tripole	T9–T10	Prodigy	40
5	53	M	Bilateral lower limb neuropathic pain	267	Tonic	2	Lamitrode Tripole	T9–T10	Prodigy MRI	40
6	52	M	Bilateral neuropathic leg pain secondary to MS	60	Burst	30	Lamitrode Tripole	T10–T12	Prodigy	40
7	61	F	Neuropathic bilateral leg pain	84	Tonic	1	Octrode	T9–T12	Prodigy	30
8	50	F	Right foot CRPS	26	Tonic	50	Octrode x 2	T9–T11	Prodigy	50
9	76	M	Neuropathic right foot pain	96	Tonic	47	Lamitrode Tripole	T12–L1	Prodigy	60
10	50	M	Neuropathic radicular left leg pain	84	Burst	1	Octrode	T9–T11	Prodigy	40
11	39	M	Neuropathic left foot and ankle pain	84	Burst	1	Octrode x 2	T8–T11	Prodigy	40
12	37	F	Neuropathic radicular left leg pain	60	Tonic	16	Octrode x 2	T8–T11	Prodigy	50
13	30	F	Neuropathic radicular left leg pain	72	Tonic	1	Lamitrode Tripole	T8–T9	Prodigy	40
14	55	F	Neuropathic left foot and ankle pain	240	Burst	24	Octrode	T10–T12	Prodigy	40
15	75	F	Neuropathic radicular left leg pain	420	Burst	8	Octrode x 2	T8–T12	Prodigy	40
16	52	M	Neuropathic radicular left leg pain	192	Burst	12	Lamitrode Tripole	T9–T10	Prodigy	40
17	52	F	Neuropathic radicular left leg pain	60	Burst	12	Octrode x 2	T9–T12	Prodigy	40
18	52	F	Neuropathic radicular left leg pain	48	Burst	12	Octrode x 2	T8–T10	Prodigy	44
19	36	F	Left foot and ankle CRPS-II	66	Burst	12	Octrode	T10–T12	Prodigy	40
20	44	M	Neuropathic radicular right leg pain	96	Tonic	19	Octrode	T10–T12	Prodigy	50

Pain duration and SCS duration measured in months. IPG = implantable pulse generator. Freq = frequency in hertz (Hz).

5.3.2 Experimental protocol

Experimental procedures were carried out in a single 2-hour session in the Pain Research Laboratory, Pain Relief Institute, Aintree University Hospital NHS Foundation Trust (Liverpool, UK). Participant's spinal cord stimulators were turned off from the time of arrival until the experiment began while EEG was applied to the head, a duration of approximately 40 minutes.

During the experiment, participants were seated in a comfortable armchair with legs raised at a 45-degree angle. The experiment consisted of 4 blocks, each consisting of 40 cycles of 4 seconds of mechanical brush stimulation followed by 4 seconds of rest. During brush periods, the experimenter manually applied brushing to the participant's pain-free leg at an approximately 45-degree angle. Brush strokes consisted of one continuous motion for 10 cm along the tibialis anterior muscle, starting at one-third of the distance between the patella and the lateral malleolus, at a rate of 5 cm/s for 2 seconds. Brushing direction was reversed was returned to the starting point using the same speed and pressure. The brush was removed during the rest period. The brush was a synthetic soft-bristled paintbrush with bristles measuring 4cm long, 6.5 cm wide and 2 cm deep (total length: 20.5 cm) which produced a distinct but painless tactile sensation. At the start and end of each block were 30-seconds of rest with no stimuli. Throughout the experiment, the times to start and stop brushing were controlled using a continuous metronome audio clip played to the experimenter through noise-cancelling headphones, which corresponded to EEG stimulus onset and offset triggers.

Each block of brushing was varied by SCS intensity as determined using the patient programmer, at the standard therapeutic intensity, low (33% of the therapeutic level), medium (66% of the therapeutic level), and no stimulation. The order of blocks was varied pseudo-randomly for each participant. After each block, SCS was turned off for two minutes. During this time, participants were asked to rate the intensity and uncomfortableness of the brushing stimuli on a numeric rating scale, from no sensation (0) to maximum sensation imaginable (intensity) or maximum uncomfortableness (100). Participants were also asked to indicate if the brushing was painful. The experiment lasted approximately 25 minutes.

After the tasks, clinical data including age, duration of pain and duration of SCS treatment were collected verbally from patients. Patients self-completed the Neuropathy Pain Scale by hand or using a tablet. Pain diaries were collected for 7 days following the visit to assess average and worst daily pain scores using a visual analogue scale from no pain (0) to worst imaginable pain (10). Patient diagnosis and SCS parameters were confirmed by a clinician.

5.3.3 EEG acquisition

Whole-scalp EEG was continuously recorded using a 63-channel system (BrainProducts GmbH, Munich, Germany). Actively shielding Ag-AgCl electrodes were mounted on an electrode cap (actiCap snap, BrainProducts) according to the International 10–20 system (Jasper, 1958). The cap was aligned with respect to three anatomical landmarks of two preauricular points and the nasion. Electrolyte gel was applied to achieve electrode-to-skin impedances of below 50 kΩ throughout the experiment. A recording band-pass filter was set at 0.001–200 Hz with a sampling rate of 1000 Hz. Electrode FCz was used as a reference electrode, and electrode FPz was used as the ground electrode. EEG average reference was applied, and signals were digitised at 1 kHz with a BrainAmp DC amplifier (actiChamp), connected to BrainVision Recorder 2.0 running on a Windows 10 laptop.

5.3.4 Spectral analysis of EEG signals

EEG data were processed using EEGLab (Delorme & Makeig, 2004) and FieldTrip (Oostenveld et al. (2011): http://fieldtriptoolbox.org). Continuous EEG data during brushing were split into 8-second epochs (4 seconds rest and 4 seconds brushing). Data were re-referenced to the common average (Lehmann, 1987) and filtered using 1 Hz high pass and 100 Hz low pass filters. For each participant, data were visually inspected for movement and muscle artefacts. Epochs containing motion, electrode or muscle artefacts were marked and excluded from further analysis. Electrode channels with large artefacts were interpolated to a maximum of <10% electrodes. The average number of epochs remaining after artefact correction for each condition were: no stimulation 33 ± 4, low intensity 34 ± 3, medium intensity 34 ± 3, therapeutic intensity 34 ± 4. A repeated measures ANOVA showed that the number of accepted trials was not significantly different between SCS intensity conditions ($F(3,54) = 0.82$, $p = .491$) or between SCS type ($F(1,18) = 0.09$, $p = .771$).

The power spectra were computed in FieldTrip using a discrete Fourier time-frequency transformation. Power spectral densities were computed using Welch's method from 1 second overlapping segments after tapering data to 1024 points. Data were smoothed using a Slepian sequence 4 Hz window prior to Fourier transformation. The spectral window was shifted in 0.1 second intervals to yield a power time series of 80 points, representing the interval from -4 to 4-seconds from the onset of brushing. Spectral power was estimated in the range 1–100 Hz with a frequency resolution of 0.977 Hz. Due to the presence of SCS artefacts due to stimulation frequencies between 40–60 Hz (see Table 1), only frequency components between 1–30 Hz were considered for statistical analysis. Relative power was evaluated using the classical ERD transformation (Pfurtscheller & Aranibar, 1979):

$$D\% = \left(100 * \frac{A - R}{R}\right)$$

where *D* represents the percentage power change during epochs following the onset of brushing *(A)* relative to a preceding baseline or reference period *(R).* Positive *D* values correspond to relative power decreases, considered to signify cortical activation (Pfurtscheller, 1977; Pfurtscheller & Aranibar, 1977). Negative *D* values correspond to increases of cortical band power and event-related synchronisation (Pfurtscheller, 1992).

5.3.5 Statistical analysis of subjective ratings

Mean subjective intensity and discomfort ratings of brushing stimuli in each condition were calculated for each participant. A 2×4 repeated measures analysis of variance (ANOVA) was computed using SPSS v. 25 (IBM Inc., USA), with independent variables of SCS Type (tonic or burst SCS) and Intensity (no stimulation, low, medium or therapeutic SCS intensity). Post-hoc t-tests were used where appropriate to follow up significant main effects.

5.3.6 Statistical analysis of EEG data

Individual and grand average topographic plots were visual inspected to identify electrodes showing prominent ERD during brushing. Grand average time-frequency plots from electrodes of interest were used to determine frequency bands showing ERD during brushing in the range 1–30 Hz. The peri-stimulus brushing interval was split into seven 0.5 second time windows from 0–3.5

seconds. For each frequency band, one-way repeated measures ANOVAs were computed to investigate the effect of SCS intensity across every electrode and time bin of interest. To control for Type I error likely to occur due to the large number of ANOVAs, the resulting statistical probability values were subject to permutation analysis using *statcond.m* with 1000 permutations.

Electrodes that exceeded a predefined threshold on the calculated *p*-values ($p < .05$) for the main effect of Intensity were entered into univariate t-tests to check that band power differed significantly from zero. Electrodes that surpassed permutation testing and t-tests were selected for further analysis and clustered based on spatial adjacency. Pairwise comparisons were computed to further investigate significant main effects. The Huynh-Feldt correction was used to tackle any violation of sphericity. Similarly, the effects of type of stimulation at each electrode and in each time bin were evaluated using unpaired Student's t-test with a corrected probability value of $p = .05$. Electrodes showing a significant main effect of SCS type or intensity were entered into mixed methods ANOVAs to analyse the presence of an interaction between conditions.

5.4 Results

5.4.1 Subjective reports

Patient's level of pain on the day of the experiment was collected using the Neuropathy Pain Scale. Patients reported a mean pain score of 45.7 ± 18.2 out of a maximum 100 points. A one-way ANOVA showed no significant difference in neuropathic pain scores between patients using burst and tonic SCS ($F(1, 19) = .049$, $p > .05$). In the 7 days following the experiment, pain diaries were collected. Five patients did not complete the pain diaries. In the completed diaries, mean average daily pain was 5.1 and mean strongest pain was 6.4 out of 10 (maximum pain). A one-way ANOVA showed no significant difference between mean average ($F(1, 13) = 4.3$, $p > .05$) and strongest ($F(1, 13) = 4.2$, $p > .05$) pain ratings between patients using burst and tonic SCS.

Two out of 20 patients reported pain resulting from brushing stimuli. Mean intensity (0–100) of brushing after each block was 31.94 ± 24.07, where 100 indicated the strongest sensation. A repeated-measures ANOVA showed no significant difference in reported brushing intensity between SCS intensity conditions ($F(3,54) = 1.27$, $p > .05$) or SCS type ($F(1,18) = 0.731$, $p > .05$). Mean uncomfortableness (0–100) during each block of brushing stimuli was 4.05 ± 11.12 out of 100. A

repeated-measures ANOVA showed no significant difference in discomfort during brushing between SCS intensity conditions ($F(3,54) = 2.01$, $p > .05$) or SCS type ($F(1,18) = 1.38$, $p > .05$), indicating that brushing was generally perceived as mild and not unpleasant, and subjective ratings were not affected by SCS type or intensity condition.

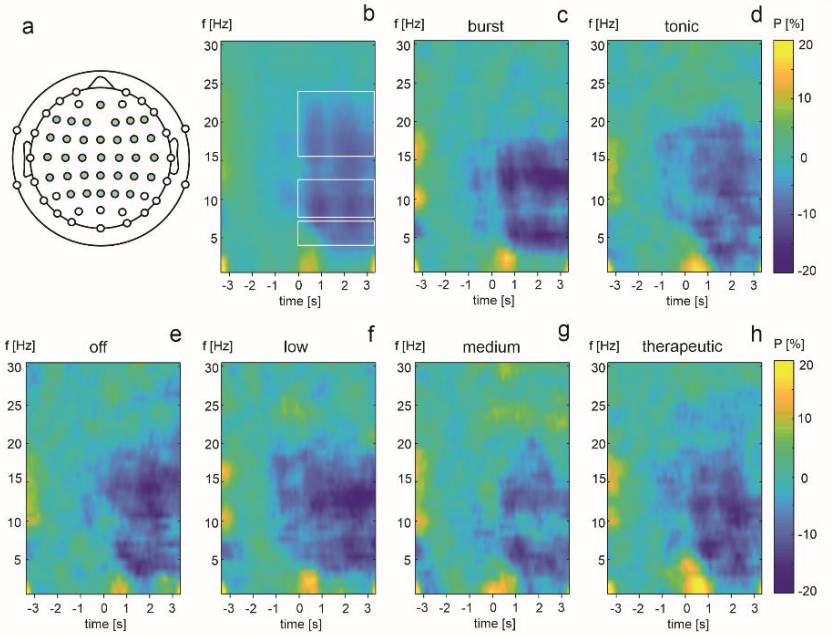

Figure 5.1. Electrodes of interest (a) and grand average time-frequency plot (b) showing brushing-related ERD between 4-24 Hz and frequency bands chosen for analyses. Time-frequency plots for burst (c) and tonic (d) SCS conditions, and each SCS intensity condition (e-h), are shown. Colour bar indicates percentage power change from baseline, with positive values indicating ERS, and negative values indicating ERD.

5.4.2 ERD during brushing

After visual inspection of individual and grand average topographic plots across all 63 electrodes, a set of 33 electrodes overlying frontal, central and parietal regions of scalp were selected (***Figure 5.1***A) to visualise the time-frequency plots in both SCS types (burst and tonic) and four SCS intensities (no stimulation, low, medium and therapeutic). The grand average time-frequency plot across all frequency components in the range 1−30 Hz (***Figure 5.1***B) showed band power decreases concentrated between 4 to 24 Hz. A qualitative comparison of time-frequency in burst and tonic SCS (***Figure 5.1***C-D) showed a similar distribution of ERD in both types of SCS, although burst SCS showed band power decreases focused around 5 Hz and 13 Hz, while tonic SCS showed a more widespread pattern of band-power reduction. ***Figure 5.1***E-H show the time-frequency plots of EEG

signals throughout the electrodes of interest (***Figure 5.1***A) in no stimulation, low, medium and therapeutic intensities of SCS. Visual analysis of time frequency plots revealed robust ERD in the frequency range of 4−24 Hz in all four SCS intensity conditions. Medium SCS intensity showed the weakest ERD during brushing, particularly at 10 Hz.

To quantify the band-power changes in both types of SCS and across four intensity conditions, ERD was computed in the frequency bands 4−7 Hz, 8−13 Hz and 16−24 Hz. These bands cover the patterns of ERD in all conditions (***Figure 5.1***B-H) and accord to previous studies reporting prominent ERD in alpha- and beta bands during brushing (Cheyne et al., 2003; Fallon et al., 2013; Gaetz & Cheyne, 2006) and altered resting 4−7 Hz oscillations in chronic pain conditions (Fallon et al., 2018; Sarnthein et al., 2006; Stern et al., 2006; Vučković et al., 2014). The ERD curves in the selected frequency bands were divided into seven 0.5 s time bins covering the peri-stimulation period from 0 to 3.5 s.

5.4.2.1 Effect of SCS type

The effect of stimulation type in all electrodes and time bins were evaluated using unpaired Student's t-test with a corrected probability value of $p = .05$.

In the 4–7 Hz band, burst SCS produced an overall larger brushing-related ERD across the right sensorimotor and midline electrodes compared to tonic SCS (***Figure 5.2***A). Burst and tonic SCS differed statistically in a cluster of two electrodes overlaying the right sensorimotor cortical area during the final period of brushing ($t(18) = -2.31$, $p = .03$; ***Figure 5.2***B-D). This difference was related to a comparatively weak band-power decrease in tonic SCS. Of note, while only the final time bin (3−3.5 s) reached statistical significance, the divergent time courses of band power in burst and tonic stimulation started 1 second earlier.

In the 8–13 Hz band, burst SCS, unlike tonic SCS, produced a widespread ERD when the brush touched the leg across the posterior parietal and right central and frontal electrodes (***Figure 5.2***E). According to the statistical analysis, burst and tonic SCS differed in brushing-induced 8–13 Hz band power changes in right frontal and left parietal electrodes during the initial period of brushing (0–0.5 s) (***Figure 5.2***F−H and J−K). Both electrodes showed a comparatively weak band-power decrease in tonic compared to burst SCS ($t(18) = -2.62$, $p = .017$; $t(18) = -2.83$, $p = .011$).

Contrastingly, burst and tonic SCS differed in left frontal central electrodes (***Figure 5.2***F), with statistically significant reduced band power in tonic compared to burst SCS (t(18) = -2.34, p = .031; ***Figure 5.2***I and L).

There was no statistically significant difference between burst and tonic SCS in any electrode or time bin in the 16–24 Hz band.

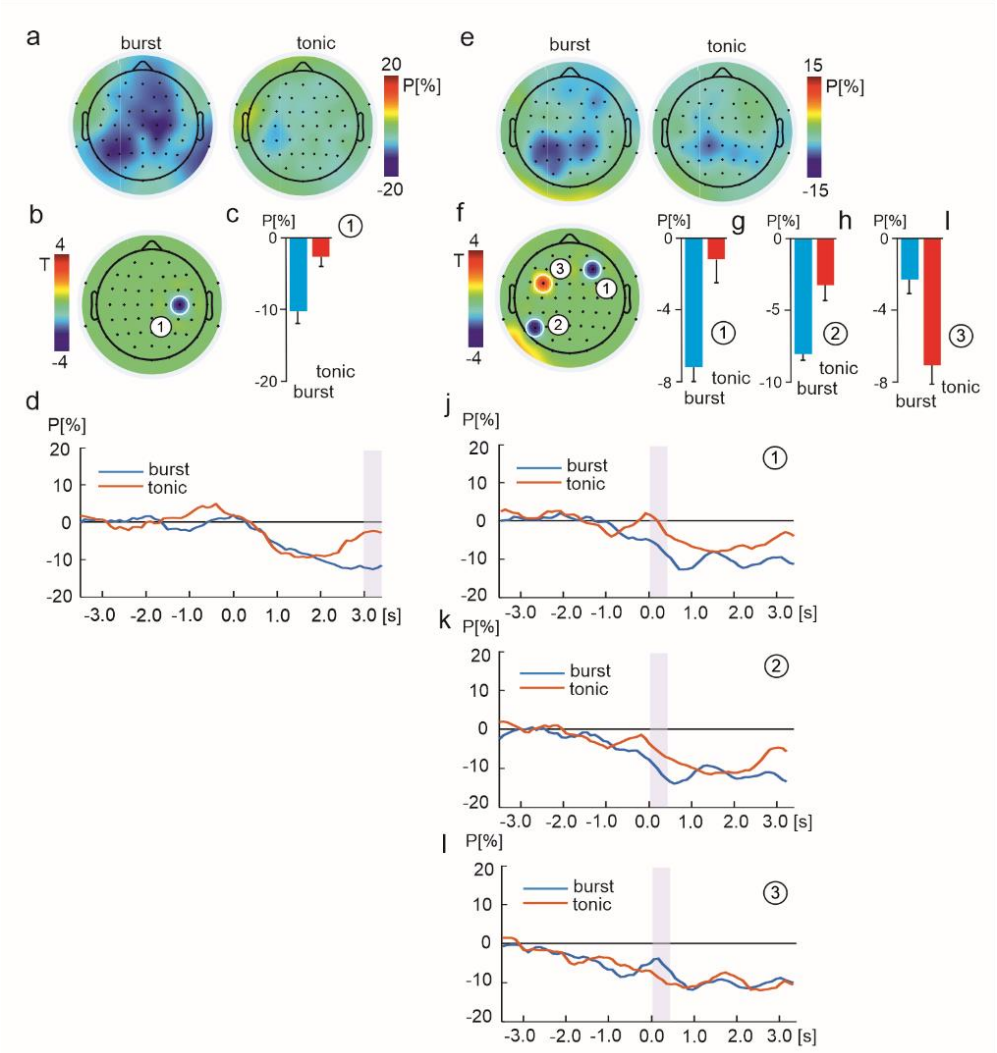

Figure 5.2. Effect of stimulation type on brushing-related ERD in theta (a-d) and alpha (e-l) frequency bands. Topographic maps (a, e) show ERD over the scalp in patients using tonic and burst SCS. Electrodes exceeding permutation test for significance are indicated and electrode clusters numbered (b, f). Bar graphs show percentage power change between stimulation types in the corresponding electrode cluster and time bin. Time courses of theta and alpha band power during brushing are shown for the corresponding electrode cluster, with statistically significant time bins highlighted.

5.4.2.2 Effect of SCS intensity

The effect of intensity was evaluated separately for each frequency band using repeated measures ANOVAs, which were carried out in all electrodes and time bins. Statistical probability values were subject to permutation analysis with 1000 permutations and a statistical threshold of p = .05.

In the 4−7 Hz band, a repeated measures ANOVA showed amplitude changes in a frontal midline and right parietal electrode in the latency epoch 0.0−0.5 s, when the brush first touched the leg (***Figure 5.3***A−F).

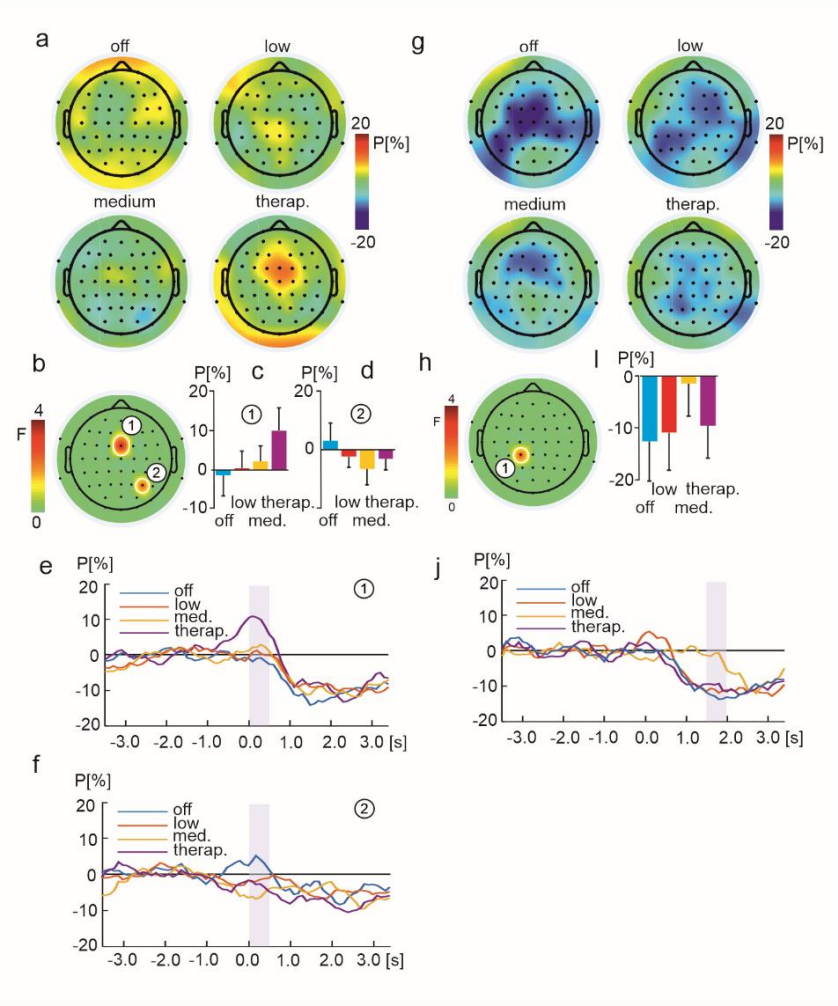

Figure 5.3. Effect of SCS intensity on brushing-related ERD in theta frequency band in time bins 0-0.5s (a-f) and 1.5-2 s (g-j). Topographic maps (a, g) show ERD over the scalp in each SCS intensity for the respective time bin. Electrodes exceeding permutation test for significance are indicated and electrode clusters numbered (b, h). Bar graphs show percentage power change between stimulation intensities in the corresponding electrode cluster and time bin. Time courses of theta band power during brushing are shown for the corresponding electrode cluster and time bin, with statistically significant time bins highlighted.

The strongest, most statistically significant effect of stimulus intensity was seen in the frontal midline electrode ($F(3,57) = 4.22$, $p = .009$, $\varepsilon = 1.0$). This effect was due to a 1 second band power increase at the onset of brushing under the strongest therapeutic intensity of SCS compared to lower SCS intensities ($p < .05$; ***Table 5.2*** and ***Figure 5.3***C and E). The statistical test of trend components confirmed that band power increased linearly with increasing SCS intensity ($F(1,19) = 9.32$, $p = .007$, ***Figure 5.3***C). To verify if increased band power in the therapeutic intensity was due to lower baseline power, a repeated measures ANOVA was computed using absolute band power in the interval used to calculate ERD values (-3 to -1) for each SCS intensity. No significant difference in baseline absolute band power was found between SCS intensities ($F(3,57) = 2.31$, $p > .05$). A smaller, statistically significant effect of SCS intensity was present in an electrode overlying the right parietal region of the scalp (***Figure 5.3***B) ($F(3,57) = 2.88$, $p = .044$, $\varepsilon = 1.0$) due to a brief increase in band power during the no stimulation condition compared to the medium intensity condition ($p < .05$). (***Figure 5.3***D and F).

Later in the brushing period (1.5−2.0 s), the medium intensity condition failed to produce a robust band-power decrease which was observed in all other intensity conditions in an electrode in the left central-parietal region of the scalp (***Figure 5.3***G–J). This effect is evidenced by topographic maps (Fig. 3h), the waveforms of 4−7 Hz band power (***Figure 5.3***J) and bar graphs representing mean band power in the four SCS intensity conditions (***Figure 5.3***I). A one-way repeated measures ANOVA confirmed a statistically significant effect of SCS intensity ($F(3,57) = 2.95$, $p = .048$, $\varepsilon = 1.0$), with stronger ERD during no stimulation and low intensity SCS compared to medium intensity SCS ($p < .05$, ***Table 5.2***).

In the 8−13 Hz band, a repeated measures one-way ANOVA showed statistically significant amplitude changes in a left parietal electrode in the latency epoch 0.0−0.5 s, when the brush first touched the leg ($F(3,57) = 5.179$, $p = .007$, $\varepsilon = .791$; ***Figure 5.4***A–D). This effect was related to a brief ERS at the strongest therapeutic intensity compared to low and medium SCS intensities ($p < .05$; ***Table 5.2*** and ***Figure 5.4***A).

Around the middle of the brushing period (1.5−2.0 s), the medium intensity condition showed amplitude changes in left central parietal and right parietal electrode clusters (***Figure 5.4***E–J). A statistically significant effect was found in left central parietal electrodes ($F(3,57) = 3.87$, $p = .015$, $\varepsilon = .949$) due to a smaller band power decrease at medium intensity SCS compared to low intensity and no stimulation ($p < 0.05$; ***Table 5.2*** and ***Figure 5.4***G and I). Notably, right parietal electrodes showed a significant effect of intensity ($F(3,57) = 3.31$, $p = .044$, $\varepsilon = .701$) due to a statistically significant increase in band power with medium intensity SCS compared to no stimulation and the strongest, therapeutic intensity ($p < .05$; ***Table 5.2*** and ***Figure 5.4***H and J).

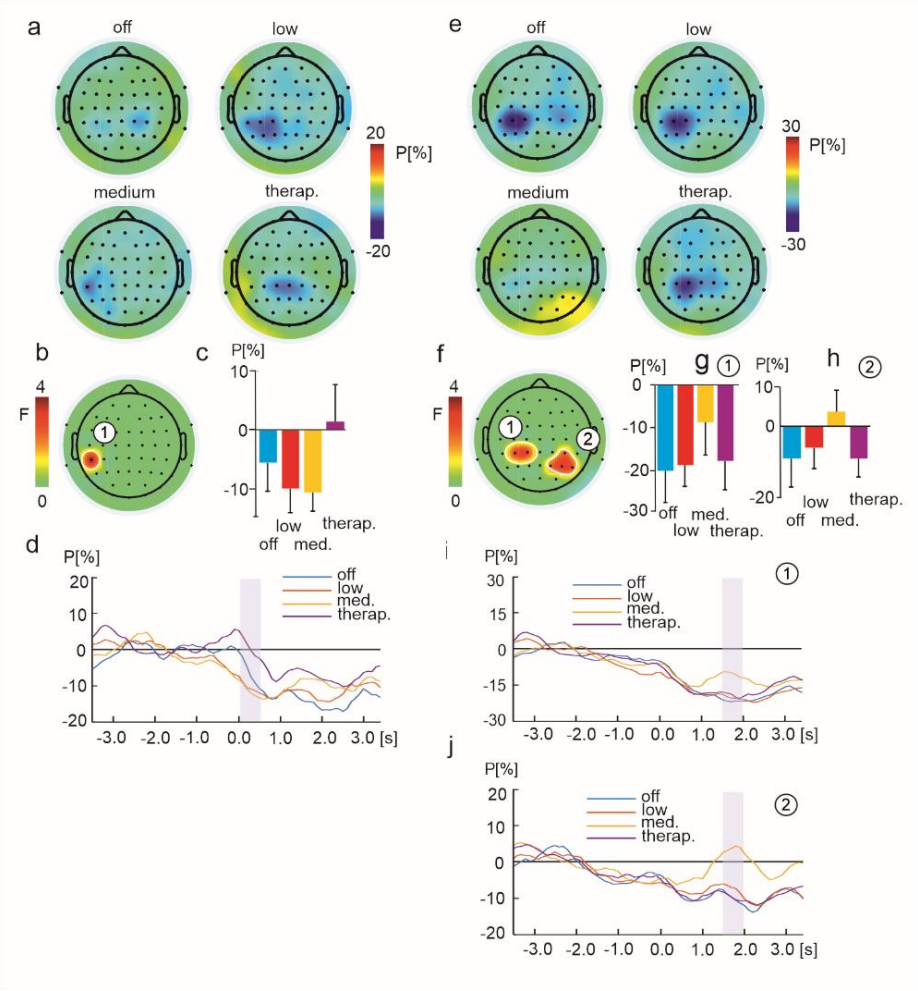

Figure 5.4. Effect of SCS intensity on brushing-related ERD in the alpha frequency band in time bins 0-0.5 s (a-d) and 1.5-2s (e-j). Topographic maps (a, e) show ERD over the scalp in each SCS intensity. Electrodes exceeding permutation test for significance are indicated and electrode clusters numbered (b, f). Bar graphs show percentage power change between stimulation intensities in the corresponding electrode cluster and time bin. Time courses of alpha band power during brushing are shown for the corresponding electrode cluster, with statistically significant time bins highlighted.

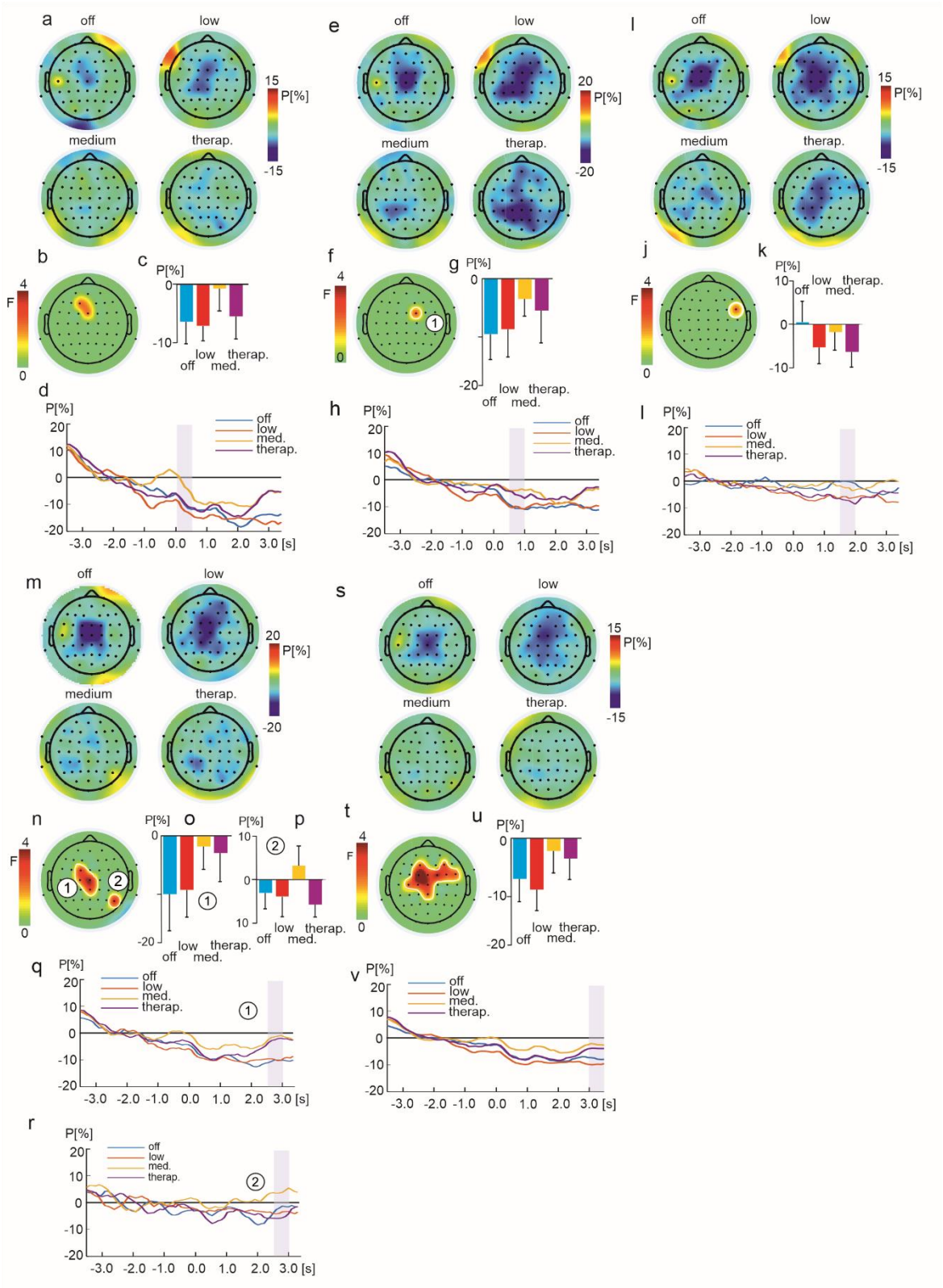

Figure 5.5. Effect of SCS intensity on brushing-related ERD in the beta frequency band in time bins 2.5-3 s (a-d) and 3-3.5 s (e-j). Topographic maps (a, e) show ERD over the scalp in each SCS intensity. Electrodes exceeding permutation test for significance are indicated and electrode clusters numbered (b, f). Bar graphs show percentage power change between stimulation intensities in the corresponding electrode cluster and time bin. Time courses of beta band power during brushing are shown for the corresponding electrode cluster, with statistically significant time bins highlighted.

Figure 5.5 illustrates the effects of four SCS intensities across the latency epochs starting from short (**Figure 5.5**A−H) to mid- (**Figure 5.5**I−L) and long-latencies (**Figure 5.5**M−V) in the 16−24 Hz band. The prevailing pattern of SCS intensity effects was a comparatively weak or non-existent 16−24 Hz ERD during medium intensity SCS predominantly in frontal and central electrodes.

In the first second of brushing, repeated measures ANOVAs showed statistically significant amplitude changes in central and left midline electrodes. The strongest, statistically significant effect at the start of brushing (0−0.5 s) was found in frontal-central regions of the scalp ($F(3,57) = 3.32$, $p = .026$, $\varepsilon = .991$), due to reduced band-power at medium intensity compared to low intensity and no stimulation ($p < .05$; ***Table 5.2*** and **Figure 5.5**A–D). Similarly, at the 0.5–1.0 s latency ($F(3,57) = 3.1$, $p = .039$, $\varepsilon = .939$; **Figure 5.5**E–H), band-power was significantly reduced at moderate intensity SCS in central electrodes compared to low intensity and no stimulation ($p < .05$).

Approaching the middle of brushing stimuli at the latency 1.5−2.0 s, there was a divergent effect of SCS intensity on 16−24 Hz band power (**Figure 5.5**I–L). A statistically significant effect was found in right central-frontal electrodes ($F(3,57) = 3.69$, $p = .022$, $\varepsilon = .872$). This effect was due to decreased band-power at low and therapeutic intensities compared to no stimulation ($p < .05$; ***Table 5.2***). In contrast, medium intensity SCS failed to show a decrease in band-power relative to baseline power or compared to no stimulation ($p < .05$).

Towards the end of brushing, the two strongest SCS intensities showed a diminution of the robust band power decrease observed in low-intensity and no- stimulation SCS in central and frontal regions of the scalp. An effect of SCS intensity was found in the latency 2.5−3 s ($F(3,57) = 6.05$, $p = .002$, $\varepsilon = .923$), with a smaller reduction in band power at the two strongest SCS intensities compared to low intensity and no stimulation ($p < .05$; **Figure 5.5**M–P). This effect was sustained towards the end of the brushing period (3−3.5 s) and extended to right frontal-central electrodes ($F(3,57) = 7.31$, $p < .001$, $\varepsilon = 1.0$; **Figure 5.5**S–V), with a relatively smaller reduction in band-power at medium and therapeutic intensities compared to no stimulation and low intensity SCS ($p < .05$; ***Table 5.2***). In parietal electrodes, a significant effect of SCS intensity was found in the 2.5−3.0 s latency window ($F(3,57) = 3.25$, $p = .032$, $\varepsilon = .915$; **Figure 5.5**P and R). This effect was due to significantly greater band power at the medium intensity compared to the other three intensities, which showed a relative

decrease in band-power during brushing ($p < .05$). However, the band power changes across four SCS intensities in cluster 2 were very weak, with only the therapeutic SCS showing an ERD different from zero.

Table 5.2. Pairwise comparisons for each frequency band of interest

Band		Electrodes	Contrast	df	t	P
4-7 Hz	Cluster 1 Time Bin 1	FCz	Off vs Low	19	3.23	0.004
			Low vs Therapeutic	19	2.42	0.026
			Medium vs Therapeutic	19	2.84	0.011
	Cluster 2 Time Bin 1	P4	Off vs Medium	19	2.98	0.008
	Cluster 3 Time Bin 4	CP1	Off vs Medium	19	2.74	0.013
			Low vs Medium	19	3.55	0.002
8-13 Hz	Cluster 1 Time Bin 1	CP5	Off vs Low	19	1.78	0.091
			Off vs Medium	19	1.97	0.026
			Medium vs Therapeutic	19	3.38	0.003
	Cluster 2 Time Bin 4	CP1 CP3	Off vs Medium	19	2.98	0.008
			Low vs Medium	19	2.84	0.011
	Cluster 3 Time Bin 4	C4 P2 P4 P6	Off vs Medium	19	4.26	< 0.001
			Medium vs Therapeutic	19	2.12	0.047
16-24 Hz	Cluster 1 Time Bin 1	FCz F1	Off vs Medium	19	2.50	0.022
			Low vs Medium	19	3.55	0.002
	Cluster 2 Time Bin 3	Pz	Low vs Medium	19	2.40	0.027
			Medium vs Therapeutic	19	4.08	< 0.001
	Cluster 3 Time Bin 4	FC6	Off vs Low	19	2.24	0.037
			Off vs Therapeutic	19	2.21	0.040
			Medium vs Therapeutic	19	2.61	0.017
	Cluster 4 Time Bin 6	FC1 C1 Cz CPz	Off vs Medium	19	3.46	0.003
			Low vs Medium	19	5.53	< 0.001
			Off vs Therapeutic	19	2.30	0.03
			Low vs Therapeutic	19	2.83	0.01
	Cluster 5 Time Bin 6	P6	Off vs Medium	19	2.26	0.036
			Low vs Medium	19	2.10	0.049
			Medium vs Therapeutic	19	2.84	0.010
	Cluster 6 Time Bin 7	F1 F4 FCz FC2 FC4 FC6 Cz C1 C3 CPz	Off vs Medium	19	3.28	0.004
			Low vs Medium	19	4.99	< 0.001
			Off vs Therapeutic	19	2.20	0.041
			Low vs Therapeutic	19	2.98	0.008

5.4.2.3 Interaction between SCS type and intensity

Electrodes showing a significant main effect of SCS type or intensity were entered into mixed methods ANOVAs to analyse the presence of an interaction between the conditions. No electrodes

showing a significant main effect showed a statistically significant interaction between SCS type and intensity ($p > .05$).

5.5 *Discussion*

The present study analysed the effects of SCS intensities (off, low, medium and therapeutic) and SCS type (burst and tonic) on brushing-related changes in cortical oscillatory activity. Results suggest an overall stronger 8−13 Hz and 4−7 Hz brushing-related ERD in burst compared to tonic SCS, with statistically significant effects in central, frontal and parietal electrodes. SCS intensity modulated brushing-related ERD with a relatively weak ERD at greater SCS intensities, most notably at the medium SCS intensity. This effect was observed in central and parietal electrodes during short- and mid-latency epochs in 4−7 Hz and 8−13 Hz bands, and in frontal and central electrodes during short- and long-latency epochs in the 16−24 Hz band.

Tonic and burst SCS differed in the overall amount of brushing-related ERD, pointing towards a difference in the processing of afferent impulses from LTMRs. While burst SCS showed widespread ERD during brushing in 4−7 Hz and 8−13 Hz frequency bands, tonic SCS was characterised by an absence of ERD in right central and right frontal electrodes, and comparatively weaker ERD in left posterior parietal regions of the scalp in the 8−13 Hz band. Somatosensory brushing stimuli is associated with alpha (8−13 Hz) ERD over bilateral sensorimotor regions (Cheyne et al., 2003; Fallon et al., 2013; Gaetz & Cheyne, 2006), which is interpreted as cortical activation of the sensory cortex to allow efficient processing of sensory stimuli (Neuper et al., 2006; Pfurtscheller & Aranibar, 1977; Pfurtscheller & Lopes da Silva, 1999). Inhibition of both tactile and nociceptive somatosensory processing by parallel LTMR input has been consistently demonstrated in EEG (Gandevia et al., 1983; Kakigi & Jones, 1986; Mancini et al., 2015), MEG (Biermann et al., 1998; Hoechstetter et al., 2001; Tamè et al., 2015), and fMRI studies (Brouwer et al., 2015; Ruben et al., 2006). In contrast, residual 8−13 Hz ERD in posterior parietal regions may reflect activation of the SI/MI foot area which has been reported with fMRI in patients using tonic SCS for leg and lower back pain (Stancak et al., 2008) and may be due to the presence of paraesthesia. Thus, attenuated brushing-related ERD suggests that tonic SCS may actively interfere with somatosensory processing by

continually activating sensorimotor processing regions, rendering them unresponsive to additional, external tactile stimuli.

Burst SCS showed widespread brushing-related ERD which was significantly greater than tonic stimulation in right frontal and left parietal electrodes in the 8−13 Hz band at the onset of brushing, and in right sensorimotor electrodes in the 4−7 Hz band towards the end of brushing. Differences in brushing-related ERD between burst and tonic SCS provides further support for the Gate Control Theory as an explanatory concept for tonic SCS (Holsheimer, 2002; Joosten & Franken, 2020; Melzack & Wall, 1965; Shealy et al., 1967). In contrast, burst stimulation may not operate via activation of the dorsal column system but rather via the spinothalamic tract, as supported by the lack of paraesthesia (Tang et al., 2014) and evidence that burst is not reliant on GABAergic processes (Crosby et al., 2015b). Burst SCS has been shown to induce greater activation of the ACC in PET (Yearwood et al., 2019) and source-localisation EEG studies (De Ridder et al., 2013; De Ridder & Vanneste, 2016), which has led to the suggestion that the analgesic effects of burst SCS may be due to modulation of affective and attentional aspects of pain via the medial pain pathway. Indeed, a recent EEG study showed differential effects of burst and tonic SCS on neural correlates of attention to tactile stimuli (Niso et al., 2021). While attention was not modulated in the current study, decreased alpha-band activity over somatosensory cortices has been reported when attention is directed towards noxious and tactile somatosensory stimuli (Anderson & Ding, 2011; May et al., 2012; Ohara et al., 2004; Peng et al., 2014), suggesting that modulation of alpha band activity acts as a gating mechanism for relevant stimuli. Taken together with previous literature, these results provide further support for different underlying mechanisms between burst and tonic SCS which may involve attentional and affective processes.

Effects of SCS intensity on brushing-related ERD were similar in both burst and tonic SCS, as shown with the absence of a significant interaction between SCS type and intensity. Brushing-related ERD was attenuated at greater SCS intensities. Reduced ERD at medium intensity SCS was found in left central-parietal electrodes in the 4−7 Hz and 8−13 Hz bands in medium-latency epochs (1.5−2 seconds), and in frontal midline electrodes in the 16−24 Hz band in short-latency epochs (0−0.5 seconds). Crucially, significantly reduced ERD at medium and therapeutic intensities was found in

a large area encompassing central midline, parietal and frontal electrodes in long-latency epochs (2.5−3.5 seconds). This robust effect suggests a nonlinear effect of SCS on somatosensory processing, with the weakest ERD suggesting the strongest interference with brushing-induced afferent impulses from LTMRs. Stronger ERD at medium intensity conditions may be due to the ceiling effect of increasing stimulus intensities on ERD, with evidence that ERD is not modulated by fine gradations of stimulus intensity (Iannetti et al., 2008; Stancak et al., 2003). Alternatively, the strongest interference of brushing-induced impulses at medium SCS intensities may reflect a potential overshoot in determining the most effective therapeutic parameters, with lower intensities being more effective at inhibiting somatosensory stimuli.

In addition to attenuated ERD at medium and therapeutic intensities, ERS in the 4−7 Hz band was sensitive to SCS intensity. At the onset of brushing, greater SCS intensities were associated with linear increases in 4−7 Hz ERS, particularly in frontal midline electrodes. Augmented resting theta (4−7 Hz) power has been consistently reported in patients with chronic pain (Fallon et al., 2018; Lim et al., 2016; Sarnthein et al., 2006; Stern et al., 2006; Vanneste et al., 2018; Vučković et al., 2014). Thalamocortical dysrhythmia, dominant low-frequency oscillations in the thalamo-cortico-thalamic network, has been proposed to be a contributing factor in the development or maintenance of a number of pathologies including chronic pain (Llinás et al., 1999, 2005) by disrupting the normal state-dependent flow of information between the thalamus and cortex, leading to disturbances of sensation, motor performance and cognition (Jones, 2010). Changes in theta activity could be relevant for patient outcomes; increased prefrontal theta activity has been shown to correlate with symptom severity in fibromyalgia (Fallon et al., 2018), and increased theta power in prefrontal, sensorimotor and cingulate cortices has been shown following the cessation of tonic pain stimuli (Rustamov et al., 2021). An investigation of a different subthreshold waveform, high-frequency SCS, showed a positive correlation between changes in disability scores and alpha/theta peak power ratios in frontal and somatosensory regions during intraoperative stimulation (Telkes et al., 2020). Thus, increased theta ERS with increasing SCS intensity could reflect an interference of pain mechanisms which are prevalent in neuropathic pain.

A limitation of the current study is the short duration between intensity conditions. SCS intensities were varied and followed by short 2-minute washout periods with no stimulation. However, the washout period of tonic and burst SCS are still poorly understood. Active-recharge burst waveforms, in contrast to passive recharge burst used in the current study, have been demonstrated to have a delayed wash-in and prolonged washout periods compared to tonic SCS (Meuwissen et al., 2018). Differences in washout periods may also be dependent on stimulus energy, which differs between participants (Abejón et al., 2015; Miller et al., 2016). SCS dosing paradigms have recently been introduced, which alternate periods of stimulation with those of no stimulation (Deer et al., 2021; Vesper et al., 2018), suggesting that the effects of stimulation outlast the stimulation itself. However, dosing waveforms have only been applied to burst SCS thus far and remain to be investigated with other SCS waveforms. However, no differences were found between burst and tonic SCS in the effect of SCS intensity, and changes were observed between intensity conditions. Furthermore, previous studies have observed that patients observe perceptual changes instantly during stimulus programming (Tan et al., 2016). Future studies could investigate differences between SCS intensities over a longer duration, which would allow for greater disentangling of possible carryover effects.

There are potentially important implications for theory and clinical practice resulting from the current findings. Firstly, in agreement with previous studies comparing burst and tonic SCS, both different and shared mechanisms are involved in somatosensory processing during SCS. Tonic SCS appears to suppress parallel inputs from brushing stimuli; although as the current study focused solely on the somatosensory paraesthesia component of SCS, it is not clear if this inhibitory effect would be equally relevant to the influence of SCS on noxious afferents. Future studies should investigate ERD patterns during burst and tonic SCS related to stimuli that primarily involve spinothalamic tract neurons, such as transient warming, cooling, or heat stimuli. Relevant for clinical practice, strong interference with transmission of afferent impulses at SCS intensities as much as one-third lower than the therapeutic level suggests that lower intensities may be equally, if not more, effective than the clinically programmed settings. SCS intensity contributes to the electrical charge transfer (Miller et al., 2016), with lower electrical charge preserving battery life and reducing any potentially unpleasant

paraesthesia sensations. Therefore, this preliminary finding suggests that EEG may have a potentially valuable role in determining optimal stimulation parameters for relieving neuropathic pain.

To conclude, burst and tonic SCS differentially modulate somatosensory processing, and changes in somatosensory processing may result from variations in the underlying therapeutic mechanisms. Unlike burst SCS, tonic SCS suppresses brushing-related cortical activity, pointing towards involvement of the dorsal column system. Greater SCS intensities within the therapeutic limits may normalise aberrant cortical oscillations which are associated with neuropathic pain; however, lower intensities than the therapeutic level may be sufficient to achieve a therapeutic benefit. These findings suggest that EEG analysis can provide an objective cue to determining the optimal SCS intensity.

Chapter 6

Inhibition of cortical somatosensory processing during and after low frequency peripheral nerve stimulation in humans

Danielle Hewitt[1], Adam Byrne[1,2], Jessica Henderson[1], Alice Newton-Fenner[1,2], John Tyson-Carr[1], Nicholas Fallon[1], Christopher Brown[1], Andrej Stancak[1]

[1] Department of Psychological Sciences, University of Liverpool, Liverpool, UK.

[2] Institute for Risk and Uncertainty, University of Liverpool, Liverpool, UK.

This experiment used source dipole modelling to investigate temporal changes in SEPs during LFS, and the effects of LFS on post-stimulation resting oscillations and pain-related evoked potentials.

This paper was published in Clinical Neurophysiology (2021), doi: https://doi.org/10.1016/j.clinph.2021.03.024

The format of the text has been modified to match the style of this thesis.

The roles of the co-authors are summarised below:

Danielle Hewitt: Conceptualisation, Methodology, Software, Investigation, Formal analysis, Writing - Original Draft, Writing - Review & Editing. **Adam Byrne:** Investigation, Writing - Review & Editing. **Jessica Henderson:** Investigation, Writing - Review & Editing. **Alice Newton-Fenner:** Investigation, Writing - Review & Editing. **John Tyson-Carr:** Software, Writing - Review & Editing. **Nicholas Fallon:** Conceptualisation, Writing - Review & Editing. **Christopher Brown:** Conceptualisation, Writing - Review & Editing. **Andrej Stancak:** Conceptualisation, Software, Formal analysis, Writing - Original Draft, Writing - Review & Editing, Supervision, Funding acquisition.

6 Inhibition of cortical somatosensory processing during and after low frequency peripheral nerve stimulation in humans

6.1 Abstract

Transcutaneous LFS elicits LTD-like effects on human pain perception. However, the neural mechanisms underlying LFS are poorly understood. We investigated cortical activation changes occurring during LFS and if changes were associated with reduced nociceptive processing and increased amplitude of spontaneous cortical oscillations post-treatment.

LFS was applied to the radial nerve of 25 healthy volunteers over two sessions using active (1 Hz) or sham (0.02 Hz) frequencies. Changes in resting EEG and LEPs were investigated before and after LFS. SEPs were recorded during LFS and source analysis was carried out.

Ipsilateral midcingulate and operculo-insular cortex source activity declined linearly during LFS. Active LFS was associated with attenuated long-latency LEP amplitude in ipsilateral frontocentral electrodes and increased resting alpha (8–12 Hz) and beta (16–24 Hz) band power in electrodes overlying operculo-insular, sensorimotor, and frontal cortical regions. Reduced ipsilateral operculo-insular cortex source activity during LFS correlated with a smaller post-treatment alpha-band power increase.

LFS attenuated somatosensory processing both during and after stimulation. Results further our understanding of the attenuation of somatosensory processing both during and after LFS.

6.2 *Introduction*

External non-invasive peripheral nerve stimulation (EN-PNS) is a palliative neurostimulation method for peripheral neuropathic pain. It utilises a small diameter electrode to deliver low frequency electrical stimulation (LFS) to peripheral nerves innervating an affected region of the limb. This allows a high current density at low frequencies of 1–2 Hz, resulting in preferential activation of Aδ nerve fibres (Inui et al., 2002; Nilsson & Schouenborg, 1999; Rottmann et al., 2008). Early case studies of LFS have reported pain relief after EN-PNS in a range of conditions including back pain, headache and trigeminal neuralgia (Rutkowski et al., 1975). More recently, therapeutic success has been reported in complex regional pain syndrome and peripheral nerve injury, and pain reduction appears to be sustained in the long-term (Johnson et al., 2015; Johnson & Goebel, 2016). Although limited, these initial studies support the value of LFS for the management of neuropathic pain.

LFS exerts its therapeutic effects via LTD of nociceptive afferents (Sandkühler et al., 1997). LTD and LTP of synaptic strength are present at many sites in the central nervous system and have been studied extensively in the hippocampus in relation to learning and memory (Bliss & Collingridge, 1993; Linden, 1994). These forms of activity-dependent plasticity can be induced using electrical stimulation in a frequency-dependent manner; high frequency electrical stimulation (HFS) can result in LTP (Bliss & Lomo, 1973), while LFS can result in LTD (Dudek & Bear, 1992; Mulkey & Malenka, 1992). Conditioning LFS of Aδ fibres in the superficial spinal dorsal horn reduces synaptic transmission for up to 2 hours both *in vitro* and *in vivo*, and this reduction is reversed with HFS (Liu et al., 1998; Randić et al., 1993; Sandkühler et al., 1997). In animal models of neuropathic pain, LFS-induced plasticity also occurs alongside reductions in mechanical allodynia (Xing et al., 2007).

Alterations in synaptic plasticity cannot be directly measured with humans *in vivo.* Thus, measures such as changes in pain ratings and cortical SEPs to noxious test stimuli after LFS have been used as surrogate markers for nociceptive LTD. In human studies, LFS was associated with decreased subjective pain ratings (Jung et al., 2009; Klein, 2004; Lindelof et al., 2010) and reduced SEP amplitudes to acute noxious test stimuli (Ellrich & Schorr, 2004). Changes in SEP components have been localised to the ACC (Jung et al., 2012). Optimal parameters for LFS have been

approximated, with maximal SEP reduction after 1200 pulses of 1 Hz stimulation at four times pain threshold (Jung et al., 2009). This indicates attenuated somatosensory processing after termination of the LFS procedure. However, as these studies have investigated only the post-stimulation effect of LFS on subsequent noxious stimuli, the acute effects of LFS on somatosensory processing are unknown. Further, as changes in synaptic efficacy in live humans cannot be directly examined, it cannot be conclusively stated that SEP reductions are due to LTD or other mechanisms such as habituation or placebo analgesia. Habituation to repeated stimuli manifests in diminished SEPs when presented at regular intervals (Condes-Lara et al., 1981; Iannetti et al., 2008; Mancini et al., 2018; Wang et al., 2010). Similarly, inert substances or sham procedures can result in placebo-induced reductions in laser-evoked potentials (LEPs) mediated by the endogenous opioid system (Eippert et al., 2009; Wager et al., 2006). To delineate the acute effects of LFS, we used a sham-controlled procedure to analyse the cortical activation changes during and after LFS, and if this was associated with selectively attenuated nociceptive processing using LEPs.

The amplitudes of cortical oscillations are known to vary with states of arousal. Task-related changes can induce decreases or increases of power in given frequency bands, known as ERD (Pfurtscheller, 1977; Pfurtscheller & Aranibar, 1977) and ERS (Pfurtscheller, 1992). ERD and ERS have been related to states of activation or inhibition within the somatosensory and motor systems (Pfurtscheller, 1992). Following somatosensory stimulation, ERD of 10 Hz and 20 Hz frequency bands occurs over bilateral SI/MI (Illman et al., 2020; Neuper & Pfurtscheller, 2001b; Nikouline et al., 2000; Pfurtscheller, 1992; Stančák, 2006), followed by post-stimulus 20 Hz ERS over contralateral precentral cortex (Brovelli et al., 2002; Illman et al., 2020; Neuper & Pfurtscheller, 2001b; Parkkonen et al., 2015; Salenius et al., 1997; Salmelin & Hari, 1994b; Stancak et al., 2003). Acute noxious stimuli induce suppression of alpha and beta power in the bands 8–14 Hz and 15–30 Hz in sensorimotor, parietal operculum and posterior and midcingulate cortices (Ploner et al., 2006; Stančák et al., 2010). This activity can be modulated with cognitive processes such as attention (May et al., 2012; Ohara et al., 2004) and expectation (Huneke et al., 2013), as well as pain intensity (Tiemann et al., 2015). As previous SEP literature suggests diminished somatosensory processing after LFS (Ellrich & Schorr, 2004; Jung et al., 2009), we investigated whether this would coincide

with a state of relative amplitude increases in sensorimotor regions in alpha and beta bands suggestive of cortical inhibition (Foxe & Snyder, 2011; Fry et al., 2016; Neuper & Pfurtscheller, 2001b; Pfurtscheller et al., 1996b).

To directly examine LFS-induced changes in cortical activity, we analysed variations in SEPs elicited by electrical stimuli applied transcutaneously to the radial nerve. Electrical stimuli activate mixed peripheral nerves which contain afferents from both LTMRs and nociceptors. Previous studies of the neural correlates of noxious stimuli have shown a shared representation for pain and touch (Colon et al., 2014; Iannetti & Mouraux, 2010; Mouraux et al., 2011). For instance, LEPs in response to noxious laser stimuli primarily originate from SII, MCC and ACC, and bilateral operculo-insular regions (Bastuji et al., 2016; Bradley et al., 2017; García-Larrea et al., 1997, 2003; Valeriani et al., 2000b). Activity in these regions reflected by LEPs is not nociceptive-specific but can be explained by a combination of multimodal and somatosensory-specific neural activity, with the magnitude determined by stimulus saliency (Mouraux & Iannetti, 2009; Wang et al., 2010) or the requirement for defensive motor actions after threatening stimuli (Moayedi et al., 2015, 2016). Furthermore, considerable literature has shown diminished SEPs to repeated stimuli (Bradley et al., 2016; Mancini et al., 2018; Wang et al., 2010). However, recent studies using intensity- and saliency-matched noxious and innocuous stimuli show preferential activation for painful stimuli in a spatially distributed subset of regions including bilateral opercular insular cortex, parietal operculum and supplementary motor area (Horing et al., 2019; Liang et al., 2019; Su et al., 2019), highlighting the importance of appropriately matched conditions. Thus, we postulated that LFS would induce suppression of activity in somatosensory processing regions of the cortex.

The goal of the present study was to investigate the attenuation of somatosensory processing during LFS, and whether this decrease of cortical activity would be associated with reduced nociceptive processing and increased power in resting state cortical oscillations after stimulation. Our hypotheses were threefold: i) LFS would be associated with a systematic decrease of SEPs in regions known to participate in nociceptive processing including the operculo-insular cortex and cingulate cortex, ii) LFS would be associated with decreases in nociceptive processing, measured with LEPs and behavioural pain ratings, and increases in cortical alpha and beta oscillations in sensorimotor

cortex, and iii) changes in LEPs, behavioural pain ratings and cortical oscillations after LFS would correlate with changes in SEPs during LFS.

6.3 Methods

6.3.1 Subjects

Twenty-five healthy subjects (14 females) with no history of chronic pain or neurological conditions were recruited from the University of Liverpool. Two subjects withdrew from the study after the first session. Four subjects were excluded during data collection: two due to an adverse skin reaction to the laser pain stimulation and two due to an exceedingly high pain threshold. Two participants were excluded in the data analysis stage due to artefactual data. The final sample included 17 participants (11 females, 12 right-handed) with a mean age of 23 ± 1 years (mean ± SD). The procedure used was approved by the Research Ethics Committee of the University of Liverpool, and all participants gave fully informed written consent at the start of the experiment in accordance with the Declaration of Helsinki. Participants were reimbursed £30 for their time and inconvenience on completion of the study.

6.3.2 Experimental protocol

Experimental procedures were carried out over two sessions in the Eleanor Rathbone Building, University of Liverpool. Sessions took place 7 days apart. Sessions were varied by the type of LFS, active or sham stimulation, with the order of conditions counterbalanced between participants. Experimental protocol and stimulus timings are illustrated in ***Figure 6.1***.

During each session, participants were seated in a dimly lit room with a 19-inch LCD monitor in front of them. Presentation of stimuli was controlled with Cogent 2000 (University College London, London, UK) in MATLAB 2010 (The Mathworks, Inc., USA). Participants were first instructed to keep their eyes open and look straight ahead for four minutes during the recording of spontaneous EEG. Following this, the participants hand was shielded from view by a cardboard box and laser pain thresholds were determined using a staircase procedure. During the laser experiment, participants were presented with a white fixation cross, followed by a black screen, at which point they were told to expect a laser stimulus on their left hand. Laser stimuli were applied pseudo-

randomly to the ulnar or radial part of the left hand by the experimenter so that participants could not predict the location of stimulation and there were an equal number of trials for each hand side. After each laser stimulus, participants were asked to rate the intensity of pain experienced by clicking on a visual analogue scale presented on the monitor with a mouse, from no sensation to maximum pain. After rating the stimulus, the fixation cross appeared again, and participants were asked to remove their hand from the mouse and place it flat on the desk. The whole block lasted approximately 15 minutes. EEG was recorded throughout.

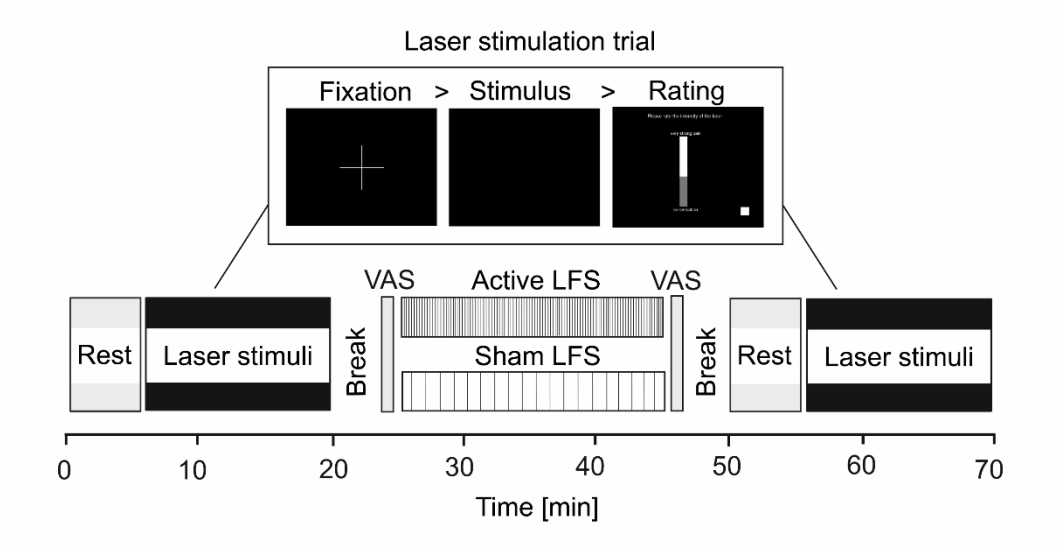

Figure 6.1. A schematic representation of the experimental protocol. Electroencephalography (EEG) was recorded from participants during rest with eyes open (4 minutes) and noxious laser stimulation (60 stimuli, ~15 minutes), both before and after conditioning low frequency stimulation (LFS). LFS was applied to the radial nerve of the left hand at 1 Hz (active condition) or 0.02 Hz (sham condition), varied by session and counterbalanced between participants (20 minutes). Subjective ratings of LFS discomfort and intensity were collected using a paper visual analogue scale (VAS). Prior to and following LFS, there was a short break while EEG impendences were checked (~5 minutes). Min = duration in minutes.

Participants were asked to report the subjective discomfort and intensity of the stimulation after a single pulse (pre-LFS) and as an average of all pulses after the block of LFS was complete (post-LFS), using a paper-based visual analogue scale from 0 (not at all intense) to 100 (maximum intensity). LFS was applied to the hand during active and sham LFS conditions. SEPs were only collected during active LFS. Both active and sham LFS blocks lasted approximately 20 minutes. Prior

to and succeeding LFS, there was a break of approximately 5 minutes during which time the electrode impedances were checked. After LFS, spontaneous EEG and LEPs were recorded again.

6.3.2.1 Electrical stimulation

Low-frequency electrical stimulation was applied to the skin in the region of the radial nerve of the left hand using a nerve mapping pen (Compex Motor Point Pen, UK) controlled by a Digitimer DS7A constant current stimulator (Digitimer, UK) and MATLAB 2010 (The Mathworks, Inc., USA). Stimulation intensity was determined at the start of each session using a staircase procedure, in which a single electrical stimulus was delivered to the test site at 0.30 milliamperes (mA). Participants were asked to verbally rate the stimulus on a scale of 0 (no sensation) to 100 (maximum discomfort), where 30 indicated uncomfortable threshold. After each stimulus, electrical stimulation intensity was raised in steps of 0.10 mA and subsequent stimuli were delivered until a threshold of 50-60/100 was reached. During the experiment, stimulation was applied to the radial nerve on the left hand at a mean intensity of 1.17 mA: 1.17 ± .08 mA in active LFS and 1.16 ± .08 mA in sham LFS conditions. In the active condition, 1200 pulses were delivered at a frequency of 1 Hz, pulse width 1 ms, duration 1 ms. In the sham condition, 20 pulses were delivered at a frequency of 0.017 Hz, at a rate of 1 per minute, duration 1 ms. Due to differences in stimulus frequency between active and sham LFS, the total number of stimuli were not equal between conditions; therefore, SEPs were only collected during active LFS.

6.3.2.2 Noxious laser stimulation

Mildly noxious laser stimuli were delivered to the dorsal surface of the left hand using a Nd–YAP laser stimulator (Stim1324, El.En., Italy). The pulse duration was 2 ms, and the spot size was 4 mm. Laser intensity was adjusted individually prior to the first block using a staircase procedure. During the staircase thresholding procedure, a single laser stimulus was delivered to the hand dorsum at 1.75 Joules (J). Participants were asked to verbally rate the stimulus intensity on a scale from 0 (no sensation) to 100 (maximum imaginable pain), where 30 indicated pain threshold. After each stimulus, laser intensity was increased in steps of 0.25 J and subsequent stimuli were delivered until a subjective pain intensity of 50-60/100 was reached, with a maximum energy of 3.0 J. After thresholding, stimuli were applied at a mean intensity of 2.71 J: 2.74 ± .25 J in active conditions, 2.69

± .31 J in sham conditions. A paired t-test revealed that the difference in laser threshold between conditions was not statistically significant, $t(16) = .64$, $p > .05$.

During the experiment, sixty laser stimuli were applied to the radial or ulnar aspect of the left-hand dorsum in a pseudorandomised order (30 ulnar, 30 radial). Stimuli were manually triggered by a second experimenter when the EEG was free from movement artefacts, resulting in inter-stimulus intervals of approximately 10 ± 5 seconds. Randomisation was determined at the start of each block using the *randperm.m* MATLAB function to shuffle an array containing 30 instances of the numbers 1 (ulnar) and 2 (radial). Prior to each trial, the upcoming hand side was indicated to the experimenter using an audio clip played through headphones. The exact location of stimuli on each hand side was varied between trials to minimise effects of receptor adaptation or local skin temperature effects.

6.3.3 EEG acquisition

Continuous EEG was recorded using a 129-channel Geodesics EGI System (Electrical Geodesics, Inc., Eugene, Oregon, USA) with a sponge-based HydroCel Sensor Net. The sensor net was aligned with respect to three anatomical landmarks of two preauricular points and the nasion. Electrode-to-skin impedances were kept below 50 kΩ throughout the experiment. A recording band-pass filter was set at 0.001–200 Hz with a sampling rate of 1000 Hz. Electrode Cz was used as a reference electrode.

6.3.4 Behavioural data analysis

Mean subjective pain ratings of laser stimuli in each condition were calculated for each participant. A 2×2×2 repeated measures analysis of variance (ANOVA) was computed using SPSS v. 25 (IBM Inc., USA), with independent variables of 'Time' (pre or post LFS), 'Condition' (active or sham), and 'Hand Side' (ulnar or radial). Subjective ratings of LFS discomfort and intensity were compared using a two-way repeated measures ANOVA. Independent variables were 'Condition' (active or sham) and 'Time' (pre or post LFS). Post-hoc t-tests were used where appropriate to follow up significant main effects.

6.3.5 EEG data analysis

EEG data were processed using BESA v. 6.1 (MEGIS GmbH, Germany). Data were filtered using 1 Hz high pass and 70 Hz low pass filters, with a notch filter of 50 Hz ± 2 Hz. Oculographic and electrocardiographic artefacts were removed with principal component analysis (Berg & Scherg, 1994). Data were visually inspected for movement and muscle artefacts. Trials containing artefacts were marked and excluded from further analysis. Electrode channels with large artefacts were interpolated to a maximum of ≤ 10% electrodes.

6.3.5.1 Spontaneous EEG

Average spectral band-power in 4-min resting EEG recordings was calculated using FieldTrip (Oostenveld et al. 2011: http://fieldtriptoolbox.org). Power spectral densities were estimated in non-overlapping 1-second epochs. Data epochs were tapered using a Hamming window. The resulting power spectral densities had a frequency resolution of 1 Hz. Mean absolute power values were transformed using a decadic logarithmic transform. The average number of 1-second epochs accepted for EEG analysis in each condition were: pre-active 237 ± 8 (mean ± SD), post-active 236 ± 10, pre-sham 244 ± 16 and post-sham 234 ± 9. A repeated-measures ANOVA showed that the average number of accepted epochs did not differ across conditions ($p > .05$).

A two-step procedure was utilised to identify electrodes for further analysis. Permutation analyses with 500 repetitions, implemented in the *statcond.m* program in the EEGLab package (Makeig et al., 2004), were carried out across electrodes for each LFS condition (Active and Sham) and Time period (pre- and post-stimulation). This was conducted to identify clusters of electrodes showing significant main effects of LFS or Time, or interactions between these variables (Maris & Oostenveld, 2007). This method provides a data-driven approach to test effects across all electrodes whilst controlling for multiple comparisons with no loss in statistical power. Next, to remove electrodes with spurious results showing only minimal changes in power from the baseline, confidence intervals for each electrode were calculated from standard error of the mean baseline period. Electrodes that exceeded a predefined threshold on the calculated *p*-values (uncorrected $p < .001$) for the main effects of, or interactions between, LFS and Time, and that exceeded baseline confidence intervals, were selected for further analysis and clustered based on spatial adjacency. Log-

transformed band power in electrodes exceeding permutation and thresholding were entered into 2×2 repeated measures ANOVA involving two Conditions (active vs. sham stimulation) and two Time periods (pre- vs. post-stimulation) in theta (4–7 Hz), alpha (8–12 Hz) and beta (16–24 Hz) bands.

6.3.5.2 Laser-evoked potentials (LEPs)

LEPs were computed by averaging single subject trials for all conditions (active vs. sham stimulation, pre- vs. post-stimulation, ulnar vs. radial hand side) in the epoch -300 pre-stimulus to 500 ms post-stimulus. The baseline period ranged from -100 to 0 ms prior to stimulus onset. Data was filtered during averaging from 1–35 Hz. Grand averages were created by averaging single subject LEPs for each condition. The average number of trials accepted for LEP analysis in each condition was 29 (Active 29 ± 1, Sham 29 ± 1, mean ± SD). A repeated-measures ANOVA showed that the average number of accepted trials did not differ across LFS conditions ($p > .05$).

To enhance the small local currents, such as those originating in the SI/MI hand area, and to arrive at reference-free data, EEG data were spatially transformed using the spline surface Laplacian operator method (Hjorth, 1975; Perrin et al., 1989) implemented with the CSD Toolbox (Kayser & Tenke, 2006). To mitigate the risk of Type 1 error due to multiple tests, ANOVAs were computed using the *statcond.m* program with 400 permutations for each condition (Active and Sham) to identify clusters of electrodes and time windows showing significant main effects of Hand Side or Time, or interactions between these variables (Maris & Oostenveld, 2007). Electrodes and time windows that exceeded a predefined threshold on the calculated *p*-values ($p < .01$) for the main effects of, or interactions between, Time and Hand Side were selected for further analysis and clustered based on spatial adjacency. The combined amplitude thresholding and permutation analysis allowed evaluation of statistically significant changes in the well-established LEP components N1, N2 and P2 whilst avoiding ad-hoc selection of epochs of interest. Only the negative components in the latency range of N1 and N2 components (100–240 ms) were interpreted, as clusters showing changes in the positive potential components mirrored that of the negative components. Likewise, only positive clusters in the latency range of the P2 component (310-340 ms) were interpreted.

6.3.5.3 Somatosensory-evoked potentials (SEPs) during LFS

SEPs were evaluated during active LFS applied to the radial nerve. All 1200 SEP responses over the 20-minute recording were divided into ten 2-minute intervals of 120 responses. SEP responses in each 2-minute interval were averaged in the epoch -100 ms pre-stimulus to 900 ms post-stimulus. The baseline period ranged from -100 to -5 ms prior to stimulus onset, and the stimulus artefact window was defined as -4 to 10 ms post stimulus. The average number of epochs containing SEP responses accepted for further analysis in each of the ten 2-minute intervals ranged from 115 ± 3 to 118 ± 2 (mean ± SD). A repeated-measures ANOVA showed that the average number of accepted epochs did not differ over time ($p > .05$). Data was filtered during averaging from 1–45 Hz.

Source modelling of SEPs was performed using BESA v. 6.1 (MEGIS GmbH, Germany). The source model was constructed using a sequential strategy, in which source dipoles were fitted consecutively starting from the first peak in global field power (Hoechstetter et al., 2000, 2001; Scherg, 1992; Stancak et al., 2002). When the residual variance was not reduced by adding another dipole, the fitting procedure was terminated. To evaluate the effect of LFS duration on SEPs, the grand average source dipole model was used to compute individual subject source waveforms in SEPs falling into 10 epochs of 2-min duration each, covering the 20 minutes of LFS. Source dipole moments in intervals surrounding peaks of equivalent current dipole (ECD) ECD waveforms were entered into a one-way repeated measures ANOVA with 10 levels of Time. The Huynh-Feldt correction was used to tackle a violation of the sphericity assumption found in the data.

6.3.6 Correlations

Bivariate Spearman's correlations were performed across subjects to investigate the relationship between source activity during LFS, behavioural ratings (laser pain scores) and electrophysiological measures (spontaneous EEG and LEPs). Spearman's non-parametric rank correlation was used due to its reduced sensitivity to outliers in comparison to parametric Pearson's correlations. In source dipoles showing a significant change in amplitude over time during active LFS, a difference index was calculated as the change in the peak amplitude of source waveforms over time (T10 minus T1). Difference in subjective laser pain ratings was calculated for each subject before and after active LFS (post-LFS minus pre-LFS). Difference in spectral band-power after active LFS in

comparison to before active LFS (post- minus pre-LFS) and change in the amplitude of LEP components (post- minus pre-LFS) were calculated for clusters of electrodes showing significant modulation by condition. For all variables, a decreased value indicated a reduction post-LFS, while an increased value indicated an increase post-LFS.

6.4 *Results*

6.4.1 Spontaneous EEG changes

Changes in spontaneous EEG were assessed over time (pre- vs. post-LFS) in both LFS conditions (Active vs. Sham) in theta (4–7 Hz), alpha (8–12 Hz) and beta (16–24 Hz) frequency bands (***Figure 6.2***A-C).

In the 4–7 Hz band, topographic maps show relatively strong band-power maxima in prefrontal electrodes and relative minima in bilateral lateral central and temporal electrodes (***Figure 6.2***A). A permutation identified a cluster of electrodes exceeding significance in frontal midline electrodes (electrodes 11, 19 and 14). These electrodes showed a main effect of Time ($F(1,16) = 28.26$, $p = .001$, $\eta^2_p = .64$), with an increase in 4–7 Hz band-power after LFS. There was also a main effect of Condition ($F(1, 16) = 4.87$, $p = .042$, $\eta^2_p = .23$), with a reduction in theta band power in the active LFS condition, in comparison to the sham condition. However, the interaction between Time and Condition was not statistically significant ($p > .05$).

Topographic maps of 8–12 Hz band power were featured by relatively low band-power in bilateral central and temporal electrodes (***Figure 6.2***B). A repeated-measures ANOVA identified a cluster of electrodes in the scalp area overlying the operculo-insular and temporal cortex (electrodes 104, 111 and 109). The location of this cluster was confirmed using 3D maps. This cluster showed a significant main effect of Time ($F(1,16) = 15.6$, $p = .001$, $\eta^2_p = .49$), with an increase in 8–12 Hz band power after LFS. There was a statistically significant interaction between Time (pre vs. post LFS) and Condition (active vs. sham) in this cluster of electrodes ($F(1,16) = 17.3$, $p = .001$, $\eta^2_p = .52$). Post-hoc t-tests revealed this interaction was caused by the statistically significant difference between active and sham stimulation after LFS ($t(16) = 2.18$, $p = .044$) but not before LFS ($t(16) = .91$, $p > .05$).

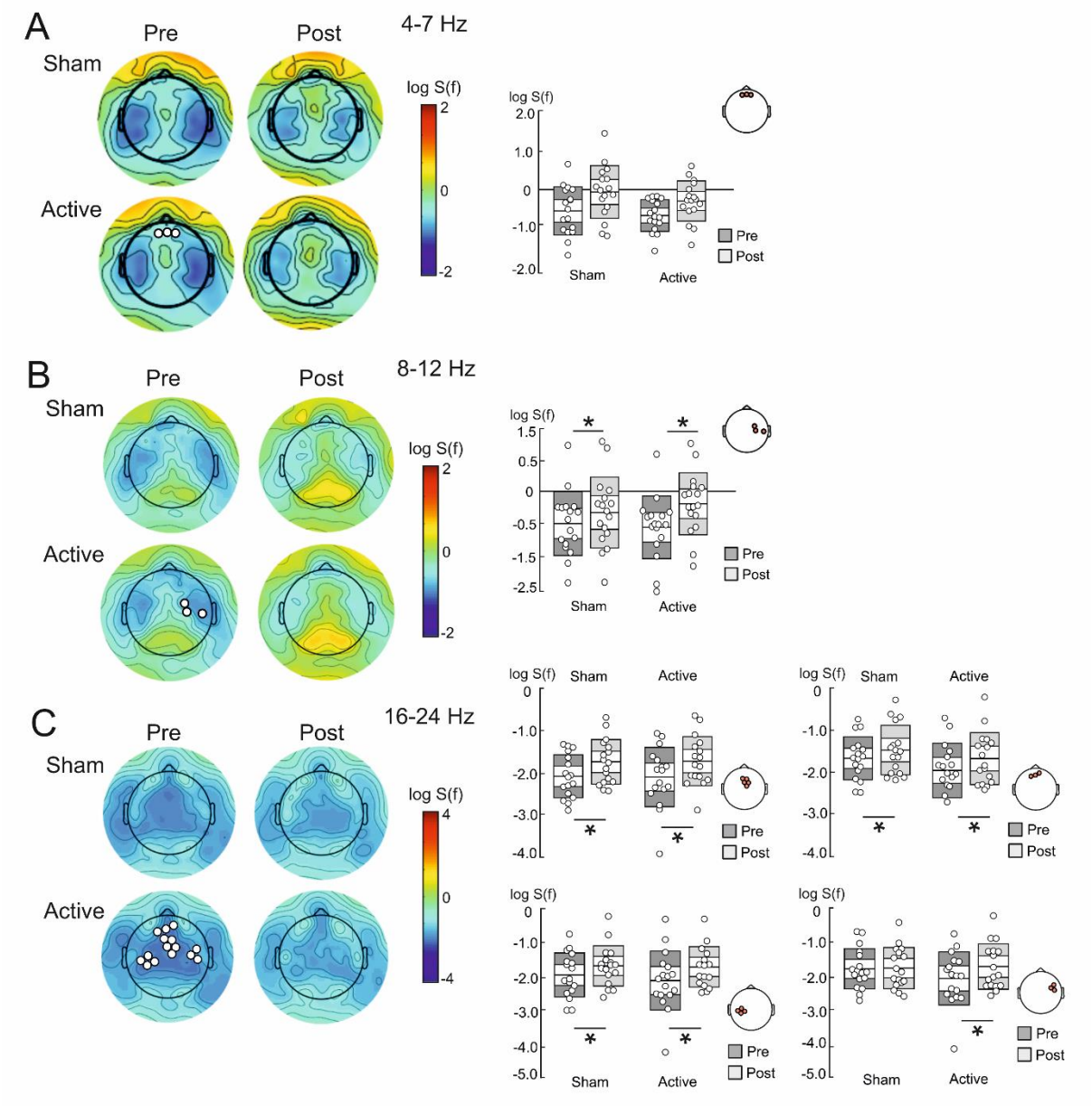

Figure 6.2. Band power changes in spontaneous EEG before (pre) and after (post) active and sham LFS. Grand average topographic maps of each frequency band of interest, 4-7 Hz (**A**), 8-12 Hz (**B**) and 16-24 Hz (**C**), are shown alongside an overhead view of electrodes showing statistically significant changes ($p < .05$) across all conditions, and box plots showing the mean band power of the cluster. Inner (white) and outer (grey) boxes represent 95% confidence intervals and 1 standard deviation, respectively. Individual subject data is overlaid as circles. Asterisks indicate results that exceeded corrected significance of $p < .05$. Hz = Hertz. Log S(f) = logarithmic power spectral density.

In the 16–24 Hz band, the topographic maps showed a large area of reduced power extending from frontal and midline electrodes to posterior parietal regions (***Figure 6.2***C). A repeated measures ANOVA identified 4 clusters of electrodes as reaching statistical significance. All four clusters,

located in the central-midline (electrodes 5, 6, 12, 106 and 112), contralateral (electrodes 103, 104 and 110) and ipsilateral central regions (electrodes 36, 37, 41 and 42) overlying sensorimotor cortex and frontal regions (electrodes 10, 11 and 19) of the scalp, showed a main effect of Time ($p < .05$) due to increases of 16–24 Hz band power after LFS. The frontal cluster also showed a significant main effect of Condition ($F(1,16) = 17.7$, $p = .001$, $\eta^2_p = .53$), with relatively lower 16–24 Hz band power in active than sham conditions, both before and after LFS. The cluster overlying the contralateral somatosensory cortex showed a significant interaction between Time (pre vs. post LFS) and Condition (active vs. sham), ($F(1,16) = 5.3$, $p = .035$, $\eta^2_p = .249$). Post-hoc t-tests revealed that this interaction was due to a significant increase in band power after active stimulation compared to before stimulation ($t(16) = 2.52$, $p = .023$) and absence of pre-post difference in the sham condition ($t(16) = 0.16$, $p > .05$). Of note, there was no statistically significant effect between sham and active conditions before LFS ($t(16) = 1.8$, $p > .05$).

6.4.2 Laser-evoked potential (LEP) changes

Differences in mean subjective pain ratings for laser stimuli were analysed using a 2×2×2 repeated measures ANOVA using factors Time, Condition and Hand Side. Mean pain ratings for each condition are shown in ***Figure 6.3***A. A statistically significant main effect of Time was found, with lower pain ratings post LFS ($F(1, 16) = 9.9$ $p = .006$, $\eta^2_p = .38$). Pain intensity during laser stimulation did not differ in active and sham Conditions ($F(1,16) = .88$, $p > .05$, $\eta^2_p = .05$) or ulnar and radial Hand Sides ($F(1, 16) = .13$, $p > .05$, $\eta^2_p = .01$).

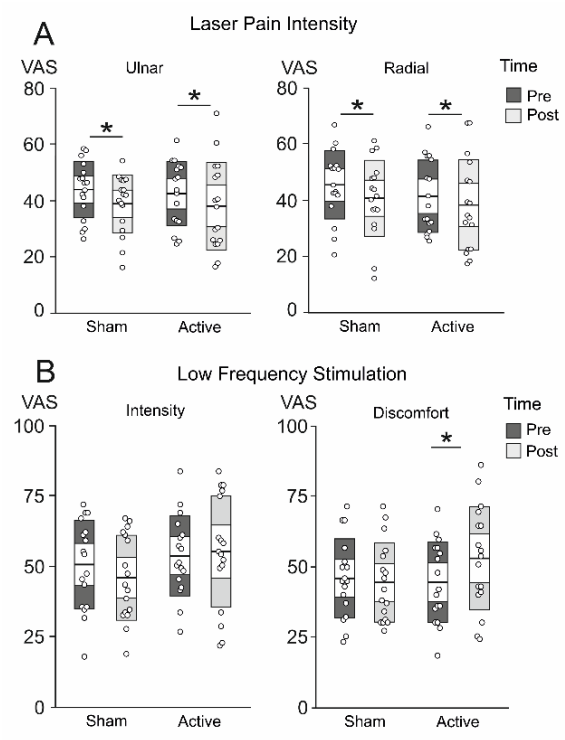

Figure 6.3. Effects of low frequency stimulation (LFS) on participants' ratings of laser pain intensity and LFS intensity and discomfort. **A.** Ratings for noxious laser stimuli applied to ulnar and radial sectors of the hand dorsum before (pre) and after (post) sham or active LFS. Pain ratings were made after each stimulus on a computerised visual analogue scale (VAS) from 0-100, with 30 indicating pain threshold. **B.** Ratings of LFS intensity and discomfort were made to a single stimulus prior to LFS (pre) and as an average score after LFS (post) on a paper VAS scale from 0-100. Box plots show mean ratings, a white inner box of 95% confidence intervals, and a grey outer box for 1 standard deviation. Individual subject data is overlaid as circles. Asterisks indicate results that exceeded corrected significance of $p < .05$.

The N1 component was present as a negative maximum in the contralateral central source derivations overlying the sensorimotor cortex and as another, comparatively weak, negative potential in contralateral temporal source derivations. The topographic maps of the N1 potential in the 140–170 ms latency epoch in active and sham conditions before and after peripheral nerve stimulation are shown in ***Figure 6.4***A. There was a significant main effect of Time in a cluster of source derivations (electrodes 105, 106, 80, 87 and 129) overlying the left central scalp region ($F(1,16) = 15.7$, $p < .001$, $\eta^2_p = .50$), with a reduction of N1 after both active and sham stimulation (***Figure 6.4***D and G). N1 amplitude did not differ by Condition ($F(1,16) = .002$, $p > .05$) or Hand Side ($F(1,16) = .004$, $p > .05$).

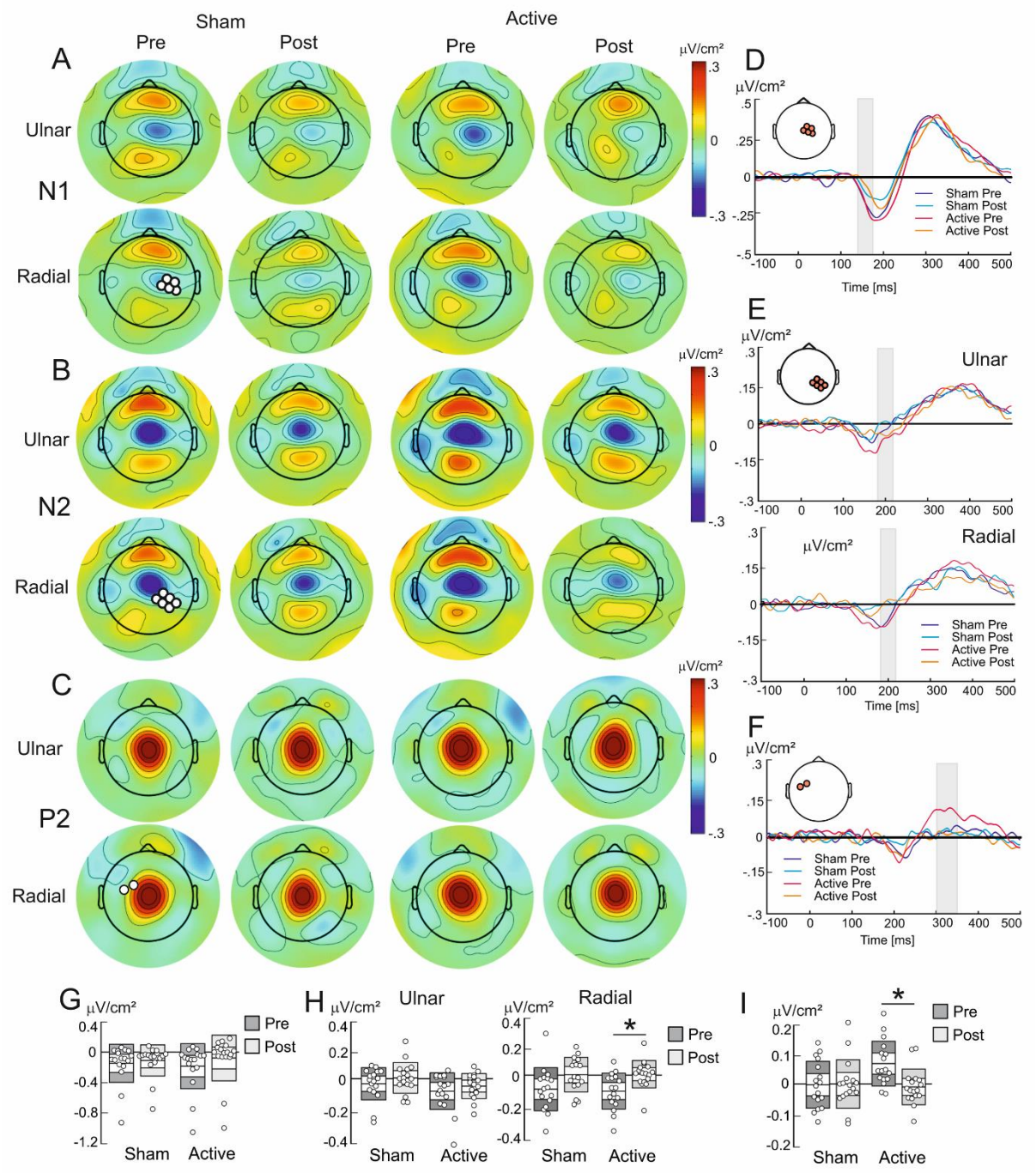

Figure 6.4 Effects of low frequency stimulation (LFS) on laser evoked potentials (LEPs) for non-conditioned (ulnar) and conditioned (radial) hand sides. LEPs were spatially smoothed using a Laplacian spherical spline operator (m = 4) to minimise effects of volume conduction (Perrin et al. 1989). Grand average topographic maps of each component of the LEP are shown (**A-C**) alongside an overhead view of electrodes showing statistically significant changes ($p < .05$) across LFS Condition and Time, averaged over hand sides (**D** and **F**), and across LFS Condition and Time for ulnar and radial hand sides (**E**). Box plots show the mean amplitude of the cluster (µV/cm²) in the selected latency window (**G-I**). Inner (white) and outer (grey) boxes represent 95% confidence intervals and 1 standard deviation, respectively. Individual subject data is overlaid as circles. Asterisks indicate results that exceeded corrected significance of $p < .05$. **A.** The N1 component between 140-160 ms in electrodes 105, 106, 80, 87 and 129. **B.** The N2 component between 180-210 ms in electrodes 79, 86,

87, 92, 93 and 98. **C.** The P2 component between 300-350 ms in electrodes 29 and 35. Ms = milliseconds. μV/cm² = microvolts per centimetre squared.

Figure 6.4B shows the topographic maps of N2 LEP components in each of four conditions in the interval 180-210 ms. Contralateral somatosensory electrodes (electrodes 79, 86, 87, 92, 93 and 98) showed a main effect of Time, with a reduction in negativity post stimulation ($F(1, 16) = 15.2$, $p = .001$, $\eta^2_p = .49$). There was no main effect of Hand Side on the N2 component ($F(1,16) = .01$, $p > .05$); however, there was a significant Time × Hand interaction ($F(1,16) = 5.4$, $p = .034$, $\eta^2_p = .25$). Post-hoc t-tests showed that the contrast between ulnar and radial stimuli was significant before LFS ($t(16) = 2.2$, $p = .041$) but not after LFS ($t(16) = 1.4$, $p = .187$), with increased amplitude N2 for stimuli on the radial hand side (***Figure 6.4***E and H). Notably, N2 amplitude was significantly reduced for radial stimuli after LFS ($t(16) = 4.6$, $p < .001$), while N2 amplitude for ulnar stimuli showed no effect ($t(16) = 1.7$, $p = .104$). However, active and sham Conditions did not differ in the amplitude of N2 component ($F(1,16) = 2.2$, $p > .05$, $\eta^2_p = .12$).

Figure 6.4C shows the topographic maps of the P2 component during the interval 300-350 ms. A cluster located at the left edge of the positive maximum of P2 component in the ipsilateral central region of the scalp (electrodes 29 and 35) showed a statistically significant main effect of Time ($F(1,16) = 11.7$, $p = .003$, $\eta^2_p = .43$), with a greater amplitude before active than sham LFS. There was a significant interaction between Time (pre vs. post LFS) and Condition (active vs. sham) ($F(1,16) = 8.6$, $p = .010$, $\eta^2_p = .34$). Post-hoc t-tests showed that there was a significant difference between active and sham stimulation before LFS ($t(16) = -3.1$, $p = .007$), with a greater amplitude prior to active LFS (***Figure 6.4***F and I). Notably, P2 amplitude was statistically reduced post LFS in the active ($t(16) = 4.2$, $p = .001$) but not sham Condition ($t(16) = -.15$, $p > .05$). There was no effect of Hand Side on P2 amplitude ($F(1,16) = 2.1$, $p > .05$, $\eta^2_p = .12$).

6.4.3 Somatosensory-evoked potential (SEP) changes during LFS

6.4.3.1 Subjective ratings of LFS

Differences in subjective ratings of LFS in active and sham conditions pre- and post-stimulation were analysed using a 2×2 repeated measures ANOVA (***Figure 6.3***B). Mean subjective intensity did not vary significantly by Time or Condition ($p > .05$). There was a statistically

significant interaction in subjective LFS discomfort between Condition and Time ($F(1, 16) = 5.51$, $p = .032$, $\eta^2_p = .26$), caused by greater ratings of discomfort after active (53 ± 19, mean ± SD) compared to sham stimulation (44 ± 14; $t(16) = 2.36$, $p = .031$). Importantly, there was no difference in subjective discomfort ratings between active and sham stimulation before LFS ($t(16) = .54$, $p > .05$).

6.4.3.2 Source dipole analysis

The changes in SEPs over 20 minutes of LFS were analysed using source dipole analysis method, which offered the possibility to quantify the changes in SEPs component irrespective of changes in topographic configurations over the duration of LFS. ***Figure 6.5***A shows the global field power in grand average SEPs computed from the data of all participants over all LFS timepoints. The first SEP component after the stimulus artefact was a P66 component showing a positive maximum in posterior parietal electrodes and a negative maximum in frontal electrodes (***Figure 6.5***D); this configuration of potentials indicate the presence of a tangential dipole in the sensorimotor cortex. In the latency epoch of 120–140 ms, the N2 component was seen in the form of a negative maximum in the contralateral (***Figure 6.5***G) and ipsilateral temporal electrodes (***Figure 6.5***J) electrodes suggesting the presence of radial dipoles located in the operculo-insular cortex. Finally, a strong positive potential was seen on the vertex in the latency period 200-250 ms (***Figure 6.5***M). This positive potential maximum was consistent with a radially orientated current dipole located in the medial frontal or parietal cortex.

The four potential components were modelled by a source dipole model shown in ***Figure 6.5***B. The four-dipole model accounted for 81.5% of the variance in the SEP. Addition of a fifth dipole with free orientation and location to the source dipole model resulted in the dipole being placed in the same location and orientation as ECD4, suggesting that the additional dipole did not explain any specific topographic aspect of the potential field; therefore, the four-dipole solution was used. ECD1 was located in the contralateral sensorimotor and premotor cortex (approximate Talairach coordinates: x = 35 mm, y = −10 mm, z = 62 mm). This source waveform had a negative peak at 66 ms (***Figure 6.5***C). ECD2 was located in the upper bank of the right Sylvian fissure comprising the secondary somatosensory cortex (approximate Talairach coordinates: x = 56 mm, y = −27 mm, z = 21 mm). The source waveform had a positive peak in frontal electrodes at 121 ms (***Figure 6.5***F). ECD3

was located in the left Sylvian fissure symmetrical to ECD2, consistent with the ipsilateral secondary somatosensory cortex (approximate Talairach coordinates: x = -56 mm, y = −27 mm, z = 21 mm). The source waveform of ECD3 (***Figure 6.5***I) waveform had a positive peak in frontal electrodes at 141 ms. Finally, ECD4 was located in the medial parietal cortex involving the mid- and posterior cingulate cortex (approximate Talairach coordinates: x = -3 mm, y = −29 mm, z = 53 mm). The ECD4 source waveform had a positive peak across the midline with a latency of 225 ms.

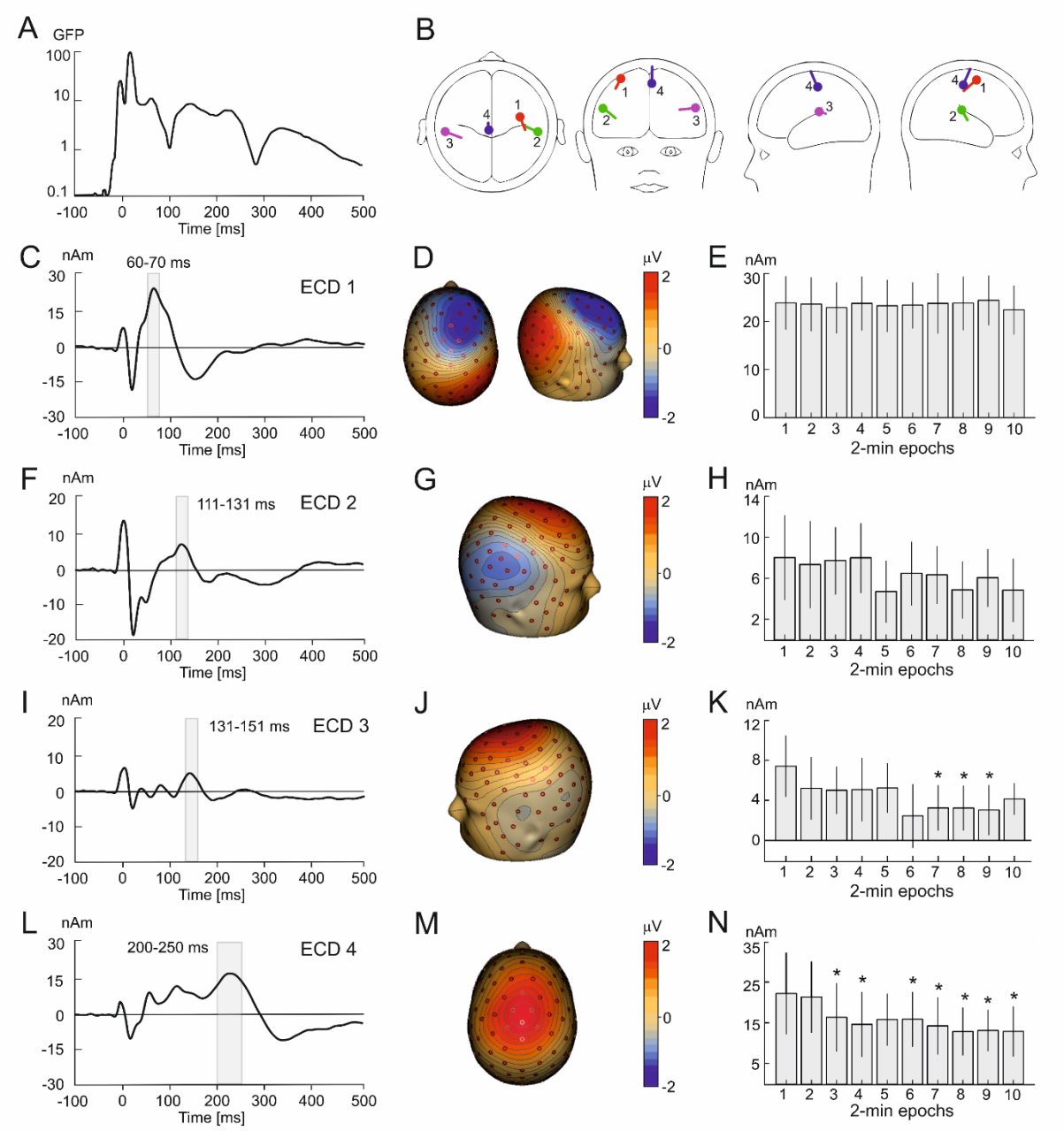

Figure 6.5. Changes in SEPs during 20-min of low frequency stimulation (LFS). **A.** Global field power (GFP) of grand average EEG potentials averaged over all participants and all 2-min epochs over the 20-min duration of LFS. **B.** Location and orientation of four equivalent current dipoles

(ECDs) in transparent glass brains determined using a data-driven sequential strategy. **C.** The time course of ECD1 with a positive peak latency of 66 ms. **D.** Potential maps of the P66 component showing a positive potential maximum in parietal area and a negative maximum in contralateral central and frontal electrodes, consistent with a tangential dipole located in the primary sensorimotor hand area. **E.** The mean amplitudes of ECD1 in the interval 60-70 ms in 10 successive epochs of 2-min duration each. **F.** The time course of ECD2 with a positive peak latency of 121 ms. **G.** Potential maps of the N2 component showing a negative maximum in contralateral temporal electrodes suggesting the presence of a radial dipole located in the operculo-insular cortex. **H.** The mean amplitudes of ECD2 in the interval 111-131 ms in 10 successive epochs of 2-min duration each. **I.** The time course of ECD3 with a positive peak latency of 141 ms. **J.** Potential maps of the N2 component showing a negative maximum in ipsilateral temporal electrodes suggesting the presence of a radial dipole located in the operculo-insular cortex. **K.** The mean amplitudes of ECD3 in the interval 131-151 ms in 10 successive epochs of 2-min duration each. **L.** The time course of ECD4 with a positive peak latency of 225 ms. **M.** Potential maps of the P225 component showing a positive potential on the vertex consistent with a radially orientated current dipole located in the medial frontal or parietal cortex. **N.** The mean amplitudes of ECD4 in the interval 200-250 ms in 10 successive epochs of 2-min duration each. Error bars represent standard error of the mean. Asterisks indicate epochs that exceeded a significant amplitude reduction from the first 2-min epoch, with corrected significance of $p < .05$. Ms = milliseconds. Min = minutes. µV = microvolts. nAm = nano-ampermeters.

6.4.3.3 Statistical analyses of SEP changes

A one-way repeated measures ANOVA was computed to assess changes in peak amplitude of source waveform over the 20-minute duration of LFS. The Huynh-Feldt correction was applied to p-values to tackle a possible violation of the sphericity assumption due to the number of levels in independent variable being larger than two. ECD1 did not show statistically significant changes during LFS ($p > .05$; ***Figure 6.5***E). ECD2 showed some reduction in source amplitude over Time, however this did not reach the statistical significance ($p > .05$; ***Figure 6.5***H). Amplitude of ECD3 was modulated by LFS duration ($F(9,144) = 2.44$, $p = .042$, $\eta^2 = .13$; ***Figure 6.5***K). Simple contrasts from T1 (1-2 minutes) indicated that this difference was significant at T7 (13-14 minutes, $p = .020$), T8 (15-16 minutes, $p = .041$) and T9 (17-18 minutes, $p = .041$). The negative linear trend was also statistically significant ($F(1,16) = 5.54$, $p = .032$, $\eta^2 = .26$). ECD4 was significantly reduced over Time ($F(9,144) = 4.49$, $p = .003$, $\eta^2 = .22$; ***Figure 6.5***N). Simple contrasts indicated that the peak amplitude decreased from T1 at all timepoints except T2 (3-4 minutes). There was a significant negative linear trend ($F(1, 16) = 9.69$, $p = .007$, $\eta^2 = .38$), indicating that as LFS duration increased, the amplitude of ECD4 decreased.

6.4.4 Correlations

We hypothesised that the changes in cortical excitability over 20 min of LFS would correlate with the changes in nociceptive processing and spontaneous cortical activity from pre- to post-LFS periods. Therefore, Spearman's correlations were computed to analyse the relationship between the changes of ECD3 and 4, evaluated as the difference in source moments between the 1st and the 10th epoch, and the changes of LEPs and band-power from pre-LFS to post-LFS periods. Only the P2 LEP component showing a statistically significant change from pre- to post-LFS in the active stimulation condition were included into correlation analysis. Similarly, only the clusters of electrodes showing a stronger band power increase after active than sham LFS were used in correlation analysis.

Figure 6.6 shows the statistically significant positive correlation between the change in ECD3 amplitudes during LFS and the change of 8–12 Hz band-power after as compared to before LFS ($r_s(15) = .77$ $p < .001$). As participants showed an increase in alpha activity after LFS, the correlation coefficient indicated that participants showing the largest reduction in source activity in the ipsilateral SII had a smaller increase of resting 8–12 Hz band power after termination of the LFS protocol. No other correlations were statistically significant.

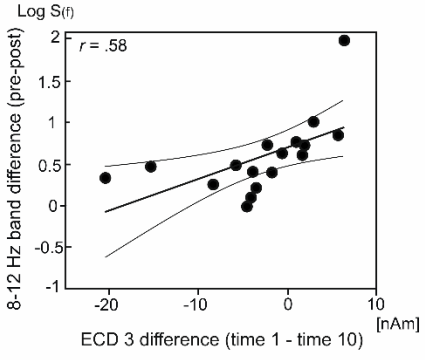

Figure 6.6. Scatter plot, linear regression line and 95% confidence lines illustrating a significant positive correlation between the changes in SEP amplitude in ECD3 and spectral power at 8-12 Hz. Change in ECD3 during LFS was calculated as the difference in amplitude in the last epoch minus the first epoch (T10 – T1), where a decreased value indicates a reduction in source amplitude during LFS, and an increased value indicates increased amplitude during LFS. Power spectra change was calculated as the difference in power in contralateral operculo-insula electrodes in the 8-12 Hz band after LFS (post – pre LFS), where an increased value indicates an increase in spectral power after LFS. ECD = equivalent current dipole. Hz = Hertz. nAm = nano-ampermeters. Log S(f) = logarithmic power spectral density.

6.5 *Discussion*

While recent studies have provided initial evidence of the value of LFS as a treatment for chronic pain, the neural substrates of LFS are poorly understood. The present study analysed electrophysiological changes during and after LFS in healthy volunteers. In line with predictions, repetitive LFS of radial nerves was associated with decreased SEPs in MCC and ipsilateral operculo-insular cortex. Likewise, after stimulation, resting oscillatory power increased in 8-12 Hz and 16-24 Hz frequency bands in source derivations overlying the contralateral operculo-insular, sensorimotor and frontal cortex. A novel component of the current study is the inclusion of an intended-sham condition, which utilised electrical stimulation at a lower frequency than active LFS. This allowed us to investigate if neural and behavioural changes were due to LFS or a more general habituation effect. While behavioural pain ratings and the amplitudes of N1 and N2 LEP components decreased equally after active and sham stimulation, there was a stronger decrease in P2 amplitude after active LFS. Similarly, greater decreases in N2 amplitude were observed on the conditioned radial hand side after LFS. Greater diminutions of source activity in the ipsilateral operculo-insular cortex during LFS positively correlated with smaller post-stimulation increases of 8–12 Hz band power in electrodes overlying the contralateral operculo-insular cortex.

Linear reductions of source activity during ongoing LFS were observed most notably in MCC (225 ms). The MCC, formerly the dorsal ACC (Vogt, 2005; Vogt et al., 2003), has been frequently implicated in nociceptive (Geuter et al., 2020; Jensen et al., 2016; Wager et al., 2013; Xu et al., 2020) and salient non-nociceptive stimulus processing (Hu et al., 2015; Liang et al., 2019; Mouraux & Iannetti, 2009). MCC shows preferential activation for onsets, rather than sustained phases, of nociceptive and innocuous sensory stimuli (Hu et al., 2015), supporting a general role in coding for stimulus novelty. Cognitively-demanding tasks have been shown to activate MCC (Devinsky et al., 1995; Silvestrini et al., 2020), and increased attentional demands during such tasks have been shown to reduce pain ratings and MCC activation to concurrent pain stimuli (Bantick et al., 2002). In contrast, MCC engagement during cognitively-demanding tasks has been shown to increase pain ratings and MCC activity to subsequent pain stimuli (Silvestrini et al., 2020). Similarly, negative expectations can enhance neural responses to noxious laser stimuli in MCC, with the effect most

pronounced in individuals with highest fear of pain (Almarzouki et al., 2017). Consequently, MCC has been linked to a variety of domain-general processes including multisensory orientation, cognitive control, negative affect, and attention to and expectation of pain (Davis et al., 1997; Shackman et al., 2011; Torta & Cauda, 2011; Vogt, 2016). Taken together with the current findings, this suggests that LFS may elicit engagement of multimodal cognitive processes involving the cingulate cortex that may act as a regulatory mechanism for pain (Silvestrini et al., 2020).

Reductions of source activity during LFS were observed to a lesser degree in the ipsilateral operculo-insular cortex (141 ms). The operculo-insular cortex has consistently been linked to pain perception based on combined evidence from electrophysiology and functional imaging studies (Duerden & Albanese, 2013; Horing et al., 2019; Hu et al., 2015; Peyron et al., 2000, 2002; Wager et al., 2013). Increased activation has been found with heightened subjective pain intensity (Segerdahl et al., 2015; Su et al., 2019), and intracortical stimulation of the insula can elicit pain (Afif et al., 2008; Mazzola et al., 2009, 2012; Ostrowsky et al., 2002). Echoing findings within the MCC, overlapping regions of the insula respond to both nociceptive and non-nociceptive stimuli such as tactile, auditory and visual stimuli (Baliki et al., 2009; Liang et al., 2019; Liberati et al., 2016; Mouraux et al., 2011), with magnitude determined by stimulus saliency (Su et al., 2019) or intensity (Baliki et al., 2009). As participants rated LFS intensity equivalently at the start and end of stimulation, reduced operculo-insular source activity is best explained by reduced saliency over repeated trials.

To probe the analgesic effects of LFS, we investigated its impact on behavioural and neural processing of laser stimuli. Reductions in pain sensitivity and cortical SEPs are generally accepted as human correlates of LTD, due to difficulties in directly measuring changes in synaptic efficacy in humans (Klein, 2004; Klein et al., 2006; Rottmann et al., 2008). In line with previous studies, our results show reduced pain ratings to noxious laser stimuli after LFS (Ellrich, 2004; Ellrich & Schorr, 2004; Jung et al., 2012; Klein, 2004; Rottmann et al., 2008). However, this effect was independent of stimulation type, with no greater effect of active or sham stimulation on pain ratings. As the aforementioned studies have compared LFS to a control of no stimulation (however, see Mucke et al. (2014) for an alternative sham design), these findings extend the literature by suggesting that decreased pain ratings may be due to central habituation rather than a correlate of LTD. However, it is

important to note that while the current study is novel in its use of intended-sham stimulation, there was a difference in total energy between sham and active stimulation due to the reduced number of pulses (12 vs 1200). These results therefore need to be interpreted with caution; future studies could investigate the effect of varying parameters for LFS.

Alongside behavioural ratings, we investigated the effect of LFS on cortical LEPs. Results indicated attenuation of the N2 component (190–210 ms) after LFS in contralateral somatosensory electrodes on the conditioned radial hand side and a reduction of P2 component (310-340 ms) amplitude in ipsilateral central electrodes after active LFS, consistent with an attentional modulation of nociceptive processing. N1 and N2 components are enhanced with selective spatial attention to the location of stimulation (Franz et al., 2015; Legrain et al., 2002), particularly in threatening contexts where defensive motor responses are required (Almarzouki et al., 2017; Moayedi et al., 2015, 2016). Reduced N2 amplitude on the radial hand side after LFS could therefore indicate reduced threat from nociceptive stimuli due to conditioning. In contrast, the P2 component is enhanced by unpredictable or rarely-presented deviant laser stimuli (Clark et al., 2008; Legrain et al., 2002, 2003), and is interpreted to reflect involuntary attentional capture by nociceptive events due to stimulus novelty and saliency (Legrain et al., 2009; Wang et al., 2010). As active LFS used a greater number of repeated stimuli in comparison to sham stimulation, reduced P2 amplitude post-treatment may be due to reduced stimulus saliency which is coded by the P2 component (Legrain et al., 2012; Mouraux & Iannetti, 2009), in line with findings of a decrease in SEPs in the operculo-insular during LFS. However, it is worth noting that P2 amplitude was also increased in the pre-LFS condition. The reason for this is not understood; as the order of sham and active sessions were varied between participants, it is unlikely to be the result of differing attention or saliency before LFS.

Due to the absence of specific and preferential effects of LFS on nociceptive processing in the conditioned (radial) hand territory, a more plausible explanation for LEP and behavioural results is integration of effects of LFS on nociceptive processing at a spinal level. Wide dynamic range (WDR) neurons in the dorsal horn show graded responses in firing rates to increasingly intense nociceptive and non-nociceptive stimulation, with stimulus-response functions in accordance with increases in subjective pain reports (Coghill et al., 1993; Mayer et al., 1975). In contrast to nociceptive-specific

neurons, WDR neurons have large, overlapping receptive fields, comprising a centre zone that responds to innocuous and noxious stimuli, and a peripheral surround zone that responds only to intense, noxious stimuli (Bushnell et al., 1984; Price et al., 1978). Innocuous stimuli increase WDR neuron firing rate in precise regions, whereas noxious stimuli activate centre zones and increasingly peripheral receptive fields which can span multiple dermatomes (Bushnell et al., 1984; Price et al., 1978; Coghill et al., 1993, 1991). This process of increased rostro-caudal recruitment is supported by primary afferent fibre projection in Lissauer's tract (Lidierth, 2007; Traub et al., 1986) and propriospinal interconnections (Coghill, 2020; Skinner et al., 1980). Increased spatial recruitment and integration of somatosensory input at the spinal level may explain the absence of preferential effects of LFS on nociceptive processing, with spreading activation between the conditioned and non-conditioned hand sides with repetitive, intense stimuli. This is supported by greater discomfort ratings after active LFS. However, integration of LFS effects could also occur at the cortical level. It should be also noted that LFS may not provide as fine-grained a somatotopic representation of radial and ulnar sides of the hand as LEPs.

Changes in resting oscillatory activity were investigated before and after LFS. LFS was followed by post-stimulus relative increases in 8–12 Hz alpha and 16–24 Hz beta band power in electrodes overlying the contralateral operculo-insular and sensorimotor cortex. Increased alpha and beta band power have been proposed as correlates of cortical idling or active inhibition (Neuper & Pfurtscheller, 2001b; Pfurtscheller et al., 1996b). Cortical inhibition after active LFS may be due to increased local concentrations of the inhibitory neurotransmitter GABA (Gaetz et al., 2011; Hall et al., 2010). Increased GABA has been shown to enhance SI/MI beta band power and reduce beta oscillation frequency after GABAergic agonist benzodiazepine administration (Jensen et al., 2005), and increase beta power and enhance beta-ERD when GABA reuptake is blocked, suggesting a GABA-A receptor mediated process (Muthukumaraswamy et al., 2013). This provides support for an increase in cortical inhibition in regions that mediate sensory perception during LFS.

While 8-12 Hz alpha band power increased after termination of LFS, a smaller increase in alpha band power in electrodes overlying the contralateral operculo-insular cortex was correlated with a stronger reduction in ipsilateral operculo-insular cortex source activity during LFS. As increased

alpha band-power has been shown to be associated with sensory gating via cortical inhibition (Foxe & Snyder, 2011; Fry et al., 2016; Neuper & Pfurtscheller, 2001b; Pfurtscheller et al., 1996b), it is possible that increased alpha band-power after LFS could reflect a habituation effect mediated by inhibition of the operculo-insular cortex (Condes-Lara et al., 1981). In contrast, in participants with the strongest inhibition of source activity, LFS may gate inhibition and enhance cortical excitation through thalamocortical and cortico-cortical pathways (Jensen & Mazaheri, 2010; Pfurtscheller & Lopes da Silva, 1999), supporting an active role of the operculo-insular cortex in the modulation of noxious and somatosensory processing after LFS. As alpha band power is tightly linked to attentional mechanisms (Foxe & Snyder, 2011; Klimesch et al., 1998), it is also possible that band-power was influenced by selective attention towards or away from stimulation. Attentional focus was not manipulated or controlled in the present study and therefore, we cannot definitively conclude that attention played a role in attenuation of SEPs; however, future studies could seek to clarify this by modulating attention during LFS.

Chronic pain is associated with alterations in structural and functional brain activity. Abnormal functional connectivity is a common feature across chronic pain conditions, with evidence of increased connectivity of the insular cortex (Baliki et al., 2014; Napadow et al., 2010) and networks including the MCC (Cauda et al., 2009) in proportion to pain intensity. Altered functional connectivity between the insula and cingulate cortex has been reported in patients with temporomandibular disorder (Ichesco et al., 2012), and increased cerebral blood flow in the anterior MCC during motor cortex stimulation for refractory neuropathic pain has been shown to correlate positively with pain relief (Peyron et al., 2007). Thus, reduced activity in the operculo-insular and MCC during LFS could reduce pain by targeting nociceptive or salience networks which are disrupted in chronic pain.

While the absence of specific analgesic effects of LFS is an important and novel finding, limitations of the study design may have contributed to this effect. Firstly, the LFS intensity used in the current study may have precluded the development of analgesia. In contrast to previous literature (Jung et al., 2009), we used an uncomfortable, non-noxious LFS intensity to reduce participant burden. Lower LFS intensities may not activate Aδ fibres, which are essential to elicit LTD of

nociception (Kaube et al., 2000; Randić et al., 1993; Sandkühler et al., 1997). To our knowledge, this is the first study investigating the effects of LFS on laser-evoked pain. Laser stimuli is phasic and short-lasting, exciting Aδ- and C-fibres (Bromm et al., 1984). However, high frequency electrical stimulation (HFS) used to induce short-lasting pain amplification (Klein, 2004; Magerl et al., 2018; Pfau et al., 2011; Randić et al., 1993) has been suggested to be ineffective at modulating Aδ- (van den Broeke & Mouraux, 2014) and C-fibre mediated pain (Lang et al., 2007), although varied protocols mean that evidence is somewhat contradictory.

In humans, reduced subjective pain ratings (Jung et al., 2009; Klein, 2004; Lindelof et al., 2010) and reduced SEP amplitudes (Ellrich & Schorr, 2004; Jung et al., 2009) have been suggested as correlates of LTD; however, as alterations in synaptic plasticity cannot be directly accessed in humans in vivo, we are unable to conclude that the neurobiological basis for MCC reduction is LTD from the present study. Due to time limitations, the current study was restricted to investigating only one post-stimulation timepoint directly after LFS. While previous studies report that reductions from LFS occur immediately after conditioning and are sustained for up to 1 hour after LFS (e.g. Ellrich and Schorr 2004; Aymanns et al. 2009) showing sustained cortical changes at subsequent timepoints would have further validated the paradigm in eliciting a LTD-like inhibition of somatosensory processing. Thus, we have been cautious in our interpretation of these results and the links with LTD. Future studies should address the question of long-term changes in cortical excitability occurring in the hours following LFS.

Results show for the first time a decreased excitability in MCC and ipsilateral operculo-insular cortex during LFS, and an increase in cortical resting oscillations in contralateral operculo-insular and SI/MI cortex after LFS. Taken together, these findings suggest that LFS is associated with decreased activations in thalamocortical nociceptive and salience networks. This study has important clinical implications for the use of LFS in palliative treatments for chronic pain, highlighting the significance of cognitive mechanisms in pain modulation. Further research could seek to clarify if these regions are also implicated in the maintenance of LTD, and in the reduction of chronic pain using LFS.

Chapter 7

Intensity-dependent modulation of cortical somatosensory processing during external, low-frequency peripheral nerve stimulation in humans

Danielle Hewitt[1], Alice Newton-Fenner[1,2], Jessica Henderson[1], Nicholas Fallon[1], Christopher Brown[1], Andrej Stancak[1]

[1] Department of Psychological Sciences, University of Liverpool, Liverpool, UK.

[2] Institute for Risk and Uncertainty, University of Liverpool, Liverpool, UK.

This experiment used source dipole modelling to investigate temporal changes in SEPs during four intensities of LFS, and investigated the effects of LFS intensity on post-stimulation resting oscillations.

This paper was published in the Journal of Neurophysiology (2022), doi: https://doi.org/10.1016/j.clinph.2021.03.024

The format of the text has been modified to match the style of this thesis.

The roles of the co-authors are summarised below:

Danielle Hewitt: Conceptualisation, Methodology, Software, Investigation, Formal analysis, Writing - Original Draft, Writing - Review & Editing. **Alice Newton-Fenner:** Investigation, Writing - Review & Editing. **Jessica Henderson:** Investigation, Writing - Review & Editing. **Nicholas Fallon:** Writing - Review & Editing. **Christopher Brown:** Writing - Review & Editing. **Andrej Stancak:** Conceptualisation, Software, Formal analysis, Writing - Original Draft, Writing - Review & Editing, Supervision, Funding acquisition.

7 Intensity-dependent modulation of cortical somatosensory processing during external, low-frequency peripheral nerve stimulation in humans

7.1 Abstract

External LFS has been proposed as a novel method for neuropathic pain relief. Previous studies have reported that LFS elicits LTD-like effects on human pain perception when delivered at noxious intensities, while lower intensities are ineffective. To shed light on cortical regions mediating the effects of LFS, we investigated changes in SEPs during four LFS intensities.

LFS was applied to the radial nerve (600 pulses, 1 Hz) of twenty-four healthy participants at perception (1×), low (5×), medium (10×) and high intensities (15× detection threshold). SEPs were recorded during LFS, and averaged SEPs in 10 consecutive one-minute epochs of LFS were analysed using source dipole modelling. Changes in resting EEG were investigated after each LFS block.

Source activity in the MCC decreased linearly during LFS, with greater attenuation at stronger LFS intensities, and in the ipsilateral operculo-insular cortex during the two lowest LFS stimulus intensities. Increased LFS intensities resulted in greater augmentation of contralateral SI/MI activity. Stronger LFS intensities were followed by increased alpha (9–11 Hz) band power in SI/MI and decreased theta (3–5 Hz) band power in MCC.

Intensity-dependent attenuation of MCC activity with LFS is consistent with a state of LTD. Sustained increases in contralateral SI/MI activity suggests that effects of LFS on somatosensory processing may also be dependent on satiation of SI/MI. Further research could clarify if the activation of SI/MI during LFS competes with nociceptive processing in neuropathic pain.

7.2 *Introduction*

Neuropathic pain, defined as pain caused by a lesion or disease in the somatosensory system (Treede et al., 2008), is characterised by spontaneous pain, heightened pain sensitivity and sensory loss (Finnerup et al., 2016; Scholz et al., 2019). Neuropathic pain syndromes affect approximately 7–10% of the general population (van Hecke et al., 2014), with considerable impacts on quality of life and functioning (Smith & Torrance, 2012). First-line pharmacological treatments for neuropathic pain are associated with modest efficacy and adverse side effects (Cavalli et al., 2019; Di Stefano et al., 2021; Finnerup et al., 2015); therefore, the development of new, effective treatments is of vital importance.

External LFS has been proposed as a novel neurostimulation method for intractable neuropathic pain syndromes (Johnson et al., 2015; Johnson & Goebel, 2016). LTD of synaptic efficacy is theorised as the neurophysiological mechanism underlying LFS (Sandkühler et al., 1997). LTD has been demonstrated at many sites in the central nervous system and can be induced in the nociceptive system after repetitive LFS (~1–2 Hz) of Aδ fibres in the spinal dorsal horn both *in vitro* (Chen & Sandkühler, 2000; Ikeda et al., 2000; Kim et al., 2015; Sandkühler et al., 1997) and *in vivo* (Liu et al., 1998). Conversely, high frequency stimulation (HFS, ~100 Hz) of primary afferent fibres induces long-term potentiation of Aδ (Randić et al., 1993) and C-fibre responses (Ikeda et al., 2003, 2006; Liu et al., 2009; Svendsen et al., 1997), and may be a mechanism for pain amplification in acute and chronic pain states (Sandkühler, 2007; Sandkühler & Gruber-Schoffnegger, 2012). Long-term potentiation in the dorsal horn can be inhibited and reversed with LFS (Ikeda et al., 2000; Liu et al., 1998; Sandkühler et al., 1997); therefore, LFS has important implications for our understanding of neuropathic pain.

Alterations in synaptic plasticity cannot be directly measured in humans, although changes in pain ratings and pain-related neural activity after LFS have been interpreted as indirect correlates of nociceptive LTD. In these studies, preferential activation of Aδ fibres through the skin is assumed with small diameter electrodes which deliver high current densities (Hugosdottir et al., 2019; Inui et al., 2002; Mørch et al., 2011; Nilsson & Schouenborg, 1999; Rottmann et al., 2008). LFS of peripheral nerve fibres in humans is associated with a sustained, homotopic decrease in perceived

pain to noxious electrical stimuli (Aymanns et al., 2009; Jung et al., 2009; Klein, 2004; Lindelof et al., 2010) and a reversal of experimentally-induced hyperalgesia (Klein, 2004; Magerl et al., 2018). LFS has been shown to decrease the amplitude of SEPs recorded with EEG during noxious electrical test stimuli (Ellrich & Schorr, 2004; Jung et al., 2009; Rottmann et al., 2008). Thus, LFS appears to elicit strong effects on somatosensory processing in humans.

While the post-stimulation effects of LFS on nociceptive processing are well established, few studies have investigated neural activation changes during the time course of LFS. We recently demonstrated in healthy volunteers that LFS is associated with source activity in SI/MI, bilateral operculo-insular cortex and MCC (Hewitt et al., 2021). By recording SEPs over the duration of LFS, we showed a linear decrease in SEP amplitude in the MCC and ipsilateral operculo-insular cortex. These findings are in line with previous studies demonstrating that LFS is associated with a linear decrease in excitatory postsynaptic potentials *in vitro* (Sandkühler et al., 1997) and gradual decreases in pain ratings during LFS conditioning in humans (Biurrun Manresa et al., 2010; Klein, 2004; Rottmann et al., 2008; Vo & Drummond, 2014). We also showed that LFS was associated with post-stimulation increases in 8–12 Hz alpha and 16–24 Hz beta band power in electrodes overlying contralateral operculo-insular and sensorimotor cortices (Hewitt et al., 2021), consistent with cortical inhibition and idling in regions that mediate sensory perception (Neuper & Pfurtscheller, 2001b; Pfurtscheller et al., 1996b). Taken together, this indicates that LFS has lasting, inhibitory effects on sensory processing that may be mediated by the midcingulate and operculo-insular cortex.

Induction of LTD has been shown to be dependent on LFS intensity. It is well established that LFS of afferent fibres at noxious intensities sufficient to activate Aδ fibres induces sustained LTD, while lower intensities activating Aβ fibres produce no inhibition (Sdrulla et al., 2015) or only a transient decrease in synaptic transmission (Liu et al., 1998; Sandkühler et al., 1997). Likewise, in human studies, maximal reduction in SEP amplitude and acute pain perception have been observed after 1200 pulses of 1 Hz stimulation at 4× pain threshold, corresponding to 15× detection threshold (Jung et al., 2009). Conversely, lower intensities at 1× and 2× pain threshold produced a smaller reduction in SEPs and pain ratings. In our recent study, we used a distinctly uncomfortable but not painful LFS intensity which may have been insufficient to activate Aδ fibres (Hewitt et al., 2021).

Thus, to examine if reduced amplitude of SEPs estimated to be generated by the MCC and operculo-insular cortex during LFS are specific to LTD, it is crucial to compare the effects of noxious intensities of LFS to stimulation at nonpainful intensities.

To shed light on the cortical regions mediating the suppression of activity during nonpainful and noxious intensities of LFS, we investigated changes in SEPs and post-stimulation resting oscillations with four intensities of continuous LFS in healthy human volunteers. Based on previous evidence that 15× detection threshold is sufficient to elicit attenuation of SEPs (Jung et al., 2009), the four intensities used were 1×, 5×, 10× and 15× detection threshold. Using source analysis, we characterised the locations of sources contributing to the SEPs and how activity in the sources changed over the duration of LFS. We predicted that LFS would be associated with a linear reduction of SEP amplitude in sources originating in the MCC and ipsilateral operculo-insular cortex, and that the greatest reduction in SEP amplitude would be found in these sources at the highest LFS intensity. We secondly investigated whether the cortical regions showing activation changes over the period of LFS would similarly show post-stimulation modulation of resting oscillatory activity. It was predicted that greater intensities of LFS would be associated with greater increases in alpha and beta band power and decreases in theta band power in source signals generated in operculo-insular and cingulate cortex.

7.3 Methods

7.3.1 Subjects

Twenty-eight healthy subjects (14 females) with no history of chronic pain or neurological conditions were recruited from a pool of undergraduate and postgraduate students at the University of Liverpool. Four subjects were excluded during data collection: three as they could not tolerate the electrical stimulation and one due to excessive movement artifacts. The final sample included 24 participants (11 females, 22 right-handed) with a mean age of 25 ± 4.2 years (mean ± SD). The procedure was approved by the Research Ethics Committee of the University of Liverpool, and all participants gave written informed consent at the start of the experiment in accordance with the Declaration of Helsinki. Participants were reimbursed with £20 for their time on completion of the study.

7.3.2 Experimental protocol

Experimental procedures were carried out in a single 2-hour session in the Eleanor Rathbone Building, University of Liverpool. Electrical detection thresholds were determined prior to the start of the experiment using the method of limits. During the experiment, participants were seated in a dimly lit room with a 19-inch LCD monitor in front of them. Participants were instructed to keep their eyes open and look straight ahead for 4 minutes during the recording of resting EEG.

LFS was applied to the dorsal aspect of the hand during four conditions, each modulated by LFS intensity: perception (1× detection threshold), low (5× detection threshold), medium (10× detection threshold) and high (15× detection threshold). Each block of LFS lasted approximately 10 minutes. Participants were randomly assigned one of six possible block orders with each block order represented four times. Presentation of LFS stimuli was controlled with Cogent 2000 (University College London, London, UK) in MATLAB 2010 (The Mathworks, Inc., USA). After each block of LFS, resting EEG was recorded for 4-minutes while participants looked straight ahead with eyes open, followed by a break of 6-minutes to ensure that participants remained alert and to allow the researcher to check electrode impedances.

Participants' ratings of electrical stimulation were collected at the start of the experiment and after each block of stimulation by applying a single electrical stimulus to the test site using the conditioning LFS electrode. Participants were informed that the intensity of test stimulation was the maximum level that they would receive during the experiment, but that their perception of the stimulus may change throughout the study. Participants were asked to rate the painfulness of the test stimuli on a verbal numeric rating scale from 0 (no pain) to 10 (maximum pain), where 3 indicated pain threshold, and unpleasantness from 0 (not at all unpleasant) to 10 (maximum unpleasantness).

7.3.2.1 Electrical stimulation

LFS was applied to the skin in the region of the radial nerve of the left hand using a nerve mapping pen electrode with 4mm diameter cathode (Compex Motor Point Pen, UK) and a distal 5cm2 flat electrode by the olecranon process which served as an anode, controlled by a Digitimer DS7A constant current stimulator (Digitimer, UK) and MATLAB 2010. Electrodes using a small cathode area such as pin, concentric or pen electrodes been designed to preferentially activate Aδ fibres

without co-activation of Aβ fibres (Bromm & Meier, 1984; Inui et al., 2002; Kaube et al., 2000; Mücke et al., 2014; Nilsson & Schouenborg, 1999). To the best of our knowledge, the proportion of Aδ and Aβ fibre involvement during low- or high-intensity LFS is not known.

Stimulus detection threshold was determined at the start of the experiment using the method of limits, where single electrical stimuli were delivered to the test site in descending and ascending steps of 0.02 milliamperes (mA) to establish the lowest threshold at which participants could perceive the stimuli (detection threshold). During the experiment, LFS was applied at four intensities calculated as multiples of detection threshold: 1×, 5×, 10×, or 15× detection threshold, with the highest intensity in line with previous studies using LFS (Jung et al., 2009; Torta et al., 2020). If participants found the high intensity condition to be intolerable, intensity was reduced to a painful but tolerable level, and medium and low intensity conditions were modified to 66% and 33% of the high intensity, respectively. Mean stimulus intensities were: perception 0.12 ± 0.04 mA, low 0.63 ± 0.32 mA, medium 1.19 ± 0.39 mA and high 1.78 ± 0.59 mA. An independent-samples t-test showed that electrical detection threshold was higher in male (M = 0.14 mV, SD = 0.04) compared to female participants (M = 0.11 mV, SD = 0.04; t(22) = 2.09, p = .048). Each block of LFS consisted of 600 pulses at delivered at a frequency of 1 Hz, pulse width 1 ms, duration 1 ms. The total number of pulses was reduced in contrast to previous studies with LFS to reduce the burden on participants, based on evidence that these parameters are sufficient to elicit a prolonged suppression of SEPs and pain ratings to electrical test stimuli (Jung et al., 2009). In addition, single electrical test stimuli were applied to the test site at the high intensity (15× detection threshold) at baseline and after each LFS block using the same electrode as the conditioning stimulus.

7.3.3 EEG acquisition

Continuous EEG was recorded using a 129-channel Geodesics EGI System (Electrical Geodesics, Inc., Eugene, Oregon, USA) with a sponge-based HydroCel Sensor Net. The sensor net was aligned with respect to three anatomical landmarks of two preauricular points and the nasion. Electrode-to-skin impedances were kept below 50 kΩ throughout the experiment. A recording band-

pass filter was set at 0.001–200 Hz with a sampling rate of 1000 Hz. Electrode Cz was used as a reference electrode during the recordings.

7.3.4 Analysis of LFS ratings

Mean ratings of pain and unpleasantness to electrical test stimuli in each condition were calculated for each participant. To assess differences in pain and unpleasantness ratings of test stimuli after each LFS intensity, 1×4 repeated measures analyses of covariance (ANCOVA) were computed using SPSS v. 27 (IBM Inc., USA) separately for pain and unpleasantness, with an independent variable of 'LFS Intensity' (perception, low, medium, high intensity) and baseline scores as a covariate. Post-hoc t-tests were used where appropriate to investigate significant main effects.

7.3.5 EEG data analysis

EEG data were processed using BESA v. 6.1 (MEGIS GmbH, Germany). Data were filtered using 1 Hz high pass and 70 Hz low pass filters, with a notch filter of 50 Hz ± 2 Hz. EEG data were spatially transformed to reference-free data using common average method (Lehmann, 1987). Oculographic and electrocardiographic artifacts were removed with principal component analysis (Berg & Scherg, 1994). Data were visually inspected for movement and muscle artifacts. Trials containing artifacts were marked and excluded from further analysis. Electrode channels with large artifacts were interpolated to a maximum of 10% of electrodes.

7.3.5.1 Analysis of SEPs during LFS

SEPs were evaluated during 10-minutes of LFS applied to the radial nerve. All 600 SEP responses over the 10-minute recording were divided into ten 1-minute intervals of 60 responses each. SEP responses in each 1-minute interval were averaged in the epoch -100 ms pre-stimulus to 900 ms post-stimulus. The baseline period ranged from -100 to -5 ms prior to stimulus onset, and the stimulus artefact window was defined as -4 to 10 ms post stimulus. Data was filtered during averaging from 1–45 Hz. The mean number of epochs containing SEP responses accepted for further analysis were 56.99 ± .27 (mean ± SE). A repeated-measures ANOVA showed that the average number of accepted epochs was significantly different between LFS intensities ($F(3,69) = 2.86$, $p = .043$) due to fewer accepted epochs during high intensity (56.45 ± .41; $p = .015$) compared to perception intensity LFS

(57.26 ± .26). Accepted epochs were significantly different over the 10-minute duration of LFS ($F(9,207) = 5.69$, $p < .001$). Pairwise comparisons showed a significant increase in the number of accepted epochs in minutes 2–10 compared to minute 1 ($p < .05$). The interaction between LFS intensity and duration was not significant ($p > .05$).

7.3.5.2 Source dipole modelling

Source dipole modelling of SEPs was performed using BESA v. 6.1 (MEGIS GmbH, Germany). The source dipole model was constructed using a sequential strategy as used in our previous study (Hewitt et al., 2021), in which equivalent current dipoles (ECDs) were fitted consecutively from the first peak in global field power (Hoechstetter et al., 2000, 2001; Scherg, 1992; Stancak et al., 2002). Due to the presence of a large stimulus artefact from LFS, dipoles were fitted between 30 ms – 900 ms post-stimulus. When residual variance was not reduced by adding another dipole, the fitting procedure was terminated. Classical LORETA analysis recursively applied (CLARA) method (Hoechstetter et al., 2010) was used as an independent source localisation method to confirm the location of ECDs.

To evaluate the effect of LFS duration on SEPs, the grand average source dipole model was used to compute individual subject source waveforms for all ten 1-minute intervals of LFS. A permutation analysis with 2000 repetitions, implemented in the *statcond.m* program in the EEGLab package (Delorme & Makeig, 2004), was utilised to identify time intervals showing significant main effects and interactions of LFS duration and intensity (Maris & Oostenveld, 2007). This method provides a data-driven approach to test effects across all timepoints whilst controlling for multiple comparisons with no loss in statistical power. Time intervals surrounding source waveform peaks were defined for each ECD (ECD1 35–75 ms, ECD2 100–150 ms, ECD3 105–155 ms, ECD4 150–260 ms). Intervals surrounding ECD peaks that exceeded a predefined threshold on the calculated *p*-values (corrected $p < .001$) for the main effect or interactions of LFS duration and intensity were selected for further analysis. Source dipole moments in intervals deemed significant by permutation tests were entered into individual 4×10 repeated measures ANOVAs involving the 4 LFS intensities (perception, low, medium and high) and each 10-minute interval (minutes 1–10) for each ECD. The

Huynh-Feldt correction was used where necessary to tackle a violation of the sphericity assumption, denoted by ε.

7.3.6 Linear regression analysis

Linear regression analysis was conducted to analyse if source dipole moments showed a systematic decrease in amplitude over time, consistent with LTD. Linear regression analysis was carried out in every subject and each level of LFS intensity, with LFS duration as a predictor variable and source dipole moments as dependent measures. As the regression analysis assessed the slope of change in ECD amplitude over time, only source dipole moments which showed a significant main effect of time were included.

The resultant regression coefficients (β) from linear regression analysis for all subjects were entered into one sample t-tests to examine if any of the 4 LFS intensities showed a significant difference from zero. Regression coefficients showing a significant difference from 0 were compared individually for each ECD using repeated measures ANOVAs to investigate changes across the 4 LFS intensities.

7.3.7 Resting EEG analysis

To evaluate the effect of LFS intensity on ongoing oscillatory activity, the grand average source dipole model was used to compute individual subject source waveforms in resting EEG recorded before LFS and after each LFS intensity. Each ECD in the source dipole model yielded, after back projection onto resting state EEG data using the surrogate model method, a continuous source signal sampled at 256 Hz. Individual continuous source signals for all LFS intensities were exported to MATLAB 2019b for spectral analysis. Power spectral density was estimated using Welch's method in the frequency range 0–128 Hz in non-overlapping 1-second segments. Data were smoothed using a Hamming window. For each subject, time samples containing artifacts were removed from the data prior to spectral analysis, and data were trimmed to the length of the shortest condition to avoid differences in data length affecting the results. The mean duration of resting EEG data for which power spectra were estimated was 231 ± 7 seconds.

Only frequency components between 1–40 Hz were considered for statistical analysis. Mean absolute power values were transformed using a decadic logarithmic transform. One-way ANOVAs were computed to investigate the effect of LFS intensity (perception, low, medium and high) on spectral power in all frequencies from 1–40 Hz in each of the four ECDs. Analyses were carried out on all frequencies from 1–40 Hz to investigate the specific frequency components showing changes in resting oscillatory activity. Resting EEG recorded prior to LFS was not included in statistical analyses as the order of this condition was not permuted. To control for Type I error likely to occur due to the large number of ANOVAs, the resulting statistical probability values were subject to permutation analysis using the *statcond.m* program with 2000 permutations. Frequency components that exceeded a predefined threshold ($p < .05$) for the main effect of LFS intensity were selected for further analysis. Pairwise comparisons were computed to investigate the direction of effects.

Next, Pearson's correlations were conducted in MATLAB to analyse the relationship between linear regression slopes (β) for change in source dipole amplitude during LFS at each of the four LFS intensities, and change in resting oscillatory band-power after stimulation. Correlations were computed individually for source waveforms showing significant differences from zero, and resting band power after each intensity of LFS in the corresponding source waveforms. To correct for individual variations in resting band power, a baseline correction was implemented by subtracting spectral power prior to stimulation from absolute power after each of the four LFS intensities.

7.4 Results

7.4.1 Mean ratings of electrical test stimuli

Painful electrical test stimuli were delivered at 15× detection threshold. Changes in ratings of electrical test stimuli after the four intensities of LFS were analysed using a 1×4 repeated measures ANCOVA, with baseline ratings as a covariate. Mean pain ratings of test stimuli prior to LFS were 4.5 ± 1.3 (mean ± SD) on a scale of 0–10, where 3 indicated pain threshold. Mean unpleasantness scores for test stimuli prior to LFS were 6.04 ± 1.9 on a scale of 0–10. Subjective pain and unpleasantness ratings for test stimuli did not significantly vary with LFS intensity ($F(3, 66) = 0.4$, $p > .05$; $F(3, 66) = 0.23$, $p > .05$).

7.4.2 Source dipole model

Changes in SEPs over the 10-minutes of LFS were analysed using source dipole analysis. ***Figure 7.1***A shows the source dipole model. Figure 1B shows the global field power in grand average SEPs computed from the data of all participants over all LFS intensities and duration. The four-dipole model accounted for 83.62% of the variance in the SEP. Addition of a fifth dipole with free orientation and location to the source dipole model resulted in an anterior dipole close to ECD4 which did not improve the residual variance; therefore, the four-dipole solution was used. CLARA method was used to verify the location of fitted ECDs. Results were highly convergent between the two models, with a maximum discrepancy of approximately 2 mm between ECD3 and the maxima of the CLARA cluster.

ECD1 was located in the contralateral SI/MI (approximate Talairach coordinates: x = 30 mm, y = -20 mm, z = 60 mm). This source waveform had a negative peak at 56 ms (***Figure 7.1***C–D). ECD2 was located in the upper bank of the right Sylvian fissure comprising the secondary somatosensory cortex (approximate Talairach coordinates: x = 40 mm, y = -23 mm, z = 17 mm). The source waveform had a positive peak in frontal electrodes at 121 ms (***Figure 7.1***E–F). ECD3 was located in the left Sylvian fissure symmetrical to ECD2, consistent with the ipsilateral secondary somatosensory cortex (approximate Talairach coordinates: x = -45 mm, y = -19 mm, z = 20 mm). The source waveform of ECD3 (***Figure 7.1***G–H) waveform had a positive peak in frontal electrodes at 126 ms. Finally, ECD4 was located in the medial parietal cortex involving the mid- and posterior cingulate cortex (approximate Talairach coordinates: x = 8 mm, y = -42 mm, z = 54 mm). The ECD4 source waveform had a positive peak across the vertex with a latency of 182 ms (***Figure 7.1***I–J).

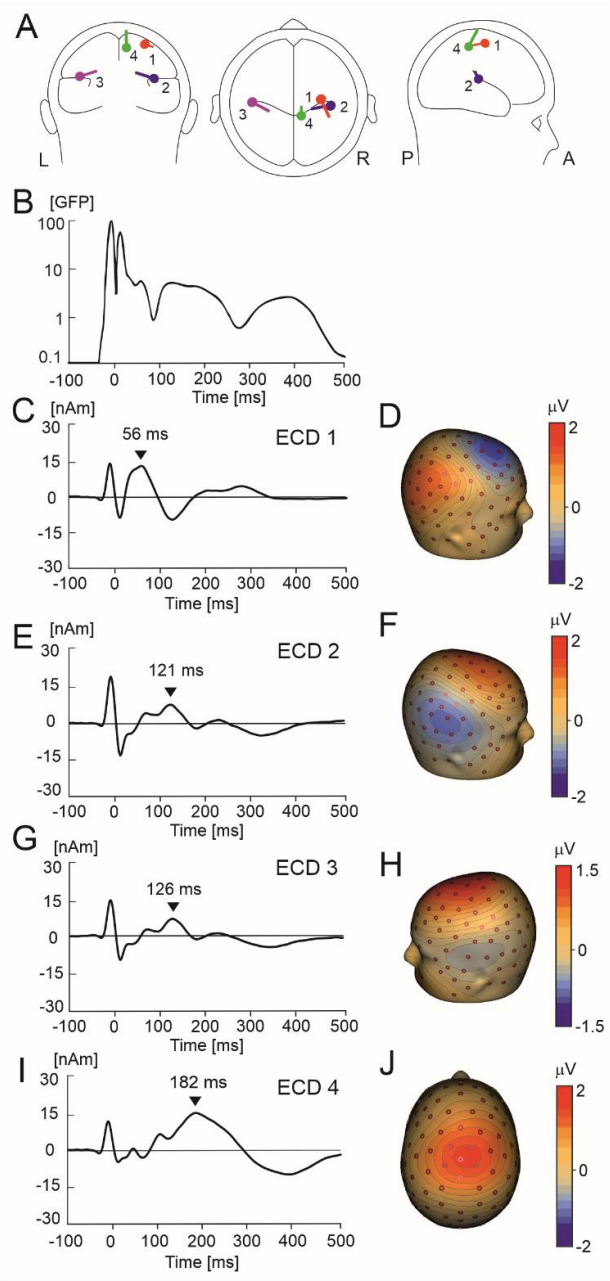

Figure 7.1. Source dipole model of SEPs during 10-mins of LFS. A. Location and orientation of four ECDs in transparent glass brains determined using a data-driven sequential strategy. B. Global field power (GFP) of grand average EEG potentials averaged over all participants (N=24, 11 females) and all 1-min epochs over the 10-min duration of LFS. C. Time course of ECD1 with a positive peak latency of 56 ms. D. Potential maps of the P56 component showing a positive potential maximum in parietal area and a negative maximum in contralateral central and frontal electrodes, consistent with a tangential dipole located in SI/MI. E. Time course of ECD2 with a positive peak latency of 121 ms. F. Potential maps of the N2 component showing a negative maximum in contralateral temporal electrodes, suggesting the presence of a radial dipole located in the contralateral operculo-insular cortex. G. Time course of ECD3 with a positive peak latency of 126 ms. H. Potential maps of the N2 component showing a negative maximum in ipsilateral temporal electrodes, suggestive of a radial dipole located in the operculo-insular cortex. I. ECD4 time course with a positive peak latency of 182 ms. J. Potential maps of the P182 component showing a positive potential on the vertex, consistent with a radially orientated current dipole located in the MCC.

7.4.2.1 Changes in SEPs during LFS

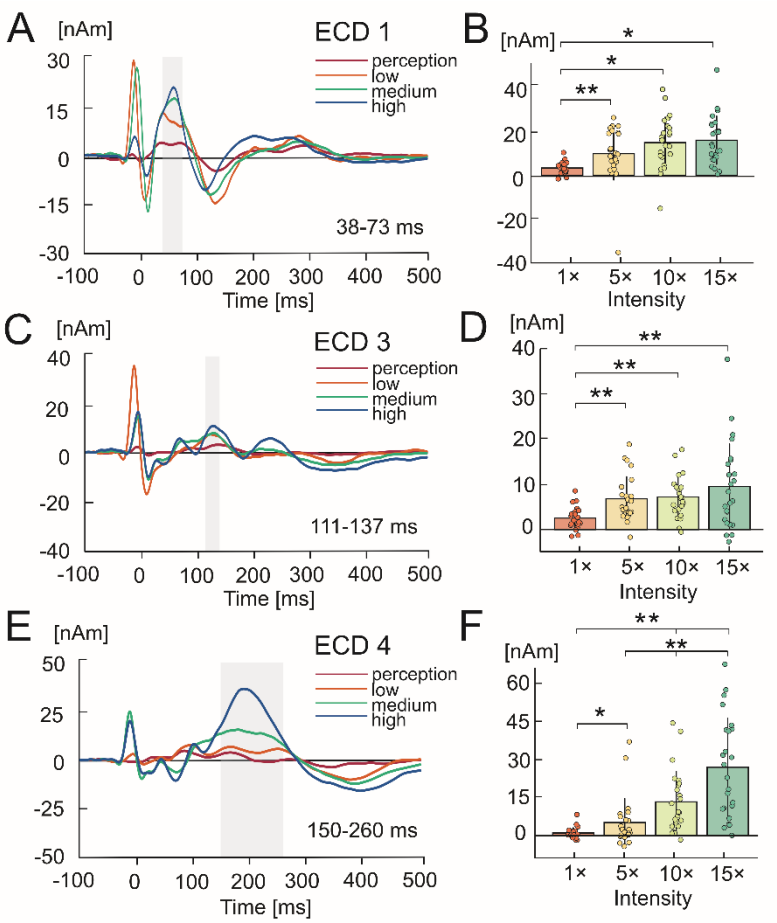

Figure 7.2. Grand average changes in SEPs at varying intensities of low-frequency stimulation (LFS). One-way ANOVAs showed a statistically significant amplitude modulation by LFS intensity for ECD1 (A), ECD3 (C) and ECD4 (E). Shaded bars indicate significant time intervals around source waveform peaks. Bar graphs show the mean amplitudes and standard deviation of ECD1 (B), ECD3 (D) and ECD4 (F) source waveforms during perception (1×), low (5×), medium (10×) and high LFS intensities (15× detection threshold) in corresponding time intervals. Individual subject data points averaged over single trials are overlaid for each condition. Pairwise comparisons were computed to identify contrasts that exceeded significance at p < .05 (*) or p < .001 (**). N=24 (11 females).

Figure 7.2A, C and E show the time intervals around source waveform peaks showing a significant effect of LFS intensity. Amplitude of ECD1 was significantly modulated by LFS intensity ($F(3,69) = 15.57$, $p < .001$, $\eta^2_p = .40$; ***Figure 7.2***B). Pairwise comparisons showed an increase in amplitude at low ($p = .010$), medium ($p < .001$) and high ($p < .001$) LFS intensities compared to the lowest perception level. ECD2 showed no statistically significant changes during LFS ($p > .05$). ECD3 was significantly modulated by LFS intensity ($F(3,69) = 10.68$, $p < .001$, $\varepsilon = .58$, $\eta^2_p = .32$; ***Figure 7.2***D), with an increase in amplitude at low, medium and high LFS intensities compared to the

lowest perception level (all $p < .001$). ECD4 also showed a significant increase in amplitude with LFS intensity ($F(3,69) = 33.76$, $p < .001$, $\varepsilon = .56$, $\eta^2_p = .60$; ***Figure 7.2***F) due to a significant increase in amplitude at greater LFS intensities (perception vs. low, $p = .028$, all other comparisons, $p < .001$). Additionally, the statistical test of trend components confirmed that amplitude increased linearly with greater LFS intensities for ECD1 ($F(1,23) = 40.03$, $p < .001$, $\eta^2_p = .64$), ECD3 ($F(1,23) = 14.04$, $p < .001$, $\eta^2_p = .38$) and ECD4 ($F(1,23) = 46.67$, $p < .001$, $\eta^2_p = .67$) but not for ECD2 ($p > 05$).

Figure 7.3A, D and G illustrate time intervals around source waveform peaks showing a significant effect of LFS duration. ECD1 amplitude was significantly modulated by LFS duration ($F(9,207) = 9.08$, $p < .001$, $\varepsilon = .74$, $\eta^2_p = .28$; ***Figure 7.3***B) in the interval 50–76 ms. Simple contrasts indicated that this effect was due to an increase in amplitude during minutes 2 ($p = .006$), 3 ($p = .031$), 5 ($p = .007$) and minutes 4 and 6–10 ($p < .001$) compared to minute 1. The linear trend was also statistically significant ($F(1,23) = 33.79$, $p < .001$, $\eta^2_p = .60$), indicating that ECD1 amplitude increased with successive LFS stimuli. ECD2 showed no statistically significant changes during LFS ($p > .05$). ECD3 was significantly modulated by LFS duration, ($F(9,207) = 4.95$, $p < .001$, $\varepsilon = .63$, $\eta^2_p = .18$; ***Figure 7.3***E) in the latency epoch 105–119 ms, with a significant linear decrease in amplitude over time ($F(1,23) = 10.12$, $p < .004$, $\eta^2_p = .31$). Simple contrasts from minute 1 indicated a significant decrease in amplitude during minutes 2 ($p = .011$), 4 ($p = .009$), 5 ($p = .040$), 7 and 8 ($p = .003$), 9 ($p = .007$) and 10 ($p = .005$). ECD4 also showed a significant linear decrease in amplitude with LFS duration ($F(9,207) = 12.94$, $p < .001$, $\varepsilon = .67$, $\eta^2_p = .36$; $F(1,23) = 20.40$, $p < .001$, $\eta^2_p = .47$; ***Figure 7.3***H) in the interval 200–261 ms. Simple contrasts from minute 1 showed a statistically significant decrease in amplitude during minutes 2 ($p = .029$), 3 and 4 ($p < .001$), 5 ($p = .002$) and minutes 6–10 ($p < .001$).

Figure 7.3A, D and G illustrate time intervals around source waveform peaks showing a significant interaction between LFS duration and intensity. ECD3 showed a statistically significant interaction between LFS duration and intensity in the window 124–142 ms, ($F(27,621) = 2.23$, $p = .003$, $\eta^2_p = .088$; ***Figure 7.3***F). Repeated measures ANOVAs showed that this effect was due to reductions in ECD3 amplitude over time both during perception ($F(9,207) = 3.72$, $p < .001$, $\eta^2_p = .14$) and low LFS intensities ($F(9,207) = 2.97$, $p = .002$, $\eta^2_p = .11$); in contrast, there was no significant

change in ECD3 amplitude during medium and high LFS intensities ($p > .05$). ECD4 showed a significant interaction between LFS duration and intensity in the window 250–256 ms, ($F(27,621) = 2.07$, $p = .012$, $\eta^2_p = .08$; ***Figure 7.3***I). Repeated measures ANOVAs showed that this was due to significant reductions in ECD4 amplitude over time during low ($F(9,207) = 7.66$, $p < .001$, $\eta^2_p = .25$), medium ($F(9,207) = 5.88$, $p < .001$, $\eta^2_p = .20$) and high ($F(9,207) = 7.89$, $p < .001$, $\eta^2_p = .26$) LFS intensities, but not perception intensity ($p > .05$).

In summary, results point towards a modulation of ECD1 and ECD4 amplitude at greater LFS intensities, and decreased ECD3 amplitude during lower LFS intensities.

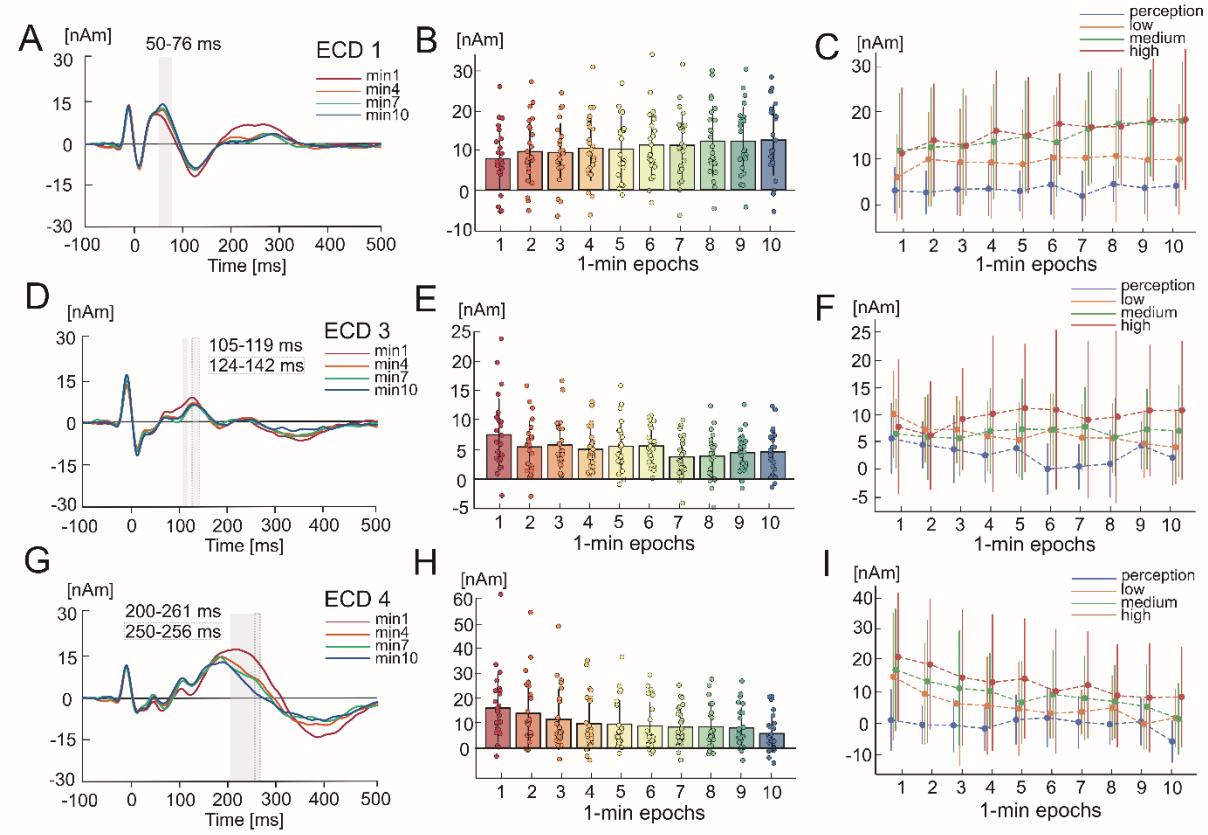

Figure 7.3. Grand average changes in SEPs during 10-mins of LFS and at varying LFS intensities. One-way ANOVAs showed a statistically significant amplitude modulation by LFS duration for ECD1 (A), ECD3 (D) and ECD4 (G). Source waveforms and standard deviations in minute 1, minute 4, minute 7 and minute 10 are shown for illustrative purposes. Bars indicate time intervals around source waveform peaks showing a significant effect of LFS duration (shaded only) or an interaction between LFS duration and intensity (shaded with outline). Bar graphs show the mean amplitudes and standard deviation of ECD1 (B), ECD3 (E) and ECD4 (H) source waveforms in 1-min intervals over the 10-min duration of LFS, averaged over all LFS intensities. Individual subject data points averaged over single trials are overlaid for each condition. Scatter graphs show mean amplitudes of ECD1 (C), ECD3 (F) and ECD4 (I) source waveforms during each of the 4 LFS intensities for all 1-min epochs of LFS. Error bars indicate standard deviation. N=24 (11 females).

7.4.3 Linear regression slopes

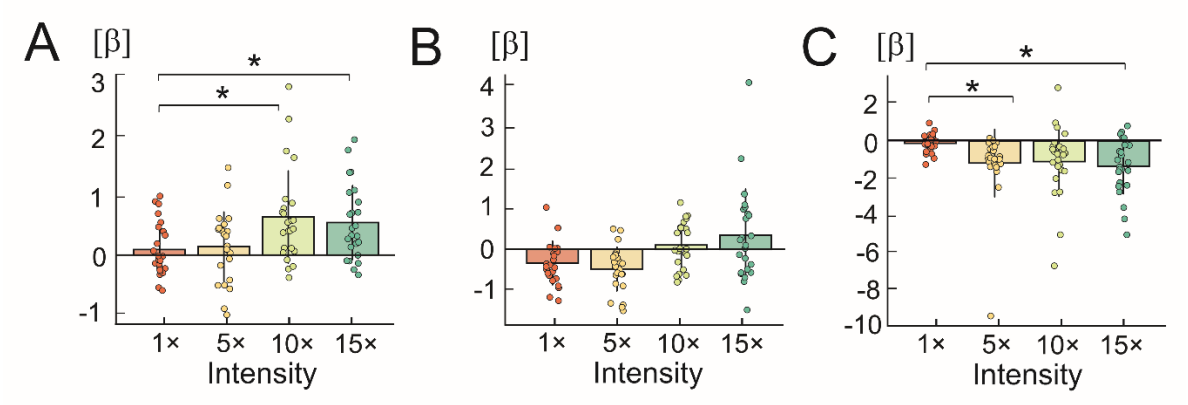

Figure 7.4. Mean linear regression coefficients (β) and standard deviation of the change in source dipole moment activity over the duration of LFS for each LFS intensity: perception (1×), low (5×), medium (10×) and high intensity (15× detection threshold). Positive values indicate an ascending slope with increased amplitude over the duration of LFS, while negative values indicate a descending slope with decreased amplitude during LFS. Pearson's correlations were conducted to analyse the relationship between regression slopes and ECD amplitude. A. ECD1 showed a significantly steeper positive slope at medium and high LFS intensities compared to perception intensity. B. Regression coefficients in ECD3 did not significantly differ between LFS intensities. C. ECD4 showed a significantly steeper negative slope at low and high LFS intensities compared to perception intensity. Asterisks indicate contrasts that exceeded significance at $p < .05$ (*). N=24 (11 females).

Repeated-measures ANOVAs were computed to assess significant differences in linear regression slopes (β) between LFS intensities for source dipole moments showing a significant difference from zero in one-way ANOVAs: ECD1, ECD3 and ECD4. Mean regression coefficients for each intensity are shown in ***Figure 7.4***A–C. ECD1 showed a statistically significant effect of LFS intensity ($F(3,69) = 5.87$, $p = .001$, $\eta^2 = .20$). Pairwise comparisons indicated that this effect was due to a significantly steeper positive slope at medium ($p = .044$) and high LFS intensities ($p = .012$) compared to perception intensity (***Figure 7.4***A). ECD3 showed a statistically significant effect of LFS intensity ($F(3,69) = 3.10$, $p = .032$, $\eta^2 = .13$), however pairwise comparisons between LFS intensities did not survive Bonferroni correction ($p > .05$) (***Figure 7.4***B). ECD4 showed a statistically significant effect of LFS intensity ($F(3,69) = 5.87$, $p = .001$, $\eta^2 = .20$). Pairwise comparisons indicated that this effect was due to a significantly steeper negative slope at low ($p = .044$) and high LFS intensities ($p = .007$) compared to perception intensity (***Figure 7.4***C).

7.4.4 Oscillatory changes in source signals after LFS

Figure 7.5 shows the power spectral densities in the resting EEG in each of the ECDs prior to any LFS stimulation (pre-LFS) and after each of four LFS intensity blocks. Resting EEG recorded prior to LFS was not included in statistical analyses and is shown only for comparison purposes. Spectral power of ECD1 was significantly modulated by LFS intensity at 9−11 Hz ($F(3,69) = 3.07$, $p = .034$, $\eta^2_p = .12$; ***Figure 7.5***A). Pairwise comparisons showed that this effect was due to an increase in band power after the strongest LFS intensity, compared to after perception ($p = .038$) and low intensities ($p = .001$). ECD2 and ECD3 showed no statistically significant changes in spectral power after each intensity of LFS ($p > .05$; ***Figure 7.5***B-C). ECD4 showed a statistically significant decrease in 3−5 Hz power with LFS intensity ($F(3,69) = 3.24$, $p < .027$, $\eta^2_p = .24$; ***Figure 7.5***D). This effect was due to a significant decrease in power after the strongest LFS intensity compared to perception intensity ($p = .014$).

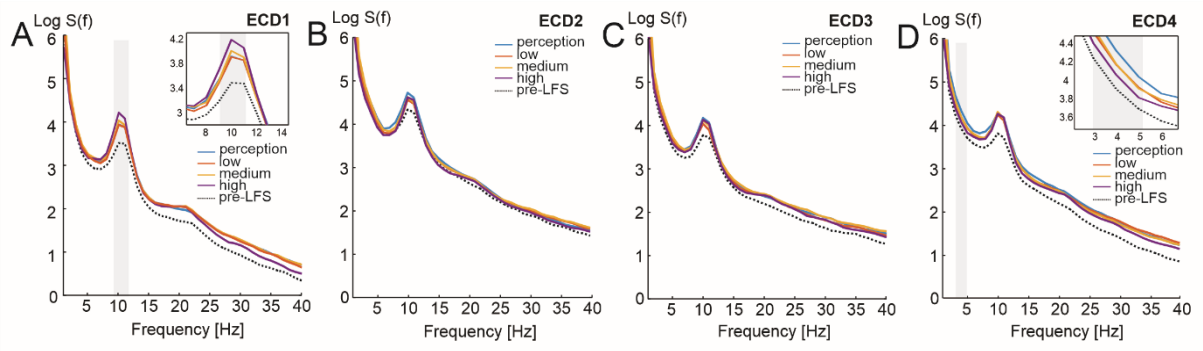

Figure 7.5. Grand average power spectral densities in resting EEG prior to LFS (pre-LFS) and following each LFS intensity block (perception, low, medium and high) for the four ECDs (A-D). One-way ANOVAs showed a significant effect of LFS intensity on spectral power in ECD1 at 9−11 Hz, and in ECD4 at 3−5 Hz. Log S(f) = logarithmic power spectral density. N=24 (11 females).

Pearson's correlations were conducted to analyse the relationship between linear regression slopes (β) in ECD1 and ECD4 at each of the four LFS intensities and normalised change in resting oscillatory band-power after stimulation. Pearson's correlations showed no statistically significant relationship between the slope of regression in ECD1 and 9−11 Hz normalised band power in ECD1 ($p > .05$), or between ECD4 and 3−5 Hz normalised band power in ECD4 ($p > .05$), at any of the four LFS intensities.

In summary, results show that LFS delivered at strong intensities (15× detection threshold) was followed by increased resting 9−11 Hz band power in ECD1 and decreased 3−5 Hz power in ECD4.

7.5 *Discussion*

The present study investigated the temporal profiles of cortical activity during four intensities of LFS and amplitudes of cortical oscillations following LFS. SEPs related to LFS of the radial nerve were modelled by four equivalent current dipoles located in contralateral SI/MI, bilateral operculo-insular cortex and MCC. Source activity in the MCC decreased linearly during LFS, with greater attenuation at increasing LFS intensities. Source activity in ipsilateral operculo-insular cortex also decreased linearly during LFS, albeit only during the two lowest stimulus intensities. In contrast, contralateral SI/MI showed a linear increase of source activity during LFS. Blocks of strong LFS intensities were followed by increased 9−11 Hz alpha band power in contralateral SI/MI and diminished 3−5 Hz theta band power in MCC.

Diminished source activity in MCC was observed during LFS intensities at greater than perception level. This furthers our previous findings (Hewitt et al., 2021), showing that changes in MCC are found at a noxious intensities. Involvement of the MCC in somatosensory processing is well established; the MCC is engaged during the anticipation (Palermo et al., 2015) and experience of acute experimental pain (Bastuji et al., 2016; Geuter et al., 2020; Vogt, 2005, 2016), as well as during nonpainful somatosensory stimuli (Hu et al., 2015; Liang et al., 2019; Mouraux & Iannetti, 2009). The MCC generates greater activity during noxious stimuli when defensive motor actions are required (Moayedi et al., 2015), and connections with the premotor cortex and intralaminar thalamic nuclei have been proposed to mediate nocifensive behaviours (Vogt, 2016). Thus, the MCC has been proposed to act as a hub between affective processing, pain, cognitive control and motor planning (Shackman et al., 2011; Vogt & Sikes, 2009). Engagement of the MCC during LFS has relevance for neuropathic pain treatments; motor cortex stimulation for neuropathic pain has been shown to increase cerebral blood flow in regions including the cingulate gyrus (Volkers et al., 2020), and transcranial magnetic stimulation over medial scalp regions corresponding to the MCC decreases

ratings of noxious electrical stimulation (D'Agata et al., 2015). Taken together, decreased MCC responses during LFS at intensities greater than perception may reflect reduced engagement of cingulate nociceptive pathways, which are implicated in neuropathic pain.

Post-stimulation amplitude of theta oscillations in the MCC were lower after periods of strong LFS. Theta oscillations have been reported to encode the intensity of acute pain and touch stimuli (Michail et al., 2016), while augmented theta power has been observed in patients with neurogenic pain (Sarnthein et al., 2006; Stern et al., 2006; Vučković et al., 2014), fibromyalgia (Fallon et al., 2018; Lim et al., 2016), and primary dysmenorrhea (Lee et al., 2017). As a result, a shift from dominant alpha to theta oscillations has been suggested as a contributing factor in the maintenance of chronic pain (Llinás et al., 1999, 2005). Greater reduction in power with increased LFS intensities suggests an inhibition within the region of MCC. This reduction in power may be related to the presence of LTD, which is a proposed mechanism of pain suppression during LFS (Klein, 2004; Sandkühler et al., 1997). Thus, reduced theta band power after LFS could reflect a reduction of aberrant processes within the MCC that potentially contribute to persistent pain states.

A novel finding in the current study was increasing slopes of activation in SI/MI during LFS, which were enhanced with greater LFS intensities. The primary somatosensory cortex has been implicated in sensory-discriminative processing of noxious and innocuous stimuli, with preferential responses for nonpainful stimulus onsets (Hu et al., 2015; Mouraux et al., 2013). Pain-related activation has also been demonstrated in the primary motor cortex (Becerra et al., 2001; Frot et al., 2013; Geuter et al., 2020; Peyron et al., 2000). Primary somatosensory cortex activation has been shown to be more resilient to stimulus repetition than other somatosensory processing regions, particularly in area 3b (Bradley et al., 2016; Klingner et al., 2011; Venkatesan et al., 2014); although some studies have reported reduced primary somatosensory cortex responses to repeated noxious stimuli (Mobascher et al., 2010). Increased amplitude of short-latency SEPs generated in SI have been reported alongside increased motor cortex excitability with high intensities of peripheral electrical stimulation, while lower intensities of peripheral electrical stimulation reduce SEP amplitude and cortical excitability (Chipchase et al., 2011; Schabrun et al., 2012). Greater cortical excitability in corticomotor pathways after high intensities of peripheral stimulation could mask subsequent parallel

inputs via an inhibitory gating mechanism (Hoechstetter et al., 2001; Huttunen et al., 1992). Findings of increased primary somatosensory cortex activation suggests that the analgesic effects of LFS that have been reported in previous studies (Aymanns et al., 2009; Jung et al., 2009; Klein, 2004; Lindelof et al., 2010; Magerl et al., 2018) may result from a combination of MCC attenuation and SI/MI facilitation.

Post-stimulation amplitude of alpha oscillations in SI/MI showed increased power after the strongest LFS intensity. Tactile and peripheral nerve stimulation are associated with amplitude attenuation of cortical 10 and 20 Hz oscillations focused primarily over contralateral sensorimotor regions (Chatrian et al., 1959; Enatsu et al., 2014; Gaetz & Cheyne, 2006; Neuper & Pfurtscheller, 2001b; Nikouline et al., 2000; Pfurtscheller, 1992; Stančák, 2006), followed by an amplitude increase or rebound after stimulus cessation (Brovelli et al., 2002; Enatsu et al., 2014; Hirata et al., 2002; Neuper & Pfurtscheller, 2001b; Pfurtscheller, 1981; Salenius et al., 1997; Salmelin & Hari, 1994b; Stancak et al., 2003). Post-stimulus increases in mu oscillatory power, particularly in the 20 Hz component, have been linked to the involvement of the dorsal column pathway (Stančák, 2006). Notably, periods of increased oscillatory band power over sensorimotor cortical areas have been found following administration of gamma-aminobutyric acid (GABA) agonist benzodiazepines (Hall et al., 2010; Jensen et al., 2005), pointing towards a direct role in sensory gating and inhibition (Jensen & Mazaheri, 2010). Pre-stimulus alpha power has been shown to be related to noxious processing, with weaker 10-12 Hz alpha power associated with higher amplitude laser-evoked potentials (Babiloni et al., 2008). Greater alpha band-power is associated with cortical inhibition (Pfurtscheller, 1992; Salmelin & Hari, 1994a). Combined, the results suggest that increased source activity in SI/MI during conditioning may inhibit post-stimulation processing, due to the possible masking of nociceptive processing by afferent impulses conveyed in ascending spinal pathways.

Ipsilateral operculo-insular source activity decreased selectively during the two lowest LFS intensities, pointing towards a differentiation between noxious and nonpainful stimulation. Operculo-insular cortex has been consistently implicated in pain processing (Duerden & Albanese, 2013; Horing et al., 2019; Hu et al., 2015; Peyron et al., 2000, 2002; Wager et al., 2013), with increased activation alongside heightened acute pain perception (Segerdahl et al., 2015; Su et al., 2019). Similar

to conditioning stimuli in the current study, repeated stimuli presented at regular intervals manifest in diminished SEPs as early as the second repetition (Condes-Lara et al., 1981; Iannetti et al., 2008; Mancini et al., 2018; Wang et al., 2010). Notably, SEPs during medium and high LFS intensities were reduced during the first minute of stimulation in contrast to the two lowest intensities. Therefore, selective attenuation of operculo-insular source activity during weaker LFS intensities may be due to immediate suppression of evoked potentials during strong stimuli, which show no further decreases during conditioning.

Activity-dependent synaptic plasticity such as LTD have been interpreted as a hallmarks of learning and memory (Bliss & Cooke, 2011; Dudek & Bear, 1992; Mulkey & Malenka, 1992), leading to the suggestion that LTD may be a process for erasing pain memory traces (Magerl et al., 2018; Rygh et al., 2002). LFS was associated with source activity in the SI/MI, bilateral operculo-insular cortex and MCC, consistent with previous studies of SEPs elicited by electrical stimulation (Cruccu et al., 2008; Shimojo et al., 2000; Valeriani et al., 2000a; Vrána et al., 2005) and our previous LFS study (Hewitt et al., 2021). While the contralateral operculo-insular cortex was not affected by intensity, activity in the SI/MI, ipsilateral operculo-insular cortex and MCC showed greater source activity as LFS intensity increased. This is in line with evidence that graded intensities of nonpainful and noxious stimuli are associated with enhanced amplitude of evoked potentials (Derbyshire et al., 1997; Iannetti et al., 2008; Loggia et al., 2012; Shimojo et al., 2000; Valeriani et al., 2000a) and greater haemodynamic responses in somatosensory processing regions (Geuter et al., 2020; Oertel et al., 2012; Peyron et al., 2000; Su et al., 2019). These findings further previous evidence of reductions in pain-related cortical activation after LFS in regions including the primary and secondary somatosensory cortices, insula, anterior cingulate cortex and inferior parietal lobule (Rottmann et al., 2010b).

The present study did not identify significant changes in pain or unpleasantness of electrical test stimuli between LFS intensities. Previous studies have reported a decrease in behavioural pain ratings to noxious stimuli after LFS (Jung et al., 2009; Klein, 2004; Lindelof et al., 2010), with the strongest attenuation after an intensity corresponding to 15× detection threshold (Jung et al., 2009). Such decreases have been interpreted as correlates of LTD of nociception in humans (Klein, 2004).

Inconsistencies may be due to variations in methodology; Jung and colleagues (Jung et al., 2009) studied the effects of LFS intensity on mean pain ratings from 0−100 during eight blocks of 15 test stimuli over 1-hour following conditioning stimulation, in comparison to single test stimuli rated from 0−10 in the present study. Ratings in the present study may also have been affected by participants' knowledge that LFS intensity was the same for each test stimulus, as cognitive processes such as expectation are well established as modulators of pain experience (Huneke et al., 2013).

A caveat of the present findings is in the use of source dipole modelling to estimate cortical generators of the observed scalp data. Source dipole modelling is an inverse solution which assumes that the scalp generated field is generated by only one or a few equivalent current dipoles in the brain (Michel & Brunet, 2019). Studies examining the accuracy of dipole source localisation methods have reported mean errors of 6–20mm (Akalin Acar & Makeig, 2013; Chen et al., 2007; Cohen et al., 1990; Cuffin et al., 1991). However, definitive identification of electrical potentials is not possible from EEG alone, and caution should be taken when interpreting the spatial locations of results.

The current findings have potential implications for neuropathic pain treatment. While preliminary investigations have demonstrated success with LFS (Johnson et al., 2015; Johnson & Goebel, 2016; Rutkowski et al., 1975), evidence is limited, and a recent randomised controlled trial in chronic peripheral nerve injury found no significant reduction in spontaneous pain symptoms following 3-months of LFS treatment (Johnson et al., 2021). However, these findings may have been affected by stimulation intensity, as patients were able to vary stimulus parameters including intensity as desired, which may have resulted in intensities below that required to activate Aδ fibres (Liu et al., 1998; Sandkühler et al., 1997). A mechanistic arm of the aforementioned trial reported significant effects of LFS on mechanical pain sensitivity and dynamic mechanical allodynia (Johnson et al., 2021). Indeed, LFS has been shown to reverse and inhibit the development of primary hyperalgesia evoked by HFS, even at very low frequencies that would not independently result in LTD (Magerl et al., 2018). This has particular relevance for neuropathic pain, with a large proportion of patients with peripheral neuropathic pain exhibiting mechanical hyperalgesia (Vollert et al., 2017).

Our study demonstrates that LFS of radial nerve fibres elicits graded effects on somatosensory processing, most notably in the MCC and SI/MI. While previous literature points

towards LTD as the neurophysiological mechanism underlying LFS, our study suggests a potential secondary mechanism involving engagement of the SI/MI. Preliminary findings of a modulation of cortical oscillations after conditioning supports sustained changes after LFS; however, the link between short-term changes in neural activity and long-lasting effects of LFS on persistent pain states has yet to be explored.

Chapter 8

8 General discussion

This thesis focused on two parallel streams of neurostimulation research: a well-established intervention for neuropathic pain, SCS, and a novel method, LFS. SCS is a palliative neurostimulation treatment to reduce intractable neuropathic pain (Duarte et al., 2020; Kriek et al., 2017; Visnjevac et al., 2017). Conventional tonic and novel burst SCS have been proposed to have different mechanisms of action (Crosby et al., 2015b; Tang et al., 2014); however, little empirical research had investigated the underlying mechanisms in humans. SCS intensity differs between burst and tonic stimulation (De Ridder et al., 2010), and intensity has been shown to modulate electrophysiological markers of somatosensory and nociceptive processing (Derbyshire et al., 1997; Iannetti et al., 2008; Lim et al., 2012; Loggia et al., 2012; Shimojo et al., 2000; Valeriani et al., 2000a).

LFS has been used as a novel neurostimulation method for peripheral neuropathic pain (Johnson et al., 2015; Johnson & Goebel, 2016). When delivered at high intensities, LFS has been proposed to elicit LTD of nociception, whereas lower intensities are ineffective (Sandkühler et al., 1997). However, cortical regions mediating the direct effects of LFS had yet to be investigated in humans. Secondly, it was unknown if cortical changes during LFS correlated with post-stimulation decreases in nociceptive processing or resting oscillatory activity.

Firstly, this thesis investigated the effects of burst and tonic SCS on resting cortical oscillations (Chapter 4) and on brushing-related ERD (Chapter 5) at four SCS intensities in neuropathic pain patients. Secondly, this thesis investigated the cortical regions mediating the direct effects of LFS and the impact of LFS on post-stimulation nociceptive processing and oscillatory activity in healthy volunteers (Chapters 6 and 7).

8.1 Summary of findings

- Stronger SCS intensities were associated with greater spontaneous beta (21–24 Hz) band power in right midline electrodes compared to low intensities, and decreased alpha band (8–

11 Hz) power in posterior parietal electrodes compared to low and medium intensities (Chapter 4).

- Stronger SCS intensities were associated with attenuated brushing-related ERD in central and parietal electrodes in theta and alpha bands, and in frontal and central electrodes in the beta (16−24 Hz) band, with the most robust effects at medium SCS intensity (Chapter 5).
- Burst SCS was associated with greater brushing-related ERD in theta (4−7 Hz) and alpha (8−13 Hz) frequency bands in central, frontal and parietal electrodes compared to tonic SCS (Chapter 5). Burst and tonic SCS did not differentially modulate the amplitudes of spontaneous cortical oscillations (Chapter 4).
- Amplitudes of SEPs originating in MCC and ipsilateral operculo-insular cortex decreased during the course of LFS (Chapters 6 and 7). Steeper decreases in SEP amplitude were observed at medium and high LFS intensities in the MCC, and at perception and low intensities in the ipsilateral operculo-insular cortex (Chapter 7).
- Amplitudes of SEPs originating in SI/MI were increased during the course of LFS, with steeper increases at medium and high LFS intensities compared to perception (Chapter 7).
- Amplitude of P2 LEP components were decreased after active LFS compared to sham LFS. Amplitude of N2 LEP components were decreased for laser stimuli on the conditioned radial hand side after LFS (Chapter 6).
- Active LFS was followed by higher amplitudes of spontaneous cortical oscillations in 8–12 Hz and 16–24 Hz frequency bands in temporal, sensorimotor and frontal electrodes compared to sham stimulation (Chapter 6). Strong LFS intensities were followed by increased 9−11 Hz alpha band power in contralateral SI/MI and diminished 3−5 Hz theta band power in MCC (Chapter 7).

8.2 Themes of findings

Individual results of four empirical studies were discussed in the experimental chapters of this thesis, and multiple overarching themes were observed. The use of EEG measures, including evoked potentials and time-frequency methods, allowed investigation of the underlying cortical processes

relating to varying intensities and types of neurostimulation. Primarily, peripheral and central neurostimulation using LFS and SCS, respectively, induced changes in cortical excitability which were modulated by stimulation intensity. Greater intensities of LFS and SCS decreased cortical excitability in widespread areas over central, sensorimotor and parietal electrodes. Analysis of changes in SEP amplitudes during stimulation enabled investigation of temporal changes in cortical excitability during repeated LFS of the radial nerve. Inspection of oscillatory activity during burst and tonic SCS supports different underlying mechanisms which are engaged during somatosensory input.

8.2.1 Graded intensity effects of SCS and LFS on cortical excitability

Across the experimental chapters in this thesis, the intensity of neurostimulation measures were found to induce changes in cortical excitability. The most robust effect was that of decreased cortical excitability at greater stimulation intensities. At the highest SCS intensity, decreased cortical excitability was observed primarily over central midline electrodes in the beta band during rest in Chapter 4, and in theta, alpha and beta frequency bands during brushing in Chapter 5. These effects suggest that therapeutic SCS induces active cortical inhibition (Fry et al., 2016; Jensen & Mazaheri, 2010; Neuper & Pfurtscheller, 2001b), in accordance with the assumption that SCS has a gating effect on somatosensory processing (Melzack & Wall, 1965). Notably, decreased cortical excitability at highest stimulation intensities were also observed during LFS in Chapter 7 in SEP dipoles generated by MCC. High LFS intensities activating Aδ fibres have been demonstrated as essential for LTD in the dorsal horn, which has been theorized as the neurobiological mechanism underlying LFS (Liu et al., 1998; Sandkühler et al., 1997). Taken together, these results suggest that high neurostimulation intensities have inhibitory effects on cortical excitability over the SI/MI, which receives sensory impulses from the periphery (Brodal, 1992). Furthermore, decreased cortical excitability in the cingulate cortex has been associated with reduced spinal potentiation and analgesia (Chen et al., 2018; Xu et al., 2008).

Additionally, medium SCS intensities had a considerable effect on cortical excitability, with the greatest decrease of cortical excitability during rest in the alpha band in Chapter 4, and during tactile brushing stimulation in theta, alpha and beta frequency bands in Chapter 5. Changes in spectral

power at medium SCS intensities were primarily observed over central and parietal regions of the scalp, suggesting that medium SCS intensities induced cortical inhibition in regions associated with somatosensory processing and multisensory integration (Foxe & Snyder, 2011; Fry et al., 2016; Neuper & Pfurtscheller, 2001b; Pfurtscheller et al., 1996b; Whitlock, 2017). These regions are consistent with activation of contralateral SI, SII and posterior parietal cortex after peripheral nerve stimulation (Forss et al., 1994; Valeriani et al., 2001). The dissociation between medium and high SCS intensities show that SCS intensity is not a simple, linear function, in line with models of strength-duration curves for neuronal activation with SCS (Miller et al., 2016). Stronger attenuation of spectral power at medium intensity conditions may be due to a ceiling effect of spectral power, in line with evidence that ERD is not modulated by fine gradations of stimulus intensity (Iannetti et al., 2008; Stancak et al., 2003), and saturation of gating effects in SI and SII at moderate intensities of electrical stimulation (Lim et al., 2012). Alternatively, greater interference of brushing-induced impulses and changes in resting oscillations at medium SCS intensities may reflect a potential overshoot in determining the most effective therapeutic parameters. Therefore, the results of Chapters 4 and 5 suggest a nonlinear effect of SCS intensity on somatosensory processing which may be due to saturation at higher intensities, or an overshoot in determining optimal SCS parameters.

Strong intensities of SCS and LFS were also associated with increased cortical excitability. In Chapter 5, enhanced brushing-related ERD over frontal central electrodes was found in the beta band at the highest SCS intensity. Similarly, Chapter 7 showed enhanced amplitude of SEPs in SI/MI over the duration of LFS, with the steepest ascending slope at medium and high intensities. When LFS was delivered at lower intensities in Chapter 6, increased source activation in SI/MI was not observed. Facilitatory effects of SCS and LFS suggest that these neurostimulation interventions for pain do not have a simple gating or inhibitory effect, as proposed by the Gate Control Theory and LTD hypotheses. Previous literature has focused primarily on the inhibitory effects of LFS on somatosensory processing, although few studies have also noted secondary mechanical hyperalgesia after LFS (Biurrun Manresa et al., 2010; Klein, 2004). Coexistence of facilitation and inhibition has been demonstrated during SCS, with activation in SI/MI somatotopically corresponding to the pain-related region, and deactivation in ipsilateral SI corresponding to unaffected regions (Stancak et al.,

2008). Heterogeneous inhibition and excitation responses during SCS have also been reported in spinal sensory projection neurons (Zhang et al., 2015). Combined, the results point towards supraspinal mechanisms beyond simple gating mechanisms with LFS and SCS.

8.2.2 Changes in cortical excitability during and following neurostimulation

Temporal changes in cortical excitability over the course of LFS were investigated in Chapters 6 and 7. LFS has been shown to elicit decreased extracellular potentials during conditioning stimulation which are sustained after stimulus cessation, consistent with LTD (Liu et al., 1998; Sandkühler et al., 1997). As hypothesized, LFS delivered at high intensities attenuated cortical somatosensory processing in regions associated with nociception (Duerden & Albanese, 2013; Jensen et al., 2016; Xu et al., 2020). In Chapters 6 and 7, SEPs related to LFS of the radial nerve were modelled by four equivalent current dipoles in contralateral SI/MI, bilateral operculo-insular cortex, and MCC, consistent with previous SEP studies (Cruccu et al., 2008; Shimojo et al., 2000; Valeriani et al., 2000a; Vrána et al., 2005). Findings from Chapters 6 and 7 showed a steady, linear decrease in MCC activity over time which started at stimulus onset and continued throughout the block. Chapter 7 furthered the findings of Chapter 6 and demonstrated that the decrease in MCC activity was sharper at greater stimulus intensities. These findings were novel, with previous studies focused solely on the post-stimulation effects of LFS on external test stimuli (Ellrich & Schorr, 2004; Jung et al., 2012; Rottmann et al., 2008).

LFS was also accompanied by relatively minor reductions in ipsilateral operculo-insular cortex activity. When averaged over all LFS intensities in Chapter 7, LFS was associated with a statistically significant decrease in ipsilateral operculo-insular cortex magnitude throughout stimulation. When LFS was delivered at an unpleasant LFS intensity, the decrease in ipsilateral operculo-insular cortex activity was not observed until later in the block. Inspection of intensity effects in Chapter 7 showed that this decrease was specific to low intensities and was maximal at 5× detection threshold. This is consistent with evidence that SII (within the operculo-insular cortex) encodes stimulus intensity until it reaches pain threshold (Frot et al., 2007). As strong, noxious LFS intensities have been shown to be necessary to elicit LTD in the dorsal horn (Liu et al., 1998;

Sandkühler et al., 1997), these findings illustrate that reductions in ipsilateral operculo-insular cortex activity are unlikely to reflect an early correlate of LTD.

In contrast to inhibitory effects in MCC and operculo-insular cortex, an increase in SI/MI amplitude was observed solely in Chapter 7 and was maximal at 10× and 15× detection threshold. Disparity between experiments may be due to reduced LFS intensity in Chapter 6 (mean 1.17 mA) which was more comparable to the medium (mean 1.19 mA) than the high intensity (mean 1.78 mA) in Chapter 7. Increased SI/MI activity suggests facilitation at greater LFS intensities (Cheron et al., 2000). Combined, findings from Chapters 6 and 7 suggest that high LFS intensities proposed to elicit LTD-like effects are mediated by a combination of SI/MI facilitation and MCC attenuation, while changes in other cortical regions including the operculo-insular cortex may reflect secondary processes from tactile input.

The theory that effects of LFS are mediated by LTD denotes lasting changes in synaptic efficacy in the spinal cord which affect the processing of nociceptive input system (Chen & Sandkühler, 2000; Dudek & Bear, 1992; Ikeda et al., 2000; Kim et al., 2015; Liu et al., 1998; Sandkühler et al., 1997). LFS modulated post-stimulation spontaneous resting oscillations, with an increase in alpha and beta band power in contralateral operculo-insular cortex and SI/MI versus sham stimulation in Chapter 6, and increased alpha power in SI/MI after greater LFS intensities in Chapter 7. These findings point towards cortical inhibition after LFS (Foxe & Snyder, 2011; Fry et al., 2016; Neuper & Pfurtscheller, 2001b; Pfurtscheller et al., 1996b). Considered alongside findings of greater cortical excitability in SI/MI during LFS, findings of the current thesis suggest that engagement of somatosensory processing regions during LFS may have an inhibitory function of gating subsequent sensory input.

Decreased theta band power in MCC was observed specifically at high LFS intensities in Chapter 7. Comparatively, no difference in theta band power was found between active and sham LFS in Chapter 6, suggesting that decreased theta oscillations in MCC reflected an intensity effect. Theta oscillations have been demonstrated to encode the intensity of acute pain and touch stimuli (Michail et al., 2016), while augmented theta power has been observed in patients with chronic pain (Fallon et al., 2018; Lim et al., 2016; Sarnthein et al., 2006; Stern et al., 2006; Vučković et al., 2014). Decreased

resting theta oscillations in fronto-central scalp regions are correlated with increased BOLD activation of regions in the default mode network (Das et al., 2022; Scheeringa et al., 2008). In contrast, increased theta is found with attention-demanding tasks (Kropotov, 2009). ACC and MCC have been strongly linked to top-down descending facilitation of spinal sensory excitatory transmission, and inhibition of the cingulate cortex is associated with reduced pain sensitisation following peripheral nerve injury (Chen et al., 2018). Therefore, findings from the two studies strengthen the argument that strong intensities of LFS induce sustained decreases in cortical excitability in MCC. Thus, augmented theta band power with increasing LFS intensity could reflect an interference of integrative sensorimotor processes, which may contribute to its effects on pain perception.

Temporal changes in cortical excitability over the duration or in the period following SCS were not investigated in Chapters 4 and 5. According to the Gate Control Theory, transmission of nociceptive information is gated at the level of the spinal cord during simultaneous somatosensory stimulation due to a disproportionate increase of large diameter over small diameter fibre activity (Melzack & Wall, 1965). Therefore, there were no specific hypotheses for changes in oscillatory band power over time, or after SCS was switched off. However, the Gate Control Theory is not a complete explanation of the mechanisms of SCS (Mendell, 2014; Nathan, 1976) and does not account for the effects of burst stimulation (De Ridder et al., 2013; Linderoth & Foreman, 2017). It is possible that changes may occur over the duration of stimulation and in the time after SCS is switched off. SCS may not have an immediate effect on spinal nociceptive processes, and effects may differ between SCS types, as illustrated by delayed onset and offset periods between active recharge burst and tonic stimulation (Meuwissen et al., 2018). Inspection of onset and offset effects were beyond the scope of this thesis but remain an important avenue for future studies.

8.2.3 Burst and tonic SCS have different effects on tactile somatosensory processing

The varying effects of burst and tonic SCS on tactile somatosensory processing and spontaneous cortical oscillations were investigated based on evidence of alternative mechanisms (De Ridder et al., 2013; De Ridder & Vanneste, 2016; Yearwood et al., 2019). Burst and tonic SCS were found to differently modulate tactile somatosensory processing in Chapter 5, although no significant

difference in spontaneous cortical oscillations was found in Chapter 4. In accordance with the Gate Control Theory, tonic SCS has been shown to stimulate the dorsal column pathway (Holsheimer, 2002; Joosten & Franken, 2020; Melzack & Wall, 1965; Shealy et al., 1967) and inhibit somatosensory processing (Bentley et al., 2016; Sankarasubramanian et al., 2019). Results from Chapter 5 of attenuated theta and alpha band ERD during brushing in right central, right frontal and left posterior parietal electrodes in patients using tonic SCS aligns with these findings. Comparatively, burst SCS is proposed to engage the spinothalamic tract without involvement of the dorsal column pathway (De Ridder & Vanneste, 2016; Joosten & Franken, 2020). In line with this theory, results from Chapter 5 showed that burst SCS did not attenuate brushing-related ERD, pointing towards alternative mechanisms which do not involve gating of LTMRs (Gandevia et al., 1983; Kakigi & Jones, 1986; Mancini et al., 2015).

Differences between burst and tonic SCS may be highlighted in their response to somatosensory inputs. EEG and fMRI responses to painful and nonpainful stimuli activating the spinothalamic tract and dorsal column pathway, respectively, originate from similar sources (Mouraux et al., 2011; Valeriani et al., 2000a), with greater magnitude for higher intensities (Baliki et al., 2009; Valeriani et al., 2000a). Therefore, SCS transmitted by the dorsal column or spinothalamic tract may not be observed independently in spontaneous EEG. Results are contrary to previous accounts of increased resting alpha and beta band power during burst compared to tonic SCS (De Ridder et al., 2013). Inconsistencies could result from variations in study design; De Ridder et al. (2013) and De Ridder & Vanneste (2016) investigated cortical oscillations during the early trial stimulation period in a small group of 5 patients. Differences observed during trial stimulation may not reflect long-term cortical changes after patients have lived with and adjusted to the device. Therefore, the results from the current thesis suggest that, to investigate the differences between burst and tonic stimulation, it is necessary to investigate their effects on external stimulation.

Conversely, the effects of SCS intensity were similar between burst and tonic stimulation, suggesting a degree of shared mechanisms between SCS waveforms. Previous investigations have identified increased theta oscillations in SI, SII, posterior cingulate cortex and the parahippocampal area, and increased gamma rhythms in ACC and prefrontal cortex after burst and tonic SCS (De

Ridder & Vanneste, 2016). A shared mechanism indicates that intensity is an important facet of SCS programming to be considered regardless of the waveform. However, the small, heterogeneous patient group under investigation may have limited the ability to find a potential difference between burst and tonic SCS. Data for Chapters 4 and 5 was taken from patients with unilateral neuropathic pain due to a range of initial causes, most commonly due to CPSS. CPSS is a generalised term used to describe patients who have not had success from spinal surgery and continue to experience neuropathic pain (Schug et al., 2019; Thomson, 2013). As a result, CPSS does not explain the initiating event leading to pain, or specific symptoms experienced by patients. To further investigate any potential differences between SCS waveforms at graded intensities, future studies could stratify patients with similar clinical presentations.

8.3 Implications for treatment of neuropathic pain

The findings in this thesis have important implications for theory and clinical practice. Strong interference with the transmission of afferent impulses at SCS intensities as much as one-third lower than the therapeutic level suggests that lower intensities may be equally or more effective than the clinically programmed settings. SCS intensity is one facet of electrical dose and electrical charge transfer, lower amounts of which preserve battery life and reduce any unpleasant paraesthesia sensations (Miller et al., 2016; Paz-Solís et al., 2022). Optimising electrical dose is crucial for effective pain relief with SCS (Chakravarthy et al., 2021; Paz-Solís et al., 2022). Currently, the method for SCS dose titration is a process of trial and error between the programmer and patient. Further understanding of the SCS therapeutic window, particularly for paraesthesia-free waveforms, is of vital importance. Therefore, these preliminary findings suggest that EEG may have a valuable role in determining optimal stimulation parameters for managing neuropathic pain.

Similarly, LFS has been shown to reduce experimentally-induced mechanical pain sensitivity and dynamic mechanical allodynia in clinical populations (Johnson et al., 2021), and reverse and inhibit the development of primary hyperalgesia (Magerl et al., 2018). This thesis demonstrates robust effects of LFS on cortical somatosensory processing at greater intensities, highlighting the importance of utilising strong LFS intensities which surpass pain threshold, as shown previously (Jung et al.,

2009; Liu et al., 1998; Sandkühler et al., 1997). These findings suggest that LFS may be integrated as a palliative treatment to manage hyperalgesia and allodynia symptoms in neuropathic pain.

8.4 Thesis Limitations

Participants' SCS parameters were not optimised at the time of data collection due to the study's observational nature, and SCS treatment duration varied widely between patients. This raises the possibility that some patients were using programmed settings that no longer treated their pain adequately. Skilful and repeated reprogramming of SCS devices is necessary to maximise the benefits of treatment, and programming approaches differ between personnel and over time (Katz et al., 2021; Sharan et al., 2002; Sheldon et al., 2021). The possibility of suboptimal SCS parameters in a subset of patients could partly explain the potential saturation or overshoot of response at medium SCS intensities captured with changes in band power. Future investigations could control for variations in treatment response by optimising and standardising SCS parameters at the start of the study.

This thesis was limited by the short timescale of studies. As the experiments in Chapters 4 and 5 took place in single sessions, the possible relationship between oscillatory changes and fluctuating pain symptoms could not be investigated. The relationship between changes in cortical excitability and pain experience is important to establish the neural underpinnings of palliative treatments for neuropathic pain. This question could have been addressed with the original plan for this thesis, which included a longitudinal study investigating changes in spontaneous cortical oscillations and suppression of brushing-induced ERD during SCS as a function of treatment response. Unfortunately, this study was not completed due to complications arising from the COVID-19 pandemic. Likewise, Chapters 6 and 7 showed an instantaneous inhibitory effect of LFS on somatosensory processing, which was accompanied by post-stimulation changes in resting oscillations. However, the phenomenon of LTD requires that lasting changes in synaptic efficacy are found. Investigation of the duration of changes in somatosensory processing after LFS would further support the notion that changes during LFS are due to LTD.

Findings did not support the analgesic effect of LFS on noxious stimulus processing. Previous studies investigating the effects of LFS on pain processing have investigated changes in pain ratings after LFS versus no stimulation (Ellrich, 2004; Ellrich & Schorr, 2004; Rottmann et al., 2008). In

Chapter 6, pain ratings for noxious laser stimuli decreased equally after active and sham stimulation, suggesting that this reduction may reflect stimulus habituation rather than LTD. In addition, analysis of LEPs revealed an absence of specific and preferential effects of active LFS on nociceptive processing in the conditioned hand territory. We speculated that this might be due to the lower intensity of LFS stimulation used in Chapter 6. Chapter 7 was designed to overcome this potential limitation; however, contrary to previous evidence of a greater reduction in pain ratings after stronger stimulus intensities (Jung et al., 2009), no changes in pain or unpleasantness ratings were found between LFS intensities. A recent study reported no significant effect of LFS on spontaneous daily pain, but reductions in allodynia and improvements in quality of life during treatment (Johnson et al., 2021). Therefore, LFS may be a potential adjunctive treatment for symptoms of neuropathic pain that are not specific to pain intensity. Taken together, the results from this thesis do not support an immediate, direct effect of LFS on acute pain perception.

8.5 *Suggestions for future research*

Contrary to burst stimulation, tonic SCS suppressed parallel inputs from brushing stimuli. Findings reaffirm the existence of alternative mechanisms of action between burst and tonic stimulation, whereby burst SCS modulates medial and lateral spinothalamic tracts, while tonic stimulation modulates activity in the lateral spinothalamic tract via the dorsal column pathway (De Ridder & Vanneste, 2016; Joosten & Franken, 2020). As the current study focused solely on the tactile processing component of SCS, it is not clear if this inhibitory effect would be equally relevant to the influence of SCS on noxious afferents. Future studies should investigate ERD patterns during burst and tonic SCS related to stimuli that primarily involve spinothalamic tract neurons, such as transient warming, cooling or heat stimuli.

Sustained changes in cortical oscillations after LFS lends support to the use of LFS in palliative treatments for chronic neuropathic pain. However, the link between short-term changes in neural activity and long-lasting effects of LFS on persistent pain states has yet to be explored. The results suggest that decreased source activity in MCC and increased source activity in SI/MI during conditioning may inhibit post-stimulation processing. However, it is not known if changes in oscillatory activity after LFS are transient or sustained after conditioning stimuli. Therefore, future

studies should investigate the duration of oscillatory changes following LFS, and if these changes correlate with clinical pain relief or other potential clinical benefits.

8.6 Concluding remarks

SCS and LFS have been used as palliative neurostimulation treatments for intractable neuropathic pain, however, the mechanisms underlying these methods are poorly understood. This thesis utilised EEG to investigate the effects of different modes of SCS and of varying intensities of SCS and LFS on resting oscillatory activity and in response to somatosensory stimuli.

The findings demonstrated that stimulation intensity is a critical factor determining response to SCS, with greater intensities inhibiting activity in somatosensory processing regions. Tonic and burst stimulation have different and shared mechanisms which were highlighted during somatosensory stimulation, and greater suppression of parallel inputs from brushing during tonic stimulation supports the gating effect of SCS. Effects of stimulation at less than therapeutic intensities warrant further investigation but suggest the possibility of implementing SCS at lower intensities to maximise treatment effectiveness.

In relation to LFS, the findings demonstrated that strong, painful intensities of LFS inhibit somatosensory processing in the MCC and operculo-insular cortex and facilitated the involvement of SI/MI. Inhibition during strong LFS was followed by augmented oscillatory band power and attenuated evoked potentials, indicating a gating of somatosensory processing. The potential relationship between change in cortical responses as a result of LFS and symptom relief in patients with chronic neuropathic pain has yet to be determined and is an avenue for future study.

In summary, this thesis advances previous understanding of the cortical processes involved in neurostimulation methods SCS and LFS, particularly in their effects on somatosensory processing. These findings may have important clinical implications for the treatment of neuropathic pain which has not been adequately managed with first-line pharmacological treatments.

9 References

Abejón, D., Rueda, P., del Saz, J., Arango, S., Monzón, E., & Gilsanz, F. (2015). Is the Introduction of Another Variable to the Strength–Duration Curve Necessary in Neurostimulation? *Neuromodulation: Technology at the Neural Interface*, *18*(3), 182–190. https://doi.org/https://doi.org/10.1111/ner.12223

Abraira, V. E., & Ginty, D. D. (2013). The sensory neurons of touch. *Neuron*, *79*(4), 618–639. https://doi.org/10.1016/j.neuron.2013.07.051

Ackerley, R., Eriksson, E., & Wessberg, J. (2013). Ultra-late EEG potential evoked by preferential activation of unmyelinated tactile afferents in human hairy skin. *Neuroscience Letters*, *535*, 62–66. https://doi.org/10.1016/j.neulet.2013.01.004

Adrian, E. D., & Matthews, B. H. C. (1934). The Berger rhythm: potential changes from the occipital lobes in man. *Brain*, *57*(4), 355–385. https://doi.org/https://doi.org/10.1093/brain/57.4.355

Afif, A., Hoffmann, D., Minotti, L., Benabid, A. L., & Kahane, P. (2008). Middle short gyrus of the insula implicated in pain processing. *Pain*, *138*(3), 546–555. https://doi.org/https://doi.org/10.1016/j.pain.2008.02.004

Akalin Acar, Z., & Makeig, S. (2013). Effects of forward model errors on EEG source localization. *Brain Topography*, *26*(3), 378–396. https://doi.org/10.1007/s10548-012-0274-6

Allison, T., McCarthy, G., & Wood, C. C. (1992). The relationship between human long-latency somatosensory evoked potentials recorded from the cortical surface and from the scalp. *Electroencephalography and Clinical Neurophysiology*, *84*(4), 301–314. https://doi.org/10.1016/0168-5597(92)90082-m

Almarzouki, A. F., Brown, C. A., Brown, R. J., Leung, M. H. K., & Jones, A. K. . (2017). Negative expectations interfere with the analgesic effect of safety cues on pain perception by priming the cortical representation of pain in the midcingulate cortex. *PLOS ONE*, *12*(6), e0180006. https://doi.org/10.1371/journal.pone.0180006

Alshelh, Z., Brusaferri, L., Saha, A., Morrissey, E., Knight, P., Kim, M., Zhang, Y., Hooker, J. M.,

Albrecht, D., Torrado-Carvajal, A., Placzek, M. S., Akeju, O., Price, J., Edwards, R. R., Lee, J., Sclocco, R., Catana, C., Napadow, V., & Loggia, M. L. (2021). Neuroimmune signatures in chronic low back pain subtypes. *Brain*. https://doi.org/10.1093/brain/awab336

Alves, P. N., Foulon, C., Karolis, V., Bzdok, D., Margulies, D. S., Volle, E., & Thiebaut de Schotten, M. (2019). An improved neuroanatomical model of the default-mode network reconciles previous neuroimaging and neuropathological findings. *Communications Biology*, *2*(1), 370. https://doi.org/10.1038/s42003-019-0611-3

Amaral, D. G., & Strick, P. L. (2013). The Organisation of the Central Nervous System. In E. R. Kandel, J. H. Schwartz, T. M. Jessell, S. A. Siegelbaum, & A. J. Hudspeth (Eds.), *Principles of neural science.* (5th ed., pp. 337–355). McGraw-Hill Medical.

Amirdelfan, K., Yu, C., Doust, M. W., Gliner, B. E., Morgan, D. M., Kapural, L., Vallejo, R., Sitzman, B. T., Yearwood, T., Bundschu, R., Yang, T., Benyamin, R., Burgher, A. H., Brooks, E. S., Powell, A. A., & Subbaroyan, J. (2018). Long-term quality of life improvement for chronic intractable back and leg pain patients using spinal cord stimulation: 12-month results from the SENZA-RCT. *Quality of Life Research*, *27*(8), 2035–2044. https://doi.org/10.1007/s11136-018-1890-8

Anderson, K. L., & Ding, M. (2011). Attentional modulation of the somatosensory mu rhythm. *Neuroscience*, *180*, 165–180. https://doi.org/https://doi.org/10.1016/j.neuroscience.2011.02.004

Andrew, C., & Pfurtscheller, G. (1997). On the existence of different alpha band rhythms in the hand area of man. *Neuroscience Letters*, *222*(2), 103–106. https://doi.org/https://doi.org/10.1016/S0304-3940(97)13358-4

Andrew, D., & Greenspan, J. D. (1999). Mechanical and heat sensitization of cutaneous nociceptors after peripheral inflammation in the rat. *Journal of Neurophysiology*, *82*(5), 2649–2656. https://doi.org/10.1152/jn.1999.82.5.2649

Arle, J. E., Mei, L., & Carlson, K. W. (2020). Fiber Threshold Accommodation as a Mechanism of Burst and High-Frequency Spinal Cord Stimulation. *Neuromodulation*, *2019*(5), 582–593. https://doi.org/10.1111/ner.13076

Aymanns, M., Yekta, S. S., & Ellrich, J. (2009). Homotopic long-term depression of trigeminal pain

and blink reflex within one side of the human face. *Clinical Neurophysiology*, *120*(12), 2093–2099. https://doi.org/10.1016/j.clinph.2009.08.027

Azevedo, F. A. C., Carvalho, L. R. B., Grinberg, L. T., Farfel, J. M., Ferretti, R. E. L., Leite, R. E. P., Jacob Filho, W., Lent, R., & Herculano-Houzel, S. (2009). Equal numbers of neuronal and nonneuronal cells make the human brain an isometrically scaled-up primate brain. *The Journal of Comparative Neurology*, *513*(5), 532–541. https://doi.org/10.1002/cne.21974

Babiloni, C., Del Percio, C., Brancucci, A., Capotosto, P., Le Pera, D., Marzano, N., Valeriani, M., Romani, G. L., Arendt-Nielsen, L., & Rossini, P. M. (2008). Pre-stimulus alpha power affects vertex N2-P2 potentials evoked by noxious stimuli. *Brain Research Bulletin*, *75*(5), 581–590. https://doi.org/10.1016/j.brainresbull.2007.09.009

Baker, M. R., & Baker, S. N. (2003). The effect of diazepam on motor cortical oscillations and corticomuscular coherence studied in man. *The Journal of Physiology*, *546*(Pt 3), 931–942. https://doi.org/10.1113/jphysiol.2002.029553

Baliki, M. N., Geha, P. Y., & Apkarian, A. V. (2009). Parsing pain perception between nociceptive representation and magnitude estimation. *Journal of Neurophysiology*, *101*(2), 875–887. https://doi.org/10.1152/jn.91100.2008

Baliki, M. N., Mansour, A. R., Baria, A. T., & Apkarian, A. V. (2014). Functional reorganization of the default mode network across chronic pain conditions. *PLoS ONE*, *9*(9), e106133–e106133. https://doi.org/10.1371/journal.pone.0106133

Bantick, S. J., Wise, R. G., Ploghaus, A., Clare, S., Smith, S. M., & Tracey, I. (2002). Imaging how attention modulates pain in humans using functional MRI. *Brain*, *125*(2), 310–319. https://doi.org/10.1093/brain/awf022

Barchini, J., Tchachaghian, S., Shamaa, F., Jabbur, S. J., Meyerson, B. A., Song, Z., Linderoth, B., & Saadé, N. E. (2012). Spinal segmental and supraspinal mechanisms underlying the pain-relieving effects of spinal cord stimulation: An experimental study in a rat model of neuropathy. *Neuroscience*, *215*, 196–208. https://doi.org/10.1016/j.neuroscience.2012.04.057

Bardouille, T., Picton, T. W., & Ross, B. (2010). Attention modulates beta oscillations during prolonged tactile stimulation. *The European Journal of Neuroscience*, *31*(4), 761–769.

https://doi.org/10.1111/j.1460-9568.2010.07094.x

Barolat, G., Zeme, S., & Ketcik, B. (1991). Multifactorial Analysis of Epidural Spinal Cord Stimulation. *Stereotactic and Functional Neurosurgery*, *56*(1–4), 77–103. https://doi.org/10.1159/000099395

Barone, J., & Rossiter, H. E. (2021). Understanding the Role of Sensorimotor Beta Oscillations. *Frontiers in Systems Neuroscience*, *15*(May), 1–7. https://doi.org/10.3389/fnsys.2021.655886

Basbaum, A. I., Bautista, D. M., Scherrer, G., & Julius, D. (2009). Cellular and molecular mechanisms of pain. *Cell*, *139*(2), 267–284. https://doi.org/10.1016/j.cell.2009.09.028

Basbaum, A. I., & Jessell, T. M. (2013). Pain. In E. R. Kandel, J. H. Schwartz, T. M. Jessell, S. A. Siegelbaum, & A. J. Hudspeth (Eds.), *Principles of neural science.* (5th ed., pp. 530–555). McGraw-Hill Medical.

Bastuji, H., Frot, M., Perchet, C., Magnin, M., & Garcia-Larrea, L. (2016). Pain networks from the inside: Spatiotemporal analysis of brain responses leading from nociception to conscious perception. *Human Brain Mapping*, *37*(12), 4301–4315. https://doi.org/10.1002/hbm.23310

Bates, D., Schultheis, B. C., Hanes, M. C., Jolly, S. M., Chakravarthy, K., Deer, T. R., Levy, R. M., & Hunter, C. W. (2019). A Comprehensive Algorithm for Management of Neuropathic Pain. *Pain Medicine*, *20*(Supplement_1), S2–S12. https://doi.org/10.1093/pm/pnz075

Becerra, L., Breiter, H. C., Wise, R., Gonzalez, R. G., & Borsook, D. (2001). Reward circuitry activation by noxious thermal stimuli. *Neuron*, *32*(5), 927–946. https://doi.org/10.1016/S0896-6273(01)00533-5

Benjamini, Y., & Hochberg, Y. (1995). Controlling the False Discovery Rate: A Practical and Powerful Approach to Multiple Testing. *Journal of the Royal Statistical Society: Series B (Methodological)*, *57*(1), 289–300. https://doi.org/10.1111/J.2517-6161.1995.TB02031.X

Bentley, L. D., Duarte, R. V., Furlong, P. L., Ashford, R. L., & Raphael, J. H. (2016). Brain activity modifications following spinal cord stimulation for chronic neuropathic pain: A systematic review. *European Journal of Pain (United Kingdom)*, *20*(4), 499–511. https://doi.org/10.1002/ejp.782

Berg, P., & Scherg, M. (1994). A multiple source approach to the correction of eye artifacts.

Electroencephalography and Clinical Neurophysiology, *90*(3), 229–241. https://doi.org/10.1016/0013-4694(94)90094-9

Berge, O.-G. (2013). Animal Models of Pain. In S. B. McMahon, M. Koltzenburg, I. Tracey, & D. Turk (Eds.), *Wall and Melzack's Textbook of Pain* (6th Ed, pp. 170–181). Elsevier.

Bessou, P., & Perl, E. R. (1969). Response of cutaneous sensory units with unmyelinated fibers to noxious stimuli. *Journal of Neurophysiology*, *32*(6), 1025–1043. https://doi.org/10.1152/jn.1969.32.6.1025

Biermann, K., Schmitz, F., Witte, O. W., Konczak, J., Freund, H. J., & Schnitzler, A. (1998). Interaction of finger representation in the human first somatosensory cortex: a neuromagnetic study. *Neuroscience Letters*, *251*(1), 13–16. https://doi.org/10.1016/s0304-3940(98)00480-7

Binder, A., & Baron, R. (2013). Complex Regional Pain Syndromes. In S. B. McMahon, M. Koltzenburg, I. Tracey, & D. Turk (Eds.), *Wall and Melzack's Textbook of Pain* (6th Ed, pp. 961–977). Saunders.

Binder, A., & Baron, R. (2016). The Pharmacological Therapy of Chronic Neuropathic Pain. *Deutsches Arzteblatt International*, *113*(37), 616–625. https://doi.org/10.3238/arztebl.2016.0616

Biurrun Manresa, J. A., Mørch, C. D., & Andersen, O. K. (2010). Long-term facilitation of nociceptive withdrawal reflexes following low-frequency conditioning electrical stimulation: A new model for central sensitization in humans. *European Journal of Pain*, *14*(8), 822–831. https://doi.org/10.1016/j.ejpain.2009.12.008

Blair, R. D. G., Lee, R. G., & Vanderlinden, G. (1975). Dorsal Column Stimulation: Its Effect on the Somatosensory Evoked Response. *Archives of Neurology*, *32*(12), 826–829. https://doi.org/10.1001/archneur.1975.00490540070009

Bliss, T. V. P., & Collingridge, G. L. (1993). A synaptic model of memory: LTP in the hippocampus. *Nature*, *361*, 31–39.

Bliss, T. V. P., & Cooke, S. F. (2011). Long-term potentiation and long-term depression: a clinical perspective. *Clinics*, *66*(Suppl 1), 3–17. https://doi.org/10.1590/S1807-59322011001300002

Bliss, T. V. P., & Lomo, T. (1973). Long-lasting potentiation of synaptic transmission in the dentate area of the anaesthetized rabbit following stimulation of the perforant path. *The Journal of*

Physiology, *232*(2), 331–356. https://doi.org/10.1113/jphysiol.1973.sp010273

Bocci, T., De Carolis, G., Paroli, M., Barloscio, D., Parenti, L., Tollapi, L., Valeriani, M., & Sartucci, F. (2018). Neurophysiological Comparison Among Tonic, High Frequency, and Burst Spinal Cord Stimulation: Novel Insights Into Spinal and Brain Mechanisms of Action. *Neuromodulation: Technology at the Neural Interface*, *2017*(2006062332 002). https://doi.org/10.1111/ner.12747

Bogduk, N. (2009). On the definitions and physiology of back pain, referred pain, and radicular pain. *PAIN*, *147*(1). https://journals.lww.com/pain/Fulltext/2009/12150/On_the_definitions_and_physiology_of_back_pain,.9.aspx

Bornhövd, K., Quante, M., Glauche, V., Bromm, B., Weiller, C., & Büchel, C. (2002). Painful stimuli evoke different stimulus-response functions in the amygdala, prefrontal, insula and somatosensory cortex: a single-trial fMRI study. *Brain: A Journal of Neurology*, *125*(Pt 6), 1326–1336. https://doi.org/10.1093/brain/awf137

Boudewyn, M. A., Luck, S. J., Farrens, J. L., & Kappenman, E. S. (2018). How many trials does it take to get a significant ERP effect? It depends. *Psychophysiology*, *55*(6), e13049–e13049. https://doi.org/10.1111/psyp.13049

Bradley, C., Bastuji, H., & García-Larrea, L. (2017). Evidence-based source modeling of nociceptive cortical responses: A direct comparison of scalp and intracranial activity in humans. *Human Brain Mapping*, *38*(12), 6083–6095. https://doi.org/10.1002/hbm.23812

Bradley, C., Joyce, N., & Garcia-Larrea, L. (2016). Adaptation in human somatosensory cortex as a model of sensory memory construction: a study using high-density EEG. *Brain Structure and Function*, *221*(1), 421–431. https://doi.org/10.1007/s00429-014-0915-5

Brinzeu, A., Cuny, E., Fontaine, D., Mertens, P., Luyet, P., Van den Abeele, C., Djian, M., Le Borgne, J., Palfi, S., Sol, J., Fowo, S., Desenclos, C., Gadan, R., Nizar, S., Simon, E., Barat, J., Blond, S., Buisset, N., Bougeard, R., … Polo, G. (2019). Spinal cord stimulation for chronic refractory pain: Long-term effectiveness and safety data from a multicentre registry. *European Journal of Pain*, *23*(5), 1031–1044. https://doi.org/10.1002/ejp.1355

Brodal, P. (1992). *The central nervous system: structure and function*. Oxford University Press.

Bromm, B., Jahnke, M., & Treede, R.-D. (1984). Responses of human cutaneous afferents to CO2 laser stimuli causing pain. *Experimental Brain Research*, *55*(1), 158–166.

Bromm, B., & Meier, W. (1984). The intracutaneous stimulus: a new pain model for algesimetric studies. *Methods and Findings in Experimental and Clinical Pharmacology*, *6*(7), 405–410.

Bromm, B., & Treede, R.-D. (1984). Nerve fibre discharges, cerebral potentials and sensations induced by CO2 laser stimulation. *Human Neurobiology*, *3*(1), 33–40.

Brouwer, G. J., Arnedo, V., Offen, S., Heeger, D. J., & Grant, A. C. (2015). Normalization in human somatosensory cortex. *Journal of Neurophysiology*, *114*(5), 2588–2599. https://doi.org/10.1152/jn.00939.2014

Brovelli, A., Battaglini, P. P., Naranjo, J. R., & Budai, R. (2002). Medium-range oscillatory network and the 20-Hz sensorimotor induced potential. *NeuroImage*, *16*(1), 130–141. https://doi.org/10.1006/nimg.2002.1058

Buonocore, M., Bodini, A., Demartini, L., & Bonezzi, C. (2012). Inhibition of somatosensory evoked potentials during spinal cord stimulation and its possible role in the comprehension of antalgic mechanisms of neurostimulation for neuropathic pain. *Minerva Anestesiologica*, *78*(3), 297–302. http://www.ncbi.nlm.nih.gov/pubmed/22095108

Buonocore, M., & Demartini, L. (2016). Inhibition of Somatosensory Evoked Potentials During Different Modalities of Spinal Cord Stimulation: A Case Report. *Neuromodulation: Technology at the Neural Interface*, *19*(8), 882–884. https://doi.org/10.1111/ner.12380

Burgess, P. R., & Perl, E. R. (1967). Myelinated afferent fibres responding specifically to noxious stimulation of the skin. *The Journal of Physiology*, *190*(3), 541–562. https://doi.org/10.1113/jphysiol.1967.sp008227

Burke, D., Mackenzie, R. A., Skuse, N. F., & Lethlean, A. K. (1975). Cutaneous afferent activity in median and radial nerve fascicles: A microelectrode study. *Journal of Neurology, Neurosurgery and Psychiatry*, *38*(9), 855–864. https://doi.org/10.1136/jnnp.38.9.855

Bushnell, M. C., Duncan, G. H., Dubner, R., & He, L. F. (1984). Activity of trigeminothalamic neurons in medullary dorsal horn of awake monkeys trained in a thermal discrimination task.

Journal of Neurophysiology, *52*(1), 170–187. https://doi.org/10.1152/jn.1984.52.1.170

Bussa, M., Mascaro, A., Cuffaro, L., & Rinaldi, S. (2017). Adult Complex Regional Pain Syndrome Type I: A Narrative Review. *PM&R*, *9*(7), 707–719. https://doi.org/10.1016/j.pmrj.2016.11.006

Buzsáki, G., Anastassiou, C. A., & Koch, C. (2012). The origin of extracellular fields and currents-EEG, ECoG, LFP and spikes. *Nature Reviews Neuroscience*, *13*(6), 407–420. https://doi.org/10.1038/nrn3241

Cambiaghi, M., & Sconocchia, S. (2018). Scribonius Largus (probably before 1CE–after 48CE). *Journal of Neurology*, *265*(10), 2466–2468. https://doi.org/10.1007/s00415-018-8739-5

Campbell, J. N., & Meyer, R. A. (1983). Sensitization of unmyelinated nociceptive afferents in monkey varies with skin type. *Journal of Neurophysiology*, *49*(1), 98–110. https://doi.org/10.1152/jn.1983.49.1.98

Campbell, J. N., Raja, S. N., Meyer, R. A., & Mackinnon, S. E. (1988). Myelinated afferents signal the hyperalgesia associated with nerve injury. *Pain*, *32*(1), 89–94. https://doi.org/10.1016/0304-3959(88)90027-9

Carmon, A., Dotan, Y., & Sarne, Y. (1978). Correlation of subjective pain experience with cerebral evoked responses to noxious thermal stimulations. *Experimental Brain Research*, *33*(3–4), 445–453. https://doi.org/10.1007/BF00235566

Cauda, F., Sacco, K., Duca, S., Cocito, D., D'Agata, F., Geminiani, G. C., & Canavero, S. (2009). Altered Resting State in Diabetic Neuropathic Pain. *PLoS ONE*, *4*(2), e4542. https://doi.org/10.1371/journal.pone.0004542

Cavalli, E., Mammana, S., Nicoletti, F., Bramanti, P., & Mazzon, E. (2019). The neuropathic pain: An overview of the current treatment and future therapeutic approaches. *International Journal of Immunopathology and Pharmacology*, *33*, 205873841983838. https://doi.org/10.1177/2058738419838383

Chakravarthy, K., Reddy, R., Al-Kaisy, A., Yearwood, T., & Grider, J. (2021). A Call to Action Toward Optimizing the Electrical Dose Received by Neural Targets in Spinal Cord Stimulation Therapy for Neuropathic Pain. *Journal of Pain Reseach*, *14*, 2767–2776. https://doi.org/10.2147/JPR.S323372

Chang, B. S., Schomer, D. L., & Niedermeyer, E. (2011). Normal EEG and Sleep: Adults and Elderly. In D. L. Schomer & F. H. Lopes da Silva (Eds.), *Niedermeyer's Electroencephalography: Basic Principles, Clinical Applications, and Related Fields* (6th ed., pp. 183–214). Wolters Kluwer/Lippincott Williams & Wilkins Health.

Chatrian, G. E., Petersen, M. C., & Lazarte, J. A. (1959). The blocking of the rolandic wicket rhythm and some central changes related to movement. *Electroencephalography and Clinical Neurophysiology*, *11*(3), 497–510. https://doi.org/10.1016/0013-4694(59)90048-3

Chen, F., Hallez, H., Hese, P. van, D'Asseler, Y., & Lemahieu, I. (2007). Dipole Estimation Errors Due to Skull Conductivity Perturbations: Simulation Study in Spherical Head Models. *2007 Joint Meeting of the 6th International Symposium on Noninvasive Functional Source Imaging of the Brain and Heart and the International Conference on Functional Biomedical Imaging*, 86–89. https://doi.org/10.1109/NFSI-ICFBI.2007.4387694

Chen, J., & Sandkühler, J. (2000). Induction of homosynaptic long-term depression at spinal synapses of sensory Aδ-fibers requires activation of metabotropic glutamate receptors. *Neuroscience*, *98*(1), 141–148. https://doi.org/10.1016/S0306-4522(00)00080-4

Chen, R., Corwell, B., & Hallett, M. (1999). Modulation of motor cortex excitability by median nerve and digit stimulation. *Experimental Brain Research*, *129*(1), 77–86. https://doi.org/10.1007/s002210050938

Chen, T., Taniguchi, W., Chen, Q.-Y., Tozaki-Saitoh, H., Song, Q., Liu, R.-H. H., Koga, K., Matsuda, T., Kaito-Sugimura, Y., Wang, J., Li, Z.-H. H., Lu, Y.-C. C., Inoue, K., Tsuda, M., Li, Y.-Q. Q., Nakatsuka, T., & Zhuo, M. (2018). Top-down descending facilitation of spinal sensory excitatory transmission from the anterior cingulate cortex. *Nature Communications*, *9*(1), 1886. https://doi.org/10.1038/s41467-018-04309-2

Cheron, G., Dan, B., & Borenstein, S. (2000). Sensory and Motor Interfering Influences on Somatosensory Evoked Potentials. *Journal of Clinical Neurophysiology*, *17*(3).

Cheyne, D., Gaetz, W., Garnero, L., Lachaux, J., Ducorps, A., Schwartz, D., & Varela, F. J. (2003). Neuromagnetic imaging of cortical oscillations accompanying tactile stimulation. *Cognitive Brain Research*, *17*(3), 599–611. https://doi.org/10.1016/S0926-6410(03)00173-3

Chien, J. H., Liu, C. C., Kim, J. H., Markman, T. M., & Lenz, F. A. (2014). Painful cutaneous laser stimuli induce event-related oscillatory EEG activities that are different from those induced by nonpainful electrical stimuli. *Journal of Neurophysiology*, *112*(4), 824–833. https://doi.org/10.1152/jn.00209.2014

Chipchase, L. S., Schabrun, S. M., & Hodges, P. W. (2011). Peripheral electrical stimulation to induce cortical plasticity: A systematic review of stimulus parameters. *Clinical Neurophysiology*, *122*(3), 456–463. https://doi.org/https://doi.org/10.1016/j.clinph.2010.07.025

Clark, J. A., Brown, C. A., Jones, A. K. ., & El-Deredy, W. (2008). Dissociating nociceptive modulation by the duration of pain anticipation from unpredictability in the timing of pain. *Clinical Neurophysiology*, *119*(12), 2870–2878. https://doi.org/10.1016/j.clinph.2008.09.022

Coghill, R. C. (2020). The Distributed Nociceptive System: A Framework for Understanding Pain. *Trends in Neurosciences*, *43*(10), 780–794. https://doi.org/10.1016/j.tins.2020.07.004

Coghill, R. C., Mayer, D. J., & Price, D. D. (1993). Wide dynamic range but not nociceptive-specific neurons encode multidimensional features of prolonged repetitive heat pain. *Journal of Neurophysiology*, *69*(3), 703–716. https://doi.org/10.1152/jn.1993.69.3.703

Coghill, R. C., Sang, C. N., Maisog, J. M., & Iadarola, M. J. (1999). Pain intensity processing within the human brain: a bilateral, distributed mechanism. *Journal of Neurophysiology*, *82*(4), 1934–1943. https://doi.org/10.1152/jn.1999.82.4.1934

Cohen, D., Cuffin, B. N., Yunokuchi, K., Maniewski, R., Purcell, C., Cosgrove, G. R., Ives, J., Kennedy, J. G., & Schomer, D. L. (1990). MEG versus EEG localization test using implanted sources in the human brain. *Annals of Neurology*, *28*(6), 811–817. https://doi.org/10.1002/ana.410280613

Cohen, M. X. (2014). *Analyzing neural time series data: theory and practice*. MIT press.

Cohen, S. P., Vase, L., & Hooten, W. M. (2021). Chronic pain: an update on burden, best practices, and new advances. *The Lancet*, *397*(10289), 2082–2097. https://doi.org/10.1016/S0140-6736(21)00393-7

Collins, W. F., Nulsen, F. E., & Randt, C. T. (1960). Relation of Peripheral Nerve Fiber Size and Sensation in Man. *Archives of Neurology*, *3*(4), 381–385.

https://doi.org/10.1001/archneur.1960.00450040031003

Colon, E., Legrain, V., & Mouraux, A. (2014). EEG Frequency Tagging to Dissociate the Cortical Responses to Nociceptive and Nonnociceptive Stimuli. *Journal of Cognitive Neuroscience*, *26*(10), 2262–2274. https://doi.org/10.1162/jocn_a_00648

Condes-Lara, M., Calvo, J. M., & Fernandez-Guardiola, A. (1981). Habituation to bearable experimental pain elicited by tooth pulp electrical stimulation. *Pain*, *11*(2), 185–200. https://doi.org/10.1016/0304-3959(81)90004-X

Crosby, N. D., Goodman Keiser, M. D., Smith, J. R., Zeeman, M. E., & Winkelstein, B. A. (2015a). Stimulation parameters define the effectiveness of burst spinal cord stimulation in a rat model of neuropathic pain. *Neuromodulation*, *18*(1), 1–8. https://doi.org/10.1111/ner.12221

Crosby, N. D., Weisshaar, C. L., Smith, J. R., Zeeman, M. E., Goodman-Keiser, M. D., & Winkelstein, B. A. (2015b). Burst and Tonic Spinal Cord Stimulation Differentially Activate GABAergic Mechanisms to Attenuate Pain in a Rat Model of Cervical Radiculopathy. *IEEE Trans Biomed Eng*, *62*(6), 1604–1613. https://doi.org/10.1109/TBME.2015.2399374

Cruccu, G., Aminoff, M. J., Curio, G., Guerit, J. M., Kakigi, R., Mauguière, F., Rossini, P. M., Treede, R.-D., & García-Larrea, L. (2008). Recommendations for the clinical use of somatosensory-evoked potentials. *Clinical Neurophysiology*, *119*(8), 1705–1719. https://doi.org/10.1016/j.clinph.2008.03.016

Cruccu, G., Sommer, C., Anand, P., Attal, N., Baron, R., Garcia-Larrea, L., Haanpaa, M., Jensen, T. S., Serra, J., & Treede, R.-D. (2010). EFNS guidelines on neuropathic pain assessment: revised 2009. *European Journal of Neurology*, *17*(8), 1010–1018. https://doi.org/10.1111/j.1468-1331.2010.02969.x

Cuffin, B. N., Cohen, D., Yunokuchi, K., Maniewski, R., Purcell, C., Cosgrove, G. R., Ives, J., Kennedy, J., & Schomer, D. L. (1991). Tests of EEG localization accuracy using implanted sources in the human brain. *Annals of Neurology*, *29*(2), 132–138. https://doi.org/10.1002/ana.410290204

Cui, J. G., Meyerson, B. A., Sollevi, A., & Linderoth, B. (1998). Effect of spinal cord stimulation on tactile hypersensitivity in mononeuropathic rats is potentiated by simultaneous GABA(B) and

adenosine receptor activation. *Neuroscience Letters*, *247*(2–3), 183–186. https://doi.org/10.1016/S0304-3940(98)00324-3

Cui, J. G., O'Connor, W. T., Ungerstedt, U., Linderoth, B., & Meyerson, B. A. (1997). Spinal cord stimulation attenuates augmented dorsal horn release of excitatory amino acids in mononeuropathy via a GABAergic mechanism. *Pain*, *73*(1), 87–95. https://doi.org/10.1016/S0304-3959(97)00077-8

D'Agata, F., Cicerale, A., Mingolla, A., Caroppo, P., Orsi, L., Mortara, P., Troni, W., & Pinessi, L. (2015). Double-cone coil TMS stimulation of the medial cortex inhibits central pain habituation. *PLOS ONE*, *10*(6), e0128765. https://doi.org/10.1371/journal.pone.0128765

Das, A., de los Angeles, C., & Menon, V. (2022). Electrophysiological foundations of the human default-mode network revealed by intracranial-EEG recordings during resting-state and cognition. *NeuroImage*, *250*, 118927. https://doi.org/https://doi.org/10.1016/j.neuroimage.2022.118927

Davis, K. D., Taylor, S. J., Crawley, A. P., Wood, M. L., & Mikulis, D. J. (1997). Functional MRI of pain- and attention-related activations in the human cingulate cortex. *Journal of Neurophysiology*, *77*(6), 3370–3380. https://doi.org/10.1152/jn.1997.77.6.3370

Dawson, G. D. (1947). Cerebral responses to electrical stimulation of peripheral nerve in man. *Journal of Neurology, Neurosurgery & Psychiatry*, *10*(3), 134–140. https://doi.org/10.1136/jnnp.10.3.134

Dawson, G. D., & Scott, J. W. (1949). The recording of nerve action potentials through skin in man. *Journal of Neurology, Neurosurgery & Psychiatry*, *12*(4), 259–267. https://doi.org/10.1136/jnnp.12.4.259

De Andrade, D. C., Bendib, B., Hattou, M., Keravel, Y., Nguyen, J. P., & Lefaucheur, J. P. (2010). Neurophysiological assessment of spinal cord stimulation in failed back surgery syndrome. *Pain*, *150*(3), 485–491. https://doi.org/10.1016/j.pain.2010.06.001

De Ridder, D., Plazier, M., Kamerling, N., Menovsky, T., & Vanneste, S. (2013). Burst spinal cord stimulation for limb and back pain. *World Neurosurg*, *80*(5), 642-649 e1. https://doi.org/10.1016/j.wneu.2013.01.040

De Ridder, D., Vancamp, T., Falowski, S. M., & Vanneste, S. (2020). All bursts are equal, but some are more equal (to burst firing): burstDR stimulation versus Boston burst stimulation. *Expert Review of Medical Devices*, *00*(00), 1–7. https://doi.org/10.1080/17434440.2020.1736560

De Ridder, D., & Vanneste, S. (2016). Burst and tonic spinal cord stimulation: Different and common brain mechanisms. *Neuromodulation*, *19*(1), 47–59. https://doi.org/10.1111/ner.12368

De Ridder, D., Vanneste, S., Plazier, M., van der Loo, E., & Menovsky, T. (2010). Burst spinal cord stimulation: Toward paresthesia-free pain suppression. *Neurosurgery*, *66*(5), 986–990. https://doi.org/10.1227/01.NEU.0000368153.44883.B3

de Vos, C. C., Bom, M. J., Vanneste, S., Lenders, M. W. P. M., & de Ridder, D. (2014). Burst Spinal Cord Stimulation Evaluated in Patients With Failed Back Surgery Syndrome and Painful Diabetic Neuropathy. *Neuromodulation: Technology at the Neural Interface*, *17*(2), 152–159. https://doi.org/10.1111/ner.12116

Deer, T., Pope, J. E., Benyamin, R., Vallejo, R., Friedman, A., Caraway, D., Staats, P., Grigsby, E., McRoberts, W. P., McJunkin, T., Shubin, R., Vahedifar, P., Tavanaiepour, D., Levy, R. M., Kapural, L., & Mekhail, N. (2016). Prospective, Multicenter, Randomized, Double-Blinded, Partial Crossover Study to Assess the Safety and Efficacy of the Novel Neuromodulation System in the Treatment of Patients With Chronic Pain of Peripheral Nerve Origin. *Neuromodulation : Journal of the International Neuromodulation Society*, *19*(1), 91–100. https://doi.org/10.1111/ner.12381

Deer, T. R., Patterson, D. G., Baksh, J., Pope, J. E., Mehta, P., Raza, A., Agnesi, F., & Chakravarthy, K. (2021). Novel Intermittent Dosing Burst Paradigm in Spinal Cord Stimulation. *Neuromodulation: Technology at the Neural Interface*, *24*(3), 566–573. https://doi.org/10.1111/ner.13143

Deer, T., Slavin, K. V., Amirdelfan, K., North, R. B., Burton, A. W., Yearwood, T., Tavel, E., Staats, P., Falowski, S., Pope, J. E., Justiz, R., Fabi, A. Y., Taghva, A., Paicius, R., Houden, T., & Wilson, D. (2018). Success Using Neuromodulation With BURST (SUNBURST) Study: Results From a Prospective, Randomized Controlled Trial Using a Novel Burst Waveform. *Neuromodulation : Journal of the International Neuromodulation Society*, *21*(1), 56–66.

https://doi.org/10.1111/ner.12698

Della Penna, S., Torquati, K., Pizzella, V., Babiloni, C., Franciotti, R., Rossini, P. M., & Romani, G. L. (2004). Temporal dynamics of alpha and beta rhythms in human SI and SII after galvanic median nerve stimulation. A MEG study. *NeuroImage*, *22*(4), 1438–1446. https://doi.org/10.1016/j.neuroimage.2004.03.045

Delorme, A., & Makeig, S. (2004). EEGLAB: an open source toolbox for analysis of single-trial EEG dynamics including independent component analysis. *Journal of Neuroscience Methods*, *134*(1), 9–21. https://doi.org/10.1016/j.jneumeth.2003.10.009

Deogaonkar, M., Sharma, M., Oluigbo, C., Nielson, D. M., Yang, X., Vera-Portocarrero, L. P., Molnar, G. F., Abduljalil, A., Sederberg, P. B., Knopp, M., & Rezai, A. R. (2016). Spinal Cord Stimulation (SCS) and Functional Magnetic Resonance Imaging (fMRI): Modulation of Cortical Connectivity with Therapeutic SCS. *Neuromodulation*, *19*(2), 142–152. https://doi.org/10.1111/ner.12346

Derbyshire, S. W. ., Jones, A. K. ., Gyulai, F., Clark, S., Townsend, D., & Firestone, L. L. (1997). Pain processing during three levels of noxious stimulation produces differential patterns of central activity. *Pain*, *73*(3), 431–445. https://doi.org/10.1016/S0304-3959(97)00138-3

Devinsky, O., Morrell, M. J., & Vogt, B. A. (1995). Contributions of anterior cingulate cortex to behaviour. *Brain*, *118*(1), 279–306. https://doi.org/10.1093/brain/118.1.279

Devor, M. (2013). Neuropathic Pain: Pathological Response of Nerves to Injury. In S. B. McMahon, M. Koltzenburg, I. Tracey, & D. Turk (Eds.), *Wall and Melzack's Textbook of Pain* (6th Ed, pp. 861–889). Saunders. https://doi.org/10.1016/B0-443-07287-6/50063-1

Di Stefano, G., Di Lionardo, A., Di Pietro, G., Cruccu, G., & Truini, A. (2021). Pharmacotherapeutic options for managing neuropathic pain: a systematic review and meta-analysis. *Pain Research and Management*, *2021*, 1–13. https://doi.org/10.1155/2021/6656863

Dodick, D. W., Silberstein, S. D., Reed, K. L., Deer, T. R., Slavin, K. V., Huh, B., Sharan, A., Narouze, S., Mogilner, A. Y., Trentman, T. L., Ordia, J., Vaisman, J., Goldstein, J., & Mekhail, N. (2015). Safety and efficacy of peripheral nerve stimulation of the occipital nerves for the management of chronic migraine: Long-term results from a randomized, multicenter, double-

blinded, controlled study. *Cephalalgia*, *35*(4), 344–358. https://doi.org/10.1177/0333102414543331

Doerr, M., Krainick, J. U., & Thoden, U. (1978). Pain perception in man after long term spinal cord stimulation. *Journal of Neurology*, *217*(4), 261–270.

Duarte, R. V., Nevitt, S., McNicol, E., Taylor, R. S., Buchser, E., North, R. B., & Eldabe, S. (2020). Systematic review and meta-analysis of placebo/sham controlled randomised trials of spinal cord stimulation for neuropathic pain. *Pain*, *161*(1), 24–35. https://doi.org/10.1097/j.pain.0000000000001689

Dudek, S. M., & Bear, M. F. (1992). Homosynaptic long-term depression in area CA1 of hippocampus and effects of N-methyl-D-aspartate receptor blockade. *Proceedings of the National Academy of Sciences*, *89*(10), 4363–4367. https://doi.org/10.1073/pnas.89.10.4363

Duerden, E. G., & Albanese, M.-C. (2013). Localization of pain-related brain activation: A meta-analysis of neuroimaging data. *Human Brain Mapping*, *34*(1), 109–149. https://doi.org/10.1002/hbm.21416

Dum, R. P., Levinthal, D. J., & Strick, P. L. (2009). The spinothalamic system targets motor and sensory areas in the cerebral cortex of monkeys. *Journal of Neuroscience*, *29*(45), 14223–14235. https://doi.org/10.1523/JNEUROSCI.3398-09.2009

Dumermuth, G., & Molinari, L. (1987). Spectral analysis of EEG background activity. In A. S. Gevins & A. Rémond (Eds.), *Handbook of Electroencephalography and Clinical Neurophysiology: Methods of Analysis of Brain Electrical and Magnetic Signals* (Volume 1, pp. 85–130). Elsevier.

Edin, B., Essick, G., Trulsson, M., & Olsson, K. A. (1995). Receptor encoding of moving tactile stimuli in humans. I. Temporal pattern of discharge of individual low-threshold mechanoreceptors. *The Journal of Neuroscience*, *15*(1), 830–847. https://doi.org/10.1523/JNEUROSCI.15-01-00830.1995

Eippert, F., Bingel, U., Schoell, E. D., Yacubian, J., Klinger, R., Lorenz, J., & Büchel, C. (2009). Activation of the Opioidergic Descending Pain Control System Underlies Placebo Analgesia. *Neuron*, *63*(4), 533–543. https://doi.org/10.1016/j.neuron.2009.07.014

El-Khoury, C., Hawwa, N., Baliki, M. N., Atweh, S. F., Jabbur, S. J., & Saadé, N. E. (2002). Attenuation of neuropathic pain by segmental and supraspinal activation of the dorsal column system in awake rats. *Neuroscience*, *112*(3), 541–553. https://doi.org/10.1016/S0306-4522(02)00111-2

Eldabe, S., Kumar, K., Buchser, E., & Taylor, R. S. (2010). An analysis of the components of pain, function, and health-related quality of life in patients with failed back surgery syndrome treated with spinal cord stimulation or conventional medical management. *Neuromodulation*, *13*(3), 201–209. https://doi.org/10.1111/j.1525-1403.2009.00271.x

Ellrich, J. (2004). Electric Low-Frequency Stimulation of the Tongue Induces Long-Term Depression of the Jaw-Opening Reflex in Anesthetized Mice. *Journal of Neurophysiology*, *92*(6), 3332–3337. https://doi.org/10.1152/jn.00156.2004

Ellrich, J., & Schorr, A. (2002). Long-term depression of the human masseter inhibitory reflex. *Neuroscience Letters*, *329*(3), 265–268. https://doi.org/10.1016/S0304-3940(02)00669-9

Ellrich, J., & Schorr, A. (2004). Low-frequency stimulation of trigeminal afferents induces long-term depression of human sensory processing. *Brain Research*, *996*(2), 255–258. https://doi.org/10.1016/j.brainres.2003.08.068

Enatsu, R., Nagamine, T., Matsubayashi, J., Maezawa, H., Kikuchi, T., Fukuyama, H., Mikuni, N., Miyamoto, S., & Hashimoto, N. (2014). The modulation of rolandic oscillation induced by digital nerve stimulation and self-paced movement of the finger: A MEG study. *Journal of the Neurological Sciences*, *337*(1–2), 201–211. https://doi.org/10.1016/j.jns.2013.12.011

Fallon, N., Chiu, Y. H., Li, X., Nurmikko, T. J., & Stancak, A. (2013). Ipsilateral cortical activation in fibromyalgia patients during brushing correlates with symptom severity. *Clinical Neurophysiology*, *124*(1), 154–163. https://doi.org/10.1016/j.clinph.2012.06.014

Fallon, N., Chiu, Y. H., Nurmikko, T. J., & Stancak, A. (2018). Altered theta oscillations in resting EEG of fibromyalgia syndrome patients. *European Journal of Pain*, *22*(1), 49–57. https://doi.org/10.1002/ejp.1076

Falowski, S. (2018). Fundamental Differences in Burst Stimulation Waveform Design: Eliminating Confusion in the Marketplace. *Neuromodulation: Technology at the Neural Interface*, *21*.

https://doi.org/10.1111/ner.12762

Farber, S. H., Han, J. L., Elsamadicy, A. A., Hussaini, Q., Yang, S., Pagadala, P., Parente, B., Xie, J., & Lad, S. P. (2017). Long-term Cost Utility of Spinal Cord Stimulation in Patients with Failed Back Surgery Syndrome. *Pain Physician*, *20*(6), E797–E805. http://www.ncbi.nlm.nih.gov/pubmed/28934786

Farrell, M. J., Laird, A. R., & Egan, G. F. (2005). Brain activity associated with painfully hot stimuli applied to the upper limb: a meta-analysis. *Human Brain Mapping*, *25*(1), 129–139. https://doi.org/10.1002/hbm.20125

Fayaz, A., Croft, P., Langford, R. M., Donaldson, L. J., & Jones, G. T. (2016). Prevalence of chronic pain in the UK: a systematic review and meta-analysis of population studies. *BMJ Open*, *6*(6), e010364. https://doi.org/10.1136/bmjopen-2015-010364

Feige, B., Scheffler, K., Esposito, F., Di Salle, F., Hennig, J., & Seifritz, E. (2005). Cortical and subcortical correlates of electroencephalographic alpha rhythm modulation. *Journal of Neurophysiology*, *93*(5), 2864–2872. https://doi.org/10.1152/jn.00721.2004

Finnerup, N. B., Attal, N., Haroutounian, S., McNicol, E., Baron, R., Dworkin, R. H., Gilron, I., Haanpää, M., Hansson, P., Jensen, T. S., Kamerman, P. R., Lund, K., Moore, A., Raja, S. N., Rice, A. S. C., Rowbotham, M. C., Sena, E., Siddall, P., Smith, B. H., & Wallace, M. S. (2015). Pharmacotherapy for neuropathic pain in adults: a systematic review and meta-analysis. *The Lancet Neurology*, *14*(2), 162–173. https://doi.org/10.1016/S1474-4422(14)70251-0

Finnerup, N. B., Haroutounian, S., Kamerman, P. R., Baron, R., Bennett, D. L. H., Bouhassira, D., Cruccu, G., Freeman, R., Hansson, P., Nurmikko, T. J., Raja, S. N., Rice, A. S. C., Serra, J., Smith, B. H., Treede, R.-D., & Jensen, T. S. (2016). Neuropathic pain: an updated grading system for research and clinical practice. *Pain*, *157*(8), 1599–1606. https://doi.org/10.1097/j.pain.0000000000000492

Forss, N., Hari, R., Salmelin, R., Ahonen, A., Hämäläinen, M., Kajola, M., Knuutila, J., & Simola, J. (1994). Activation of the human posterior parietal cortex by median nerve stimulation. *Experimental Brain Research*, *99*(2), 309–315. https://doi.org/10.1007/BF00239597

Forss, N., Narici, L., & Hari, R. (2001). Sustained activation of the human SII cortices by stimulus

trains. *NeuroImage*, *13*(3), 497–501. https://doi.org/10.1006/nimg.2000.0700

Foxe, J. J., & Snyder, A. C. (2011). The Role of Alpha-Band Brain Oscillations as a Sensory Suppression Mechanism during Selective Attention. *Frontiers in Psychology*, *2*, 1–13. https://doi.org/10.3389/fpsyg.2011.00154

Franz, M., Nickel, M. M., Ritter, A., Miltner, W. H. R., & Weiss, T. (2015). Somatosensory spatial attention modulates amplitudes, latencies, and latency jitter of laser-evoked brain potentials. *Journal of Neurophysiology*, *113*(7), 2760–2768. https://doi.org/10.1152/jn.00070.2015

Frederico, T. N., & da Silva Freitas, T. (2020). Peripheral Nerve Stimulation of the Brachial Plexus for Chronic Refractory CRPS Pain of the Upper Limb: Description of a New Technique and Case Series. *Pain Medicine*, *21*(Supplement_1), S18–S26. https://doi.org/10.1093/pm/pnaa201

Friebel, U., Eickhoff, S. B., & Lotze, M. (2011). Coordinate-based meta-analysis of experimentally induced and chronic persistent neuropathic pain. *NeuroImage*, *58*(4), 1070–1080. https://doi.org/10.1016/j.neuroimage.2011.07.022

Frot, M., Magnin, M., Mauguière, F., & Garcia-Larrea, L. (2013). Cortical representation of pain in primary sensory-motor areas (S1/M1)-a study using intracortical recordings in humans. *Human Brain Mapping*, *34*(10), 2655–2668. https://doi.org/10.1002/hbm.22097

Fry, A., Mullinger, K. J., O'Neill, G. C., Barratt, E. L., Morris, P. G., Bauer, M., Folland, J. P., & Brookes, M. J. (2016). Modulation of post-movement beta rebound by contraction force and rate of force development. *Human Brain Mapping*, *37*(7), 2493–2511. https://doi.org/10.1002/hbm.23189

Fuchs, P. N., Campbell, J. N., & Meyer, R. A. (2000). Secondary hyperalgesia persists in capsaicin desensitized skin. *Pain*, *84*(2–3), 141–149. https://doi.org/10.1016/s0304-3959(99)00194-3

Gaetz, W., & Cheyne, D. (2006). Localization of sensorimotor cortical rhythms induced by tactile stimulation using spatially filtered MEG. *NeuroImage*, *30*(3), 899–908. https://doi.org/10.1016/j.neuroimage.2005.10.009

Gaetz, W., Edgar, J. C., Wang, D. J., & Roberts, T. P. L. (2011). Relating MEG measured motor cortical oscillations to resting γ-Aminobutyric acid (GABA) concentration. *NeuroImage*, *55*(2), 616–621. https://doi.org/10.1016/j.neuroimage.2010.12.077

Gandevia, S. C., Burke, D., & McKeon, B. B. (1983). Convergence in the somatosensory pathway between cutaneous afferents from the index and middle fingers in man. *Experimental Brain Research*, *50*(2–3), 415–425. https://doi.org/10.1007/BF00239208

Garcia-Larrea, L., Convers, P., Magnin, M., André-Obadia, N., Peyron, R., Laurent, B., & Mauguière, F. (2002). Laser-evoked potential abnormalities in central pain patients: The influence of spontaneous and provoked pain. *Brain*, *125*(12), 2766–2781. https://doi.org/10.1093/brain/awf275

García-Larrea, L., Frot, M., & Valeriani, M. (2003). Brain generators of laser-evoked potentials: From dipoles to functional significance. *Clinical Neurophysiology*, *33*(6), 279–292. https://doi.org/10.1016/j.neucli.2003.10.008

García-Larrea, L., Peyron, R., Merlet, I., Laurent, B., & Mauguière, F. (1997). Nociceptive evoked potentials or cognitive evoked potentials? A mapping/modeling study of cortical responses to painful and innocuous stimulation under attentive and distractive conditions. *Electroencephalography and Clinical Neurophysiology*, *103*(1), 179.

Gardner, E. P., & Johnson, K. O. (2013). The Somatosensory System: Receptors and Central Pathways. In E. R. Kandel, J. H. Schwartz, T. M. Jessell, S. A. Siegelbaum, & A. J. Hudspeth (Eds.), *Principles of neural science.* (5th ed., pp. 475–497). McGraw-Hill Medical.

Gasser, T., Bächer, P., & Möcks, J. (1982). Transformations towards the normal distribution of broad band spectral parameters of the EEG. *Electroencephalography and Clinical Neurophysiology*, *53*(1), 119–124. https://doi.org/10.1016/0013-4694(82)90112-2

Gastaut, H. (1952). [Electrocorticographic study of the reactivity of rolandic rhythm]. *Revue neurologique*, *87*(2), 176–182.

Geurts, J. W., Smits, H., Kemler, M. A., Brunner, F., Kessels, A. G. H., & van Kleef, M. (2013). Spinal Cord Stimulation for Complex Regional Pain Syndrome Type I: A Prospective Cohort Study With Long-Term Follow-Up. *Neuromodulation: Technology at the Neural Interface*, *16*(6), 523–529. https://doi.org//10.1111/ner.12024

Geuter, S., Reynolds Losin, E. A., Roy, M., Atlas, L. Y., Schmidt, L., Krishnan, A., Koban, L., Wager, T. D., & Lindquist, M. A. (2020). Multiple brain networks mediating stimulus–pain

relationships in humans. *Cerebral Cortex*, *30*(7), 4204–4219. https://doi.org/10.1093/cercor/bhaa048

Gevins, A. S. (1987). Overview of computer analysis. In A. S. Gevins & A. Rémond (Eds.), *Handbook of Electroencephalography and Clinical Neurophysiology: Methods of Analysis of Brain Electrical and Magnetic Signals1* (Volume 1, pp. 31–84). Elsevier.

Gibson, W., Wand, B. M., Meads, C., Catley, M. J., & O'connell, N. E. (2019). Transcutaneous electrical nerve stimulation (TENS) for chronic pain - An overview of Cochrane Reviews. *Cochrane Database of Systematic Reviews*, *2019*(2). https://doi.org/10.1002/14651858.CD011890.pub2

Goroszeniuk, T., Pang, D., Shetty, A., Eldabe, S., O'Keeffe, D., & Racz, G. (2014). Percutaneous Peripheral Neuromodulation Lead Insertion Using a Novel Stimulating Coudé Needle. *Neuromodulation: Technology at the Neural Interface*, *17*(5), 506–509. https://doi.org/10.1111/ner.12126

Goudman, L., Linderoth, B., Nagels, G., Huysmans, E., & Moens, M. (2020). Cortical Mapping in Conventional and High Dose Spinal Cord Stimulation: An Exploratory Power Spectrum and Functional Connectivity Analysis With Electroencephalography. *Neuromodulation: Technology at the Neural Interface*, *23*(1), 74–81. https://doi.org/10.1111/ner.12969

Gracely, R. H. (2013). Studies of Pain in Human Subjects. In S. B. McMahon, M. Koltzenburg, I. Tracey, & D. Turk (Eds.), *Wall and Melzack's Textbook of Pain* (6th Ed, pp. 283–300). Saunders.

Graimann, B., & Pfurtscheller, G. (2006). Quantification and visualization of event-related changes in oscillatory brain activity in the time-frequency domain. *Progress in Brain Research*, *159*, 79–97. https://doi.org/10.1016/S0079-6123(06)59006-5

Grider, J. S., Manchikanti, L., Carayannopoulos, A., Sharma, M. L., Balog, C. C., Harned, M. E., Grami, V., Justiz, R., Nouri, K. H., Hayek, S. M., Vallejo, R., & Christo, P. J. (2016). Effectiveness of Spinal Cord Stimulation in Chronic Spinal Pain: A Systematic Review. *Pain Physician*, *19*(1), E33–E54.

Groppe, D. M., Urbach, T. P., & Kutas, M. (2011). Mass univariate analysis of event-related brain

potentials/fields I: A critical tutorial review. *Psychophysiology*, *48*(12). https://onlinelibrary.wiley.com/doi/full/10.1111/j.1469-8986.2011.01273.x

Guerra, A., Pogosyan, A., Nowak, M., Tan, H., Ferreri, F., Di Lazzaro, V., & Brown, P. (2016). Phase Dependency of the Human Primary Motor Cortex and Cholinergic Inhibition Cancelation during Beta tACS. *Cerebral Cortex*, *26*(10), 3977–3990. https://doi.org/10.1093/cercor/bhw245

Haanpää, M., Attal, N., Backonja, M., Baron, R., Bennett, M. I., Bouhassira, D., Cruccu, G., Hansson, P., Haythornthwaite, J. A., Iannetti, G. D., Jensen, T. S., Kauppila, T., Nurmikko, T. J., Rice, A. S. C., Rowbotham, M. C., Serra, J., Sommer, C., Smith, B. H., & Treede, R.-D. (2011). NeuPSIG guidelines on neuropathic pain assessment. *PAIN*, *152*(1).

Hadi, M. A., McHugh, G. A., & Closs, S. J. (2019). Impact of Chronic Pain on Patients' Quality of Life: A Comparative Mixed-Methods Study. *Journal of Patient Experience*, *6*(2), 133–141. https://doi.org/10.1177/2374373518786013

Halata, Z., Grim, M., & Bauman, K. I. (2003). Friedrich Sigmund Merkel and his "Merkel cell", morphology, development, and physiology: Review and new results. *The Anatomical Record Part A: Discoveries in Molecular, Cellular, and Evolutionary Biology*, *271A*(1), 225–239. https://doi.org/10.1002/ar.a.10029

Hall, M., Kidgell, D., Perraton, L., Morrissey, J., & Jaberzadeh, S. (2021). Pain Induced Changes in Brain Oxyhemoglobin: A Systematic Review and Meta-Analysis of Functional NIRS Studies. *Pain Medicine*, *22*(6), 1399–1410. https://doi.org/10.1093/pm/pnaa453

Hall, S. D., Barnes, G. R., Furlong, P. L., Seri, S., & Hillebrand, A. (2010). Neuronal network pharmacodynamics of GABAergic modulation in the human cortex determined using pharmaco-magnetoencephalography. *Human Brain Mapping*, *31*, 581–594. https://doi.org/10.1002/hbm.20889

Hämäläinen, M., Hari, R., Ilmoniemi, R. J., Knuutila, J., & Lounasmaa, O. V. (1993). Magnetoencephalography theory, instrumentation, and applications to noninvasive studies of the working human brain. In *Reviews of Modern Physics* (Vol. 65, Issue 2, pp. 413–497). https://doi.org/10.1103/RevModPhys.65.413

Handwerker, H. O., Kilo, S., & Reeh, P. W. (1991). Unresponsive afferent nerve fibres in the sural

nerve of the rat. *The Journal of Physiology*, *435*, 229–242. https://doi.org/10.1113/jphysiol.1991.sp018507

Hansen, N., Obermann, M., Üçeyler, N., Zeller, D., Mueller, D., Yoon, M. S., Reiners, K., Sommer, C., & Katsarava, Z. (2012). Klinische Anwendung schmerzevozierter Potenziale. *Der Schmerz*, *26*(1), 8–15. https://doi.org/10.1007/s00482-011-1117-1

Harden, N. R., Bruehl, S., Galer, B. S., Saltz, S., Bertram, M., Backonja, M., Gayles, R., Rudin, N., Bhugra, M. K., & Stanton-Hicks, M. (1999). Complex regional pain syndrome: are the IASP diagnostic criteria valid and sufficiently comprehensive? *Pain*, *83*(2), 211–219. https://doi.org/10.1016/s0304-3959(99)00104-9

Harden, N. R., Bruehl, S., Perez, R. S. G. M., Birklein, F., Marinus, J., Maihöfner, C., Lubenow, T., Buvanendran, A., Mackey, S., Graciosa, J., Mogilevski, M., Ramsden, C., Chont, M., & Vatine, J.-J. (2010). Validation of proposed diagnostic criteria (the "Budapest Criteria") for Complex Regional Pain Syndrome. *Pain*, *150*(2), 268–274. https://doi.org/10.1016/j.pain.2010.04.030

Hardy, J. D., Wolff, H. G., & Goodell, H. (1950). Experimental evidence on the nature of cutaneous hyperalgesia. *The Journal of Clinical Investigation*, *29*(1), 115–140. https://doi.org/10.1172/JCI102227

He, J., Barolat, G., Holsheimer, J., & Struijk, J. J. (1994). Perception threshold and electrode position for spinal cord stimulation. *Pain*, *59*(1), 55–63. https://doi.org/10.1016/0304-3959(94)90047-7

Herrmann, C. S., Grigutsch, M., & Busch, N. A. (2005). EEG oscillations and wavelet analysis. In T. C. Handy (Ed.), *Event-related potentials: A methods handbook* (pp. 229–258). MIT Press. http://www-e.uni-magdeburg.de/cherrman/pdfs/MIT-Bookchapter.pdf

Hewitt, D., Byrne, A., Henderson, J., Newton-Fenner, A., Tyson-Carr, J., Fallon, N., Brown, C. A., & Stancak, A. (2021). Inhibition of cortical somatosensory processing during and after low frequency peripheral nerve stimulation in humans. *Clinical Neurophysiology*, *132*(7), 1481–1495. https://doi.org/10.1016/j.clinph.2021.03.024

Hirata, M., Kato, A., Taniguchi, M., Ninomiya, H., Cheyne, D., Robinson, S. E., Maruno, M., Kumura, E., Ishii, R., Hirabuki, N., Nakamura, H., & Yoshimine, T. (2002). Frequency-dependent spatial distribution of human somatosensory evoked neuromagnetic fields.

Neuroscience Letters, *318*(2), 73–76. https://doi.org/10.1016/S0304-3940(01)02483-1

Hjorth, B. (1975). An on-line transformation of EEG scalp potentials into orthogonal source derivations. *Electroencephalography and Clinical Neurophysiology*, *39*, 526–530. https://doi.org/10.1016/0013-4694(75)90056-5

Hoechstetter, K., Berg, P., & Scherg, M. (2010). BESA research tutorial 4: distributed source imaging. In *BESA Research Tutorial*.

Hoechstetter, K., Rupp, A., Meinck, H.-M., Weckesser, D., Bornfleth, H., Stippich, C., Berg, P., & Scherg, M. (2000). Magnetic source imaging of tactile input shows task-independent attention effects in SII. *NeuroReport*, *11*(11), 2461–2465. https://doi.org/10.1097/00001756-200008030-00024

Hoechstetter, K., Rupp, A., Stančák, A., Meinck, H.-M., Stippich, C., Berg, P., & Scherg, M. (2001). Interaction of Tactile Input in the Human Primary and Secondary Somatosensory Cortex—A Magnetoencephalographic Study. *NeuroImage*, *14*(3), 759–767. https://doi.org/10.1006/nimg.2001.0855

Hollingworth, W., Turner, J. A., Welton, N. J., Comstock, B. A., & Deyo, R. A. (2011). Costs and Cost-Effectiveness of Spinal Cord Stimulation (SCS) for Failed Back Surgery Syndrome. *Spine*, *36*(24), 2076–2083. https://doi.org/10.1097/BRS.0b013e31822a867c

Holsheimer, J. (2002). Which neuronal elements are activated directly by spinal cord stimulation. *Neuromodulation*, *5*(1), 25–31. https://doi.org/10.1046/j.1525-1403.2002._2005.x

Horing, B., Sprenger, C., & Büchel, C. (2019). The parietal operculum preferentially encodes heat pain and not salience. *PLOS Biology*, *17*(8), e3000205. https://doi.org/10.1371/journal.pbio.3000205

Hu, L., Cai, M. M., Xiao, P. R., Luo, F., & Iannetti, G. D. (2014). Human brain responses to concomitant stimulation of Aδ and C nociceptors. *The Journal of Neuroscience : The Official Journal of the Society for Neuroscience*, *34*(34), 11439–11451. https://doi.org/10.1523/JNEUROSCI.1355-14.2014

Hu, L., Peng, W., Valentini, E., Zhang, Z., & Hu, Y. (2013). Functional Features of Nociceptive-Induced Suppression of Alpha Band Electroencephalographic Oscillations. *The Journal of Pain*,

14(1), 89–99. https://doi.org/10.1016/j.jpain.2012.10.008

Hu, L., Zhang, L., Chen, R., Yu, H., Li, H., & Mouraux, A. (2015). The primary somatosensory cortex and the insula contribute differently to the processing of transient and sustained nociceptive and non-nociceptive somatosensory inputs. *Human Brain Mapping*, *36*(11), 4346–4360. https://doi.org/10.1002/hbm.22922

Hugosdottir, R., Mørch, C. D., Andersen, O. K., & Arendt-Nielsen, L. (2019). Investigating stimulation parameters for preferential small-fiber activation using exponentially rising electrical currents. *Journal of Neurophysiology*, *122*(4), 1745–1752. https://doi.org/10.1152/jn.00390.2019

Huneke, N. T. M., Brown, C. A., Burford, E., Watson, A., Trujillo-Barreto, N. J., El-Deredy, W., & Jones, A. K. . (2013). Experimental placebo analgesia changes resting-state alpha oscillations. *PLoS ONE*, *8*(10), e78278. https://doi.org/10.1371/journal.pone.0078278

Huttunen, J., Ahlfors, S., & Hari, R. (1992). Interaction of afferent impulses in the human primary sensorimotor cortex. *Electroencephalography and Clinical Neurophysiology*, *82*(3), 176–181. https://doi.org/10.1016/0013-4694(92)90165-E

Hyder, R., Kamel, N., Boon, T. T., & Reza, F. (2015). Mapping of language brain areas in patients with brain tumors. *2015 37th Annual International Conference of the IEEE Engineering in Medicine and Biology Society (EMBC)*, 626–629. https://doi.org/10.1109/EMBC.2015.7318440

Iannetti, G. D., Hughes, N. P., Lee, M. C., & Mouraux, A. (2008). Determinants of laser-evoked EEG responses: pain perception or stimulus saliency? *Journal of Neurophysiology*, *100*(2), 815–828. https://doi.org/10.1152/jn.00097.2008

Iannetti, G. D., & Mouraux, A. (2010). From the neuromatrix to the pain matrix (and back). *Experimental Brain Research*, *205*(1), 1–12. https://doi.org/10.1007/s00221-010-2340-1

Iannetti, G. D., Truini, A., Romaniello, A., Galeotti, F., Rizzo, C., Manfredi, M., & Cruccu, G. (2003). Evidence of a specific spinal pathway for the sense of warmth in humans. *Journal of Neurophysiology*, *89*(1), 562–570. https://doi.org/10.1152/jn.00393.2002

Ichesco, E., Quintero, A., Clauw, D. J., Peltier, S., Sundgren, P. C., Gerstner, G. E., & Schmidt-Wilcke, T. (2012). Altered Functional Connectivity Between the Insula and the Cingulate Cortex

in Patients With Temporomandibular Disorder: A Pilot Study. *Headache*, *52*(3), 441–454. https://doi.org/10.1111/j.1526-4610.2011.01998.x

Ikeda, H., Asai, T., & Murase, K. (2000). Robust changes of afferent-induced excitation in the rat spinal dorsal horn after conditioning high-frequency stimulation. *Journal of Neurophysiology*, *83*(4), 2412–2420. https://doi.org/10.1152/jn.2000.83.4.2412

Ikeda, H., Heinke, B., Ruscheweyh, R., & Sandkühler, J. (2003). Synaptic olasticity in spinal lamina I projection neurons that mediate hyperalgesia. *Science*, *299*(5610), 1237–1240. https://doi.org/10.1126/science.1080659

Ikeda, H., Stark, J., Fischer, H., Wagner, M., Drdla, R., Jäger, T., & Sandkühler, J. (2006). Synaptic amplifier of inflammatory pain in the spinal dorsal horn. *Science*, *312*(5780), 1659–1662. https://doi.org/10.1126/science.1127233

Ille, N., Berg, P., & Scherg, M. (2002). Artifact Correction of the Ongoing EEG Using Spatial Filters Based on Artifact and Brain Signal Topographies. *Journal of Clinical Neurophysiology*, *19*(2), 113–124. https://doi.org/10.1097/00004691-200203000-00002

Illman, M., Laaksonen, K., Liljeström, M., Jousmäki, V., Piitulainen, H., & Forss, N. (2020). Comparing MEG and EEG in detecting the ~20-Hz rhythm modulation to tactile and proprioceptive stimulation. *NeuroImage*, *215*, 116804. https://doi.org/10.1016/j.neuroimage.2020.116804

Inoue, S., Kamiya, M., Nishihara, M., Arai, Y.-C. P., Ikemoto, T., & Ushida, T. (2017). Prevalence, characteristics, and burden of failed back surgery syndrome: the influence of various residual symptoms on patient satisfaction and quality of life as assessed by a nationwide Internet survey in Japan. *Journal of Pain Research*, *10*, 811–823. https://doi.org/10.2147/JPR.S129295

Inui, K., Tran, T. D., Hoshiyama, M., & Kakigi, R. (2002). Preferential stimulation of Aδ fibers by intra-epidermal needle electrode in humans. *Pain*, *96*(3), 247–252. https://doi.org/10.1016/S0304-3959(01)00453-5

Janssen, S. P., Gerard, S., Raijmakers, M. E., Truin, M., van Kleef, M., & Joosten, E. A. J. (2012). Decreased intracellular GABA levels contribute to spinal cord stimulation-induced analgesia in rats suffering from painful peripheral neuropathy: the role of KCC2 and GABA(A) receptor-

mediated inhibition. *Neurochemistry International*, *60*(1), 21–30. https://doi.org/10.1016/j.neuint.2011.11.006

Jasper, H. H. (1958). The Ten-Twenty Electrode System of the International Federation. *Electroencephalography and Clinical Neurophysiology*, *10*, 371–375.

Jensen, K. B., Regenbogen, C., Ohse, M. C., Frasnelli, J., Freiherr, J., & Lundström, J. N. (2016). Brain activations during pain. *Pain*, *157*(6), 1279–1286. https://doi.org/10.1097/j.pain.0000000000000517

Jensen, O., Goel, P., Kopell, N., Pohja, M., Hari, R., & Ermentrout, B. (2005). On the human sensorimotor-cortex beta rhythm: Sources and modeling. *NeuroImage*, *26*(2), 347–355. https://doi.org/10.1016/j.neuroimage.2005.02.008

Jensen, O., & Mazaheri, A. (2010). Shaping Functional Architecture by Oscillatory Alpha Activity: Gating by Inhibition. *Frontiers in Human Neuroscience*, *4*, 1–8. https://doi.org/10.3389/fnhum.2010.00186

Johansson, R. S., Trulsson, M., Olsson, K. A., & Westberg, K. G. (1988). Mechanoreceptor activity from the human face and oral mucosa. *Experimental Brain Research*, *72*(1), 204–208. https://doi.org/10.1007/BF00248518

Johnson, S., Ayling, H., Sharma, M. L., & Goebel, A. (2015). External noninvasive peripheral nerve stimulation treatment of neuropathic pain: A prospective audit. *Neuromodulation*, *18*(5), 384–391. https://doi.org/10.1111/ner.12244

Johnson, S., & Goebel, A. (2016). Long-term treatment of chronic neuropathic pain using external noninvasive external peripheral nerve stimulation in five patients. *Neuromodulation: Technology at the Neural Interface*, *19*(8), 893–896. https://doi.org/10.1111/ner.12365

Johnson, S., Marshall, A. A., Hughes, D., Holmes, E., Henrich, F., Nurmikko, T. J., Sharma, M. L., Frank, B., Bassett, P., Marshall, A. A., Magerl, W., & Goebel, A. (2021). Mechanistically informed non-invasive peripheral nerve stimulation for peripheral neuropathic pain: a randomised double-blind sham-controlled trial. *Journal of Translational Medicine*, *19*(1), 1–15. https://doi.org/10.1186/s12967-021-03128-2

Jones, E. G. (2010). Thalamocortical dysrhythmia and chronic pain. *Pain*, *150*(1), 4–5.

https://doi.org/10.1016/j.pain.2010.03.022

Joosten, E. A. J., & Franken, G. (2020). Spinal cord stimulation in chronic neuropathic pain: mechanisms of action, new locations, new paradigms. *Pain*, *161*, S104–S113. https://doi.org/10.1097/j.pain.0000000000001854

Jung, K., Larsen, L. E., Rottmann, S., & Ellrich, J. (2011). Heterotopic low-frequency stimulation induces nociceptive LTD within the same central receptive field in man. *Experimental Brain Research*, *212*(2), 189–198. https://doi.org/10.1007/s00221-011-2718-8

Jung, K., Lelic, D., Rottmann, S., Drewes, A. M., Petrini, L., & Ellrich, J. (2012). Electrical low-frequency stimulation induces central neuroplastic changes of pain processing in man. *European Journal of Pain*, *16*(4), 509–521. https://doi.org/10.1016/j.ejpain.2011.08.006

Jung, K., Rottmann, S., & Ellrich, J. (2009). Long-term depression of spinal nociception and pain in man: Influence of varying stimulation parameters. *European Journal of Pain*, *13*(2), 161–170. https://doi.org/10.1016/j.ejpain.2008.04.001

Jung, T.-P., Makeig, S., Humphries, C., Lee, T. W., McKeown, M. J., Iragui, V., & Sejnowski, T. J. (2000). Removing electroencephalographic artifacts by blind source separation. *Psychophysiology*, *37*(2), 163–178.

Kakigi, R., & Jones, S. J. (1986). Influence of concurrent tactile stimulation on somatosensory evoked potentials following posterior tibial nerve stimulation in man. *Electroencephalography and Clinical Neurophysiology/Evoked Potentials Section*, *65*(2), 118–129. https://doi.org/https://doi.org/10.1016/0168-5597(86)90044-4

Karakaş, S. (2020). A review of theta oscillation and its functional correlates. *International Journal of Psychophysiology*, *157*, 82–99. https://doi.org/10.1016/j.ijpsycho.2020.04.008

Katz, N., Dworkin, R. H., North, R. B., Thomson, S., Eldabe, S., Hayek, S. M., Kopell, B. H., Markman, J., Rezai, A. R., Taylor, R. S., Turk, D. C., Buchser, E., Fields, H., Fiore, G., Ferguson, M., Gewandter, J., Hilker, C., Jain, R., Leitner, A., … Venkatesan, L. (2021). Research design considerations for randomized controlled trials of spinal cord stimulation for pain: Initiative on Methods, Measurement, and Pain Assessment in Clinical Trials/Institute of Neuromodulation/International Neuromodulation Society recommendati. *Pain*, *162*(7), 1935–

1956. https://doi.org/10.1097/j.pain.0000000000002204

Kaube, H., Katsarava, Z., Käufer, T., Diener, H. C., & Ellrich, J. (2000). A new method to increase nociception specificity of the human blink reflex. *Clinical Neurophysiology*, *111*(3), 413–416. https://doi.org/10.1016/S1388-2457(99)00295-3

Kayser, J., & Tenke, C. E. (2006). Principal components analysis of Laplacian waveforms as a generic method for identifying ERP generator patterns: I. Evaluation with auditory oddball tasks. *Clinical Neurophysiology*, *117*(2), 348–368. https://doi.org/10.1016/j.clinph.2005.08.034

Kemler, M. A., Barendse, G. A., van Kleef, M., de Vet, H. C., Rijks, C. P., Furnée, C. A., & Van Den Wildenberg, F. A. J. M. (2000). Spinal cord stimulation in patients with chronic reflex sympathetic dystrophy. *The New England Journal of Medicine*, *343*(9), 618–624. https://doi.org/10.1056/NEJM200008313430904

Kemler, M. A., Raphael, J. H., Bentley, A., & Taylor, R. S. (2010). The cost-effectiveness of spinal cord stimulation for complex regional pain syndrome. *Value in Health*, *13*(6), 735–742. https://doi.org/10.1111/j.1524-4733.2010.00744.x

Kim, D., Chae, Y., Park, H. J., & Lee, I. S. (2021). Effects of Chronic Pain Treatment on Altered Functional and Metabolic Activities in the Brain: A Systematic Review and Meta-Analysis of Functional Neuroimaging Studies. *Frontiers in Neuroscience*, *15*(July), 1–15. https://doi.org/10.3389/fnins.2021.684926

Kim, H. Y., Jun, J., Wang, J., Bittar, A., Chung, K., & Chung, J. M. (2015). Induction of long-term potentiation and long-term depression is cell-type specific in the spinal cord. *Pain*, *156*(4), 618–625. https://doi.org/10.1097/01.j.pain.0000460354.09622.ec

Kiriakopoulos, E. T., Tasker, R. R., Nicosia, S., Wood, M. L., & Mikulis, D. J. (1997). Functional magnetic resonance imaging: A potential tool for the evaluation of spinal cord stimulation: Technical case report. *Neurosurgery*, *41*(2), 501–504. https://doi.org/10.1097/00006123-199708000-00042

Kishima, H., Saitoh, Y., Oshino, S., Hosomi, K., Ali, M., Maruo, T., Hirata, M., Goto, T., Yanagisawa, T., Sumitani, M., Osaki, Y., Hatazawa, J., & Yoshimine, T. (2010). Modulation of neuronal activity after spinal cord stimulation for neuropathic pain; H215O PET study.

NeuroImage, *49*(3), 2564–2569. https://doi.org/10.1016/j.neuroimage.2009.10.054

Kisler, L. B., Kim, J. A., Hemington, K. S., Rogachov, A., Cheng, J. C., Bosma, R. L., Osborne, N. R., Dunkley, B. T., Inman, R. D., & Davis, K. D. (2020). Abnormal alpha band power in the dynamic pain connectome is a marker of chronic pain with a neuropathic component. *NeuroImage: Clinical*, *26*, 102241. https://doi.org/10.1016/j.nicl.2020.102241

Klein, T. (2004). Perceptual correlates of nociceptive long-term potentiation and long-term depression in humans. *Journal of Neuroscience*, *24*(4), 964–971. https://doi.org/10.1523/JNEUROSCI.1222-03.2004

Klein, T., Magerl, W., & Treede, R.-D. (2006). Perceptual Correlate of Nociceptive Long-Term Potentiation (LTP) in Humans Shares the Time Course of Early-LTP. *Journal of Neurophysiology*, *96*(6), 3551–3555. https://doi.org/10.1152/jn.00755.2006

Klem, G. H., Lüders, H. O., Jasper, H. H., & Elger, C. (1999). The ten-twenty electrode system of the International Federation. The International Federation of Clinical Neurophysiology. *Electroencephalography and Clinical Neurophysiology. Supplement*, *52*, 3–6.

Klimesch, W. (1999). EEG alpha and theta oscillations reflect cognitive and memory performance: a review and analysis. *Brain Research Reviews*, *29*(2–3), 169–195. https://doi.org/10.1016/S0165-0173(98)00056-3

Klimesch, W., Doppelmayr, M., Russegger, H., Pachinger, T., & Schwaiger, J. (1998). Induced alpha band power changes in the human EEG and attention. *Neuroscience Letters*, *244*(2), 73–76. https://doi.org/10.1016/S0304-3940(98)00122-0

Klimesch, W., Freunberger, R., Sauseng, P., & Gruber, W. (2008). A short review of slow phase synchronization and memory: Evidence for control processes in different memory systems? *Brain Research*, *1235*, 31–44. https://doi.org/https://doi.org/10.1016/j.brainres.2008.06.049

Klimesch, W., Sauseng, P., & Hanslmayr, S. (2007). EEG alpha oscillations: the inhibition-timing hypothesis. *Brain Research Reviews*, *53*(1), 63–88. https://doi.org/10.1016/j.brainresrev.2006.06.003

Klingner, C. M., Nenadic, I., Hasler, C., Brodoehl, S., & Witte, O. W. (2011). Habituation within the somatosensory processing hierarchy. *Behavioural Brain Research*, *225*(2), 432–436.

https://doi.org/10.1016/j.bbr.2011.07.053

Koes, B. W., van Tulder, M. W., & Thomas, S. (2006). Diagnosis and treatment of low back pain. *BMJ (Clinical Research Ed.)*, *332*(7555), 1430–1434. https://doi.org/10.1136/bmj.332.7555.1430

Koltzenburg, M., Lundberg, L. E. R., & Torebjörk, E. H. (1992). Dynamic and static components of mechanical hyperalgesia in human hairy skin. *Pain*, *51*(2), 207–219. https://doi.org/10.1016/0304-3959(92)90262-A

Koltzenburg, M., Stucky, C. L., & Lewin, G. R. (1997). Receptive properties of mouse sensory neurons innervating hairy skin. *Journal of Neurophysiology*, *78*(4), 1841–1850. https://doi.org/10.1152/jn.1997.78.4.1841

Konno, S., & Sekiguchi, M. (2018). Association between brain and low back pain. *Journal of Orthopaedic Science*, *23*(1), 3–7. https://doi.org/https://doi.org/10.1016/j.jos.2017.11.007

Kothari, S., & Goroszeniuk, T. (2006). External neuromodulation (EN) as a diagnostic test and therapeutic procedure. *European Journal of Pain*, *10*(S1), S158a – S158. https://doi.org/10.1016/S1090-3801(06)60605-8

Koyama, S., Xia, J., Leblanc, B. W., Gu, J. W., & Saab, C. Y. (2018). Sub-paresthesia spinal cord stimulation reverses thermal hyperalgesia and modulates low frequency EEG in a rat model of neuropathic pain. *Scientific Reports*, *8*(1), 7181. https://doi.org/10.1038/s41598-018-25420-w

Krames, E. S., Monis, S., Poree, L., Deer, T., & Levy, R. M. (2011). Using the SAFE Principles When Evaluating Electrical Stimulation Therapies for the Pain of Failed Back Surgery Syndrome. *Neuromodulation: Technology at the Neural Interface*, *14*(4), 299–311. https://doi.org/10.1111/j.1525-1403.2011.00373.x

Kregel, J., Meeus, M., Malfliet, A., Dolphens, M., Danneels, L., Nijs, J., & Cagnie, B. (2015). Structural and functional brain abnormalities in chronic low back pain: A systematic review☆. *Seminars in Arthritis and Rheumatism*, *45*(2), 229–237. https://doi.org/10.1016/j.semarthrit.2015.05.002

Kress, M., Koltzenburg, M., Reeh, P. W., & Handwerker, H. O. (1992). Responsiveness and

functional attributes of electrically localized terminals of cutaneous C-fibers in vivo and in vitro. *Journal of Neurophysiology*, *68*(2), 581–595. https://doi.org/10.1152/jn.1992.68.2.581

Kriek, N., Groeneweg, J. G., Stronks, D. L., de Ridder, D., & Huygen, F. J. P. M. (2017). Preferred frequencies and waveforms for spinal cord stimulation in patients with complex regional pain syndrome: A multicentre, double-blind, randomized and placebo-controlled crossover trial. *European Journal of Pain*, *21*(3), 507–519. https://doi.org/10.1002/ejp.944

Kropotov, J. D. (2009). *Quantitative EEG, Event-Related Potentials and Neurotherapy*. Academic Press. https://doi.org/https://doi.org/10.1016/B978-0-12-374512-5.00027-X

Kruger, L., Perl, E. R., & Sedivec, M. J. (1981). Fine structure of myelinated mechanical nociceptor endings in cat hairy skin. *The Journal of Comparative Neurology*, *198*(1), 137–154. https://doi.org/10.1002/cne.901980112

Kuhlman, W. N. (1978). Functional topography of the human mu rhythm. *Neuropsychology*, *44*(1), 83–93. https://doi.org/10.1016/0013-4694(78)90107-4

Kumar, K., Taylor, R. S., Jacques, L., Eldabe, S., Meglio, M., Molet, J., Thomson, S., O'Callaghan, J., Eisenberg, E., Milbouw, G., Buchser, E., Fortini, G., Richardson, J., & North, R. B. (2008). The effects of spinal cord stimulation in neuropathic pain are sustained: a 24-month follow-up of the prospective randomized controlled multicenter trial of the effectiveness of spinal cord stimulation. *Neurosurgery*, *63*(4), 762–770; discussion 770. https://doi.org/10.1227/01.NEU.0000325731.46702.D9

Kumar, K., Taylor, R. S., Jacques, L., Eldabe, S., Meglio, M., Molet, J., Thomson, S., O'Callaghan, J., Eisenberg, E., Milbouw, G., Buchser, E., Fortini, G., Richardson, J., North, R. B., O'Callaghan, J., Eisenberg, E., Milbouw, G., Buchser, E., Fortini, G., … North, R. B. (2007). Spinal cord stimulation versus conventional medical management for neuropathic pain: A multicentre randomised controlled trial in patients with failed back surgery syndrome. *Pain*, *132*(1–2), 179–188. https://doi.org/10.1016/j.pain.2007.07.028

Kumar, K., Toth, C., & Nath, R. K. (1996). Spinal cord stimulation for chronic pain in peripheral neuropathy. *Surgical Neurology*, *46*(4), 363–369. https://doi.org/10.1016/S0090-3019(96)00191-7

Kunitake, A., Iwasaki, T., Hidaka, N., Nagamachi, S., Katsuki, H., Uno, T., & Takasaki, M. (2005). The effects of spinal cord stimulation on the neuronal activity of the brain in patients with chronic neuropathic pain. *Pain Research*, *20*(3), 117–125. https://doi.org/10.11154/pain.20.117

Lagerlund, T. D., Sharbrough, F. W., & Busacker, N. E. (1997). Spatial Filtering of Multichannel Electroencephalographic Recordings Through Principal Component Analysis by Singular Value Decomposition. *Journal of Clinical Neurophysiology*, *14*(1), 73–82.

LaMotte, R. H., Shain, C. N., Simone, D. A., & Tsai, E. F. (1991). Neurogenic hyperalgesia: psychophysical studies of underlying mechanisms. *Journal of Neurophysiology*, *66*(1), 190–211. https://doi.org/10.1152/jn.1991.66.1.190

LaMotte, R. H., Thalhammer, J. G., & Robinson, C. J. (1983). Peripheral neural correlates of magnitude of cutaneous pain and hyperalgesia: a comparison of neural events in monkey with sensory judgments in human. *Journal of Neurophysiology*, *50*(1), 1–26. https://doi.org/10.1152/jn.1983.50.1.1

LaMotte, R., Thalhammer, J., Torebjork, H., & Robinson, C. (1982). Peripheral neural mechanisms of cutaneous hyperalgesia following mild injury by heat. *The Journal of Neuroscience*, *2*(6), 765–781. https://doi.org/10.1523/JNEUROSCI.02-06-00765.1982

Lang, S., Klein, T., Magerl, W., & Treede, R.-D. (2007). Modality-specific sensory changes in humans after the induction of long-term potentiation (LTP) in cutaneous nociceptive pathways. *Pain*, *128*(3), 254–263. https://doi.org/10.1016/j.pain.2006.09.026

Lanz, S., Seifert, F., & Maihöfner, C. (2011). Brain activity associated with pain, hyperalgesia and allodynia: an ALE meta-analysis. *Journal of Neural Transmission*, *118*(8), 1139–1154. https://doi.org/10.1007/s00702-011-0606-9

Latremoliere, A., & Woolf, C. J. (2009). Central Sensitization: A Generator of Pain Hypersensitivity by Central Neural Plasticity. *The Journal of Pain*, *10*(9), 895–926. https://doi.org/10.1016/j.jpain.2009.06.012

Law, J. D., Swett, J., & Kirsch, W. M. (1980). Retrospective analysis of 22 patients with chronic pain treated by peripheral nerve stimulation. *Journal of Neurosurgery*, *52*(4), 482–485. https://doi.org/10.3171/jns.1980.52.4.0482

Leandri, M., Saturno, M., Spadavecchia, L., Iannetti, G. D., Cruccu, G., & Truini, A. (2006). Measurement of skin temperature after infrared laser stimulation. *Neurophysiologie Clinique/Clinical Neurophysiology*, *36*(4), 207–218. https://doi.org/10.1016/j.neucli.2006.08.004

Lee, P.-S., Low, I., Chen, Y.-S., Tu, C.-H., Chao, H.-T., Hsieh, J.-C., & Chen, L.-F. (2017). Encoding of menstrual pain experience with theta oscillations in women with primary dysmenorrhea. *Scientific Reports*, *7*(1), 15977. https://doi.org/10.1038/s41598-017-16039-4

Legrain, V., Bruyer, R., Guérit, J.-M., & Plaghki, L. (2003). Nociceptive processing in the human brain of infrequent task-relevant and task-irrelevant noxious stimuli. A study with event-related potentials evoked by CO2 laser radiant heat stimuli. *Pain*, *103*, 237–248.

Legrain, V., Guérit, J.-M. M., Bruyer, R., & Plaghki, L. (2002). Attentional modulation of the nociceptive processing into the human brain: selective spatial attention, probability of stimulus occurrence, and target detection effects on laser evoked potentials. *Pain*, *99*(1–2), 21–39. https://doi.org/10.1016/S0304-3959(02)00051-9

Legrain, V., Mancini, F., Sambo, C. F., Torta, D. M., Ronga, I., & Valentini, E. (2012). Cognitive aspects of nociception and pain. Bridging neurophysiology with cognitive psychology. *Neurophysiologie Clinique/Clinical Neurophysiology*, *42*(5), 325–336. https://doi.org/10.1016/j.neucli.2012.06.003

Legrain, V., Perchet, C., & García-Larrea, L. (2009). Involuntary Orienting of Attention to Nociceptive Events: Neural and Behavioral Signatures. *Journal of Neurophysiology*, *102*(4), 2423–2434. https://doi.org/10.1152/jn.00372.2009

Lehmann, D. (1984). EEG assessment of brain activity: Spatial aspects, segmentation and imaging. *International Journal of Psychophysiology*, *1*(3), 267–276. https://doi.org/10.1016/0167-8760(84)90046-1

Lehmann, D. (1987). Principles of spatial analysis. In A. S. Gevins & A. Remond (Eds.), *Handbook of Electroencephalography and Clinical Neurophysiology: Methods of Analysis of Brain Electrical and Magnetic Signals* (pp. 309–354). Elsevier.

Lelic, D., Mørch, C. D., Hennings, K., Andersen, O. K., & Drewes, A. M. (2012). Differences in

perception and brain activation following stimulation by large versus small area cutaneous surface electrodes. *European Journal of Pain*, *16*(6), 827–837. https://doi.org/10.1002/j.1532-2149.2011.00063.x

Lemm, S., Müller, K.-R., & Curio, G. (2009). A Generalized Framework for Quantifying the Dynamics of EEG Event-Related Desynchronization. *PLOS Computational Biology*, *5*(8), e1000453. https://doi.org/10.1371/journal.pcbi.1000453

Lenoir, D., Cagnie, B., Verhelst, H., & De Pauw, R. (2021). Graph Measure Based Connectivity in Chronic Pain Patients: A Systematic Review. *Pain Physician*, *24*(7), E1037–E1058.

Lenoir, D., Willaert, W., Coppieters, I., Malfliet, A., Ickmans, K., Nijs, J., Vonck, K., Meeus, M., & Cagnie, B. (2020). Electroencephalography During Nociceptive Stimulation in Chronic Pain Patients: A Systematic Review. *Pain Medicine*, *21*(12), 3413–3427. https://doi.org/10.1093/pm/pnaa131

Levy, R., Deer, T. R., Poree, L., Rosen, S. M., Kapural, L., Amirdelfan, K., Soliday, N., Leitner, A., & Mekhail, N. (2019). Multicenter, Randomized, Double-Blind Study Protocol Using Human Spinal Cord Recording Comparing Safety, Efficacy, and Neurophysiological Responses Between Patients Being Treated With Evoked Compound Action Potential–Controlled Closed-Loop Spinal Cord Sti. *Neuromodulation: Technology at the Neural Interface*, *22*(3), 317–326. https://doi.org/10.1111/ner.12932

Liang, M., Su, Q., Mouraux, A., & Iannetti, G. D. (2019). Spatial Patterns of Brain Activity Preferentially Reflecting Transient Pain and Stimulus Intensity. *Cerebral Cortex*, *29*(5), 2211–2227. https://doi.org/10.1093/cercor/bhz026

Liberati, G., Klöcker, A., Safronova, M. M., Ferrão Santos, S., Ribeiro-Vaz, J. G., Raftopoulos, C., & Mouraux, A. (2016). Nociceptive Local Field Potentials Recorded from the Human Insula Are Not Specific for Nociception. *PLOS Biology*, *14*(1), e1002345. https://doi.org/10.1371/journal.pbio.1002345

Lidierth, M. (2007). Long-range projections of Aδ primary afferents in the Lissauer tract of the rat. *Neuroscience Letters*, *425*(2), 126–130. https://doi.org/10.1016/j.neulet.2007.08.029

Light, A. R., & Perl, E. R. (1977). Differential termination of large-diameter and small-diameter

primary afferent fibers in the spinal dorsal gray matter as indicated by labeling with horseradish peroxidase. *Neuroscience Letters*, *6*(1), 59–63. https://doi.org/10.1016/0304-3940(77)90065-9

Lim, M., Kim, J. S., & Chung, C. K. (2012). Modulation of somatosensory evoked magnetic fields by intensity of interfering stimuli in human somatosensory cortex: An MEG study. *NeuroImage*, *61*(3), 660–669. https://doi.org/10.1016/j.neuroimage.2012.04.003

Lim, M., Kim, J. S., Kim, D. J., & Chung, C. K. (2016). Increased low-and high-frequency oscillatory activity in the prefrontal cortex of fibromyalgia patients. *Frontiers in Human Neuroscience*, *10*(MAR2016). https://doi.org/10.3389/fnhum.2016.00111

Lind, G., Meyerson, B. A., Winter, J., & Linderoth, B. (2004). Intrathecal baclofen as adjuvant therapy to enhance the effect of spinal cord stimulation in neuropathic pain: A pilot study. *European Journal of Pain*, *8*(4), 377–383. https://doi.org/10.1016/j.ejpain.2003.11.002

Lind, G., Schechtmann, G., Winter, J., Meyerson, B. A., & Linderoth, B. (2008). Baclofen-enhanced spinal cord stimulation and intrathecal baclofen alone for neuropathic pain: Long-term outcome of a pilot study. *Eur J Pain*, *12*(1), 132–136. https://doi.org/10.1016/j.ejpain.2007.03.011

Lindelof, K., Jung, K., Ellrich, J., Jensen, R., & Bendtsen, L. (2010). Low-frequency electrical stimulation induces long-term depression in patients with chronic tension-type headache. *Cephalalgia*, *30*(7), 860–867. https://doi.org/10.1177/0333102409354783

Linden, D. J. (1994). Long-term synaptic depression in the mammalian brain. *Neuron*, *12*(3), 457–472. https://doi.org/10.1016/0896-6273(94)90205-4

Linderoth, B., & Foreman, R. D. (2017). Conventional and Novel Spinal Stimulation Algorithms: Hypothetical Mechanisms of Action and Comments on Outcomes. *Neuromodulation*, *20*(6), 525–533. https://doi.org/10.1111/ner.12624

Linderoth, B., Stiller, C., Gunasekera, L., O'Connor, W. T., Ungerstedt, U., & Brodin, E. (1994). Gamma-aminobutyric acid is released in the dorsal horn by electrical spinal cord stimulation: an in vivo microdialysis study in the rat. *Neurosurgery*, *34*(3), 484–489. https://doi.org/10.1227/00006123-199403000-00014

Liu, W. T., Han, Y., Li, H. C., Adams, B., Zheng, J. H., Wu, Y. P., Henkemeyer, M., & Song, X. J. (2009). An in vivo mouse model of long-term potentiation at synapses between primary afferent

C-fibers and spinal dorsal horn neurons: Essential role of EphB1 receptor. *Molecular Pain*, *5*, 29. https://doi.org/10.1186/1744-8069-5-29

Liu, X. G., Morton, C. R., Azkue, J. J., Zimmermann, M., & Sandkühler, J. (1998). Long-term depression of C-fibre-evoked spinal field potentials by stimulation of primary afferent Aδ-fibres in the adult rat. *European Journal of Neuroscience*, *10*(10), 3069–3075. https://doi.org/10.1046/j.1460-9568.1998.00310.x

Llinás, R. R., Ribary, U., Jeanmonod, D., Kronberg, E., & Mitra, P. P. (1999). Thalamocortical dysrhythmia: A neurological and neuropsychiatric syndrome characterized by magnetoencephalography. *Proceedings of the National Academy of Sciences*, *96*(26), 15222–15227. https://doi.org/10.1073/pnas.96.26.15222

Llinás, R. R., Urbano, F. J., Leznik, E., Ramírez, R. R., & van Marle, H. J. F. (2005). Rhythmic and dysrhythmic thalamocortical dynamics: GABA systems and the edge effect. *Trends in Neurosciences*, *28*(6), 325–333. https://doi.org/10.1016/j.tins.2005.04.006

Loggia, M. L., Edwards, R. R., Kim, J., Vangel, M. G., Wasan, A. D., Gollub, R. L., Harris, R. E., Park, K., & Napadow, V. (2012). Disentangling linear and nonlinear brain responses to evoked deep tissue pain. *Pain*, *153*(10), 2140–2151. https://doi.org/10.1016/j.pain.2012.07.014

Logothetis, N. K. (2008). What we can and what we cannot do with fMRI. *Nature*, *453*(7197), 869–878. https://doi.org/10.1038/nature06976

Löken, L. S., Wessberg, J., Morrison, I., McGlone, F., & Olausson, H. (2009). Coding of pleasant touch by unmyelinated afferents in humans. *Nature Neuroscience*, *12*(5), 547–548. https://doi.org/10.1038/nn.2312

Lømo, T. (2003). The discovery of long-term potentiation. *Philosophical Transactions of the Royal Society of London. Series B, Biological Sciences*, *358*(1432), 617–620. https://doi.org/10.1098/rstb.2002.1226

Long, D. M. (2013). Surgery for Back and Neck Pain (Including Radiculopathies). In S. B. McMahon, M. Koltzenburg, I. Tracey, & D. Turk (Eds.), *Wall and Melzack's Textbook of Pain* (6th Ed, pp. 1012–1028). Saunders.

Lopes da Silva, F. H. (2011a). Biophysical Aspects of EEG and Magnetoencephalogram Generation.

In D. L. Schomer & F. H. Lopes da Silva (Eds.), *Niedermeyer's Electroencephalography: Basic Principles, Clinical Applications, and Related Fields* (6th ed., pp. 91–110). Wolters Kluwer/Lippincott Williams & Wilkins Health.

Lopes da Silva, F. H. (2011b). Event-related potentials: General aspects of methodology and quantification. In D. L. Schomer & F. H. Lopes da Silva (Eds.), *Niedermeyer's Electroencephalography: Basic Principles, Clinical Applications, and Related Fields* (6th ed., pp. 923–934). Wolters Kluwer/Lippincott Williams & Wilkins Health.

Lopes da Silva, F. H., & Pfurtscheller, G. (1999). Basic concepts on EEG synchronization and desynchronization. In F. H. Lopes da Silva & G. Pfurtscheller (Eds.), *Handbook of Electroencephalography and Clinical Neurophysiology: Event-Related Desynchronization* (6th ed., pp. 3–12). Elsevier Science B.V.

Luck, S. J. (2014). An introduction to the event-related potential technique. In *MIT Press*. MIT press.

Luu, P., & Ferree, T. (2005). *Determination of the HydroCel Geodesic Sensor Nets' Average Electrode Positions and Their 10 – 10 International Equivalents*.

Madden, V. J., Catley, M. J., Grabherr, L., Mazzola, F., Shohag, M., & Moseley, G. L. (2016). The effect of repeated laser stimuli to ink-marked skin on skin temperature—recommendations for a safe experimental protocol in humans. *PeerJ*, *4*, e1577. https://doi.org/10.7717/peerj.1577

Magerl, W., Fuchs, P. N., Meyer, R. A., & Treede, R.-D. (2001). Roles of capsaicin-insensitive nociceptors in cutaneous pain and secondary hyperalgesia. *Brain*, *124*(9), 1754–1764. https://doi.org/10.1093/brain/124.9.1754

Magerl, W., Hansen, N., Treede, R.-D., & Klein, T. (2018). The human pain system exhibits higher-order plasticity (metaplasticity). *Neurobiology of Learning and Memory*, *154*, 112–120. https://doi.org/10.1016/j.nlm.2018.04.003

Maihöfner, C., & Handwerker, H. O. (2005). Differential coding of hyperalgesia in the human brain: a functional MRI study. *NeuroImage*, *28*(4), 996–1006. https://doi.org/10.1016/j.neuroimage.2005.06.049

Makeig, S., Bell, A. J., Jung, T.-P., & Sejnowski, T. J. (1996). Independent Component Analysis of Electroencephalographic Data. *Advances in Neural Information Processing Systems*, *8*(8), 145–

151. https://papers.nips.cc/paper/1091-independent-component-analysis-of-electroencephalographic-data.pdf

Makeig, S., Debener, S., Onton, J., & Delorme, A. (2004). Mining event-related brain dynamics. *Trends in Cognitive Sciences*, *8*(5), 204–210. https://doi.org/10.1016/j.tics.2004.03.008

Mancini, F., Beaumont, A.-L., Hu, L., Haggard, P., & Iannetti, G. D. (2015). Touch inhibits subcortical and cortical nociceptive responses. *Pain*, *156*(10), 1936–1944. https://doi.org/10.1097/j.pain.0000000000000253

Mancini, F., Pepe, A., Bernacchia, A., Di Stefano, G., Mouraux, A., & Iannetti, G. D. (2018). Characterizing the Short-Term Habituation of Event-Related Evoked Potentials. *ENeuro*, *5*(5), 1–14. https://doi.org/10.1523/ENEURO.0014-18.2018

Maniadakis, N., & Gray, A. (2000). The economic burden of back pain in the UK. *Pain*, *84*(1), 95–103. https://doi.org/10.1016/S0304-3959(99)00187-6

Marinus, J., Moseley, G. L., Birklein, F., Baron, R., Maihöfner, C., Kingery, W. S., & van Hilten, J. J. (2011). Clinical features and pathophysiology of complex regional pain syndrome. *The Lancet. Neurology*, *10*(7), 637–648. https://doi.org/10.1016/S1474-4422(11)70106-5

Maris, E., & Oostenveld, R. (2007). Nonparametric statistical testing of EEG- and MEG-data. *Journal of Neuroscience Methods*, *164*(1), 177–190. https://doi.org/10.1016/j.jneumeth.2007.03.024

Matharu, M. S., Bartsch, T., Ward, N., Frackowiak, R. S. J., Weiner, R. L., & Goadsby, P. J. (2004). Central neuromodulation in chronic migraine patients with suboccipital stimulators: a PET study. *Brain*, *127*(1), 220–230. https://doi.org/10.1093/brain/awh022

May, E. S., Butz, M., Kahlbrock, N., Hoogenboom, N., Brenner, M., & Schnitzler, A. (2012). Pre- and post-stimulus alpha activity shows differential modulation with spatial attention during the processing of pain. *NeuroImage*, *62*(3), 1965–1974. https://doi.org/10.1016/j.neuroimage.2012.05.071

Mayer, D. J., Price, D. D., & Becker, D. P. (1975). Neurophysiological characterization of the anterolateral spinal cord neurons contributing to pain perception in man. *Pain*, *1*(1), 51–58. https://doi.org/10.1016/0304-3959(75)90004-4

Mazzola, L., Isnard, J., Peyron, R., Guénot, M., & Mauguière, F. (2009). Somatotopic organization of

pain responses to direct electrical stimulation of the human insular cortex. *Pain*, *146*(1–2), 99–104. https://doi.org/10.1016/j.pain.2009.07.014

Mazzola, L., Isnard, J., Peyron, R., & Mauguière, F. (2012). Stimulation of the human cortex and the experience of pain: Wilder Penfield's observations revisited. *Brain*, *135*(2), 631–640. https://doi.org/10.1093/brain/awr265

Mazzone, P., Pisani, R., Pizio, N., Arrigo, A., & Nobili, F. (1994). Cerebral blood flow and somatosensory evoked response changes induced by spinal cord stimulation: preliminary follow-up observations. *Stereotactic and Functional Neurosurgery*, *62*(1–4), 179–185. https://doi.org/10.1159/000098615

McGlone, F., & Reilly, D. (2010). The cutaneous sensory system. *Neuroscience and Biobehavioral Reviews*, *34*(2), 148–159. https://doi.org/10.1016/j.neubiorev.2009.08.004

Mekhail, N., Levy, R. M., Deer, T. R., Kapural, L., Li, S., Amirdelfan, K., Hunter, C. W., Rosen, S. M., Costandi, S. J., Falowski, S. M., Burgher, A. H., Pope, J. E., Gilmore, C. A., Qureshi, F. A., Staats, P., Scowcroft, J., Carlson, J., Kim, C. K., Yang, M. I., … Soliday, N. (2020). Long-term safety and efficacy of closed-loop spinal cord stimulation to treat chronic back and leg pain (Evoke): a double-blind, randomised, controlled trial. *The Lancet Neurology*, *19*(2), 123–134. https://doi.org/10.1016/S1474-4422(19)30414-4

Melzack, R. (1999). From the gate to the neuromatrix. *Pain*, *82*(Supplement 1), S121–S126. https://doi.org/10.1016/S0304-3959(99)00145-1

Melzack, R., & Wall, P. D. (1965). Pain Mechanisms: A New Theory. *Science*, *150*(c), 1–4. https://doi.org/10.15713/ins.mmj.3

Mendell, L. M. (2014). Constructing and deconstructing the gate theory of pain. *Pain*, *155*(2), 210–216. https://doi.org/10.1016/j.pain.2013.12.010

Metting van Rijn, A. C., Peper, A., & Grimbergen, C. A. (1990). High-quality recording of bioelectric events. *Medical and Biological Engineering and Computing*, *28*(5), 389–397. https://doi.org/10.1007/BF02441961

Meuwissen, K. P. V, Gu, J. W., Zhang, T. C., & Joosten, E. A. J. (2018). Burst Spinal Cord Stimulation in Peripherally Injured Chronic Neuropathic Rats: A Delayed Effect. *Pain Practice*,

18(8), 988–996. https://doi.org/10.1111/papr.12701

Meyer, R. A., & Campbell, J. N. (1981). Myelinated Nociceptive Afferents Account for the Hyperalgesia That Follows a Burn to the Hand. *Science*, *213*(4515), 1527–1529. https://doi.org/10.1126/science.7280675

Michail, G., Dresel, C., Witkovský, V., Stankewitz, A., & Schulz, E. (2016). Neuronal Oscillations in Various Frequency Bands Differ between Pain and Touch. *Frontiers in Human Neuroscience*, *10*, 1–8. https://doi.org/10.3389/fnhum.2016.00182

Michel, C. M., & Brunet, D. (2019). EEG Source Imaging: A Practical Review of the Analysis Steps. *Frontiers in Neurology*, *10*, 1–18. https://doi.org/10.3389/fneur.2019.00325

Miller, J. P., Eldabe, S., Buchser, E., Johanek, L. M., Guan, Y., & Linderoth, B. (2016). Parameters of Spinal Cord Stimulation and Their Role in Electrical Charge Delivery: A Review. *Neuromodulation: Technology at the Neural Interface*, *19*(4), 373–384. https://doi.org/10.1111/ner.12438

Misidou, C., & Papagoras, C. (2019). Complex Regional Pain Syndrome: An update. *Mediterranean Journal of Rheumatology*, *30*(1), 16–25. https://doi.org/10.31138/mjr.30.1.16

Moayedi, M., Di Stefano, G., Stubbs, M. T., Djeugam, B., Liang, M., & Iannetti, G. D. (2016). Nociceptive-Evoked Potentials Are Sensitive to Behaviorally Relevant Stimulus Displacements in Egocentric Coordinates. *ENeuro*, *3*(3), 1–12. https://doi.org/10.1523/ENEURO.0151-15.2016

Moayedi, M., Liang, M., Sim, A. L., Hu, L., Haggard, P., & Iannetti, G. D. (2015). Laser-Evoked Vertex Potentials Predict Defensive Motor Actions. *Cerebral Cortex*, *25*(12), 4789–4798. https://doi.org/10.1093/cercor/bhv149

Mobascher, A., Brinkmeyer, J., Warbrick, T., Musso, F., Schlemper, V., Wittsack, H. J., Saleh, A., Schnitzler, A., & Winterer, G. (2010). Brain activation patterns underlying fast habituation to painful laser stimuli. *International Journal of Psychophysiology*, *75*(1), 16–24. https://doi.org/10.1016/j.ijpsycho.2009.10.008

Moens, M., Sunaert, S., Mariën, P., Brouns, R., De Smedt, A., Droogmans, S., Van Schuerbeek, P., Peeters, R., Poelaert, J., & Nuttin, B. (2012). Spinal cord stimulation modulates cerebral function: An fMRI study. *Neuroradiology*, *54*(12), 1399–1407. https://doi.org/10.1007/s00234-

012-1087-8

Mor, J., & Carmon, A. (1975). Laser emitted radiant heat for pain research. *Pain*, *1*(3), 233–237. https://doi.org/https://doi.org/10.1016/0304-3959(75)90040-8

Mørch, C. D., Hennings, K., & Andersen, O. K. (2011). Estimating nerve excitation thresholds to cutaneous electrical stimulation by finite element modeling combined with a stochastic branching nerve fiber model. *Medical and Biological Engineering and Computing*, *49*(4), 385–395. https://doi.org/10.1007/s11517-010-0725-8

Mouraux, A., De Paepe, A. L., Marot, E., Plaghki, L., Iannetti, G. D., & Legrain, V. (2013). Unmasking the obligatory components of nociceptive event-related brain potentials. *Journal of Neurophysiology*, *110*(10), 2312–2324. https://doi.org/10.1152/jn.00137.2013

Mouraux, A., Diukova, A., Lee, M. C., Wise, R. G., & Iannetti, G. D. (2011). A multisensory investigation of the functional significance of the "pain matrix." *NeuroImage*, *54*(3), 2237–2249. https://doi.org/10.1016/j.neuroimage.2010.09.084

Mouraux, A., & Iannetti, G. D. (2009). Nociceptive Laser-Evoked Brain Potentials Do Not Reflect Nociceptive-Specific Neural Activity. *Journal of Neurophysiology*, *101*(6), 3258–3269. https://doi.org/10.1152/jn.91181.2008

Mücke, M., Cuhls, H., Radbruch, L., Weigl, T., Rolke, R., Mu, M., Mücke, M., Cuhls, H., Radbruch, L., Weigl, T., & Rolke, R. (2014). Evidence of heterosynaptic LTD in the human nociceptive system: Superficial skin neuromodulation using a matrix lectrode reduces deep pain sensitivity. *PLoS ONE*, *9*(9), 1–12. https://doi.org/10.1371/journal.pone.0107718

Mulkey, R. M., & Malenka, R. C. (1992). Mechanisms underlying induction of homosynaptic long-term depression in area CA1 of the hippocampus. *Neuron*, *9*(5), 967–975. https://doi.org/10.1016/0896-6273(92)90248-C

Muthukumaraswamy, S. D., Myers, J. F. M., Wilson, S. J., Nutt, D. J., Lingford-Hughes, A., Singh, K. D., & Hamandi, K. (2013). The effects of elevated endogenous GABA levels on movement-related network oscillations. *NeuroImage*, *66*, 36–41. https://doi.org/10.1016/j.neuroimage.2012.10.054

Nagamachi, S., Fujita, S., Nishii, R., Futami, S., & Wakamatsu, H. (2006). Alteration of regional

cerebral blood flow in patients with chronic pain reEvaluation before and after epidural spinal cord stimulation. *Annals of Nuclear Medicine*, *20*(4), 303–310.

Napadow, V., LaCount, L., Park, K., As-Sanie, S., Clauw, D. J., & Harris, R. E. (2010). Intrinsic brain connectivity in fibromyalgia is associated with chronic pain intensity. *Arthritis and Rheumatism*, *62*(8), 2545–2555. https://doi.org/10.1002/art.27497

Nathan, P. W. (1976). The gate-control theory of pain. *Brain*, *99*(1), 123–158. https://doi.org/10.1093/brain/99.1.123

National Institute for Health and Care Excellence. (2008). Spinal cord stimulation for chronic pain of neuropathic or ischaemic origin. In *NICE guidance*. https://doi.org/10.3310/hta13170

National Institute for Health and Care Excellence. (2013). *Percutaneous electrical nerve stimulation for refractory neuropathic pain*. https://doi.org/10.1159/000509621

National Institute for Health and Care Excellence. (2021a). *Duloxetine*. BNF. https://bnf.nice.org.uk/drug/duloxetine.html

National Institute for Health and Care Excellence. (2021b). *Gabapentin*. BNF. https://bnf.nice.org.uk/drug/gabapentin.html

National Institute for Health and Care Excellence. (2021c). *NICE Pathways: Neuropathic pain overview*.

National Institute for Health and Care Excellence. (2021d). *Pregabalin*. BNF. https://bnf.nice.org.uk/drug/pregabalin.html

National Institute for Health and Care Excellence. (2021e). *Tramadol hydrochloride*. BNF. https://doi.org/10.1097/00002508-199103000-00069

Neuper, C., & Pfurtscheller, G. (2001a). Evidence for distinct beta resonance frequencies in human EEG related to specific sensorimotor cortical areas. *Clinical Neurophysiology*, *112*(11), 2084–2097. https://doi.org/10.1016/S1388-2457(01)00661-7

Neuper, C., & Pfurtscheller, G. (2001b). Event-related dynamics of cortical rhythms: frequency-specific features and functional correlates. *International Journal of Psychophysiology*, *43*(1), 41–58. https://doi.org/10.1016/S0167-8760(01)00178-7

Neuper, C., Wörtz, M., & Pfurtscheller, G. (2006). ERD/ERS patterns reflecting sensorimotor

activation and deactivation. *Progress in Brain Research*, *159*, 211–222. https://doi.org/10.1016/S0079-6123(06)59014-4

Ng, S. K., Urquhart, D. M., Fitzgerald, P. B., Cicuttini, F. M., Hussain, S. M., & Fitzgibbon, B. M. (2017). The Relationship between Structural and Functional Brain Changes and Altered Emotion and Cognition in Chronic Low Back Pain: A Systematic Review of MRI and fMRI Studies. *Clinical Journal of Pain*, *34*(3), 237–261. https://doi.org/10.1097/AJP.0000000000000534

NHS. (2019). *Peripheral neuropathy*. https://www.nhs.uk/conditions/peripheral-neuropathy/

Nicholas, M., Vlaeyen, J. W. S., Rief, W., Barke, A., Aziz, Q., Benoliel, R., Cohen, M., Evers, S., Giamberardino, M. A., Goebel, A., Korwisi, B., Perrot, S., Svensson, P., Wang, S.-J., & Treede, R.-D. (2019). The IASP classification of chronic pain for ICD-11: chronic primary pain. *Pain*, *160*(1), 28–37. https://doi.org/10.1097/j.pain.0000000000001390

Nikouline, V. V., Linkenkaer-Hansen, K., Wikström, H., Kesäniemi, M., Antonova, E. V., Ilmoniemi, R. J., & Huttunen, J. (2000). Dynamics of mu-rhythm suppression caused by median nerve stimulation: a magnetoencephalographic study in human subjects. *Neuroscience Letters*, *294*(3), 163–166. https://doi.org/10.1016/S0304-3940(00)01562-7

Nilsson, H. J., & Schouenborg, J. (1999). Differential inhibitory effect on human nociceptive skin senses induced by local stimulation of thin cutaneous fibers. *Pain*, *80*(1–2), 103–112. https://doi.org/10.1016/s0304-3959(98)00205-x

Niso, G., Tjepkema-Cloostermans, M. C., Lenders, M. W. P. M., & de Vos, C. C. (2021). Modulation of the Somatosensory Evoked Potential by Attention and Spinal Cord Stimulation. *Frontiers in Neurology*, *12*, 1–11. https://doi.org/10.3389/fneur.2021.694310

North, R. B., Ewend, M. G., Lawton, M. T., & Piantadosi, S. A. (1991). Spinal cord stimulation for chronic, intractable pain: Superiority of "multi-channel" devices. *Pain*, *44*(2), 119–130. https://doi.org/10.1016/0304-3959(91)90125-H

Nunez, P. L., Silberstein, R. B., Cadusch, P. J., Wijesinghe, R. S., Westdorp, A. F., & Srinivasan, R. (1994). A theoretical and experimental study of high resolution EEG based on surface Laplacians and cortical imaging. *Electroencephalography and Clinical Neurophysiology*, *90*(1),

40–57. https://doi.org/10.1016/0013-4694(94)90112-0

Nunez, P. L., & Srinivasan, R. (2006). *Electric Fields of the Brain* (2nd ed.). Oxford University Press. https://doi.org/10.1093/acprof:oso/9780195050387.001.0001

Nunez, P. L., Wingeier, B. M., & Silberstein, R. B. (2001). Spatial-temporal structures of human alpha rhythms: Theory, microcurrent sources, multiscale measurements, and global binding of local networks. *Human Brain Mapping*, *13*(3), 125–164. https://doi.org/10.1002/hbm.1030

Oakley, J. C. (2006). Spinal Cord Stimulation in Axial Low Back Pain: Solving the Dilemma. *Pain Medicine*, *7*(S1), S58–S63. https://doi.org/10.1111/j.1526-4637.2006.00123.x

Oertel, B. G., Preibisch, C., Martin, T., Walter, C., Gamer, M., Deichmann, R., & Lötsch, J. (2012). Separating brain processing of pain from that of stimulus intensity. *Human Brain Mapping*, *33*(4), 883–894. https://doi.org/10.1002/hbm.21256

Ohara, S., Crone, N. ., Weiss, N., & Lenz, F. A. (2004). Attention to a painful cutaneous laser stimulus modulates electrocorticographic event-related desynchronization in humans. *Clinical Neurophysiology*, *115*(7), 1641–1652. https://doi.org/10.1016/j.clinph.2004.02.023

Oostenveld, R., Fries, P., Maris, E., & Schoffelen, J.-M. (2011). FieldTrip: Open Source Software for Advanced Analysis of MEG, EEG, and Invasive Electrophysiological Data. *Computational Intelligence and Neuroscience*, *2011*, 1–9. https://doi.org/10.1155/2011/156869

Opsommer, E., Weiss, T., Plaghki, L., & Miltner, W. H. R. (2001). Dipole analysis of ultralate (C-fibres) evoked potentials after laser stimulation of tiny cutaneous surface areas in humans. *Neuroscience Letters*, *298*(1), 41–44. https://doi.org/10.1016/s0304-3940(00)01718-3

Ostrowsky, K., Magnin, M., Ryvlin, P., Isnard, J., Guenot, M., & Mauguière, F. (2002). Representation of Pain and Somatic Sensation in the Human Insula: a Study of Responses to Direct Electrical Cortical Stimulation. *Cerebral Cortex*, *12*(4), 376–385. https://doi.org/10.1093/cercor/12.4.376

Ottestad, E., & Orlovich, D. S. (2020). History of Peripheral Nerve Stimulation—Update for the 21st Century. *Pain Medicine*, *21*, S3–S5. https://doi.org/10.1093/pm/pnaa165

Palermo, S., Benedetti, F., Costa, T., & Amanzio, M. (2015). Pain anticipation: An activation likelihood estimation meta-analysis of brain imaging studies. *Human Brain Mapping*, *36*(5),

1648–1661. https://doi.org/10.1002/hbm.22727

Palva, S., Linkenkaer-Hansen, K., Näätänen, R., & Palva, J. M. (2005). Early Neural Correlates of Conscious Somatosensory Perception. *The Journal of Neuroscience*, *25*(21), 5248 LP – 5258. https://doi.org/10.1523/JNEUROSCI.0141-05.2005

Parker, J. L., Karantonis, D. M., Single, P., Obradovic, M., & Cousins, M. J. (2012). Compound action potentials recorded in the human spinal cord during neurostimulation for pain relief. *Pain*, *153*(3), 593–601. https://doi.org/10.1016/j.pain.2011.11.023

Parkkonen, E., Laaksonen, K., Piitulainen, H., Parkkonen, L., & Forss, N. (2015). Modulation of the ~20-Hz motor-cortex rhythm to passive movement and tactile stimulation. *Brain and Behavior*, *5*(5), e00328. https://doi.org/10.1002/brb3.328

Pascual-Marqui, R. D., Michel, C. M., & Lehmann, D. (1994). Low resolution electromagnetic tomography: a new method for localizing electrical activity in the brain. *International Journal of Psychophysiology*, *18*(1), 49–65. https://doi.org/10.1016/0167-8760(84)90014-X

Patel, E. A., & Perloff, M. D. (2018). Radicular Pain Syndromes: Cervical, Lumbar, and Spinal Stenosis. *Seminars in Neurology*, *38*(6), 634–639. https://doi.org/10.1055/s-0038-1673680

Paz-Solís, J., Thomson, S., Jain, R., Chen, L., Huertas, I., & Doan, Q. (2022). Exploration of High- and Low-Frequency Options for Subperception Spinal Cord Stimulation Using Neural Dosing Parameter Relationships: The HALO Study. *Neuromodulation: Technology at the Neural Interface*, *25*(1), 94–102. https://doi.org/10.1111/ner.13390

Pazzaglia, C., & Valeriani, M. (2009). Brain-evoked potentials as a tool for diagnosing neuropathic pain. *Expert Review of Neurotherapeutics*, *9*(5), 759–771. https://doi.org/10.1586/ern.09.16

Peng, W., Hu, L., Zhang, Z., & Hu, Y. (2014). Changes of spontaneous oscillatory activity to tonic heat pain. *PLoS ONE*, *9*(3), 1–11. https://doi.org/10.1371/journal.pone.0091052

Perchet, C., Godinho, F., Mazza, S., Frot, M., Legrain, V., Magnin, M., & Garcia-Larrea, L. (2008). Evoked potentials to nociceptive stimuli delivered by CO2 or Nd:YAP lasers. *Clinical Neurophysiology*, *119*(11), 2615–2622. https://doi.org/10.1016/j.clinph.2008.06.021

Perrin, F., Pernier, J., Bertrand, O., & Echallier, J. F. (1989). Spherical splines for scalp potential and current density mapping. *Electroencephalography and Clinical Neurophysiology*, *72*(2), 184–

187. https://doi.org/10.1016/0013-4694(89)90180-6

Peyron, R., Faillenot, I., Mertens, P., Laurent, B., & Garcia-Larrea, L. (2007). Motor cortex stimulation in neuropathic pain. Correlations between analgesic effect and hemodynamic changes in the brain. A PET study. *NeuroImage*, *34*(1), 310–321. https://doi.org/10.1016/j.neuroimage.2006.08.037

Peyron, R., Frot, M., Schneider, F., García-Larrea, L., Mertens, P., Barral, F. G., Sindou, M., Laurent, B., & Mauguière, F. (2002). Role of Operculoinsular Cortices in Human Pain Processing: Converging Evidence from PET, fMRI, Dipole Modeling, and Intracerebral Recordings of Evoked Potentials. *NeuroImage*, *17*(3), 1336–1346. https://doi.org/10.1006/nimg.2002.1315

Peyron, R., Laurent, B., & García-Larrea, L. (2000). Functional imaging of brain responses to pain. A review and meta-analysis (2000). *Neurophysiologie Clinique/Clinical Neurophysiology*, *30*(5), 263–288. https://doi.org/10.1016/S0987-7053(00)00227-6

Pfannmöller, J., & Lotze, M. (2019). Review on biomarkers in the resting-state networks of chronic pain patients. *Brain and Cognition*, *131*, 4–9. https://doi.org/10.1016/j.bandc.2018.06.005

Pfau, D. B., Klein, T., Putzer, D., Pogatzki-Zahn, E. M., Treede, R.-D., & Magerl, W. (2011). Analysis of hyperalgesia time courses in humans after painful electrical high-frequency stimulation identifies a possible transition from early to late LTP-like pain plasticity. *Pain*, *152*(7), 1532–1539. https://doi.org/10.1016/j.pain.2011.02.037

Pfurtscheller, G. (1977). Graphical display and statistical evaluation of event-related desynchronization (ERD). *Electroencephalography and Clinical Neurophysiology*, *43*, 757–760.

Pfurtscheller, G. (1981). Central beta rhythm during sensorimotor activities in man. *Electroencephalography and Clinical Neurophysiology*, *51*(3), 253–264. https://doi.org/10.1016/0013-4694(81)90139-5

Pfurtscheller, G. (1992). Event-related synchronization (ERS): an electrophysiological correlate of cortical areas at rest. *Electroencephalography and Clinical Neurophysiology*, *83*(1), 62–69. https://doi.org/10.1016/0013-4694(92)90133-3

Pfurtscheller, G. (1999). Quantification of ERD and ERS in the time domain. In G. Pfurtscheller & F. H. Lopes da Silva (Eds.), *Handbook of Electroencephalography and Clinical Neurophysiology:*

Event-Related Desynchronization (6th ed., pp. 89–105). Elsevier BV.

Pfurtscheller, G. (2003). Induced Oscillations in the Alpha Band: Functional Meaning. *Epilepsia*, *44*(12), 2–8. https://doi.org/10.1111/j.0013-9580.2003.12001.x

Pfurtscheller, G., & Aranibar, A. (1977). Event-related cortical desynchronization detected by power measurements of scalp EEG. *Electroencephalography and Clinical Neurophysiology*, *42*(6), 817–826. https://doi.org/10.1016/0013-4694(77)90235-8

Pfurtscheller, G., & Aranibar, A. (1979). Evaluation of event-related desynchronization (ERD) preceding and following voluntary self-paced movement. *Electroencephalography and Clinical Neurophysiology*, *46*(2), 138–146. https://doi.org/10.1016/0013-4694(79)90063-4

Pfurtscheller, G., & Lopes da Silva, F. H. (1999). Event-related EEG/MEG synchronization and desynchronization: basic principles. *Clinical Neurophysiology*, *110*(11), 1842–1857. https://doi.org/10.1016/S1388-2457(99)00141-8

Pfurtscheller, G., Neuper, C., & Krausz, G. (2000). Functional dissociation of lower and upper frequency mu rhythms in relation to voluntary limb movement. *Clinical Neurophysiology*, *111*(10), 1873–1879. https://doi.org/10.1016/S1388-2457(00)00428-4

Pfurtscheller, G., Pichler-Zalaudek, K., & Neuper, C. (1999). ERD and ERS in voluntary movement of different limbs. In *Event-Related Desynchronization. Handbook of Electroenceph. and Clin. Neurophysiol.* (pp. 245–268). Elsevier BV.

Pfurtscheller, G., Stancak, A., & Neuper, C. (1996a). Post-movement beta synchronization. A correlate of an idling motor area? *Electroencephalography and Clinical Neurophysiology*, *98*(4), 281–293. https://doi.org/10.1016/0013-4694(95)00258-8

Pfurtscheller, G., Stancak, A., & Neuper, C. (1996b). Event-related synchronization (ERS) in the alpha band—an electrophysiological correlate of cortical idling: a review. *International Journal of Psychophysiology*, *24*(1–2), 39–46. https://doi.org/10.1016/S0167-8760(96)00066-9

Pfurtscheller, G., Woertz, M., Müller, G., Wriessnegger, S., & Pfurtscheller, K. (2002). Contrasting behavior of beta event-related synchronization and somatosensory evoked potential after median nerve stimulation during finger manipulation in man. *Neuroscience Letters*, *323*(2), 113–116. https://doi.org/10.1016/S0304-3940(02)00119-2

Pilitsis, J. G., Chakravarthy, K., Will, A. J., Trutnau, K. C., Hageman, K. N., Dinsmoor, D. A., & Litvak, L. M. (2021). The Evoked Compound Action Potential as a Predictor for Perception in Chronic Pain Patients: Tools for Automatic Spinal Cord Stimulator Programming and Control. *Frontiers in Neuroscience*, *15*, 673998. https://doi.org/10.3389/fnins.2021.673998

Pineda, J. A. (2005). The functional significance of mu rhythms: Translating "seeing" and "hearing" into "doing." *Brain Research Reviews*, *50*(1), 57–68. https://doi.org/10.1016/j.brainresrev.2005.04.005

Pinheiro, E. S. D. S., Queirós, F. C. De, Montoya, P., Santos, C. L., Do Nascimento, M. A., Ito, C. H., Silva, M., Santos, D. B. N., Benevides, S., Miranda, J. G. V., Sá, K. N., & Baptista, A. F. (2016). Electroencephalographic patterns in chronic pain: A systematic review of the literature. *PLoS ONE*, *11*(2), 1–26. https://doi.org/10.1371/journal.pone.0149085

Plaghki, L., & Mouraux, A. (2003). How do we selectively activate skin nociceptors with a high power infrared laser? Physiology and biophysics of laser stimulation. *Neurophysiologie Clinique/Clinical Neurophysiology*, *33*(6), 269–277. https://doi.org/10.1016/j.neucli.2003.10.003

Ploner, M., Gross, J., Timmermann, L., Pollok, B., & Schnitzler, A. (2006). Pain Suppresses Spontaneous Brain Rhythms. *Cerebral Cortex*, *16*(4), 537–540. https://doi.org/10.1093/cercor/bhj001

Ploner, M., Sorg, C., & Gross, J. (2017). Brain Rhythms of Pain. *Trends in Cognitive Sciences*, *21*(2), 100–110. https://doi.org/10.1016/j.tics.2016.12.001

Poláček, H., Kozák, J., Vrba, I., Vrána, J., & Stančák, A. (2007). Effects of spinal cord stimulation on the cortical somatosensory evoked potentials in failed back surgery syndrome patients. *Clinical Neurophysiology*, *118*(6), 1291–1302. https://doi.org/10.1016/j.clinph.2007.02.029

Poulsen, A. H., Tigerholm, J., Andersen, O. K., & Morch, C. D. (2021). Increased preferential activation of small cutaneous nerve fibers by optimization of electrode design parameters. *Journal of Neural Engineering*, *18*(1). https://doi.org/10.1088/1741-2552/abd1c1

Prato, V., Taberner, F. J., Hockley, J. R. F., Callejo, G., Arcourt, A., Tazir, B., Hammer, L., Schad, P., Heppenstall, P. A., Smith, E. S., & Lechner, S. G. (2017). Functional and Molecular

Characterization of Mechanoinsensitive “Silent” Nociceptors. *Cell Reports*, *21*(11), 3102–3115. https://doi.org/10.1016/j.celrep.2017.11.066

Price, D. D., Hayes, R. L., Ruda, M., & Dubner, R. (1978). Spatial and temporal transformations of input to spinothalamic tract neurons and their relation to somatic sensations. *Journal of Neurophysiology*, *41*(4), 933–947. https://doi.org/10.1152/jn.1978.41.4.933

Raij, T. T., Forss, N., Stančák, A., & Hari, R. (2004). Modulation of motor-cortex oscillatory activity by painful Adelta- and C-fiber stimuli. *NeuroImage*, *23*(2), 569–573. https://doi.org/10.1016/j.neuroimage.2004.06.036

Raja, S. N., Campbell, J. N., & Meyer, R. A. (1984). Evidence for different mechanisms of primary and secondary hyperalgesia following heat injury to the glabrous skin. *Brain*, *107*(4), 1179–1188. https://doi.org/10.1093/brain/107.4.1179

Raja, S. N., Carr, D. B., Cohen, M., Finnerup, N. B., Flor, H., Gibson, S., Keefe, F. J., Mogil, J. S., Ringkamp, M., Sluka, K. A., Song, X. J., Stevens, B., Sullivan, M. D., Tutelman, P. R., Ushida, T., & Vader, K. (2020). The revised International Association for the Study of Pain definition of pain: concepts, challenges, and compromises. *Pain*, *161*(9), 1976–1982. https://doi.org/10.1097/j.pain.0000000000001939

Randić, M., Jiang, M. C., & Cerne, R. (1993). Long-term potentiation and long-term depression of primary afferent neurotransmission in the rat spinal cord. *The Journal of Neuroscience*, *13*(12), 5228–5241. https://doi.org/10.1523/JNEUROSCI.13-12-05228.1993

Reeh, P. W., Bayer, J., Kocher, L., & Handwerker, H. O. (1987). Sensitization of nociceptive cutaneous nerve fibers from the rat’s tail by noxious mechanical stimulation. *Experimental Brain Research*, *65*(3), 505–512. https://doi.org/10.1007/BF00235973

Ren, B., Linderoth, B., & Meyerson, B. A. (1996). Effects of spinal cord stimulation on the flexor reflex and involvement of supraspinal mechanisms: an experimental study in mononeuropathic rats. *Journal of Neurosurgery*, *84*(2), 244–249. https://doi.org/10.3171/jns.1996.84.2.0244

Reverberi, C., Bonezzi, C., & Demartini, L. (2009). Peripheral subcutaneous neurostimulation in the management of neuropathic pain: Five case reports. *Neuromodulation*, *12*(2), 146–155. https://doi.org/10.1111/j.1525-1403.2009.00201.x

Rexed, B. (1952). The cytoarchitectonic organization of the spinal cord in the cat. *Journal of Comparative Neurology*, *96*(3), 415–495. https://doi.org/10.1002/cne.900960303

Rice, A. S. C., Smith, B. H., & Blyth, F. M. (2016). Pain and the global burden of disease. *Pain*, *157*(4), 791–796. https://doi.org/10.1097/j.pain.0000000000000454

Ringkamp, M., Raja, S. N., Campbell, J. N., & Meyer, R. A. (2013). Peripheral Mechanisms of Cutaneous Nociception. In S. B. McMahon, M. Koltzenburg, I. Tracey, & D. Turk (Eds.), *Wall and Melzack's Textbook of Pain* (6th ed, pp. 1–30). Saunders.

Rottmann, S., Jung, K., & Ellrich, J. (2008). Electrical low-frequency stimulation induces homotopic long-term depression of nociception and pain from hand in man. *Clinical Neurophysiology*, *119*(8), 1895–1904. https://doi.org/10.1016/j.clinph.2008.02.022

Rottmann, S., Jung, K., & Ellrich, J. (2010a). Electrical low-frequency stimulation induces long-term depression of sensory and affective components of pain in healthy man. *European Journal of Pain*, *14*(4), 359–365. https://doi.org/10.1016/j.ejpain.2009.06.001

Rottmann, S., Jung, K., Vohn, R., & Ellrich, J. (2010b). Long-term depression of pain-related cerebral activation in healthy man: An fMRI study. *European Journal of Pain*, *14*(6), 615–624. https://doi.org/10.1016/j.ejpain.2009.10.006

Ruben, J., Krause, T., Taskin, B., Blankenburg, F., Moosmann, M., & Villringer, A. (2006). Subarea-specific Suppressive Interaction in the BOLD Responses to Simultaneous Finger Stimulation in Human Primary Somatosensory Cortex: Evidence for Increasing Rostral-to-caudal Convergence. *Cerebral Cortex*, *16*(6), 819–826. https://doi.org/10.1093/cercor/bhj025

Rustamov, N., Sharma, L., Chiang, S. N., Burk, C., Haroutounian, S., & Leuthardt, E. C. (2021). Spatial and Frequency-specific Electrophysiological Signatures of Tonic Pain Recovery in Humans. *Neuroscience*, *465*, 23–37. https://doi.org/10.1016/j.neuroscience.2021.04.008

Rutkowski, B., Niedzialkowska, T., & Otto, J. (1975). Electrostimulation in the management of chronic pain. *Anaesthesist*, *24*(10), 457–460. http://www.ncbi.nlm.nih.gov/pubmed/1081351

Rygh, L. J., Tjølsen, A., Hole, K., & Svendsen, F. (2002). Cellular memory in spinal nociceptive circuitry. *Scandinavian Journal of Psychology*, *43*(2), 153–159. https://doi.org/10.1111/1467-9450.00281

Saadé, N. E., Tabet, M. S., Soueidan, S. A., Bitar, M., Atweh, S. F., & Jabbur, S. J. (1986). Supraspinal modulation of nociception in awake rats by stimulation of the dorsal column nuclei. *Brain Research*, *369*(1–2), 307–310. https://doi.org/10.1016/0006-8993(86)90540-8

Saber, M., Schwabe, D., Park, H.-J., Tessmer, J., Khan, Z., Ding, Y., Robinson, M., Hogan, Q. H., & Pawela, C. P. (2021). Tonic, Burst, and Burst Cycle Spinal Cord Stimulation Lead to Differential Brain Activation Patterns as Detected by Functional Magnetic Resonance Imaging. *Neuromodulation: Technology at the Neural Interface*, *n/a*(n/a). https://doi.org/10.1111/ner.13460

Salenius, S., Schnitzler, A., Salmelin, R., Jousmäki, V., & Hari, R. (1997). Modulation of human cortical rolandic rhythms during natural sensorimotor tasks. *NeuroImage*, *5*(3), 221–228. https://doi.org/10.1006/nimg.1997.0261

Salmelin, R., & Hari, R. (1994a). Characterization of spontaneous MEG rhythms in healthy adults. *Electroencephalography and Clinical Neurophysiology*, *91*(4), 237–248. https://doi.org/10.1016/0013-4694(94)90187-2

Salmelin, R., & Hari, R. (1994b). Spatiotemporal characteristics of rhythmic neuromagnetic activity related to thumb movement. *Neuroscience*, *60*(94), 537–550. https://doi.org/10.1016/0306-4522(94)90263-1

Salmelin, R., & Hari, R. (1994c). Spatiotemporal characteristics of sensorimotor neuromagnetic rhythms related to thumb movement. *Neuroscience*, *60*(94), 537–550. https://doi.org/10.1016/0306-4522(94)90263-1

Sandkühler, J. (2007). Understanding LTP in pain pathways. *Molecular Pain*, *3*, 1–9. https://doi.org/10.1186/1744-8069-3-9

Sandkühler, J., Chen, J. G., Cheng, G., & Randić, M. (1997). Low-frequency stimulation of afferent Aδ-fibers induces long-term depression at primary afferent synapses with substantia gelatinosa neurons in the rat. *The Journal of Neuroscience*, *17*(16), 6483–6491. https://doi.org/10.1523/JNEUROSCI.17-16-06483.1997

Sandkühler, J., & Gruber-Schoffnegger, D. (2012). Hyperalgesia by synaptic long-term potentiation (LTP): An update. *Current Opinion in Pharmacology*, *12*(1), 18–27.

https://doi.org/10.1016/j.coph.2011.10.018

Sandkühler, J., & Liu, X. G. (1998). Induction of long-term potentiation at spinal synapses by noxious stimulation or nerve injury. *European Journal of Neuroscience*, *10*(7), 2476–2480. https://doi.org/10.1046/j.1460-9568.1998.00278.x

Sandroni, P., Benrud-Larson, L. M., McClelland, R. L., & Low, P. A. (2003). Complex regional pain syndrome type I: incidence and prevalence in Olmsted county, a population-based study. *Pain*, *103*(1–2), 199–207. https://doi.org/10.1016/s0304-3959(03)00065-4

Sang, C. N., Max, M. B., & Gracely, R. H. (2003). Stability and Reliability of Detection Thresholds for Human A-Beta and A-Delta Sensory Afferents Determined by Cutaneous Electrical Stimulation. *Journal of Pain and Symptom Management*, *25*(1), 64–73. https://doi.org/10.1016/S0885-3924(02)00541-9

Sankarasubramanian, V., Harte, S. E., Chiravuri, S., Harris, R. E., Brummett, C. M., Patil, P. G., Clauw, D. J., & Lempka, S. F. (2019). Objective Measures to Characterize the Physiological Effects of Spinal Cord Stimulation in Neuropathic Pain: A Literature Review. *Neuromodulation: Technology at the Neural Interface*, *22*(2), 227–248. https://doi.org/10.1111/ner.12804

Sarnthein, J., Stern, J., Aufenberg, C., Rousson, V., & Jeanmonod, D. (2006). Increased EEG power and slowed dominant frequency in patients with neurogenic pain. *Brain*, *129*(1), 55–64. https://doi.org/10.1093/brain/awh631

Sato, K. L., Johanek, L. M., Sanada, L. S., & Sluka, K. A. (2014). Spinal cord stimulation reduces mechanical hyperalgesia and glial cell activation in animals with neuropathic pain. *Anesthesia and Analgesia*, *118*(2), 464–472. https://doi.org/10.1213/ANE.0000000000000047

Scadding, J. W., & Koltzenburg, M. (2013). Painful Peripheral Neuropathies. In S. B. McMahon, M. Koltzenburg, I. Tracey, & D. Turk (Eds.), *Wall and Melzack's Textbook of Pain* (6th Ed, pp. 926–951). Saunders.

Scalone, L., Zucco, F., Lavano, A., Costantini, A., De Rose, M., Poli, P., Fortini, G., Demartini, L., De Simone, E., Menardo, V., Meglio, M., Cozzolino, P., Cortesi, P. A., & Mantovani, L. G. (2018). Benefits in pain perception, ability function and health-related quality of life in patients with failed back surgery syndrome undergoing spinal cord stimulation in a clinical practice

setting. *Health and Quality of Life Outcomes*, *16*(1), 1–14. https://doi.org/10.1186/s12955-018-0887-x

Schabrun, S. M., Ridding, M. C., Galea, M. P., Hodges, P. W., & Chipchase, L. S. (2012). Primary Sensory and Motor Cortex Excitability Are Co-Modulated in Response to Peripheral Electrical Nerve Stimulation. *PLoS ONE*, *7*(12), 1–7. https://doi.org/10.1371/journal.pone.0051298

Schaible, H. G., & Schmidt, R. (1983). Responses of fine medial articular nerve afferents to passive movements of knee joints. *Journal of Neurophysiology*, *49*(5), 1118–1126. https://doi.org/10.1152/jn.1983.49.5.1118

Schechtmann, G., Lind, G., Winter, J., Meyerson, B. A., & Linderoth, B. (2010). Intrathecal Clonidine and Baclofen Enhance the Pain-Relieving Effect of Spinal Cord Stimulation. *Neurosurgery*, *67*(1), 173–181. https://doi.org/10.1227/01.NEU.0000370249.41634.4F

Scheeringa, R., Bastiaansen, M. C. M., Petersson, K. M., Oostenveld, R., Norris, D. G., & Hagoort, P. (2008). Frontal theta EEG activity correlates negatively with the default mode network in resting state. *International Journal of Psychophysiology*, *67*(3), 242–251. https://doi.org/10.1016/j.ijpsycho.2007.05.017

Scherg, M. (1992). Functional imaging and localization of electromagnetic brain activity. *Brain Topography*, *5*(2), 103–111. https://doi.org/10.1007/BF01129037

Scherg, M., & Berg, P. (1996). New concepts of brain source imaging and localization. *Electroencephalography and Clinical Neurophysiology. Supplement*, *46*, 127–137.

Scherg, M., Hoechstetter, K., & Berg, P. (2010). BESA Research Tutorial 1: Introduction to Discrete Source Analysis. In *BESA Research Tutorial*.

Schlaier, J. R., Eichhammer, P., Langguth, B., Doenitz, C., Binder, H., Hajak, G., & Brawanski, A. (2007). Effects of spinal cord stimulation on cortical excitability in patients with chronic neuropathic pain: A pilot study. *European Journal of Pain*, *11*(8), 863–868. https://doi.org/10.1016/j.ejpain.2007.01.004

Schmidt, R., Schmelz, M., Forster, C., Ringkamp, M., Torebjork, E., & Handwerker, H. (1995). Novel classes of responsive and unresponsive C nociceptors in human skin. *The Journal of Neuroscience*, *15*(1), 333–341. https://doi.org/10.1523/JNEUROSCI.15-01-00333.1995

Schnitzler, A., & Gross, J. (2005). Normal and pathological oscillatory communication in the brain. *Nature Reviews Neuroscience*, *6*(4), 285–296. https://doi.org/10.1038/nrn1650

Scholz, J., Finnerup, N. B., Attal, N., Aziz, Q., Baron, R., Bennett, M. I., Benoliel, R., Cohen, M., Cruccu, G., Davis, K. D., Evers, S., First, M., Giamberardino, M. A., Hansson, P., Kaasa, S., Korwisi, B., Kosek, E., Lavand'homme, P., Nicholas, M., … (NeuPSIG), C. C. of the N. P. S. I. G. (2019). The IASP classification of chronic pain for ICD-11: chronic neuropathic pain. *Pain*, *160*(1), 53–59. https://doi.org/10.1097/j.pain.0000000000001365

Schu, S., Slotty, P. J., Bara, G., von Knop, M., Edgar, D., & Vesper, J. (2014). A Prospective, Randomised, Double-blind, Placebo-controlled Study to Examine the Effectiveness of Burst Spinal Cord Stimulation Patterns for the Treatment of Failed Back Surgery Syndrome. *Neuromodulation: Technology at the Neural Interface*, *17*(5), 443–450. https://doi.org/10.1111/ner.12197

Schug, S. A., Lavand'homme, P., Barke, A., Korwisi, B., Rief, W., & Treede, R.-D. (2019). The IASP classification of chronic pain for ICD-11: chronic postsurgical or posttraumatic pain. *Pain*, *160*(1), 45–52. https://doi.org/10.1097/j.pain.0000000000001413

Schulman, J. J., Ramirez, R. R., Zonenshayn, M., Ribary, U., & Llinás, R. R. (2005). Thalamocortical dysrhythmia syndrome: MEG imaging of neuropathic pain. *Thalamus and Related Systems*, *3*(1), 33–39. https://doi.org/10.1017/S1472928805000063

Sdrulla, A. D., Xu, Q., He, S.-Q., Tiwari, V., Yang, F., Zhang, C., Shu, B., Shechter, R., Raja, S. N., Wang, Y., Dong, X., & Guan, Y. (2015). Electrical stimulation of low-threshold afferent fibers induces a prolonged synaptic depression in lamina II dorsal horn neurons to high-threshold afferent inputs in mice. *Pain*, *156*(6), 1008–1017. https://doi.org/10.1097/01.j.pain.0000460353.15460.a3

Sebaaly, A., Lahoud, M.-J., Rizkallah, M., Kreichati, G., & Kharrat, K. (2018). Etiology, Evaluation, and Treatment of Failed Back Surgery Syndrome. *Asian Spine Journal*, *12*(3), 574–585. https://doi.org/10.4184/asj.2018.12.3.574

Segerdahl, A. R., Mezue, M., Okell, T. W., Farrar, J. T., & Tracey, I. (2015). The dorsal posterior insula subserves a fundamental role in human pain. *Nature Neuroscience*, *18*(4), 499–500.

https://doi.org/10.1038/nn.3969

Shackman, A. J., Salomons, T. V., Slagter, H. A., Fox, A. S., Winter, J. J., & Davidson, R. J. (2011). The integration of negative affect, pain and cognitive control in the cingulate cortex. *Nature Reviews Neuroscience*, *12*(3), 154–167. https://doi.org/10.1038/nrn2994

Sharan, A., Cameron, T., & Barolat, G. (2002). Evolving Patterns of Spinal Cord Stimulation in Patients Implanted for Intractable Low Back and Leg Pain. *Neuromodulation: Technology at the Neural Interface*, *5*(3), 167–179. https://doi.org/10.1046/j.1525-1403.2002.02027.x

Shealy, C. N., Mortimer, J. T., & Reswick, J. B. (1967). Electrical inhibition of pain by stimulation of the dorsal columns: preliminary clinical report. *Anesthesia and Analgesia*, *46*(4), 489–491. https://doi.org/10.3109/15360288.2012.678473

Sheldon, B., Staudt, M. D., Williams, L., Harland, T. A., & Pilitsis, J. G. (2021). Spinal cord stimulation programming: a crash course. *Neurosurgical Review*, *44*(2), 709–720. https://doi.org/10.1007/s10143-020-01299-y

Shimojo, M., Svensson, P., Arendt-Nielsen, L., & Chen, A. C. N. (2000). Dynamic brain topography of somatosensory evoked potentials and equivalent dipoles in response to graded painful skin and muscle stimulation. *Brain Topography*, *13*(1), 43–58. https://doi.org/10.1023/a:1007834319135

Silvestrini, N., Chen, J.-I., Piché, M., Roy, M., Vachon-Presseau, E., Woo, C.-W., Wager, T. D., & Rainville, P. (2020). Distinct fMRI patterns colocalized in the cingulate cortex underlie the after-effects of cognitive control on pain. *NeuroImage*, *217*, 116898. https://doi.org/10.1016/j.neuroimage.2020.116898

Simopoulos, T., Aner, M., Sharma, S., Ghosh, P., & Gill, J. S. (2019). Explantation of Percutaneous Spinal Cord Stimulator Devices: A Retrospective Descriptive Analysis of a Single-Center 15-Year Experience. *Pain Medicine*, *20*(7), 1355–1361. https://doi.org/10.1093/pm/pny245

Skinner, R. D., Adams, R. J., & Remmel, R. S. (1980). Responses of long descending propriospinal neurons to natural and electrical types of stimuli in cat. *Brain Research*, *196*(2), 387–403. https://doi.org/10.1016/0006-8993(80)90403-5

Slavin, K. V., Colpan, M. E., Munawar, N., Wess, C., & Nersesyan, H. (2006). Trigeminal and

occipital peripheral nerve stimulation for craniofacial pain: a single-institution experience and review of the literature. *Neurosurgical Focus*, *21*(6), 1–5. https://doi.org/10.3171/foc.2006.21.6.8

Slepian, D. (1978). Prolate Spheroidal Wave Functions, Fourier Analysis, and Uncertainty-V: The Discrete Case. *Bell System Technical Journal*, *57*(5), 1371–1430. https://doi.org/10.1002/j.1538-7305.1978.tb02104.x

Smallwood, R. F., Laird, A. R., Ramage, A. E., Parkinson, A. L., Lewis, J., Clauw, D. J., Williams, D. A., Schmidt-Wilcke, T., Farrell, M. J., Eickhoff, S. B., & Robin, D. A. (2013). Structural brain anomalies and chronic pain: a quantitative meta-analysis of gray matter volume. *The Journal of Pain*, *14*(7), 663–675. https://doi.org/10.1016/j.jpain.2013.03.001

Smith, B. H., & Torrance, N. (2012). Epidemiology of Neuropathic Pain and Its Impact on Quality of Life. *Current Pain and Headache Reports*, *16*(3), 191–198. https://doi.org/10.1007/s11916-012-0256-0

Smith, E. S., & Lewin, G. R. (2009). Nociceptors: a phylogenetic view. *Journal of Comparative Physiology A*, *195*(12), 1089–1106. https://doi.org/10.1007/s00359-009-0482-z

Song, Z., Ansah, O. B., Meyerson, B. A., Pertovaara, A., & Linderoth, B. (2013). The rostroventromedial medulla is engaged in the effects of spinal cord stimulation in a rodent model of neuropathic pain. *Neuroscience*, *247*, 134–144. https://doi.org/10.1016/j.neuroscience.2013.05.027

Speckmann, E.-J., Elger, C. E., & Gorji, A. (2011). Neurophysiologic Basis of EEG and DC Potentials. In D. L. Schomer & F. H. Lopes da Silva (Eds.), *2Niedermeyer's Electroencephalography: Basic Principles, Clinical Applications, and Related Fields* (6th ed., pp. 17–32). Wolters Kluwer/Lippincott Williams & Wilkins Health.

Srinivasan, R., Nunez, P. L., & Silberstein, R. B. (1998). Spatial filtering and neocortical dynamics: Estimates of EEG coherence. *IEEE Transactions on Biomedical Engineering*, *45*(7), 814–826. https://doi.org/10.1109/10.686789

Stančák, A. (2006). Cortical oscillatory changes occurring during somatosensory and thermal stimulation. In C. Neuper & W. Klimesch (Eds.), *Event-Related Dynamics of Brain Oscillations*

(Vol. 159, pp. 237–252). Elsevier. https://doi.org/10.1016/S0079-6123(06)59016-8

Stancak, A., Cook, S., Wright, H., & Fallon, N. (2016). Mapping multidimensional pain experience onto electrophysiological responses to noxious laser heat stimuli. *NeuroImage*, *125*, 244–255. https://doi.org/10.1016/j.neuroimage.2015.10.028

Stancak, A., & Fallon, N. (2013). Emotional modulation of experimental pain: a source imaging study of laser evoked potentials. *Frontiers in Human Neuroscience*, *7*, 552. https://doi.org/10.3389/fnhum.2013.00552

Stancak, A., Fallon, N., Fenu, A., Kokmotou, K., Soto, V., & Cook, S. (2018). Neural Mechanisms of Attentional Switching Between Pain and a Visual Illusion Task: A Laser Evoked Potential Study. *Brain Topography*, *31*(3), 430–446. https://doi.org/10.1007/s10548-017-0613-8

Stancak, A., Hoechstetter, K., Tintěra, J., Vrána, J., Rachmanová, R., Kralik, J., & Scherg, M. (2002). Source activity in the human secondary somatosensory cortex depends on the size of corpus callosum. *Brain Research*, *936*(1–2), 47–57. https://doi.org/10.1016/S0006-8993(02)02502-7

Stancak, A., Kozák, J., Vrba, I., Tintěra, J., Vrána, J., Poláček, H., & Stančák, M. (2008). Functional magnetic resonance imaging of cerebral activation during spinal cord stimulation in failed back surgery syndrome patients. *European Journal of Pain*, *12*(2), 137–148. https://doi.org/10.1016/j.ejpain.2007.03.003

Stancak, A., & Pfurtscheller, G. (1996). Mu-rhythm changes in brisk and slow self-paced finger movements. *NeuroReport*, *7*, 1161–1164.

Stančák, A., Poláček, H., & Bukovský, S. (2010). Bursts of 15–30 Hz oscillations following noxious laser stimulus originate in posterior cingulate cortex. *Brain Research*, *1317*, 69–79. https://doi.org/10.1016/j.brainres.2009.12.064

Stančák, A., Raij, T. T., Pohja, M., Forss, N., & Hari, R. (2005). Oscillatory motor cortex-muscle coupling during painful laser and nonpainful tactile stimulation. *NeuroImage*, *26*(3), 793–800. https://doi.org/10.1016/j.neuroimage.2005.02.047

Stancak, A., Svoboda, J., Rachmanová, R., Vrána, J., Kralik, J., & Tintěra, J. (2003). Desynchronization of cortical rhythms following cutaneous stimulation: effects of stimulus repetition and intensity, and of the size of corpus callosum. *Clinical Neurophysiology*, *114*(10),

1936–1947. https://doi.org/10.1016/S1388-2457(03)00201-3

Stern, J., Jeanmonod, D., & Sarnthein, J. (2006). Persistent EEG overactivation in the cortical pain matrix of neurogenic pain patients. *NeuroImage*, *31*(2), 721–731. https://doi.org/10.1016/j.neuroimage.2005.12.042

Stiller, C., Cui, J. G., O'Connor, W. T., Brodin, E., Meyerson, B. A., & Linderoth, B. (1996). Release of γ-aminobutyric acid in the dorsal horn and suppression of tactile allodynia by spinal cord stimulation in mononeuropathic rats. *Neurosurgery*, *39*(2), 367–375. https://doi.org/10.1097/00006123-199608000-00026

Su, Q., Qin, W., Yang, Q. Q., Yu, C. S., Qian, T. Y., Mouraux, A., Iannetti, G. D., & Liang, M. (2019). Brain regions preferentially responding to transient and iso-intense painful or tactile stimuli. *NeuroImage*, *192*, 52–65. https://doi.org/10.1016/j.neuroimage.2019.01.039

Sufianov, A. A., Shapkin, A. G., Sufianova, G. Z., Elishev, V. G., Barashin, D. A., Berdichevskii, V. B., & Churkin, S. V. (2014). Functional and Metabolic Changes in the Brain in Neuropathic Pain Syndrome against the Background of Chronic Epidural Electrostimulation of the Spinal Cord. *Bulletin of Experimental Biology and Medicine*, *157*(4), 462–465. https://doi.org/10.1007/s10517-014-2591-0

Sufka, K. J., & Price, D. D. (2002). Gate Control Theory Reconsidered. *Brain and Mind*, *3*, 277–290. https://doi.org/10.1023/A:1019996809849

Sun, L., Peng, C., Joosten, E. A. J., Cheung, C. W., Tan, F., Jiang, W., & Shen, X. (2021). Spinal Cord Stimulation and Treatment of Peripheral or Central Neuropathic Pain: Mechanisms and Clinical Application. *Neural Plasticity*, *2021*, 5607898. https://doi.org/10.1155/2021/5607898

Svendsen, F., Tjølsen, A., & Hole, K. (1997). LTP of spinal Aβ and C-fibre evoked responses after electrical sciatic nerve stimulation. *NeuroReport*, *8*(16), 3427–3430. https://doi.org/10.1097/00001756-199711100-00002

Sweet, W. H., & Wepsic, J. G. (1968). Treatment of chronic pain by stimulation of fibers of primary afferent neuron. *Transactions of the American Neurological Association*, *93*, 103–107.

Tallon-Baudry, C., Bertrand, O., Delpuech, C., & Pernía-Andrade, A. J. (1996). Stimulus specificity of phase-locked and non-phase-locked 40 Hz visual responses in human. *Journal of*

Neuroscience, *16*(13), 4240–4249. https://doi.org/10.1523/jneurosci.16-13-04240.1996

Tamè, L., Pavani, F., Papadelis, C., Farnè, A., & Braun, C. (2015). Early integration of bilateral touch in the primary somatosensory cortex. *Human Brain Mapping*, *36*(4), 1506–1523. https://doi.org/10.1002/hbm.22719

Tan, D., Tyler, D. J., Sweet, J., & Miller, J. P. (2016). Intensity Modulation: A Novel Approach to Percept Control in Spinal Cord Stimulation. *Neuromodulation*, *19*(3), 254–259. https://doi.org/10.1111/ner.12358

Tanasescu, R., Cottam, W. J., Condon, L., Tench, C. R., & Auer, D. P. (2016). Functional reorganisation in chronic pain and neural correlates of pain sensitisation: A coordinate based meta-analysis of 266 cutaneous pain fMRI studies. *Neuroscience and Biobehavioral Reviews*, *68*, 120–133. https://doi.org/10.1016/j.neubiorev.2016.04.001

Tang, R., Martinez, M., Goodman-Keiser, M., Farber, J. P., Qin, C., & Foreman, R. D. (2014). Comparison of burst and tonic spinal cord stimulation on spinal neural processing in an animal model. *Neuromodulation*, *17*(2), 143–151. https://doi.org/10.1111/ner.12117

Taylor, R. S., Desai, M. J., Rigoard, P., & Taylor, R. J. (2014). Predictors of pain relief following spinal cord stimulation in chronic back and leg pain and failed back surgery syndrome: A systematic review and meta-regression analysis. *Pain Practice*, *14*(6), 489–505. https://doi.org/10.1111/papr.12095

Tazawa, T., Kamiya, Y., Kobayashi, A., Saeki, K., Takiguchi, M., Nakahashi, Y., Shinbori, H., Funakoshi, K., & Goto, T. (2015). Spinal cord stimulation modulates supraspinal centers of the descending antinociceptive system in rats with unilateral spinal nerve injury. *Molecular Pain*, *11*, 36. https://doi.org/10.1186/s12990-015-0039-9

Telkes, llknur, Hancu, M., Paniccioli, S., Grey, R., Briotte, M., McCarthy, K., Raviv, N., & Pilitsis, J. G. (2020). Differences in EEG patterns between tonic and high frequency spinal cord stimulation in chronic pain patients. *Clinical Neurophysiology*, *131*(8), 1731–1740. https://doi.org/10.1016/j.clinph.2020.03.040

Thalhammer, J. G., & LaMotte, R. H. (1982). Spatial properties of nociceptor sensitization following heat injury of the skin. *Brain Research*, *231*(2), 257–265. https://doi.org/10.1016/0006-

8993(82)90364-x

The British Pain Society. (2010). *National Pain Audit Final Report: 2010 - 2012*. 66.

Theuvenet, P. J., Dunajski, Z., Peters, M. J., & van Ree, J. M. (1999). Responses to median and tibial nerve stimulation in patients with chronic neuropathic pain. *Brain Topogr*, *11*(4), 305–313. https://doi.org/10.1023/a:1022210704505

Thomson, S. (2013). Failed back surgery syndrome – definition, epidemiology and demographics. *British Journal of Pain*, *7*(1), 56–59. https://doi.org/10.1177/2049463713479096

Tiemann, L., May, E. S., Postorino, M., Schulz, E., Nickel, M. M., Bingel, U., & Ploner, M. (2015). Differential neurophysiological correlates of bottom-up and top-down modulations of pain. *Pain*, *156*(2), 289–296. https://doi.org/10.1097/01.j.pain.0000460309.94442.44

Tölle, T. R., Kaufmann, T., Siessmeier, T., Lautenbacher, S., Berthele, A., Munz, F., Zieglgänsberger, W., Willoch, F., Schwaiger, M., Conrad, B., & Bartenstein, P. (1999). Region-specific encoding of sensory and affective components of pain in the human brain: A positron emission tomography correlation analysis. *Annals of Neurology*, *45*(1), 40–47. https://doi.org/10.1002/1531-8249(199901)45:1<40::AID-ART8>3.0.CO;2-L

Torta, D. M., & Cauda, F. (2011). Different functions in the cingulate cortex, a meta-analytic connectivity modeling study. *NeuroImage*, *56*(4), 2157–2172. https://doi.org/10.1016/j.neuroimage.2011.03.066

Torta, D. M., De Laurentis, M., Eichin, K. N., von Leupoldt, A., van den Broeke, E. N., & Vlaeyen, J. W. S. (2020). A highly cognitive demanding working memory task may prevent the development of nociceptive hypersensitivity. *Pain*, *161*(7), 1459–1469. https://doi.org/10.1097/j.pain.0000000000001841

Traub, R. J., Sedivec, M. J., & Mendell, L. M. (1986). The rostral projection of small diameter primary afferents in Lissauer's tract. *Brain Research*, *399*(1), 185–189. https://doi.org/10.1016/0006-8993(86)90617-7

Treede, R.-D., Jensen, T. S., Campbell, J. N., Cruccu, G., Dostrovsky, J. O., Griffin, J. W., Hansson, P., Hughes, R., Nurmikko, T. J., & Serra, J. (2008). Neuropathic pain: redefinition and a grading system for clinical and research purposes. *Neurology*, *70*(18), 1630–1635.

https://doi.org/10.1212/01.wnl.0000282763.29778.59

Treede, R.-D., Kenshalo, D. R., Gracely, R. H., & Jones, A. K. . (1999). The cortical representation of pain. *Pain*, *79*(2–3), 105–111. https://doi.org/10.1016/s0304-3959(98)00184-5

Treede, R.-D., Meyer, R. A., & Campbell, J. N. (1998). Myelinated mechanically insensitive afferents from monkey hairy skin: heat-response properties. *Journal of Neurophysiology*, *80*(3), 1082–1093. https://doi.org/10.1152/jn.1998.80.3.1082

Treede, R.-D., Meyer, R. A., Raja, S. N., & Campbell, J. N. (1992). Peripheral and central mechanisms of cutaneous hyperalgesia. *Progress in Neurobiology*, *38*(4), 397–421. https://doi.org/10.1016/0301-0082(92)90027-c

Treede, R.-D., Rief, W., Barke, A., Aziz, Q., Bennett, M. I., Benoliel, R., Cohen, M., Evers, S., Finnerup, N. B., First, M. B., Giamberardino, M. A., Kaasa, S., Korwisi, B., Kosek, E., Lavand'homme, P., Nicholas, M., Perrot, S., Scholz, J., Schug, S., … Wang, S.-J. (2019). Chronic pain as a symptom or a disease: the IASP Classification of Chronic Pain for the International Classification of Diseases (ICD-11). *Pain*, *160*(1), 19–27. https://doi.org/10.1097/j.pain.0000000000001384

Treede, R.-D., Rief, W., Barke, A., Aziz, Q., Bennett, M. I., Benoliel, R., Cohen, M., Evers, S., Finnerup, N. B., First, M. B., Giamberardino, M. A., Kaasa, S., Kosek, E., Lavand'homme, P., Nicholas, M., Perrot, S., Scholz, J., Schug, S., Smith, B. H., … Wang, S.-J. (2015). A classification of chronic pain for ICD-11. *Pain*, *156*(6), 1003–1007. https://doi.org/10.1097/j.pain.0000000000000160

Treede, R. D., Meyer, R. A., Raja, S. N., & Campbell, J. N. (1995). Evidence for two different heat transduction mechanisms in nociceptive primary afferents innervating monkey skin. *The Journal of Physiology*, *483*(3), 747–758. https://doi.org/10.1113/jphysiol.1995.sp020619

Truini, A., Galeotti, F., Romaniello, A., Virtuoso, M., Iannetti, G. D., & Cruccu, G. (2005). Laser-evoked potentials: Normative values. *Clinical Neurophysiology*, *116*(4), 821–826. https://doi.org/10.1016/j.clinph.2004.10.004

Tsui, B. C. H. (2008). Electrical Nerve Stimulation. In V. Chan, B. Finucane, T. Grau, & A. Walji (Eds.), *Atlas of Ultrasound- and Nerve Stimulation-Guided Regional Anesthesia* (pp. 9–18).

Springer. https://doi.org/10.1007/978-3-7091-3271-5

Urasaki, E., Tsuda, M., Nakane, S., Toyoda, K., Umeno, T., & Yamakawa, Y. (2014). Spinal cord stimulation for intractable pain evaluated by a collision study using somatosensory evoked potentials: A preliminary report. *Neuromodulation*, *17*(8), 746–752. https://doi.org/10.1111/ner.12205

Urits, I., Burshtein, A., Sharma, M., Testa, L., Gold, P. A., Orhurhu, V., Viswanath, O., Jones, M. R., Sidransky, M. A., Spektor, B., & Kaye, A. D. (2019). Low Back Pain, a Comprehensive Review: Pathophysiology, Diagnosis, and Treatment. *Current Pain and Headache Reports*, *23*(3), 23. https://doi.org/10.1007/s11916-019-0757-1

Valeriani, M., Le Pera, D., Niddam, D., Arendt-Nielsen, L., & Chen, A. C. N. (2000a). Dipolar source modeling of somatosensory evoked potentials to painful and nonpainful median nerve stimulation. *Muscle & Nerve*, *23*(8), 1194–1203. https://doi.org/10.1002/1097-4598(200008)23:8<1194::AID-MUS6>3.0.CO;2-E

Valeriani, M., Le Pera, D., & Tonali, P. (2001). Characterizing somatosensory evoked potential sources with dipole models: Advantages and limitations. *Muscle & Nerve*, *24*(3), 325–339. https://doi.org/10.1002/1097-4598(200103)24:3<325::AID-MUS1002>3.0.CO;2-0

Valeriani, M., Pazzaglia, C., Cruccu, G., & Truini, A. (2012). Clinical usefulness of laser evoked potentials. *Neurophysiologie Clinique/Clinical Neurophysiology*, *42*(5), 345–353. https://doi.org/10.1016/j.neucli.2012.05.002

Valeriani, M., Restuccia, D., Barba, C., Le Pera, D., Tonali, P. A., & Mauguière, F. (2000b). Sources of cortical responses to painful CO2 laser skin stimulation of the hand and foot in the human brain. *Clinical Neurophysiology*, *111*(6), 1103–1112. https://doi.org/10.1016/S1388-2457(00)00273-X

Vallbo, Å., Olausson, H., Wessberg, J., & Norrsell, U. (1993). A system of unmyelinated afferents for innocuous mechanoreception in the human skin. *Brain Research*, *628*(1–2), 301–304. https://doi.org/10.1016/0006-8993(93)90968-S

Vallejo, R., Chakravarthy, K., Will, A. J., Trutnau, K. C., & Dinsmoor, D. (2021). A New Direction for Closed-Loop Spinal Cord Stimulation: Combining Contemporary Therapy Paradigms with

Evoked Compound Action Potential Sensing. *Journal of Pain Research*, *14*, 3909–3918. https://doi.org/10.2147/JPR.S344568

van den Broeke, E. N., & Mouraux, A. (2014). High-frequency electrical stimulation of the human skin induces heterotopical mechanical hyperalgesia, heat hyperalgesia, and enhanced responses to nonnociceptive vibrotactile input. *Journal of Neurophysiology*, *111*(8), 1564–1573. https://doi.org/10.1152/jn.00651.2013

van Hecke, O., Austin, S. K., Khan, R. A., Smith, B. H., & Torrance, N. (2014). Neuropathic pain in the general population: A systematic review of epidemiological studies. *Pain*, *155*(4), 654–662. https://doi.org/10.1016/j.pain.2013.11.013

Vanneste, S., Song, J. J., & De Ridder, D. (2018). Thalamocortical dysrhythmia detected by machine learning. *Nature Communications*, *9*(1). https://doi.org/10.1038/s41467-018-02820-0

Veldman, P. H. J. ., Reynen, H. ., Arntz, I. ., & Goris, R. J. . (1993). Signs and symptoms of reflex sympathetic dystrophy: prospective study of 829 patients. *The Lancet*, *342*(8878), 1012–1016. https://doi.org/10.1016/0140-6736(93)92877-V

Venkatesan, L., Barlow, S. M., Popescu, M., & Popescu, A. (2014). Integrated approach for studying adaptation mechanisms in the human somatosensory cortical network. *Experimental Brain Research*, *232*(11), 3545–3554. https://doi.org/10.1007/s00221-014-4043-5

Vesper, J., Slotty, P. J., Schu, S., Poeggel-Kraemer, K., Littges, H., Van Looy, P., Agnesi, F., Venkatesan, L., Van Havenbergh, T., Looy, P. Van, Agnesi, F., Venkatesan, L., & Havenbergh, T. Van. (2018). Burst SCS Microdosing Is as Efficacious as Standard Burst SCS in Treating Chronic Back and Leg Pain: Results From a Randomized Controlled Trial. *Neuromodulation: Technology at the Neural Interface*, *2018*(2), 3–6. https://doi.org/10.1111/ner.12883

Visnjevac, O., Costandi, S., Patel, B. A., Azer, G., Agarwal, P., Bolash, R., & Mekhail, N. (2017). A Comprehensive Outcome-Specific Review of the Use of Spinal Cord Stimulation for Complex Regional Pain Syndrome. *Pain Practice*, *17*(4), 533–545. https://doi.org/10.1111/papr.12513

Vo, L., & Drummond, P. D. (2014). Analgesia to pressure-pain develops in the ipsilateral forehead after high- and low-frequency electrical stimulation of the forearm. *Experimental Brain Research*, *232*(2), 685–693. https://doi.org/10.1007/s00221-013-3776-x

Vogt, B. A. (2005). Pain and emotion interactions in subregions of the cingulate gyrus. *Nature Reviews Neuroscience*, *6*(7), 533–544. https://doi.org/10.1038/nrn1704

Vogt, B. A. (2016). Midcingulate cortex: Structure, connections, homologies, functions and diseases. *Journal of Chemical Neuroanatomy*, *74*, 28–46. https://doi.org/10.1016/j.jchemneu.2016.01.010

Vogt, B. A., Berger, G. R., & Derbyshire, S. W. G. (2003). Structural and functional dichotomy of human midcingulate cortex. *European Journal of Neuroscience*, *18*(11), 3134–3144. https://doi.org/10.1111/j.1460-9568.2003.03034.x

Vogt, B. A., & Sikes, R. W. (2009). Cingulate nociceptive circuitry and roles in pain processing: the cingulate premotor pain model. In B. A. Vogt (Ed.), *Cingulate neurobiology and disease* (pp. 312–339). Oxford University Press.

Volkers, R., Giesen, E., van der Heiden, M., Kerperien, M., Lange, S., Kurt, E., van Dongen, R., Schutter, D., Vissers, K. C. P., & Henssen, D. (2020). Invasive Motor Cortex Stimulation Influences Intracerebral Structures in Patients With Neuropathic Pain: An Activation Likelihood Estimation Meta-Analysis of Imaging Data. *Neuromodulation: Technology at the Neural Interface*, *23*(4), 436–443. https://doi.org/10.1111/ner.13119

Vollert, J., Maier, C., Attal, N., Bennett, D. L. H., Bouhassira, D., Enax-Krumova, E. K., Finnerup, N. B., Freynhagen, R., Gierthmühlen, J., Haanpää, M., Hansson, P., Hüllemann, P., Jensen, T. S., Magerl, W., Ramirez, J. D., Rice, A. S. C., Schuh-Hofer, S., Segerdahl, M., Serra, J., … Baron, R. (2017). Stratifying patients with peripheral neuropathic pain based on sensory profiles: algorithm and sample size recommendations. *Pain*, *158*(8), 1446–1455. https://doi.org/10.1097/j.pain.0000000000000935

Vraa, M. L., Myers, C. A., Young, J. L., & Rhon, D. I. (2022). More Than 1 in 3 Patients With Chronic Low Back Pain Continue to Use Opioids Long-term After Spinal Fusion. *The Clinical Journal of Pain*, *38*(3), 222–230. https://doi.org/10.1097/AJP.0000000000001006

Vrána, J., Poláček, H., & Stancak, A. (2005). Somatosensory-evoked potentials are influenced differently by isometric muscle contraction of stimulated and non-stimulated hand in humans. *Neuroscience Letters*, *386*(3), 170–175. https://doi.org/10.1016/j.neulet.2005.06.005

Vučković, A., Hasan, M. A., Fraser, M., Conway, B. A., Nasseroleslami, B., & Allan, D. B. (2014).

Dynamic oscillatory signatures of central neuropathic pain in spinal cord injury. *Journal of Pain*, *15*(6), 645–655. https://doi.org/10.1016/j.jpain.2014.02.005

Wager, T. D., Atlas, L. Y., Lindquist, M. A., Roy, M., Woo, C.-W., & Kross, E. (2013). An fMRI-Based Neurologic Signature of Physical Pain. *New England Journal of Medicine*, *368*(15), 1388–1397. https://doi.org/10.1056/NEJMoa1204471

Wager, T. D., Matre, D., & Casey, K. L. (2006). Placebo effects in laser-evoked pain potentials. *Brain, Behavior, and Immunity*, *20*(3), 219–230. https://doi.org/10.1016/j.bbi.2006.01.007

Wall, P. D. (1978). The gate control theory of pain mechanisms: A re-examination and re-statement. *Brain*, *101*(1), 1–18. https://doi.org/10.1093/brain/101.1.1

Wall, P. D., & Sweet, W. H. (1967). Temporary Abolition of Pain in Man. *Science*, *155*(3758), 108–109. https://doi.org/10.1126/science.155.3758.108

Wallin, J., Cui, J. G., Yakhnitsa, V., Schechtmann, G., Meyerson, B. A., & Linderoth, B. (2002). Gabapentin and pregabalin suppress tactile allodynia and potentiate spinal cord stimulation in a model of neuropathy. *European Journal of Pain*, *6*(4), 261–272. https://doi.org/10.1053/eujp.2002.0329

Wang, A. L., Mouraux, A., Liang, M., & Iannetti, G. D. (2010). Stimulus Novelty, and Not Neural Refractoriness, Explains the Repetition Suppression of Laser-Evoked Potentials. *Journal of Neurophysiology*, *104*(4), 2116–2124. https://doi.org/10.1152/jn.01088.2009

Watkins, R. H., Dione, M., Ackerley, R., Backlund Wasling, H., Wessberg, J., & Löken, L. S. (2020). Evidence for sparse C-tactile afferent innervation of glabrous human hand skin. *Journal of Neurophysiology*, *125*(1), 232–237. https://doi.org/10.1152/jn.00587.2020

Weiner, R. L., & Reed, K. L. (1999). Peripheral Neurostimulation for Control of Intractable Occipital Neuralgia. *Neuromodulation: Technology at the Neural Interface*, *2*(3), 217–221. https://doi.org/10.1046/j.1525-1403.1999.00217.x

Weir, S., Samnaliev, M., Kuo, T.-C., Tierney, T. S., Manca, A., Taylor, R. S., Bruce, J., Eldabe, S., & Cumming, D. (2020). Persistent postoperative pain and healthcare costs associated with instrumented and non-instrumented spinal surgery: a case-control study. *Journal of Orthopaedic Surgery and Research*, *15*(1), 127. https://doi.org/10.1186/s13018-020-01633-6

Welch, P. D. (1967). The Use of Fast Fourier Transform for the Estimation of Power Spectra: A Method Based on Time Averaging Over Short, Modified Periodograms. *IEEE Transactions on Audio and Electroacoustics*, *15*(2), 70–73. https://doi.org/10.1109/TAU.1967.1161901

Whitlock, J. R. (2017). Posterior parietal cortex. *Current Biology*, *27*(14), R691–R695. https://doi.org/10.1016/j.cub.2017.06.007

Wolter, T., Kieselbach, K., Sircar, R., & Gierthmuehlen, M. (2013). Spinal cord stimulation inhibits cortical somatosensory evoked potentials significantly stronger than transcutaneous electrical nerve stimulation. *Pain Physician*, *16*(4), 405–414. http://www.ncbi.nlm.nih.gov/pubmed/23877457

Woolf, C. J. (1983). Evidence for a central component of post-injury pain hypersensitivity. *Nature*, *306*(5944), 686–688. https://doi.org/10.1038/306686a0

Woolf, C. J. (2011). Central sensitization: implications for the diagnosis and treatment of pain. *Pain*, *152*(3 Suppl), S2–S15. https://doi.org/10.1016/j.pain.2010.09.030

World Health Organisation. (2020). *Global Health Estimates 2019: Disease burden by Cause, Age, Sex, by Country and by Region, 2000-2019*.

Xiao, X., & Zhang, Y.-Q. (2018). A new perspective on the anterior cingulate cortex and affective pain. *Neuroscience and Biobehavioral Reviews*, *90*, 200–211. https://doi.org/10.1016/j.neubiorev.2018.03.022

Xing, G.-G., Liu, F.-Y., Qu, X.-X., Han, J.-S., & Wan, Y. (2007). Long-term synaptic plasticity in the spinal dorsal horn and its modulation by electroacupuncture in rats with neuropathic pain. *Experimental Neurology*, *208*(2), 323–332. https://doi.org/10.1016/j.expneurol.2007.09.004

Xu, A., Larsen, B., Baller, E. B., Scott, J. C., Sharma, V., Adebimpe, A., Basbaum, A. I., Dworkin, R. H., Edwards, R. R., Woolf, C. J., Eickhoff, S. B., Eickhoff, C. R., & Satterthwaite, T. D. (2020). Convergent neural representations of experimentally-induced acute pain in healthy volunteers: A large-scale fMRI meta-analysis. *Neuroscience & Biobehavioral Reviews*, *112*, 300–323. https://doi.org/10.1016/j.neubiorev.2020.01.004

Xu, A., Larsen, B., Henn, A., Baller, E. B., Scott, J. C., Sharma, V., Adebimpe, A., Basbaum, A. I., Corder, G., Dworkin, R. H., Edwards, R. R., Woolf, C. J., Eickhoff, S. B., Eickhoff, C. R., &

Satterthwaite, T. D. (2021). Brain Responses to Noxious Stimuli in Patients With Chronic Pain: A Systematic Review and Meta-analysis. *JAMA Network Open*, *4*(1), e2032236. https://doi.org/10.1001/jamanetworkopen.2020.32236

Xu, H., Wu, L.-J., Wang, H., Zhang, X., Vadakkan, K. I., Kim, S. S., Steenland, H. W., & Zhuo, M. (2008). Presynaptic and Postsynaptic Amplifications of Neuropathic Pain in the Anterior Cingulate Cortex. *Journal of Neuroscience*, *28*(29), 7445–7453. https://doi.org/10.1523/JNEUROSCI.1812-08.2008

Yakhnitsa, V., Linderoth, B., & Meyerson, B. A. (1999). Spinal cord stimulation attenuates dorsal horn neuronal hyperexcitability in a rat model of mononeuropathy. *Pain*, *79*(2–3), 223–233. https://doi.org/10.1016/S0304-3959(98)00169-9

Yang, F., Xu, Q., Cheong, Y.-K. K., Shechter, R., Sdrulla, A. D., He, S.-Q. Q., Tiwari, V., Dong, X., Wacnik, P. W., Meyer, R. A., Raja, S. N., & Guan, Y. (2014). Comparison of intensity-dependent inhibition of spinal wide-dynamic range neurons by dorsal column and peripheral nerve stimulation in a rat model of neuropathic pain. *European Journal of Pain*, *18*(7), 978–988. https://doi.org/10.1002/j.1532-2149.2013.00443.x

Yearwood, T., Hershey, B., Bradley, K., & Lee, D. (2010). Pulse width programming in spinal cord stimulation: a clinical study. *Pain Physician*, *13*(4), 321–335.

Yearwood, T., Ridder, D. De, Yoo, H. Bin, Falowski, S., Venkatesan, L., To, W. T., Vanneste, S., De Ridder, D., Yoo, H. Bin, Falowski, S., Venkatesan, L., Ting To, W., & Vanneste, S. (2019). Comparison of Neural Activity in Chronic Pain Patients During Tonic and Burst Spinal Cord Stimulation Using Fluorodeoxyglucose Positron Emission Tomography. *Neuromodulation: Technology at the Neural Interface*, *2019*(1), 56–63. https://doi.org/10.1111/ner.12960

Yekta, S. S., Lamp, S., & Ellrich, J. (2006). Heterosynaptic long-term depression of craniofacial nociception: Divergent effects on pain perception and blink reflex in man. *Experimental Brain Research*, *170*(3), 414–422. https://doi.org/10.1007/s00221-005-0226-4

Zhang, H.-M., Zhou, L.-J., Hu, X.-D., Hu, N.-W., Zhang, T., & Liu, X.-G. (2004). Acute nerve injury induces long-term potentiation of C-fiber evoked field potentials in spinal dorsal horn of intact rat. *Sheng Li Xue Bao*, *56*(5), 591–596. http://www.ncbi.nlm.nih.gov/pubmed/15497039

Zhang, T. C., Janik, J. J., Peters, R. V., Chen, G., Ji, R. R., & Grill, W. M. (2015). Spinal sensory projection neuron responses to spinal cord stimulation are mediated by circuits beyond gate control. *Journal of Neurophysiology*, *114*(1), 284–300. https://doi.org/10.1152/jn.00147.2015